
The Rich Legacy of Isothiocyanates and Arenediazonium Salts in Metal- Free Cascade Reactions

Submitted by

Anjali Dahiya

Roll No. 166122028




Department of Chemistry
Indian Institute of Technology Guwahati
Guwahati-781039, Assam, India
August, 2022





DEDICATED WITH LOVE

**To Mom, Dad & My Brother, For Their Endless
Love, Support & Encouragement.**







INDIAN INSTITUTE OF TECHNOLOGY GUWAHATI

Department of Chemistry

STATEMENT

I do hereby declare that the matter embodied in this thesis is the result of investigations carried out by me in the Department of Chemistry, Indian Institute of Technology Guwahati, India, under the guidance of Professor Bhisma K. Patel. This thesis has been submitted by me to the Department of Chemistry, Indian Institute of Technology Guwahati for the award of the degree of Doctor of Philosophy.

In keeping with the general practice of reporting scientific observations, due acknowledgements have been made wherever the work described is based on the findings of other investigators. I further declare that this work has not been submitted anywhere else for any degree diploma, associateship or membership etc. of any Institute or University to the best of my knowledge.

August 2022
IIT Guwahati

Anjali Dahiya





INDIAN INSTITUTE OF TECHNOLOGY GUWAHATI

Department of Chemistry

CERTIFICATE

This is to certify that Anjali Dahiya has been working under my supervision since July 2016 as a regular registered Ph. D. student. Her thesis entitled “**The Rich Legacy of Isothiocyanates and Arenediazonium Salts in Metal-Free Cascade Reactions**” is an authentic record of the results obtained from the research work in the Department of Chemistry, Indian Institute of Technology Guwahati, Assam, India. I am forwarding her thesis to submit for the Ph.D. (Science) degree from this institute. I certify that she has fulfilled all the requirements according to the rules of this institute regarding the investigations embodied in her thesis and this work has not been submitted elsewhere for a degree.

August, 2022

Prof. Bhisma K. Patel
(Thesis Supervisor)
Department of Chemistry
IIT Guwahati



ACKNOWLEDGEMENTS

If suffer we must, let's suffer on the heights- Victor Hugo.

A wise person once said that 'doing a Ph.D. is like climbing a mountain'. And no one climbs the mountain alone. So, standing at the final stage of a truly unforgettable journey, I would like to acknowledge and thank the people who climbed with me, supported me, believed in me, and pushed me to the finish line. I wouldn't have reached the summit without you.

First and foremost, I would like to express my deepest respect and appreciation to my supervisor Prof. Bhisma K. Patel for allowing me to work in his group. His scientific ideas, tutelage, endless encouragement, and deep insights have encouraged me to take up the hard and demanding challenges. I feel fortunate to have him as my mentor who gave me unconditional love, a timely morale boost, and total freedom in choosing the work of domain assembled in this thesis.

Besides my mentor, I would like to extend my sincere gratitude to my doctoral committee members, Prof. Bhubaneswar Mandal, Prof. Subhas Chandra Pan, and Dr. Shyam Prosad Biswas for assessing my work timely. Their insightful advice and suggestions helped me to widen my research perspectives and improve my work. Thanks to the Chemistry Department staff for their co-operative nature. Especially Imdadul da for the help he has rendered in NMR analysis and Dr. Babulal Das for discharging his duties whenever I needed help in Single Crystal XRD studies. My sincere thanks to the staff members of the Central Instrument Facility, for their help and guidance with several analytical instruments, required during my research work. Thanks to IIT Guwahati for fellowships and its administration for being kind enough to advise and help in their respective roles.

The entire Patel Lab, past and present, deserves tremendous credit for making my journey so wonderful. I have been fortunate that I came across wonderful lab seniors; Saurav da, Wajid bhai, Ahalya di, Anju di, Suresh da, Bilal bhai, and Prasenjit da who provided enormous help and support during my initial days. Especially, Wajid bhai who nurtured in me the basic lab techniques and provided precious advice even when you were across the sea in South Korea. I also feel lucky to have shared most of my moments with my batchmates Subhendu and my best friend Amitava. When you guys go off to do unbelievable things after your Ph.D., I can't wait to brag that we were batchmates. Without a modicum of doubt, my fabulous and talented lab juniors Tipu, Ashish, Nikita, Tamanna, Bubul, Hiru, Pritishree, and Raju deserve the best and utmost respect for their hard work, diligence, and indispensable input into the research work. From sharing the morning tea to evening snacks, all the lab shenanigans, city parties, and our picnics, I have lived my life to the fullest with these fellow warriors. I am also thankful to the postdoctoral fellow Joy da, Suman Da, Ritush bhai, Gaurav bhai, Kamal da and Binoy bhai. I also had the opportunity to work with some dedicated summer and M.Sc. trainees like Poonam, Arihant,

Mona di, Kunika, Prashant, Pankaj, Shreyasi, Priyabrata, Abhishek, and Akshar. For younger members in the lab: I cannot wait to see how you direct the course of our program and only regret that I can't see your stories unfold firsthand!

No words would suffice to express my feelings toward my teachers to whom I owe my obligations for their great teachings and philosophy to be a good human; Prof. Dinesh Rawat, Prof. Akhilesh K. Verma, Prof. Mahendra Nath, Prof. Indrajit Roy, Dr. Sujata, Dr. Renu Parasher, Dr. Ambika Soni, Dr. Satish Chand and the entire fraternity from my school, Hansraj College (DU), and University of Delhi.

I've also had the benefit of tremendous friendships during my time at IIT-G; Nehal, Jinat, Amitava, Archana, and Sandeep. I am especially grateful to my besties Nehal and Jinat for always being there by my side during the high and lows of my Ph.D. as I am not an easy person to handle. From sharing jokes to watching late-night movies, making fun of each other, partying on the smallest occasion, or when the mess food was not to our liking, it was always great to have you two by my side. I will always cherish these memories throughout my life. Words fall short to express my love to my college buddies, Neha, Himani, Ruhi, Sangeeta, Jyoti, Subodh, Riya, and Annu, your love and care have been the constant source of inspiration during my frustrating times even though you were far apart during this tenure. I would like to extend my gratitude to my friends, seniors, and colleagues at IIT-G, Adil bhai, Shaad bhai, Adil bhai, Ishani di, Gaurangi di, Sumana di, Saumita di, Megha di, Nimisha di, Tushar bhai, Sujan di, Jumi di, Baquir bhai, Akhtar, Shoaib, Adit, Tanumay, Rabindranath, Gobinda, Nasim, Debojit, Kaustav, Bikash, Kanu, Ananya, Subhajit, Mihir, Bipin, Manoj, Subhamoy, Bikoshita, Pallab, Sudip, Surjya, Sabina, Santa, Sonbidya, Manmath, Manideepa, Kavita, Debika, Priyanka, Chandrakanta and Amit.

Lastly, and most importantly, I want to thank my entire family for their unwavering support, and prayers over the past years. The tripods of my life: Mom, Dad, and my brother Arvind. I can't believe you put up with me and my chemistry pipedreams! Your love means the world to me and I always felt more confident pursuing just about anything with you in my corner. Dedicating this thesis to them is a minor recognition for their support and encouragement. Special thanks to my lovely grandmother and my cousin Akshey for their endless love and untiring smile. I can't think of a better support system than you two.

I am always thankful to almighty the creator of everything for giving me a great life, the strength to chase my dreams, and for being with me in all my failures and success.

As I stand on this summit, looking behind reminds me of all the hardships, the milestones, the laughs, the tears, the prayers, and most importantly, the growth that this ascent has allowed. I made it! I can't help but to look forward and set for the new mountains and summits this world has to offer me.

Anjali Dahiya

SYNOPSIS

The contents of this thesis have been divided into four chapters based on the experimental works performed and results obtained during the course of research period. The introductory chapter of the thesis represents a summary of isothiocyanates and aryl diazonium salts as a precursor in metal-free organic synthesis. For simplicity and brevity, Chapter I is divided into two parts. Chapter IA includes an overview of metal-free cascade strategies for the construction of C–C, C–N, C–O and C–S bonds using isothiocyanates. The subsections of Chapter IA are based on the mode of reactivity of aroyl isothiocyanates. Whereas, Chapter IB deals with the different aspects of arenediazonium salts in construction of C–C, C–heteroatom bonds and heterocycles *via* traditional and modern approaches.

Chapter II demonstrates a greener and atom economic route for the synthesis of 2-iminothiazolidines *via* domino ring opening cyclization. Aroyl isothiocyanates and unactivated aziridines were used as a precursor under catalyst and solvent free condition.

Chapter III illustrates a cascade synthesis of *S*-allyl benzoylcarbamothioates *via* mumm-type rearrangement utilizing aroyl isothiocyanates and baylis-hilman alcohols.

Chapter IV describes a visible-light-driven synthesis of isoindolinones using isocyanides and *o*-alkenylanilines. The reaction proceeds *via* intermolecular radical insertion of isocyanides to *in situ* diazotized *o*-alkenylanilines

Each of these chapters comprises of seven subsections which includes introduction, previous work, present work, experimental section, references, spectral data and few representative spectra.

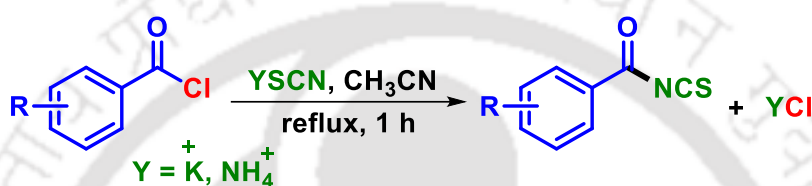
CHAPTER I. An Overview of Isothiocyanates and Arene-diazonium Salts in Metal-Free Cascade Reactions

Part A: The introductory chapter includes the brief understanding of cascade strategies, their advantages, limitations and applications in synthetic organic chemistry. The first part of this chapter includes metal-free reactions of isothiocyanates for the construction of C–C, C–N, C–O and C–S bonds in a cascade manner.

Cascade reactions with 100% atom economy are integral part of contemporary organic chemistry for the synthesis of complex and biologically active natural products. The stepwise synthesis of a target organic compound comprises of purification/isolation of the intermediates at each step. However, cascade reaction is a well-orchestrated sequence of individual reactions that enables the one-pot construction of several bonds without workup and isolation of any of the intermediates. The practicality of any cascade reaction is correlated to the bond-forming efficacy, increase in structural complexity and its suitability for a general application. Bond forming efficacy is the number of bonds which are formed in one sequence. Synthesis of palytoxin is one of the most remarkable examples of cascade reactions. The structural complexity involves 64 stereogenic centres, from which over 10^{19} different stereoisomers could exist.

Catalyst and solvent-less technology has a number of advantages from the perspective of both academia and industry. Two of the twelve principles of “green chemistry” are to “use safer solvent and reaction conditions” and to “prevent waste”. The poisonous and volatile nature of many organic solvents particularly chlorinated hydrocarbons, which are commonly used in huge quantities for organic reactions, have created a serious risk to human health and the environment. Thus, the proposed use of solvent-less catalytic reactions has gained undisputed attention in recent times in the area of green synthesis. Another important advantage of many of these methods are that they are simple and efficient and they exclude any important additional expenditure, which is very attractive for potential industrial applications.

In many cascade approaches, aroyl isothiocyanates are important synthon and have found extensive use in the construction of biologically active acyclic and cyclic frameworks. Isothiocyanates, well-known as a key reagent in the Edman peptide sequencing and a very useful synthons in organic chemistry, especially in the architecture of heterocycles such as functionalized thiazoles, thiadiazoles, triazoles, benzimidazoles, dithiolane, spiro-fused oxazolines, triazines, and oxazines, etc. The methods of synthesis of isothiocyanates have drawn the attention of chemists. Aroyl isothiocyanates, in particular, are easily accessible by the reaction of acyl chlorides with thiocyanate salts such as potassium thiocyanate and ammonium thiocyanate (Scheme IA.1).



Scheme IA.1. Synthesis of aroyl isothiocyanates.

Aroyl isothiocyanate constitute a group of hetero-cumulenes containing an acyl group and a thiocyanate group. Due to the presence of four reactive sites *viz.* the nucleophilic *S* and *N*-atoms, the electrophilic carbonyl and thiocarbonyl groups they serve either as an electrophile or an ambident nucleophile (Figure IA.1). Especially, the carbonyl group in aroyl isothiocyanates divulges unique structural features and it shows differential reactivity under various reaction conditions. The strong electron-withdrawing nature of the adjacent aroyl group enhances the reactivity of the isothiocyanate group and promotes nucleophilic addition at this site.

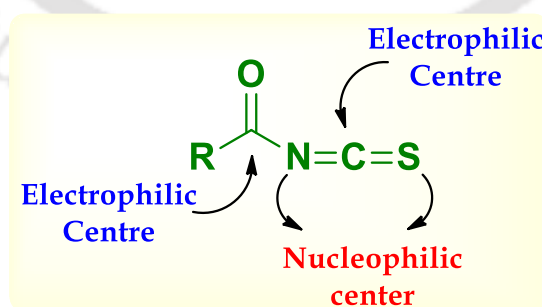


Figure IA.1. Differential reactivity of aroyl isothiocyanates.

Based on the reactive centres of aroyl isothiocyanates its reactions can be divided into following groups:

- Cyclization reactions involving both electrophilic centers
- Cyclization reactions involving the thiocarbonyl group
- Cyclization reactions involving azomethine linkage
- Aroyl isothiocyanates as acyl/thiocyanate transfer reagents

IA.1. Cyclization reactions involving both electrophilic centers

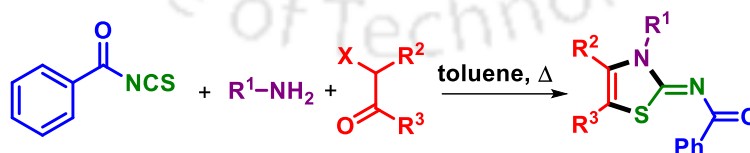
In 2006, Insuasty *et al.* have reported synthesis of pyrazolo[1,5-*a*]-[1,3,5]-triazines derivatives employing the chemistry of aroyl isothiocyanates. This two-step reaction proceeds via formation of thiourea derivatives from 5-amino-3-methylpyrazole and aroyl isothiocyanates, which after *S*-ethylation and cyclization afforded pyrazolo[1,5-*a*]-[1,3,5]-triazines (Scheme I.1.1).



Scheme IA.1.1. Synthesis of pyrazolo[1,5-*a*][1,3,5]triazines.

IA.2. Cyclization reactions involving the thiocarbonyl group

In 2010, Manaka group reported a one-pot three-component condensation of aroyl isothiocyanates, amines and α -halocarbonyls affording the 2-acylimino-alkyl-3*H*-thiazoline ring system. The synthesized 2-imino-thiazoline moiety was further modified to low-molecular-weight β -turn mimics (Scheme I.2.1).

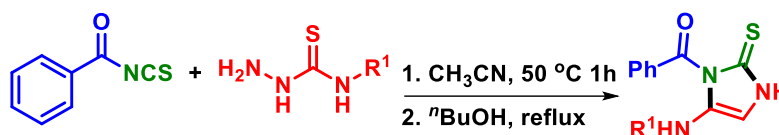


Scheme IA.2.1. Synthesis of 2-imino-thiazolines.

IA.3. Cyclization reactions involving the azomethine linkage

Tolpygin and co-workers reported a two-step reaction of 4-arylalkyl- and 4-arylthiosemicarbazides with aroyl isothiocyanates to give the substituted 1,2-

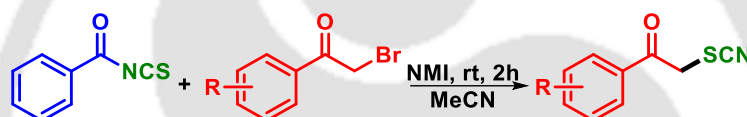
bis(thiocarbamoyl)hydrazines which is readily cyclize to 4-aryl 5-arylalkyl- and 4-aryl-5-arylamino-2H-1,2,4-triazole-3-thiones, respectively (Scheme I.3.1).



Scheme IA.3.1. Synthesis of 2-imino-thiazolines.

IA.4. Aryl isothiocyanates as acyl/thiocyanate transfer reagents

Since 2007, our group is actively involved in the chemistry of aryl isothiocyanates. In 2009, we have established the efficacy of aryl isothiocyanates as a nucleophile with α -bromoketones in the presence of a tertiary amine (*N*-methyl imidazole). This process is most effective when the bromomethyl proton is less acidic, while the presence of a more acidic proton gives 1,3-oxathiol-2-ylidene and other related products (Scheme IA.4.1).

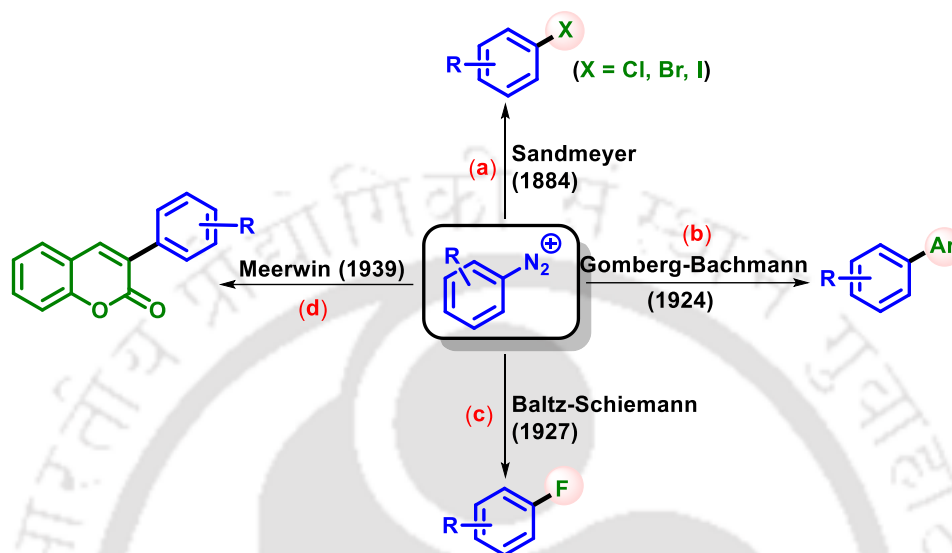


Scheme IA.4.1. Synthesis of α -thiocyanatoacetophenone.

Part B: The second part of this chapter gives a brief synopsis on exploring the chemistry of arenediazonium salts towards the construction of C–C, C–heteroatom bonds and heterocycles *via* traditional and modern approaches.

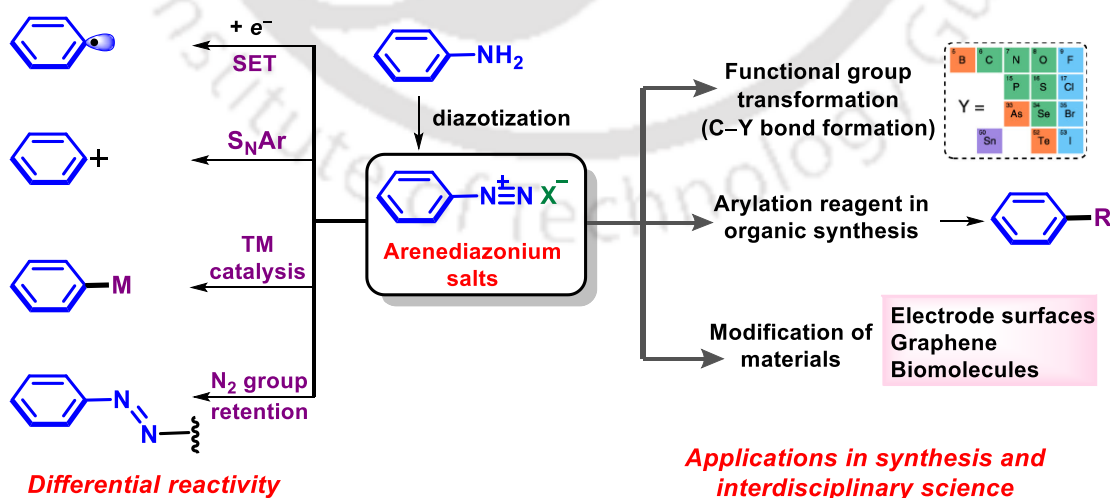
Diazonium compounds, represent a large group of organic compounds with the general formula $R-N\equiv N^+X^-$, in which R can be alkyl or aryl and X is an organic or an inorganic anion such as a halogen. Diazonium salts, especially those where R is an aryl group, are important intermediates and have found wide applications in organic synthesis. Since their first discovery in 1858, several prominent named reactions associated with arene diazonium salts have evolved throughout the development of more than one century (Scheme IB.1). In 1884, Sandmeyer disclosed that by treatment with Cu (I) halides, benzenediazonium salt can be easily converted to aryl halides (Scheme IB.1a). In 1924, Gomberg and Bachmann developed an intermolecular biaryl synthesis via insertion of aryl radical to benzene (Scheme IB.1b). Only three years later, an important innovation was achieved by Balz and Schiemann, where they reported thermal decomposition of aromatic diazonium

tetrafluoroborates to aromatic fluorides, which cannot be accessed by the Sandmeyer reaction (Scheme IB.1c). In 1939, Meerwein and co-workers reported an extensive study on the reaction of aromatic diazonium salts with α,β -unsaturated carbonyl compounds. The reaction was later known as Meerwein arylation, in which the aryl group adds across the double bond (Scheme IB.1d).



Scheme IB.1. Evolution of arene diazonium salts chemistry.

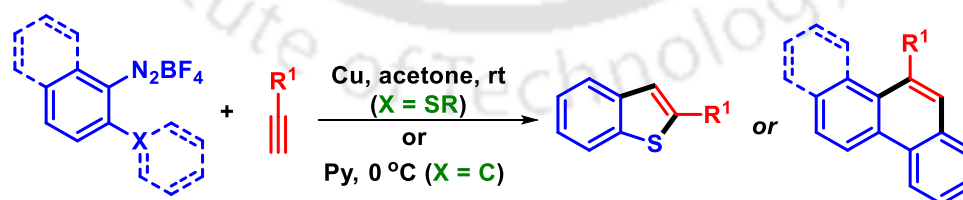
Besides the above-mentioned classical examples, the reactions of arenediazonium salts can be categorized into four classes, including thermal or electro/photochemical transformations via aryl radical, transformations via aryl cation, transition-metal-catalyzed processes, and transformations with retention of the dinitrogen group.



Scheme IB.2. Differential reactivity and applications of arene diazonium salts.

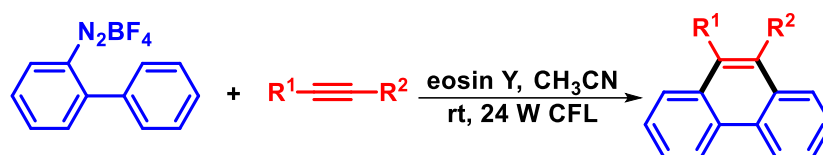
The first three reaction classes are based on the intrinsic electrophilicity of diazonium salts with N_2 as an excellent leaving group. In the last reaction type, in the presence of nucleophiles such as phenols and anilines, the arenediazonium ion can serve as a nitrogen electrophile, giving rise to products with dinitrogen retention (Scheme IB.2). Owing to its ability to serve as aryl halide surrogates, diazonium salts have been widely employed in Pd-catalyzed cross-coupling reactions for C–C bond and C–heteroatom bond formation. These coupling reactions have been well established over the past 40 years since the pioneering work of Kikukawa and Matsuda in 1977, and are comprehensively documented in a series of excellent reviews. The mesomeric stabilization renders many arenediazonium salts stable which can be easily handled under ambient conditions and therefore entertain rich chemistry of aromatic ipso-substitution, *N*-terminal addition reactions, and cycloadditions. In addition, diazonium salts are also highly useful in the dye and pigment industries for the preparation of azo-compounds.

Aryl diazonium salts are prone to undergo a homolytic dediazonation to provide aryl radicals, and the in situ generated aryl radicals can be trapped by other reactive species to form the desired products. Among many different approaches to aryl radicals, the photo-induced reduction of aryl diazonium salts through electron transfer is particularly attractive. The condensed (hetero)aryl ring systems can be generated via homolytic annulation reactions between suitable *ortho* substituted arenediazonium salts and alkynes via radical addition–cyclization sequences. Such annulation reactions were first demonstrated by Zanardi's group in 1984 with *ortho*-methylthio or *o*-phenyl arenediazonium salts and terminal alkynes to produce 2-arylbenzothiophenes and condensed polycyclic aromatic hydrocarbons (PAHs) respectively (Scheme IB.3).



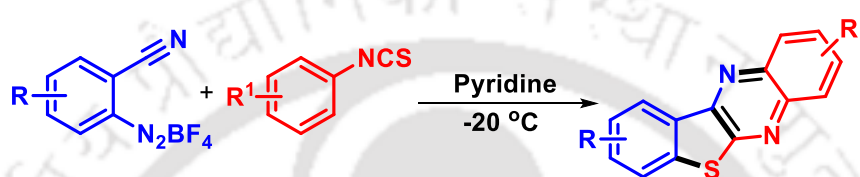
Scheme IB.3. Radical annulation *o*-substituted arenediazonium salts.

In 2012, Zhou group documented a visible-light-induced [4 + 2] benzannulation of biaryldiazonium salts with alkynes, using eosin Y as photoredox catalyst, a variety of 9-substituted or 9,10-disubstituted phenanthrenes were obtained (Scheme IB.4).



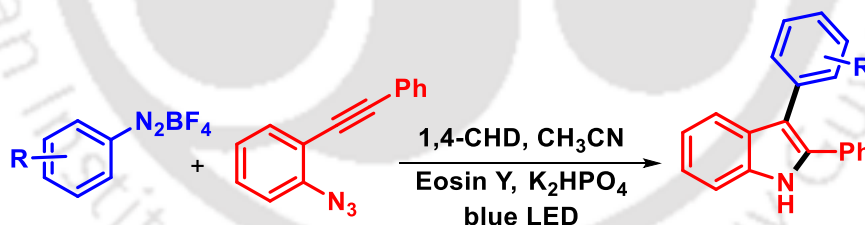
Scheme IB.4. Visible-light-induced [4 + 2] benzannulation of biaryldiazonium salts.

In 1997, Zanardi's group reported a synthesis of benzothienoquinoxalines via a [3 + 2] radical cascade annulation reaction using *o*-cyano arenediazonium salts and aryl isothiocyanates. The benzothienoquinoxalines were obtained in good to moderate yields (Scheme IB.5).



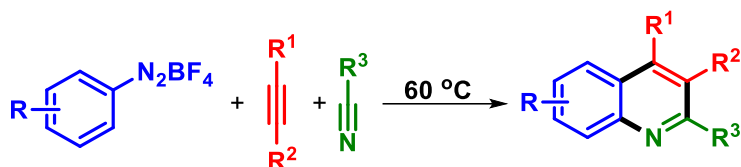
Scheme IB.5. Synthesis of benzothienoquinoxalines using aryl isothiocyanates.

In 2017, Cheng group reported visible-light mediated cyclization reaction of *o*-azidoarylalkynes and aryl diazonium salts. The procedure provides a metal-free approach for the synthesis of unsymmetrical 2,3-diaryl-substituted indoles at room temperature from readily available starting materials. These reactions exhibit excellent substrate scope and predictable regioselectivity (Scheme IB.6).



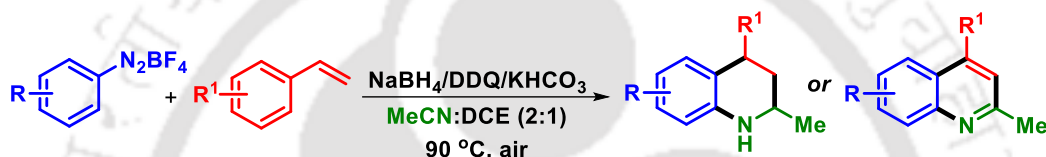
Scheme IB.6. Photocatalytic synthesis of free *N*-H 2,3-disubstituted indoles.

Yu group reported a three-component cascade annulation of readily available aryl diazonium salts, nitriles, and alkynes to give an efficient and rapid synthesis of multiply substituted quinolones. The methodology is catalyst- and additive-free. Various aryl diazonium salts, nitriles, and alkynes can participate in this transformation which shows the broad substrate scope, and up to 83% yield (Scheme IB.7).



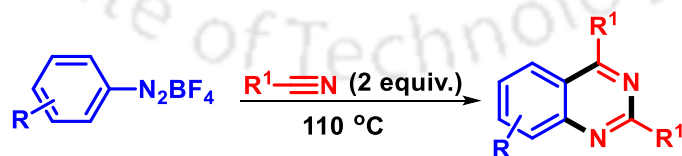
Scheme IB.7. Metal-free synthesis of multi-substituted quinolines.

In 2018, Lee *et al.* documented a similar metal-free, one-pot synthesis of diversely substituted (tetrahydro)quinolines through a three-component assembly reaction of arenediazonium salts, nitriles, and styrenes. The titled compound could be further transformed to quinolines and tetrahydroquinolines depending on the reaction conditions. The advantages of this protocol include its simplicity, metal-free and mild conditions, readily available starting materials, and good functional group tolerance (Scheme IB.8).



Scheme IB.8. Metal-free synthesis of multi-substituted quinolones.

Liu group described a [2 + 2 + 2] modular synthesis of multi-substituted quinazolines by the direct reaction of aryldiazonium salts with two equivalent of nitriles. In the proposed mechanism, reaction of aryldiazonium salt with a nitrile provides the initial formation of a reactive nitrilium ion, which is attacked by another molecule of nitrile followed by electrophilic cyclization to deliver the desired product. Notable feature of the present methodology is flexibility in the substitution patterns, readily available substrates, short reaction time, metal-free, and gram-scale synthesis (Scheme IB.9).



Scheme IB.9. Metal-free synthesis of quinazolines.

In summary the use of aroyl isothiocyanates and arenediazonium salts in metal free cascade reactions has bought the renaissance in the contemporary organic chemistry. Regardless of the rich legacy, the aroyl isothiocyanates and arenediazonium salts still attract

considerable attention and new developments have been emerging constantly via employing modern techniques. Further improvement in this field may open up new avenues to straightforward and efficient synthesis of various complex structures that may find applications in pharmaceuticals or other industries.

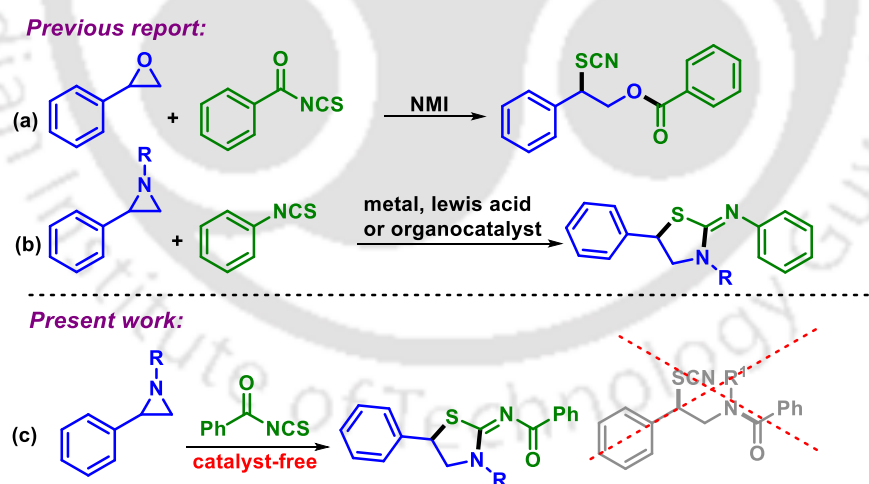
CHAPTER II: Catalyst and Solvent Free Domino Ring Opening Cyclization: A Greener and Atom Economic Route to 2-Iminothiazolidines

This chapter demonstrates a domino ring opening cyclization approach for the synthesis of 2-iminothiazolidines by reacting unactivated aziridines and aroyl isothiocyanates under catalyst and solvent free conditions. The reactions ensue through nucleophilic addition of aziridines on sp carbon of heterocumulene NCS followed by concomitant ring opening of aziridines in a S_N^2 manner.

Heterocycles, including both aromatic and non-aromatic ring systems are ubiquitous in pharmaceuticals and natural products that shows immense biological properties with potential use in medicinal chemistry. Heterocyclic compounds are very widely spread in nature and are crucial to life; vast number of pharmacologically active heterocycles are in regular medical use. For example, penicillin and cephalosporins are commonly used antibiotics. Alkaloids such as vinblastine (chemotherapy medication), morphine (analgesic), and reserpine (anti-hypertensive effect) etc. have heterocyclic moiety. Heterocycles are integral part of genetic material DNA and RNA, bio-macromolecules *viz.*, protein and enzymes. Besides these heterocyclic compounds are also utilized as anti-cancer agents, analeptics, analgesics, antidepressants, hypnotics, pesticides, insecticides, weedicides, rodenticides etc. Heterocyclic compounds have also found enormous applications in material science as analytical reagents, fluorescent sensors, organic conductors and semiconductors, photovoltaic cells etc. For that reasons, great efforts have been devoted over many decades for the development of novel and efficient methods for their synthesis and represents one of the major domains in contemporary organic chemistry. Among these, iminothiazolidines are important structural scaffolds found in many biologically active compounds possessing a wide range of activity such as anti-inflammatory, antidepressant, and anti-Alzheimer. They also act as a nitric oxide synthase (NOS) inhibitor and find applications as a γ -radioprotective agent. These moieties have also been used as organo-catalyst in many reactions. As a consequence, significant efforts have been devoted for the synthesis of 2-

iminothiazolidines from aziridines and isothiocyanates employing various catalytic systems involving either metals or Lewis acids or organo-catalysts. Nevertheless, many of these methods suffer from certain drawbacks such as prolonged reaction time and use of organic solvents and harsh reaction conditions or expensive catalytic systems. In this context, development of greener and atom economic approaches for the synthesis of iminothiazolidine is deemed worthy of investigation.

Due to their unique structural features aroyl isothiocyanates can serve either as electrophiles (ArCO-) or ambident nucleophiles ($-\text{SCN}$). In our previous reports, we have demonstrated the utility of aroyl isothiocyanates as a nucleophile with α -bromoketone while both as an electrophile and a nucleophile with oxirane through a concomitant transfer of thiocyanate as the nucleophile and the aroyl moiety as an electrophile. Thus, it will be interesting to see the outcome of the reaction, if aziridine is used in lieu of the oxirane. Will it form thiazolidine moiety via a $[3 + 2]$ cycloaddition similar to aryl isothiocyanates or undergo a double group transfer similar to oxirane? Both the possibilities exist for aziridine since it is susceptible to undergo double group transfer in a nucleophile less-nucleophilic substitution fashion or undergo a $[3 + 2]$ cycloaddition with heterocumulene ($\text{N}=\text{C}=\text{S}$) of aroyl isothiocyanate leading to 2-iminothiazolidines (Scheme II.1).

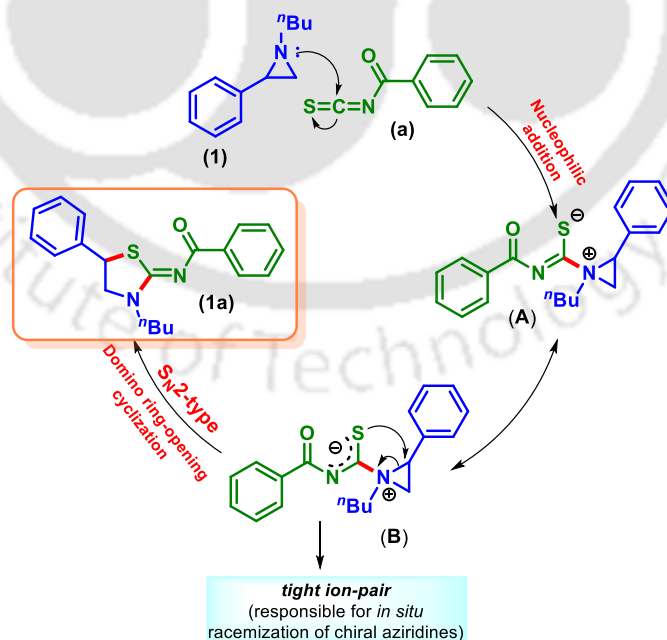


Scheme II.1. Differential reactivity of aroyl isothiocyanates.

In our previous double group transfer process, a *tert*-amine such as *N*-methyl imidazole (NMI) was used as the organo-catalyst for the simultaneous double group transfer reaction involving an oxirane. However, in the present strategy one of the starting materials (aziridine) itself is a *tert*-amine, so it might act similar to NMI and serve as a substrate

become organo-catalyst, eliminating the need for an extra catalyst. Herein, we report a simple and efficient approach for the synthesis of a diverse array of 2-iminothiazolidines *via* domino ring opening cyclization of unactivated aziridines.

To reach the suitable conditions for the synthesis of 2-iminothiazolidines, various solvents were screened. Since all the reagents are liquid at room temperature, it was found that neat condition is the optimal reaction condition. This makes the present methodology an eco-friendly and greener route from the synthetic and environmental point of view. Having established a solvent free optimized reaction condition, this protocol was subsequently applied for [3 + 2] cycloaddition of various *N*-alkyl-2-phenyl aziridines and aroyl isothiocyanates. Regardless of steric and electronic effect, most of the substrates provided moderate to excellent yield. It was observed that electron-donating substituents (EDGs) on the phenyl ring of the aroyl isothiocyanates provided relatively inferior yields of the corresponding products. However, the presence of EDGs on the phenyl ring of the aziridines increases the product yield. The reaction of benzoyl isothiocyanate with activated aziridine *viz.*, 2-phenyl-1-tosylaziridine gave only 17% of the anticipated product. This might be due to the unavailability of activated aziridine lone pair toward nucleophilic attack at the thiocyanate carbon for triggering subsequent ring opening via the attack of thiolate onto the aziridine.



Scheme II.2. Plausible mechanism for the synthesis of 2-iminothiazolidines.

To ascertain the nucleophilic (S_N2) path of aziridine ring opening, reactions were commenced with enantiomerically pure aziridines and aroyl isothiocyanates. The isolated products were found to be optically active but the enantioselectivity was very poor (51-54%). The formation of opposite enantiomers with low enantioselectivity may be due to the presence of a tight ion-pair present in dipolar intermediate (**A**). Since no other reagent is present in the reaction medium that can stabilize **A** which is responsible for the partial *in situ* racemization of chiral aziridines. Based on the earlier reports and our experimental findings a plausible reaction mechanism has been proposed as shown in Scheme II.2. Because of the nucleophilicity of aziridine its lone pair first attacks at the sp carbon of heterocumulene NCS forming a thiourea intermediate **A**. This negative charge on sulfur then attacks onto the benzylic site of aziridine associated with concurrent ring opening giving the 2-iminothiazolidine moiety.

In summary, we have established an elegant catalyst free domino ring opening cyclization approach for the synthesis of 2-iminothiazolidine. This methodology allows the useful synthesis of many valuable 2-iminothiazolidine via catalyst and solvent free approach. In this protocol, C–N and C–S bonds are assembled at the same time and have the merits of wide-ranging substrate scope, greener approach, and shorter reaction time.

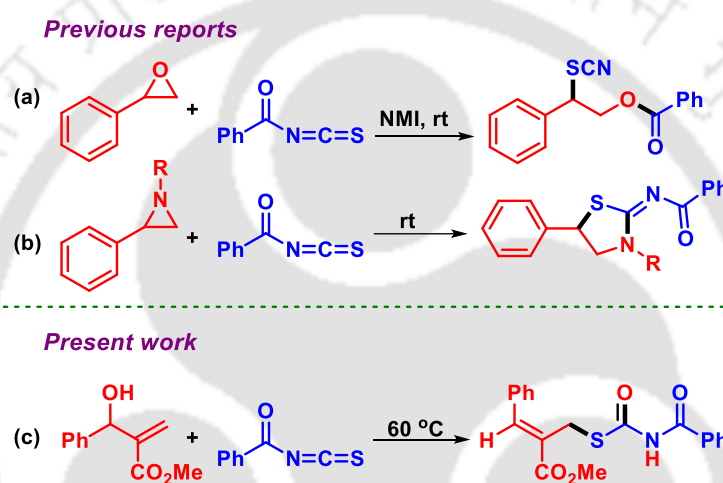
CHAPTER III: A Cascade Synthesis of *S*-Allyl Benzoylcarbamothioates via Mumm-type Rearrangement

This chapter illustrates a catalyst and solvent free synthesis of *S*-allyl benzoylcarbamothioates from the *in situ* generated benzoylcarbonimidothioates obtained by reacting Morita-Baylis-Hilman (MBH) alcohols with aroyl isothiocyanates. This cascade reaction involves an intramolecular thia-Michael addition of the *in situ* generated adduct followed by a Mumm-type of rearrangement leading to a stereoselective synthesis of highly functionalized *S*-allyl benzoylcarbamothioates.

The progress of cascade synthetic methods, where structural divergence is selectively congregated at the molecular level from multifunctional small molecules in one pot, has been established as one of the key epitomes of modern organic chemistry. Toward this endeavour, cascade processes have found wide applications because they successfully implement the goal and principle of sustainability. In many cascade approaches, aroyl isothiocyanates are

important synthon and have found extensive use in the construction of biologically active acyclic and cyclic frameworks.

In our previous reports, we have established the efficacy of aroyl isothiocyanates as a nucleophile with α -bromoketones. While, both as an electrophile and a nucleophile during ring opening of oxiranes and aziridines. In the former a concomitant transfer of a thiocyanate (as nucleophile) and an aroyl moiety (as electrophile) occurs (Scheme III.1a) while in the later a domino ring opening cyclisation of aziridine takes place (Scheme III.1b). Taking cues from the reactivity of aroyl isothiocyanate, we articulated that this could be the precursor to afford *S*-allyl benzoylcarbamothioate upon reaction with MBH alcohol.



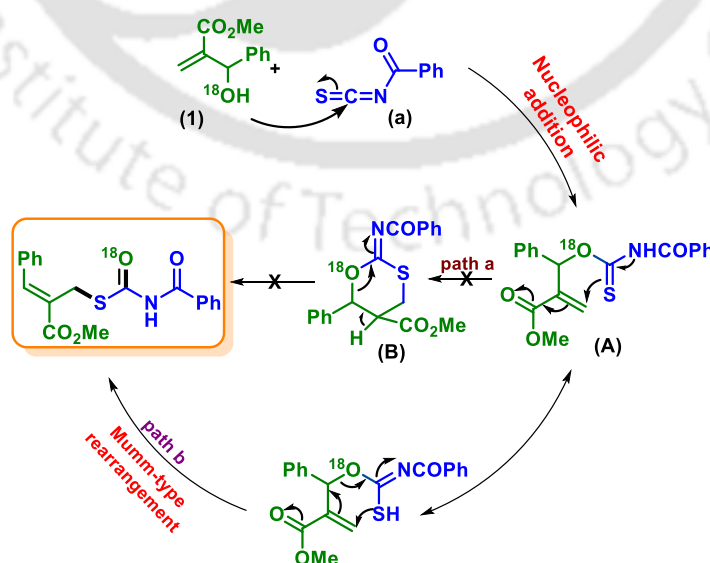
Scheme III.1. Differential reactivity of aroyl isothiocyanates.

In pursuit to accomplish an appropriate reaction condition for this unparalleled transformation, other reaction parameters such as solvents and temperature were screened. Since all the reagents are liquid at room temperature, it was found that at 60 °C a neat condition is the optimal reaction condition. Encouraged by this catalyst and solvent free condition, various aroyl isothiocyanates were reacted with different MBH alcohols to enhance the scope and generality of this rearrangement reaction. To our delight, moderate to excellent yield was observed for the synthesized products. The presence of an electron-donating substituents (EDGs) on the phenyl ring of the MBH alcohols increase the nucleophilicity due to the +I and +R effects and hence better yield was observed compared to substrates bearing electron-withdrawing groups. While, aroyl isothiocyanates bearing EDGs follows a reverse yield pattern which might be due to the decrease in electrophilicity of heterocumulene (N=C=S) owing to the +I and +R effects of EDGs. To our dismay, reaction

was not productive at all when isatin derived MBH alcohols were reacted with benzoyl isothiocyanate. This might be due to the steric hindrance of MBH alcohols that prevents the nucleophilic addition at the sp^2 carbon of $-N=C=S$.

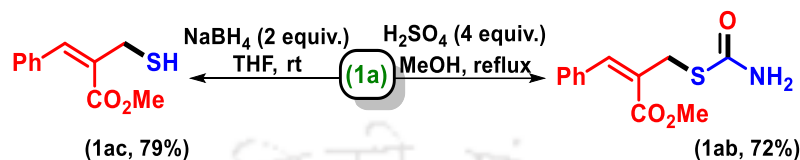
The 1D NOE experiment suggested that *Z*-isomer of *S*-allyl benzoylcarbamothioate was obtained exclusively. The origin of carbonyl oxygen was confirmed by reacting a preformed ^{18}O -labeled MBH alcohol and benzoyl isothiocyanate. ^{13}C NMR analysis of ^{18}O -labeled *S*-allyl benzoylcarbamothioate shows two signals (δ 169.622 and 169.658 ppm) due to both labelled and unlabelled carbonyl group of carbamothioate. This observation suggests that the carbonyl oxygen is originating from the $-OH$ of MBH alcohol.

There are two possible paths that can account for this migration. The first possible route is the generation of a benzoylcarbonimidothioate intermediate (**A**) after nucleophilic addition of MBH alcohol (**1**) with benzoyl isothiocyanate (**a**) which undergo thia-Michael addition to form a cyclic intermediate 1,3-oxathiane (**B**). The intermediate (**B**) opens up to give an *S*-allyl benzoylcarbamothioate (**1a**) (Scheme II.2, path a). However, a careful examination of 1H NMR of the reaction mixture obtained by reacting (**1**) and (**a**) at different time intervals rules out the possible formation of any cyclic intermediate (**B**) (see ESI). The other possibility is that the intermediate (**A**) undergo a thia-Michael addition with concurrent Mumm-type of rearrangement. The Mumm rearrangement involves 1,3 acyl migration of an acyl imidate to an imide. The ^{18}O labelling experiment supports the occurrence of Mumm-type rearrangement.



Scheme III.2. Plausible mechanism for the synthesis of *S*-allyl benzoylcarbamothioates.

To demonstrate the applicability of our protocol, the *S*-allyl benzoylcarbamothioate (**1a**) was subjected to a few useful organic transformations (Scheme III.3). An acid hydrolysis of (**1a**) was carried out which furnished (**1ab**) by cleavage of the imide bond. When (**1a**) was treated with NaBH₄, selective cleavage of C–S bond takes place giving (**1ac**) in moderate yield. Other transformations are still under process.



Scheme III.3. Synthetic utility of *S*-allyl benzoylcarbamothioates.

In summary, we have developed an elegant approach for the synthesis of *S*-allyl benzoylcarbamothioate *via* Mumm-type rearrangement. This methodology allows the useful synthesis of many valuable *S*-allyl benzoylcarbamothioate under mild condition and avoids the use of costly and harmful materials or cumbersome multi-stepped processes. The 18O labeling experiments supports the proposed mechanistic pathway. In this protocol, C=O and C–S bonds are assembled simultaneously and have the merits of wide range of substrate scope, neat condition and simple purification.

CHAPTER IV: Visible-Light-Driven Isocyanide Insertion to *o*-Alkenylanilines: A Route to Isoindolinone Synthesis

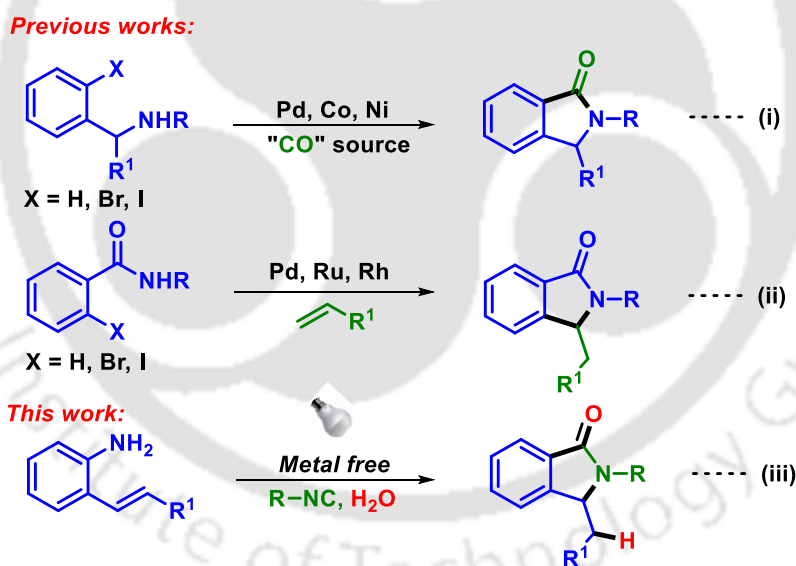
This chapter focuses on intermolecular radical insertion of isocyanides to electron-deficient *o*-alkenylanilines leading to isoindolinones. This photo cascade methodology is overall redox-neutral process and proceeds via isocyanides insertion to *in situ* diazotized *o*-alkenylanilines.

Recently, visible-light mediated functionalizations have emerged as significant tools in modern organic chemistry. Much of the potential of visible-light photoredox catalysis centres on its ability to accomplish remarkable, if not exotic bond formations that are not possible using conventional approaches. However, most organic compounds do not absorb visible light efficiently has limited the application of photochemical synthesis. Therefore, a photocatalyst is often utilized to sensitize organic molecules to carry out required photochemical reactions. The use of visible light sensitization has reduced the side reaction often linked with photochemical reactions conducted with high energy UV light. Some of the

commonly used photocatalysts includes Ru and Ir polypyridyl complexes along with organic dyes that absorbed in the visible-light region.

The wealth of *N*-containing heterocycles in bioactive molecules and pharmaceuticals has inspired synthetic organic chemists to develop novel and efficient methods toward their synthesis. Quaternization of the nitrogen atom is the most common route to enhance the solubility of commercially available drugs which is important for the oral absorption and bioavailability. Hence, most of the drugs contain at least one *N*-heterocycle within their core structures and are thus considered as privileged targets by medicinal chemists.

Among nitrogenous heterocycles, isoindolinone (phthalimidines) scaffold having a C(sp³)-N bond represents a growing class of benzo fused γ -lactam natural products. Synthetic and natural isoindolinones are medicinally relevant possessing various biological activities such as inhibitors for the production of tumour necrosis factor (TNF- α), 4 MGR-1 antagonist, anti-tumour, anti-inflammatory, antimicrobial, antioxidant, antifungal, anxiolytic, antiviral etc.



Scheme IV.1. Various approaches for the synthesis of isoindolinones.

The prerequisite isoindolinone derivatives are synthesized via lactamization of *o*-(aminomethyl)benzoic acids, reductive/condensative cyclizations, halogenation (or direct C-H activation) and cyclization of *o*-methylbenzamides, and carbonylative strategies {Scheme IV.1 (i)}. The C-H functionalization strategies for isoindolinone synthesis requires the use of *N*-substituted benzamides as reactants bearing either activating or directing groups {Scheme IV.1 (ii)}. The common synthetic precursor for the synthesis of isoindolinone is *N*-

substituted benzamides which are synthesized via carbonylative coupling using aryl halides or aryl diazonium salts as electrophile and primary or secondary amines as nucleophiles.

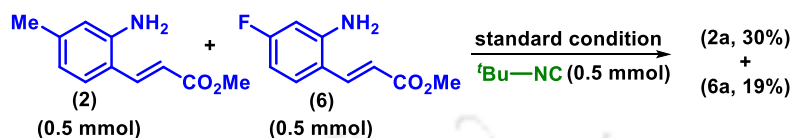
Isocyanides are a class of highly versatile and irreplaceable reagents that can act as both a nucleophile and an electrophile. Structurally, isocyanides are isoelectronic equivalents of carbon monoxide and are widely used in palladium-catalyzed insertion reactions. The literature revealed that the reaction of aryl diazonium salts and isocyanides generates imidoyl radicals that can be used for subsequent reactions. Thus, we anticipated that the in situ generated 2-alkenylaryldiazonium salts could be used as a suitable precursor in this photocatalytic isocyanide insertion followed by intramolecular cyclization to give the corresponding isoindolinones.

To realize our hypothesis, a preliminary reaction was conducted between methyl 3-(2-aminophenyl) acrylate and *tert*-butyl isocyanide. Herein, methyl 3-(2-aminophenyl)acrylate was first diazotized to the corresponding 2-alkenylaryldiazonium tosylates followed by the addition of *tert*-butyl isocyanide, eosin Y (2 mol%) as photocatalyst, base Cs₂CO₃ (2 equiv.), DMSO (2 mL) and stirred under the irradiation of 2 x 10 W white LEDs at room temperature. A new compound was isolated in a satisfactory yield of 82%. The IR spectra (peaks at 1683 and 1735 cm⁻¹), ¹H NMR (absence of alkene protons) and ¹³C NMR revealed the product structure to be a benzo fused lactam. Finally, the single X-ray crystallographic diffraction study of one of the derivatives re-established its structure to be methyl 2-(2-(naphthalen-2-yl)-3-oxoisoindolin-1-yl)acetate. In the pursuit to accomplish an appropriate reaction condition for this transformation, extensive optimization studies involving the selection of different catalytic systems, bases and solvents were carried out. After a series of optimizations, we found that eosin Y (2 mol %), Cs₂CO₃ (2 equiv.), equivalent amount of *in situ* diazotized *o*-alkenylanilines and isocyanides in 2 mL DMSO is the optimal condition for the reaction.

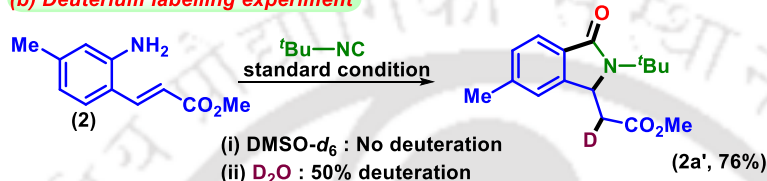
With the optimized condition in hand, the viability of the reaction was subsequently applied for various *o*-alkenylanilines using different isocyanides. The anticipated isoindolinones were obtained in good to moderate yield irrespective of electronic and steric bulk of *o*-alkenylanilines and isocyanides. Nevertheless, under the standard conditions the reaction with an electron-rich alkene *viz.* 2-styrylaniline failed to give the desired isoindolinone instead, the (*E*)-*N*-(*tert*-butyl)-2-styrylbenzamide intermediate was obtained in 83% yield. To find out the reason, CV of the (*E*)-*N*-(*tert*-butyl)-2-styrylbenzamide was

performed. The $E_{1/2 \text{ oxd}}$ (+1.48 V vs. SCE) of (*E*)-*N*-(*tert*-butyl)-2-styrylbenzamide was found to be higher than the $E_{1/2 \text{ red}}$ (+0.83 V vs. SCE) of excited EY. The higher $E_{1/2 \text{ oxd}}$ of (*E*)-*N*-(*tert*-butyl)-2-styrylbenzamide prevents the ET process and further cyclization in the case of 2-styrylaniline.

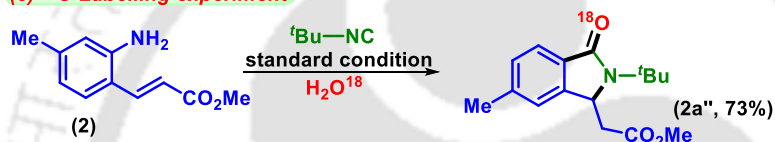
(a) Intermolecular competitive experiment



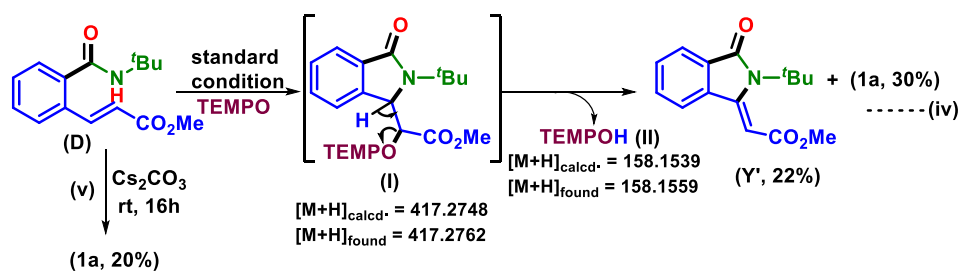
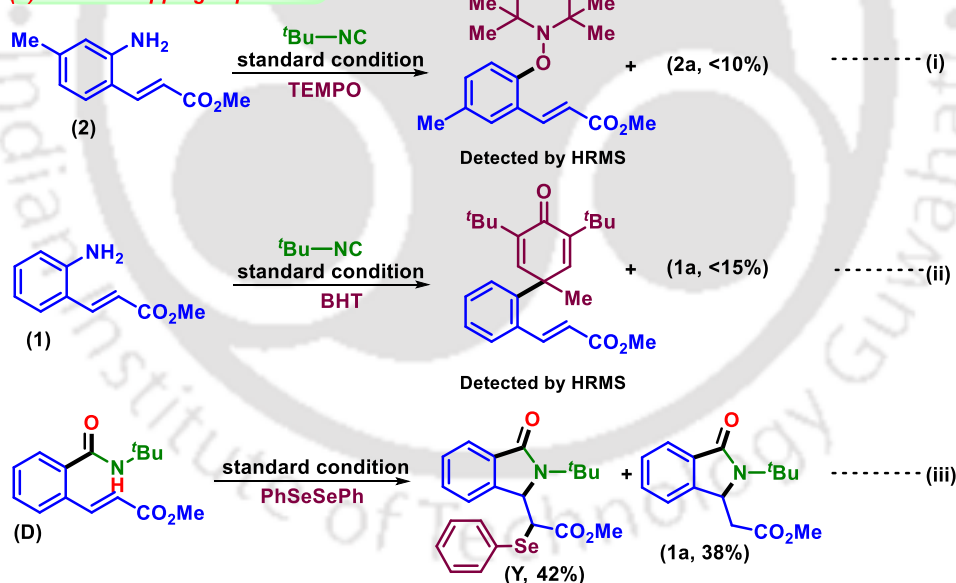
(b) Deuterium labelling experiment



(c) ^{18}O Labelling experiment



(d) Radical-trapping experiment

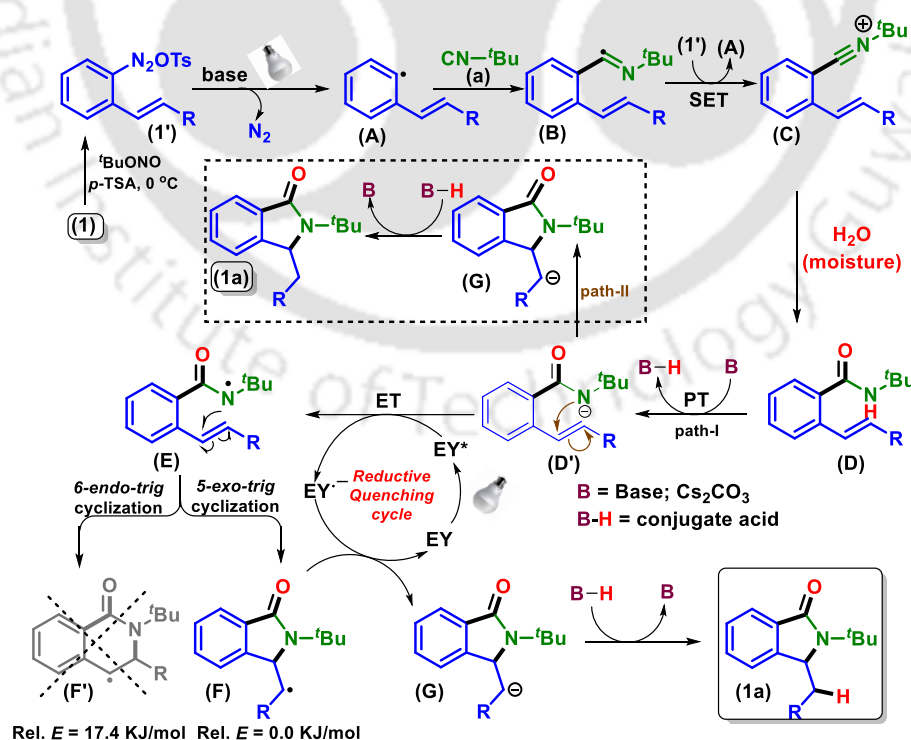


Scheme IV.2. Intermolecular competitive experiment and mechanistic investigations.

The intermolecular competitive experiments reveal that *o*-alkenylanilines possessing EDGs show better reactivity compared to EWGs. This might be due to the $-M$ and $-I$ effect of EWGs which possibly destabilize the aryl radical intermediate after the dediazotization step (Scheme IV.2a). To unearth the origin of extra hydrogen and carbonyl oxygen of the product, few labelling experiments were carried out. The deuterium labelling experiment with D_2O gave 50% deuteration at α position of ester group. This supports that the moisture present in solvent (DMSO) is the possible source of hydrogen (Scheme IV.2b). The ^{18}O labelling experiment with equivalent amount of H_2O^{18} confirms water to be the source of carbonyl oxygen (Scheme IV.2b). The reaction in the presence of radical scavenger 2,2,6,6-tetramethylpiperidine-1-oxyl (TEMPO) and 2,6-di-*tert*butyl-4-methyl phenol (BHT) turned out to be messy. The formation of trapped TEMPO and BHT adducts of aryl radical intermediate (confirmed by HRMS analysis of the reaction mixture) affirms the radical nature of the reaction {Scheme IV.2d (i) and (ii)}. From 2-alkenyl carboxamide the reaction can either proceed via radical or an anionic pathway (aza-Michael addition). Thus, few radical trapping experiments were conducted with 2-alkenyl carboxamide under standard reaction condition. The reaction with TEMPO and diphenyldiselenide failed to give corresponding isoindolinone product which supports the radical nature of the reaction {Scheme IV.2d (iii) and (iv)}. The reaction of carboxamide **D** in the absence of EY and light gave only 20% of isoindolinone (**1a**) after 16 h {Scheme III.3d (v)}. This suggests that in addition to the anionic mechanism a predominant radical path is operating concurrently under this photochemical condition. Stern-Volmer quenching and CV experiments further supports the photochemical nature of the reaction. In the Stern-Volmer plot, a linear quenching in excitation of eosin Y in presence of Cs_2CO_3 and 2-alkenylcarboxamide (**D**) was observed. This indicates the electron transfer between excited state of eosin Y (EY^*) and **D** where Cs_2CO_3 is acting as a Brønsted base and helping in the stepwise PT/ET pathway for the generation of an amidyl radical. Similarly, the addition of equivalent amount of Cs_2CO_3 , the $E_{1/2\text{ oxd}}$ of **D** was found to be +0.286 V vs. SCE (+0.33 V vs. Ag/AgCl sat. KCl), which is lower than the $E_{1/2\text{ red}}$ of excited EY, *i.e.*, +0.83 V vs. SCE. This confirms the base mediated PT/ET process between the excited state of eosin Y (EY^*) and **D** to generate $EY^{\cdot-}$ radical anion and an amidyl radical.

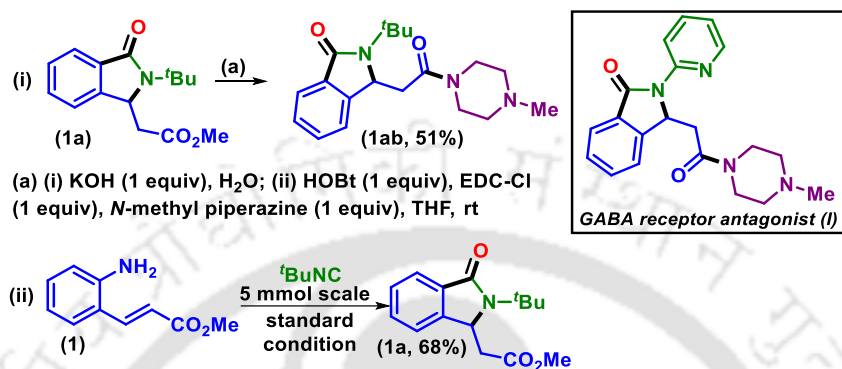
Based on the above experimental results and literature precedents, a plausible mechanism is proposed for this photochemical reaction (Scheme IV.3). Initially, the *in situ*

generated 2-alkenyl arenediazonium salt (**1'**) forms an aryl radical (**A**) via a visible-light-induced deamination process. The aryl radical (**A**) is then trapped by isocyanide (**a**) to give an imidoyl radical (**B**) followed by a single electron transfer (SET) between 2-alkenyl arenediazonium salt (**1'**) and **B** to give a nitrilium intermediate (**C**) and aryl radical (**A**). The nucleophilic addition of water and concurrent tautomerization gives a 2-alkenyl carboxamide species (**D**). As evident from the Stern-Volmer (SV) and CV experiments, the carbonate base induces PT from 2-alkenyl carboxamide (**D**) to give intermediate **D'** followed by ET between the excited state of eosin Y (**EY***) and **D'** to give an amidyl radical (**E**) and a radical anion of eosin Y (**EY⁻**). The intermediate **E** can undergo 5-*exo-trig* or 6-*endo-trig* cyclization. The DFT calculations energetically favours the formation of **F** (5-*exo-trig*) instead of **F'** (6-*endo-trig*) by 17.4 KJ/mol. Thus, a 5-*exo-trig* cyclization of **E** gives intermediate (**F**) which is reduced by radical anion of eosin Y to give intermediate (**G**), thereby maintaining the reductive catalytic cycle of eosin Y. Finally, the intermediate (**G**) abstracts a proton from the conjugate acid of base (B-H) to give the corresponding isoindolinone (**1a**) (Scheme IV.3). Based on the control experiment {Scheme IV.2d (v)} it is apparent that without photochemical conditions an anionic reaction pathway cannot be completely ruled out (path-II). Notably, the present photocatalytic cycle is a redox-neutral process without the addition of any external oxidant.



Scheme IV.3. Plausible mechanism for the synthesis of isoindolinones.

To demonstrate the synthetic utility of the isoindolinone products, **1a** was transformed to a useful analogue (**1ab**) of a GABA receptor antagonist (**I**) {Scheme IV.4 (i)}. To check the scalability of the present protocol, a standard reaction was carried out at a 5 mmol scale. Delightfully, the anticipated isoindolinone (**1a**) was obtained in 68% yield {Scheme IV.4 (ii)}.



Scheme IV.3. Post-synthetic modification of isoindolinone.

In conclusion, we have demonstrated a photocatalytic approach for accessing isoindolinones via PT/ET-assisted amidyl radical formation. The photochemical nature of this protocol was confirmed by SV and CV experiments. Mechanistic investigations confirm water as –H and –O sources. This photo cascade methodology is overall a redox neutral process featuring metal-free condition and substrate scope is demonstrated with 32 examples. This method is amenable to gram-scale synthesis. The practical utility of the present protocol is demonstrated by synthesizing analogue of GABA receptor antagonist.

CONTENTS

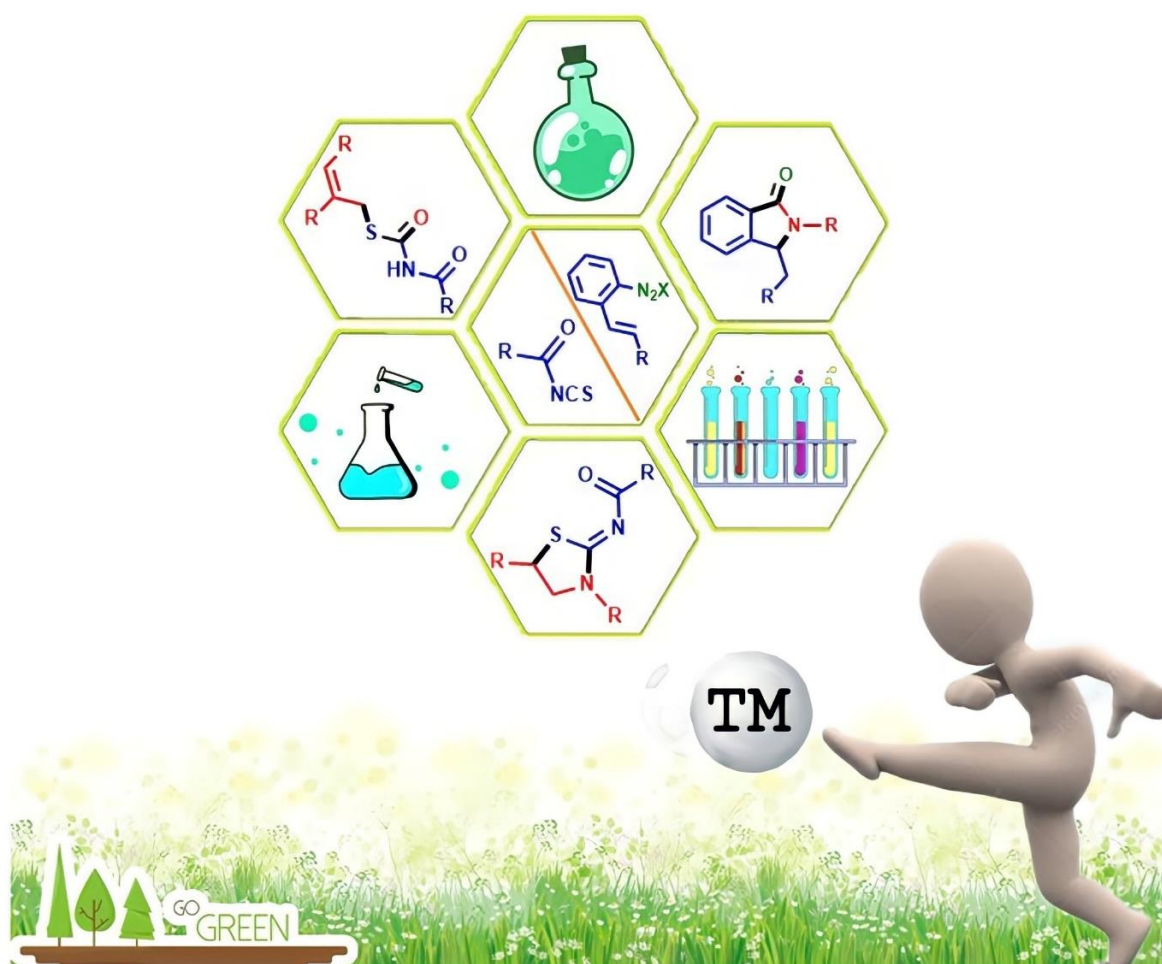
Chapter I—An Overview of Isothiocyanates and Arenediazonium Salts in Metal-Free Cascade Reactions	1
IA. An Overview of Isothiocyanates in Metal-Free Cascade Reactions	03
I.A.1. Introduction	03
I.A.2. Historical Background	04
I.A.3. Classification of Cascade Reactions	06
I.A.4. Transition Metal-Free Cascade Reactions	07
I.A.4. IA.5. Representative Examples of Transition Metal-Free Cascade Reactions of Isothiocyanates	08
IA.5.1. Cyclization reactions involving both electrophilic centers	11
IA.5.2. Cyclization reactions involving the thiocarbonyl group	12
IA.5.3. Cyclization reactions involving the azomethine linkage	15
IA.5.4. Acyl isothiocyanates as acyl/thiocyanate transfer reagents	17
I.A.6. References	19
IB. An Outline of Metal-Free Cascade Reactions of Arenediazonium Salts	25
IB.1. Introduction	25
IB.2. Historical Background	26
IB.3. Reactivity and Modern Applications	27
IB.4. Representative Examples of Transition Metal-Free Cascade Reactions of Arenediazonium Salts	29
IB.4.1. C–C bonds formation	29
IB.4.2. C–O bonds formation	33
IB.4.3. C–N bonds formation	35
IB.4.4. C–S bonds formation	41
IB.4.5. C–Y bonds formation (Y = B, Se, Te, Sn, P)	45
IB.5. Arenediazonium Salts: An Archetype for Modification of Functional Materials and Molecules	45
IB.7. References	48

Chapter II– Catalyst and Solvent Free Domino Ring Opening Cyclization: A Greener and Atom Economic Route to 2-Iminothiazolidines	55
II.1. Introduction	55
II.2. Differential Strategies Towards the Synthesis of 2-Iminothiazolidines	56
II.3. Present work	64
II.4. Experimental section	71
II.4.1. General information	71
II.4.2. Crystallographic Description	72
II.4.3. General procedure for synthesis of (1a)	72
II.4.4. General procedure for synthesis of (a-k)	72
II.5. References	73
II.6. Spectral data	75
II.7. Spectra	91
Chapter III A Cascade Synthesis of S-Allyl Benzoylcarbamothioates via Mumm-type Rearrangement	103
III.1. Introduction	103
III.2. Ideas Toward the Synthesis of S-Aryl Carbamothioates	104
III.3. Present work	110
III.4. Experimental section	117
III.4.1. General information	117
III.4.2. Crystallographic Description	117
III.4.3. General procedure for synthesis of (1a)	117
III.4.4. General procedure for synthesis of (a-k)	118
III.4.5. General procedure for synthesis of (1-18)	118
III.4.6. General procedure for synthesis of (1ab)	118
III.4.7. General procedure for synthesis of (1ac)	119
III.4.8. NOE Experiment	119
III.4.9. Mechanistic Investigation	121
III.4.10. ¹⁸ O Labelling Experiment	122
III.5. References	124
III.6. Spectral Data	126

III.7. Spectra	141
Chapter IV- Visible-Light-Driven Isocyanide Insertion to <i>o</i>-Alkenylanilines: A Route to Isoindolinone Synthesis	151
IV.1. Introduction	151
IV.2 Differential Strategies for Synthesis of Isoindolinones	152
IV.3. Present work	159
IV.4. Experimental section	170
IV.4.1. General information	170
IV.4.2. Crystallographic Description	170
IV.4.3. General procedure for synthesis of (1a)	171
IV.4.4. Intermolecular Competitive Experiment	171
IV.4.5. Deuterium Labelling Experiment	172
IV.4.6. ¹⁸ O Labelling Experiment	174
IV.4.7. Radical-trapping Experiment	176
IV.4.8. Stern-Volmer Quenching Studies	183
IV.4.9. Cyclic Voltammetry Experiments	185
IV.4.10. Post-Synthetic Modification	187
IV.4.11. DFT Study	187
IV.5. References	190
IV.6. Spectral data	195
IV.7. Spectra	209
List of Publications	217

CHAPTER I

An Overview of Isothiocyanates and Arenediazonium Salts in Metal-Free Cascade Reactions





CHAPTER IA

IA. An Overview of Isothiocyanates in Metal-Free Cascade Reactions**IA.1. Introduction**

Nature's biosynthetic systems have progressed over billions of years that are competent in efficient one-pot multi-step catalysis. Compared with biosynthesis, organic synthesis is still in its initial stages having started only in the early 1800s. The complexity and structural diversity of natural products have fascinated organic chemists for a very long time. The underlying mechanisms that simplify these biological reactions have become the main driving force in synthetic chemistry. The blueprints of biosynthetic systems are founded on some key fundamentals, *viz.* cascade reactions and the avoidance of protecting-group strategies, which, when combined have a huge impact on the efficiency of biosynthetic systems.¹

The traditional approach for the synthesis of a target molecule is the stepwise construction of individual bonds towards the synthesis of the target organic compound. The stepwise synthesis comprises purification/isolation of the intermediates at each step. Thus, it would be much more efficient if a single step in a concurrent fashion can construct several bonds without isolating the intermediates. Such processes would be more economic by requiring fewer reagents, solvents, energy, and labor together with a minimized waste generation. These "one-pot" reactions have been described in various contexts and different terms, which are discussed below.²

Type-1 processes comprise 'domino' or 'cascade' reactions which involve a well-orchestrated sequence of individual reactions that enables the one-pot construction of several bonds without workup and isolation of any of the intermediates. The term domino/cascade indicates that the individual reactions are difficult to perform in a stepwise fashion as they belong tightly together. Therefore, the intermediates of individual steps are most likely unstable which eludes isolation and characterization (Figure IA.1.1).

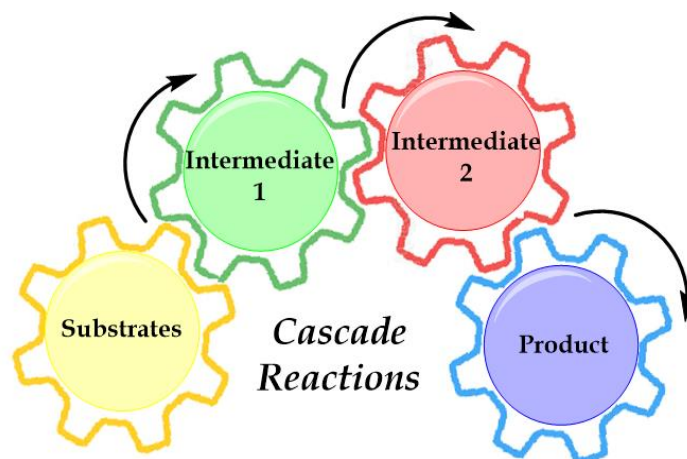


Figure IA.1.1. Cascade or domino reaction.

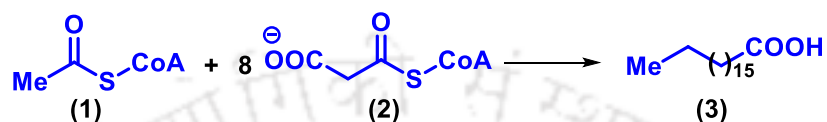
Type II processes include two-step (or more) reactions that proceed in a sequential manner where each of the steps can be performed separately. Such reactions are denoted as ‘*sequential*’ or ‘*tandem*’ reactions. Thus, it can be expected that the intermediate will be a stable species that can be isolated and characterized.

The practicality of any reaction is correlated to the bond-forming efficacy, increase in structural complexity and its suitability for a general application. Bond forming efficacy is the number of bonds that are formed in one sequence. The synthesis of palytoxin is one of the most remarkable examples of a cascade reaction. The structural complexity involves 64 stereogenic centers, out of which over 10^{19} different stereoisomers could exist.³ With all these utilities cascade reactions have vastly contributed to both the science and art of total synthesis. This brings not only the improved practical efficiency and its suitability for a general application but also enhanced aesthetic appeal to synthetic planning.⁴

IA.2. Historical Background

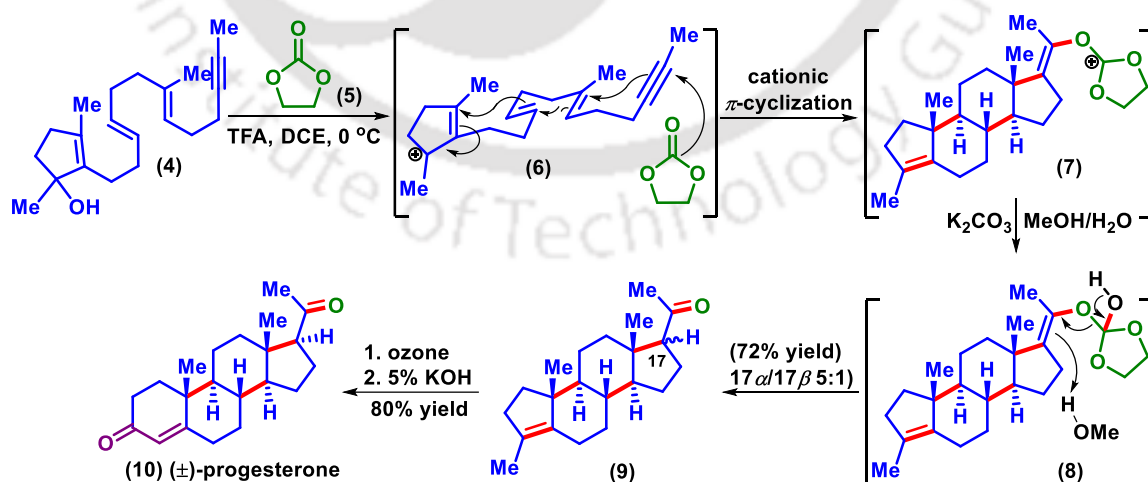
In nature, domino reactions are rather common. Nature has synthesized a variety of compounds viz. fatty acids from acetate, steroid,⁵ progesterone,⁶ daphnilactone A,⁷ and (+)-codaphniphylline⁸ via cascade strategies. Since the evolution, the forces of nature have cultivated and enhanced the properties of biological macromolecules to contribute to the survival of their host organism. These adaptive forces have stimulated enzymes with the ability to catalyze reactions at rate accelerations of up to 10^{17} fold. Because of the involvement of multienzymes and fast reaction rate, a direct comparison of reactions in a flask to biosynthesis is not possible. Incidentally, the biosynthesis of fatty acids starting

from acetate presents a beautiful example of a natural cascade reaction. Remarkably, the reaction stops after putting together the acetate (1) and 7 or 8 equiv. of malonyl-S-CoA (2) to give either palmitic acid or stearic acid (3). Such control is rather difficult to mimic in a reaction flask (Scheme IA.2.1).⁹ Another example of a natural cascade reaction includes the biosynthesis of steroids from squalene epoxide which is transformed selectively into lanosterol with the formation of four C–C bonds and generation of six stereogenic centers.¹⁰



Scheme IA.2.1. Biosynthesis of fatty acids.

The cascade/domino reactions either anticipated or serendipitous discoveries have attracted significant attention of synthetic organic chemists since the formative years of total synthesis. The first seminal cascade synthesis was reported by Schöpf and Robinson (1917) by reacting succindialdehyde, acetone dicarboxylic acid, and methylaminopropionone through double Mannich reactions to give tropinone.¹¹ Thus, the Mannich reaction is apparently the first cascade reaction described in the literature.¹² Subsequent typical examples of cascade reactions include the synthesis of progesterone via cationic polyolefin cyclization developed by Johnson and co-workers.⁶ This approach is based on the Stork–Eschenmoser hypothesis (Scheme IA.2.2).¹³



Scheme IA.2.2. Total synthesis of (±)-progesterone via polyolefin cyclization.

IA.3. Classifications of Cascade Reactions

Classification of cascade reactions is sometimes difficult due to the diverse nature of the many steps involved in the transformation. All the reactions do not meet the criteria set by its definition. According to L. F. Tietze's definition, a cascade reaction is understood as;

'A process involving two or more bond-forming transformations which take place under the same reaction conditions without adding additional reagents and catalysts and in which the subsequent reactions result as a consequence of the functionality formed in the previous step.' -L. F. Tietze

If a starting precursor have several functionalities and all of them underwent an individual transformation in the same pot then such reactions will not be regarded as cascade reaction. For example, the well-developed Diels–Alder reaction may not be accredited as a cascade reaction, although two bonds are usually formed in one sequence. The preliminary step of any reaction, involving the generation of reactive intermediates, for example, carbocation and carbanion are not counted as the step of the reaction. However, the generation of diene through retro-Diels-Alder reaction with a concurrent cycloaddition step would be considered a cascade reaction.^{1a} To further simplify things, L. F. Tietze classified the cascades reactions based on the nature of the first step in the mechanism into the following categories:

- Anionic Cascade Reactions
- Cationic Cascade Reactions
- Pericyclic Cascade Reactions
- Radical Cascade Reactions
- Transition-Metal-Induced Cascade Reactions
- Enzymatic Cascade Reactions
- Photochemical-Induced Cascade Reactions
- Cascade Reactions Induced by Oxidation/Reduction

Combination of the reactions with a similar mechanism in each step is termed as homo-domino reactions and such reactions occur more often in the literature e.g., cationic-cationic, anionic-anionic, pericyclic-pericyclic, radical-radical, and transition metal-catalyzed reactions. On the contrary, reactions involving different types of mechanisms are

called hetero-domino reactions. Such reactions are less frequent but there are a few important hetero-domino reactions that have both been investigated thoroughly *viz.* the anionic-pericyclic sequence and the anionic-pericyclic-pericyclic reactions.^{1a}

Since the work delineated in this dissertation solely belongs to metal-free nucleophilic cascade reactions of isothiocyanates, and traditional and photochemical induced cascade reactions of arene diazonium salts, the description pertaining to these is only discussed here.

IA.4. Transition Metal-Free Cascade Reactions

Earlier, chemists used to synthesize simple and small molecules but cascade approaches have opened the avenues to construct complex molecules in terms of creating many bonds, rings, and stereocenters in a single transformation.¹⁴ Regardless of this great achievement and its importance to our daily life, the public image of chemistry has deteriorated due to the increasing importance of environmental issues and the perception that it could negatively affect the ecological balance. So, today's challenge is not *what we can synthesize* but *how we do it sustainably*. Major problems associated with chemical production are waste management and the search for environment-friendly procedures that preserve resources and increase the efficiency of the protocol. These issues are nicely summarized in the ideal synthesis as proposed by Wender *et al* (Figure IA.4.1).¹⁵

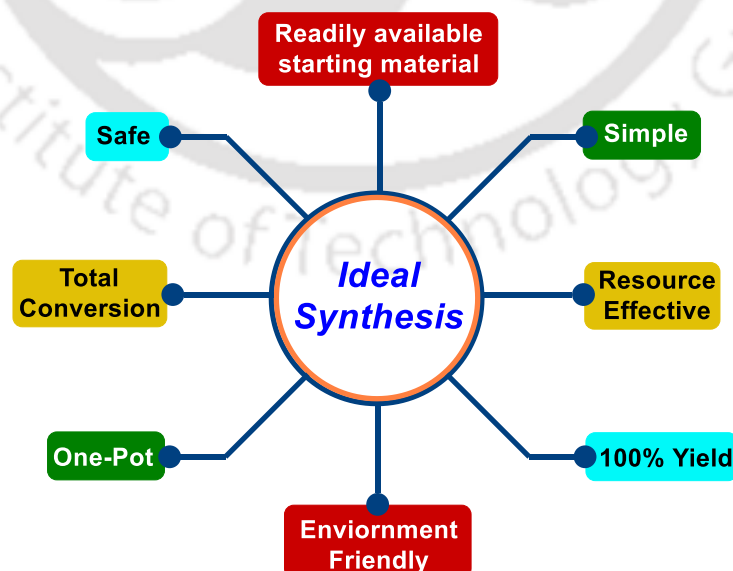


Figure IA.4.1. The principle of ideal synthesis as proposed by Wender *et al*.

In terms of an ideal synthesis, metal-catalyzed reactions sometimes face predicaments in terms of either cost or toxicity. As an alternative, catalyst and solvent-less technology have made significant progress and are recognized as powerful tools in the chemist's arsenal. Two of the twelve principles of "green chemistry" are to "use safer solvent and reaction conditions" and to "prevent waste." Thus, the domain of metal-free reactions has become significant for avoiding expenses and environmental issues. The poisonous and volatile nature of many organic solvents particularly chlorinated hydrocarbons, which are commonly used in large quantities for organic reactions, have created a serious risk to human health and the environment. Thus, the proposed use of solvent-less and metal-free reactions has gained undisputed attention in recent times in the area of green synthesis. Another important advantage of many of these methods is that they are simple and efficient and they exclude any important additional expenditure, which is very attractive for potential industrial applications.¹⁶

With these merits, metal-free C–C, C–O, C–N, and C–S bond-forming cascade reactions have undoubtedly witnessed important progress in recent years and there is no dearth of prospects in the synthetic chemist's arsenal. Such types of reactions have epitomized a paradigm shift and the synthetic community has witnessed an unparalleled advancement in the field of C–C and C-heteroatom bond-forming reactions. In the following chapters, the chemistry of isothiocyanates and arene diazonium salts are discussed separately. Chapter IA includes an overview of metal-free cascade strategies for the construction of heterocycles (via C–C, C-heteroatom bond formations) using isothiocyanates. Whereas, Chapter IB deals with the different aspects of aryl diazonium salts in the construction of C–C, C-heteroatom bonds via traditional and photochemical approaches.

IA.5. Representative Examples of Transition Metal-Free Cascade Reactions of Isothiocyanates

Isothiocyanates (ITC) are highly versatile reagents having widespread applications in organic, medicinal, and combinatorial chemistry. Owing to this, isothiocyanates as synthons have gained the significant attraction of synthetic organic chemists. Isothiocyanates are easily available and compared to their oxygen analogous, isocyanates, are less unpleasant and to some extent less harmful to work with. Naturally occurring

isothiocyanates are limited in number. Conversely, there is a large number of synthetic isothiocyanates which constitute an important class of compounds. Isothiocyanates are usually found to be present in some species of cruciferous vegetables (e.g., broccoli, kale, brussels sprouts, cabbage, mustard, garden cress, and cauliflower) as progenitors, called glucosinolates, and are released from the injured plant by the enzyme myrosinase. The cruciferous vegetables are a rich source of benzyl-ITC (BITC), phenethyl-ITC (PEITC), allyl-ITC (AITC), and sulforaphane (SFN) (Figure IA.5.1). The isothiocyanates have some biological activities as well, such as to exhibit anticancer activity in animals treated with chemical carcinogens due to their inhibition of carcinogen metabolic activation.¹⁷

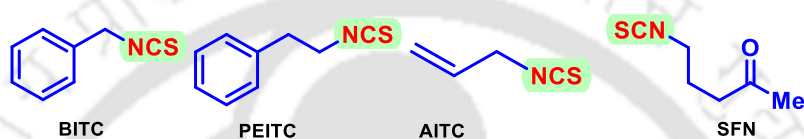
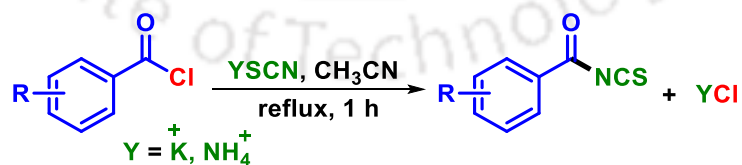


Figure IA.5.1. Examples of naturally found isothiocyanates.

Isothiocyanates are recognized as an important reagent in the Edman peptide sequencing and very valuable synthons in synthetic organic chemistry.¹⁸ In many cascade approaches, isothiocyanates have found extensive use in the construction of biologically active acyclic and cyclic frameworks, e.g., functionalized thiazoles, thiadiazoles, triazoles, benzimidazoles, dithiolane, spiro-fused oxazolines, triazines, and oxazines, etc.¹⁹ Therefore, the synthesis of isothiocyanates has also drawn the attention of chemists. Compared to aryl isothiocyanates, acyl isothiocyanates are easy to synthesize by reacting acyl chlorides with thiocyanate salts such as lead thiocyanate ($\text{Pb}(\text{SCN})_2$), potassium thiocyanate (KSCN) and ammonium thiocyanate (NH_4SCN) as shown in Scheme IA.5.1.²⁰



Scheme IA.5.1. Synthesis of acyl isothiocyanates.

The rich legacy of isothiocyanates is well documented in the literature. The presence of a carbonyl group in acyl isothiocyanates imparts unique reactivity to acyl isothiocyanates compared to aryl isothiocyanates. Structurally, acyl isothiocyanate constitutes a group of

hetero-cumulenes containing an acyl group and a thiocyanate group. Due to the presence of four reactive sites *viz.* the nucleophilic S and N-atoms, the electrophilic carbonyl and thiocarbonyl groups serve either as an electrophile or an ambident nucleophile (Figure IA.5.2).²¹ Especially, the carbonyl group in aroyl isothiocyanates divulges unique structural features and it shows differential reactivity under various reaction conditions. The strong electron-withdrawing nature of the adjacent acyl group enhances the reactivity of the isothiocyanate group and promotes nucleophilic addition at this site. There is evidence that suggests a slight conjugative donation in the case of acyl isothiocyanates.²²

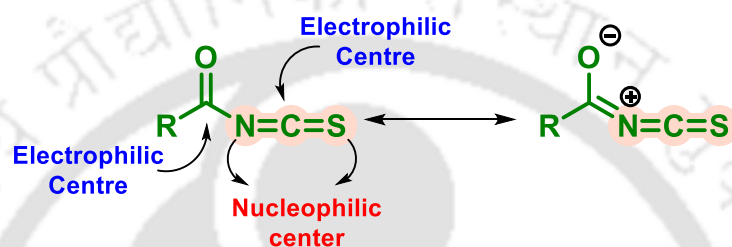


Figure IA.5.2. Differential reactivity of acyl isothiocyanates.

Goerdeler *et al.* reported that a thermal 1,3-shift of substituent R in acyl isothiocyanates is possible via the transition state TS (Figure IA.5.3). The isomerization of aroyl isothiocyanates to thioacyl isocyanates takes place in solution phase at temperatures around 100 °C. Even though the acyl isothiocyanates are more stable than thioacyl isocyanates, an equilibrium between the two may be attained from either side under favorable conditions. The migratory aptitude observed for this equilibrium is: R = Alk)₂N–, Alk(Ar)N– > ArS– > AlkS– > ArO– > AlkO– (If R was *tert*-butyl, or CCl₃, no rearrangement was observed).²³

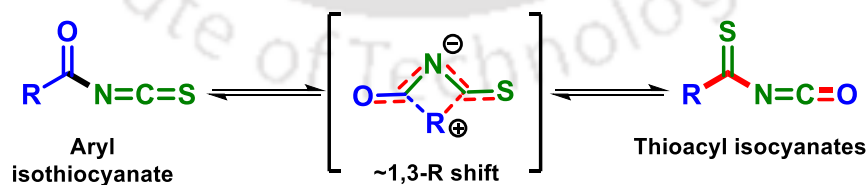


Figure IA.5.3. Thermal 1,3-rearrangement of acyl isothiocyanates.

Due to the strong electron-withdrawing nature of the adjacent acyl group, the reactivity of the isothiocyanate group increases and helps in the nucleophilic addition at this position. The most common nucleophiles that have been frequently explored in metal-free cascade reactions of acyl isothiocyanates are nitrogen-based nucleophiles *viz.* –NH₂,

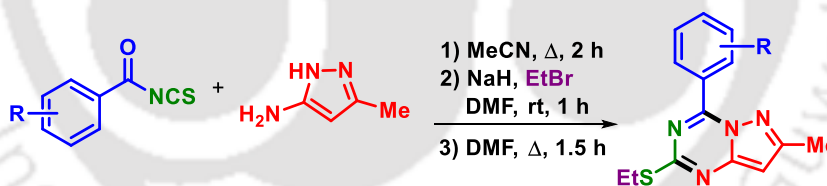
-N₂H₄, hydrazides, amidines, etc. The subsequent cyclization of the resulting adducts (according to the mode of reactivity) provides access to various five or six-membered heterocycles including bicyclic condensed ring systems, for example, 1,2,4-triazoline, thiazolidine, benzothiazole, benzoxazine, benzimidazole, benzoxazole, etc.

Based on the reactive centres of aroyl isothiocyanates its reactions can be divided into the following groups:

- Cyclization involving both electrophilic centers
- Cyclization involving the thiocarbonyl group
- Cyclization involving azomethine linkage
- Aroyl isothiocyanates as thiocyanate/acyl transfer reagents

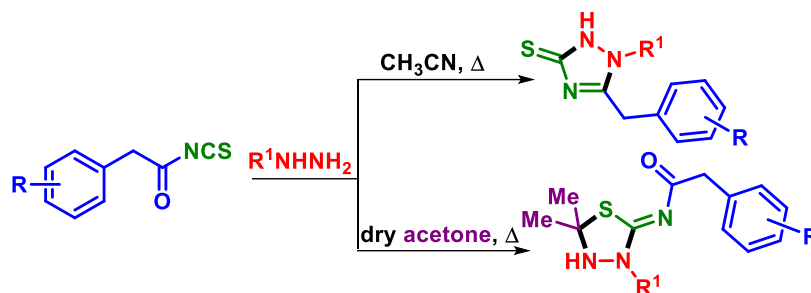
IA.5.1. Cyclization reactions involving both electrophilic centers

In 2006, Insuasty *et al.* reported the synthesis of pyrazolo[1,5-*a*]-[1,3,5]-triazines derivatives employing the chemistry of aroyl isothiocyanates. This two-step reaction proceeds via the formation of thiourea derivatives from 5-amino-3-methylpyrazole and aroyl isothiocyanates, which after *S*-ethylation and cyclization afforded pyrazolo[1,5-*a*]-[1,3,5]-triazines (Scheme IA.5.1.1).²⁴



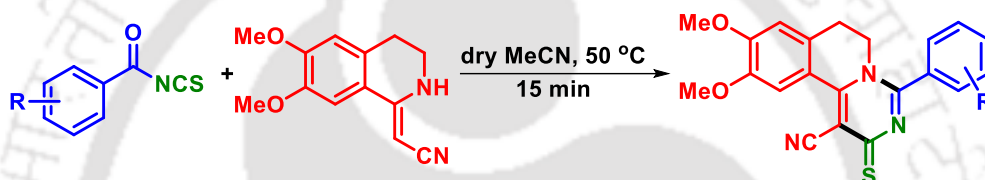
Scheme IA.5.1.1. Synthesis of pyrazolo[1,5-*a*][1,3,5]triazines.

Hemdan and co-workers demonstrated a solvent-dependent, metal-free synthesis of 1,2,4-triazoline-3-thione and thiadiazolidine derivatives using 2-phenylacetyl isothiocyanate, benzoylhydrazine, and hydrazine as reactants. The reaction proceeds via an addition-cyclization sequence. The reaction of isothiocyanate with phenylhydrazine in acetonitrile solvent provided the 1,2,4-triazoline derivative whereas, in dry acetone, thiadiazolidine derivatives were obtained (Scheme IA.5.1.2).²⁵



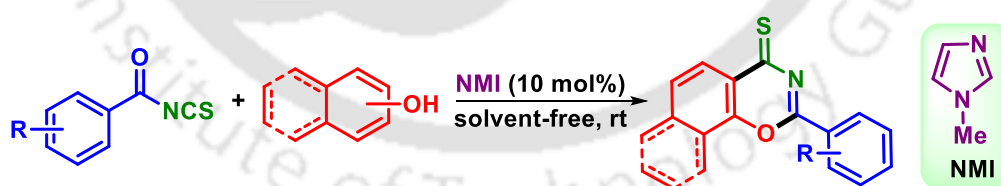
Scheme IA.5.1.2. Synthesis of 1,2,4-triazoline-3-thiones and thiadiazolidines.

In 2011, Afon'kin *et al.* reported a metal-free synthesis of 1,2-fused oxo- and thioxodihydropyrimidoisoquinolines and thiouracyloisoquinoline by reacting acyl isothiocyanates and enamine 6,7-dimethoxy-3,4-dihydroisoquinolin-1-ylacetonitrile under anhydrous acetonitrile (Scheme IA.5.1.3).²⁶



Scheme IA.5.1.3. Synthesis of thioxodihydropyrimidoisoquinolines.

An excellent metal and solvent-free method for the synthesis of benz- and naphthoxazine-4-thiones is developed by Khalilzadeh's group by reacting phenols and naphthols with acyl isothiocyanates in the presence of *N*-methylimidazole (NMI) as an organocatalyst (Scheme IA.5.1.4).²⁷

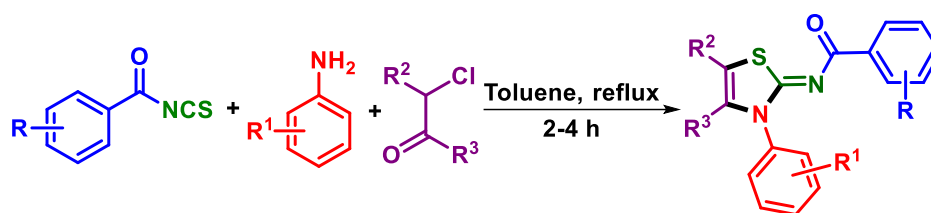


Scheme IA.5.1.4. Synthesis of naphthoxazine-4-thiones.

IA.5.2. Cyclization reactions involving the thiocarbonyl group

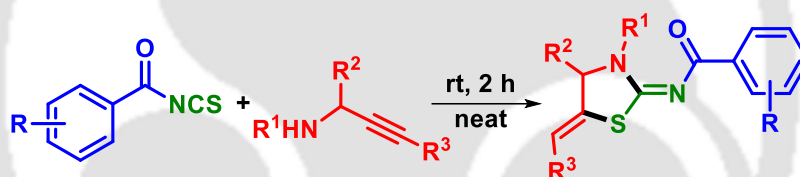
Manaka group reported a metal-free, three-component synthesis of 2-acylimino-3-alkyl-3*H*-thiazoline derivatives by reacting aroylthiourea, primary amine, and α -halocarbonyl derivatives. The method was further used to synthesize β -turn tripeptide

mimics by introducing various functional groups at 4-positions in the 3*H*-thiazoline scaffold (Scheme IA.5.2.1).²⁸



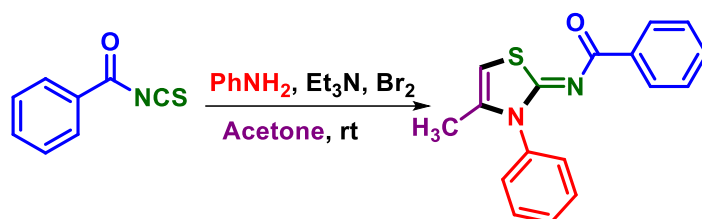
Scheme IA.5.2.1. Synthesis of 2-acylimino-3-alkyl-3*H*-thiazolines.

In 2017, Dethé *et al.* disclosed a metal-free thiol-yne coupling for the synthesis of thiazolidin-2-ylideneamine using propargylamine and acyl isothiocyanate as coupling partners. The *in situ* generated propargylthiourea undergoes 5-*exo-dig* cyclization to give thiazolidin-2-ylideneamine under a neat condition. The present protocol provided a wide variety of thiazolidin-2-ylideneamine derivatives under metal-free, solvent-free conditions with no requirement for additional additives (Scheme IA.5.2.2).²⁹



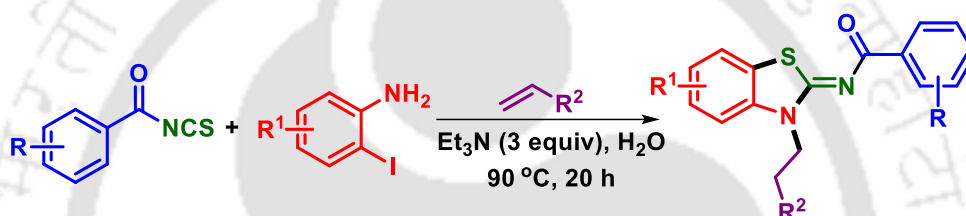
Scheme IA.5.2.2. Synthesis of 2-iminothiazolidines via thiol-yne coupling.

In 2006, our group reported the synthesis of thiazolidene-2-imine by reacting 1-benzoyl-3-phenylthiourea (from benzoyl isothiocyanate and aniline) with enolizable ketones such as acetone in the presence of bromine and triethylamine. Instead of bromine a more safer and efficient brominating agent, 1,1'-(ethane-1,2-diyl)dipyridinium dibromide (EDPBT), also provided the 2-iminothiazolidines in excellent yields.³⁰ Before this work, Zou's group reported the formation of imidazole-2-thione under present conditions.³¹ However, in this work, we have unambiguously proved that the final product is a 2-iminothiazolidine scaffold and not an imidazole-2-thione (Scheme IA.5.2.3).



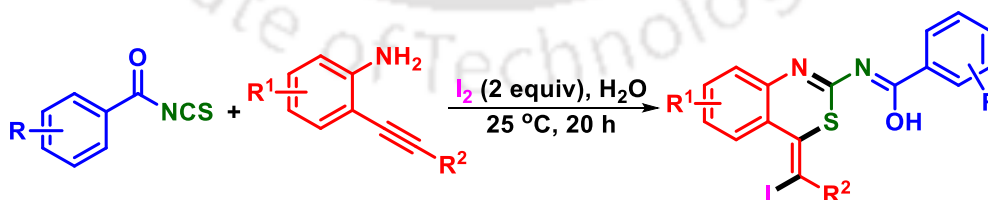
Scheme IA.5.2.3. Multicomponent synthesis of thiazolidene-2-imine.

A metal-free, one-pot, three-component synthesis of functionalized benzo[*d*]thiazol-2(3*H*)-ylidene benzamide was accomplished by Verma *et al.*, using *ortho*-iodoanilines, aryl isothiocyanates, and activated alkenes. The “on-water” methodology proceeds via the *in situ* generations of thiourea intermediate followed by base-mediated intramolecular S_NAr displacement and a successive Michael addition to activated alkenes (Scheme IA.5.2.4).³²



Scheme IA.5.2.4. Synthesis of functionalized benzo[*d*]thiazol-2(3*H*)-ylidene benzamides.

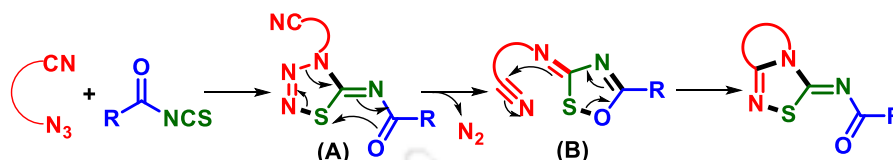
In the same year, Verma’s group developed an iodine-mediated “on-water” synthesis of diversely substituted 1,3-benzothiazines by reacting *ortho*-alkynylanilines and aryl isothiocyanates. This metal- and base-free cascade strategy proceeds via regioselective 6-*exo-dig* cyclization of the *in situ* generated *ortho*-alkynylthiourea. The final product 1,3-benzothiazines preserves the iodo-olefin substitution pattern which can be used for further late-stage derivatization (Scheme IA.5.2.5).³³



Scheme IA.5.2.5. Synthesis of substituted 1,3-benzothiazines.

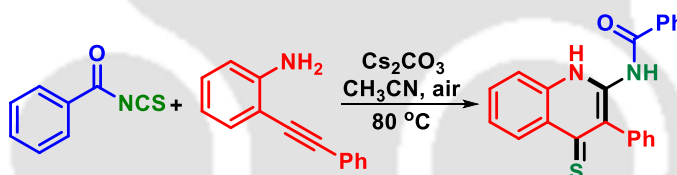
L'abbe and coworkers reported the cascade reaction of acyl isothiocyanates with organic azides having a nitrile group at the γ - or δ -positions to give the fused dihydro-1,2,4-thiadiazolimines. The intermediate dihydrothiadiazoles (**A**) were obtained by

cycloaddition of azides across the C=S bond of the acyl isothiocyanates. However, due to the anchimeric assistance of the carbonyl group these intermediates are unstable. Upon decomposition, dihydrothiatrazoles generates a stable fused thiadiazole via 1,2,4-oxathiazol-3-imine intermediate (**B**) (Scheme IA.5.2.6).³⁴



Scheme IA.5.2.6. Synthesis of fused dihydro-1,2,4-thiadiazolines.

In 2017, our group reported a base-mediated synthesis of diversely functionalized quinoline-4(1*H*)-thiones by reacting *ortho*-alkynylanilines with aroyl isothiocyanates. The reaction proceeds through a 6-*exo-dig*S-cyclization of the *in situ* generated *ortho*-alkynylthiourea followed by rearrangement. This metal-free cascade approach is 100% atom-economic, and have wide functional group tolerance with good to excellent yields of quinoline-4(1*H*)-thiones (Scheme IA.5.2.7).³⁵



Scheme IA.5.2.7. Base mediated synthesis of quinoline-4(1*H*)-thiones.

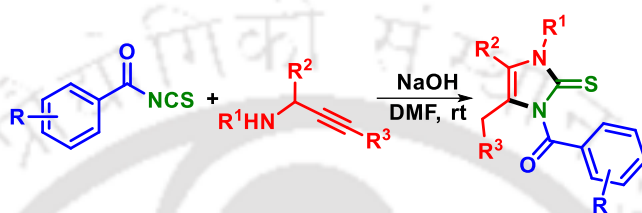
IA.5.3. Cyclization reactions involving the azomethine linkage

Tolpygin and co-workers reported a two-step reaction of 4-arylalkyl- and 4-arylthiosemicarbazides with aroyl isothiocyanates to give the substituted 1,2-bis(thiocarbamoyl)hydrazines, which are readily cyclized to 4-aryl 5-arylalkyl- and 4-aryl-5-arylamino-2*H*-1,2,4-triazole-3-thiones, respectively (Scheme IA.5.3.1).³⁶



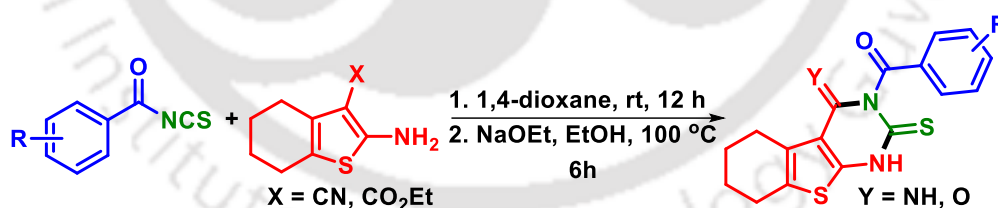
Scheme IA.5.3.1. Synthesis of 2-imino-thiazolines.

A metal-free and base-mediated intramolecular hydroamination strategy for the synthesis of diversely substituted imidazole-2-thione and spiro-cyclic imidazolidine-2-thione is reported by Dethe and co-workers. Herein, propargylamine and isothiocyanate are used as reacting partners. This regioselective intramolecular 5-*exo-dig* cycloisomerization reaction is atom economic and an array of imidazole-2-thiones are synthesized, which could be used as precursors for the synthesis of novel *N*-heterocyclic carbenes (NHCs) (Scheme IA.5.3.2).³⁷



Scheme IA.5.3.2. Synthesis of imidazole-2-thiones.

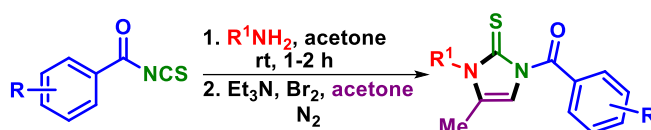
El-Sharkawi *et al.* accomplished a two-step synthesis of annulated thiophenes containing tetrahydropyrimidines by reacting aroyl isothiocyanates with 2-amino tetrahydrobenzothiophenes under metal-free conditions. In the first step, the reaction of aroyl isothiocyanates with 2-amino-4,5,6,7-tetrahydrobenzo[*b*]thiophenes generates *N*-benzoylthiourea derivatives. Under basic conditions, thioureas undergo cyclization to give the tetrahydrobenzo[*b*]thieno[2,3-*d*]pyrimidine derivatives (Scheme IA.5.3.3).³⁸



Scheme IA.5.3.3. Synthesis of tetrahydrobenzo[*b*]thieno[2,3-*d*]pyrimidines.

Due to their various pharmacological and bioactivities, derivatives of the imidazole-2-thione scaffold have attracted widespread attention. In this regard, a base-catalyzed condensation reaction was reported by Saeed and Batool for the synthesis of 1-(isomeric methyl) benzoyl-3-aryl-4-methylimidazole-2-thiones. The reaction of acetone with thioureas (obtained from aroyl isothiocyanates and anilines) in the presence of Et₃N and

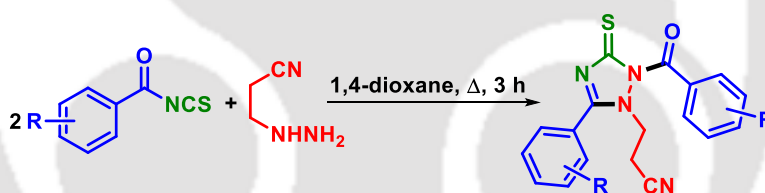
Br₂ provided 1-tolyl-3-aryl-4-methylimidazole-2-thiones in reasonable yields (Scheme IA.5.3.4).³⁹



Scheme IA.5.3.4. Synthesis of imidazole-2-thiones.

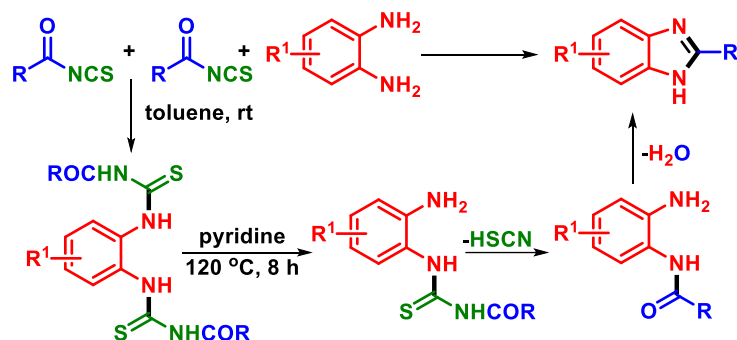
IA.5.4. Acyl isothiocyanates as acyl/thiocyanate transfer reagents

Elmoghayar and co-workers disclosed a metal-free, one-step cascade synthesis of 5-thioxo-1,2,4-triazole derivatives by reacting β -cyanoethylhydrazine with aroyl isothiocyanates in dioxane at room temperature. Herein, two molecules of aroyl isothiocyanates are used. Initially, β -cyanoethyl hydrazine reacts with benzoyl isothiocyanate to give 5-thioxo-1,2,4-triazole. Treatment of 5-thioxo-1,2,4-triazole with another molecule of benzoyl isothiocyanate resulted in the formation of imidazole-3-thione derivative via loss of HSCN (Scheme IA.5.4.1).⁴⁰



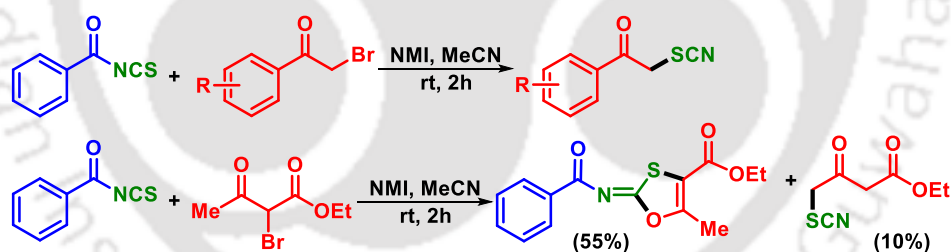
Scheme IA.5.4.1. Synthesis of imidazole-3-thiones.

The reaction of aroyl isothiocyanates with 1,2-phenylenediamines (2:1 molar ratio) results in the formation of 2-aryl benzimidazoles via *N,N'*-bis(benzoylthiocarbamoyl)-1,2-phenylene diamines as intermediates. Initially, the nucleophilic attack of 1,2-phenylenediamines to C=S linkage of isothiocyanate provided a bis-thiourea moiety. Next, the removal of one aroyl isothiocyanate moiety leads to the formation of *N*-(benzoylthiocarbamoyl)-1,2-phenylenediamines. A subsequent dethiocyanation and concomitant cyclodehydration gave 2-arylbenzimidazoles (Scheme IA.5.4.2).⁴¹



Scheme IA.5.4.2. Synthesis of 2-aryl benzimidazoles.

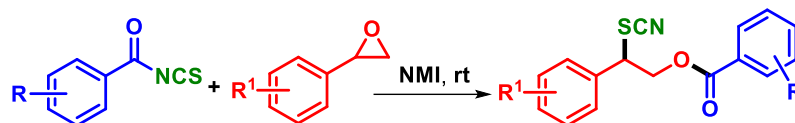
In 2009, our group reported the organocatalyzed thiocyanation of alkyl or benzylic bromide. Herein, aroyl isothiocyanate acts as a $-SCN$ transfer agent in the presence of *N*-methyl imidazole (NMI) as a catalyst. In this process, the α -haloketone serves as an electrophile and the aroyl isothiocyanate as the source of nucleophile ($-SCN$). The acidity of bromomethyl proton dictates the fate of the reaction. This process is most effective when the bromomethyl proton is less acidic. When acidity increases, usually a 1,3-oxathiol-2-ylidene skeleton or $NH-C=S$ is inserted, and the 1,3-oxathiol-2-ylidene products are obtained (Scheme IA.5.4.3).⁴²



Scheme IA.5.4.3. Aroyl isothiocyanate as $-SCN$ transfer agent.

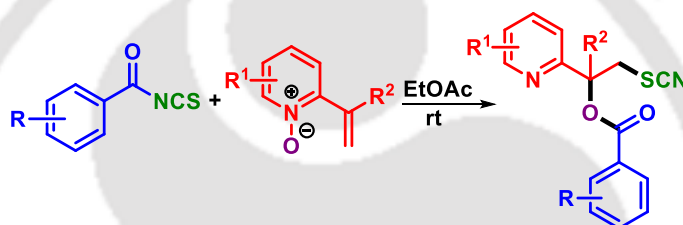
Inspired by above work on biomimetic thiocyanate group transfer from aroyl isothiocyanate, our group developed a regioselective method for concomitant transfer of thiocyanate ($-SCN$) and aroyl ($-COR$) groups from aroyl isothiocyanates onto oxiranes using NMI as a catalyst. In the absence of any real nucleophile, a nucleophilic substitution product was observed with α -haloketones. In this metal-free, atom-economic, simultaneous electrophilic–nucleophilic reaction, the thiocyanate ($-SCN$) of aroyl isothiocyanate acts as the nucleophile, while the aroyl part serves as the electrophilic partner. The methodology shows broad substrate scope with aroyl isothiocyanates and epoxide resulting in the

formation of a plethora of diversely functionalized 2-phenyl-2-thiocyanatoethyl benzoates (Scheme IA.5.4.4).⁴³



Scheme IA.5.4.4. Synthesis of 2-phenyl-2-thiocyanatoethyl benzoates.

In 2019, Li and Hong's group reported a bis-functionalization strategy of alkenylpyridine *N*-oxides using aroyl isothiocyanates as a thiocyanate (–SCN) and aroyl (–COR) group transfer agent. The reaction proceeds via a tandem addition/Boekelheide rearrangement. This metal and base-free strategy simultaneously constructs the C–O and C–S bonds at the α - and β -positions with 100% atom economy (Scheme IA.4.4.5).⁴⁴



Scheme IA.5.4.5. Difunctionalization of alkenylpyridine *N*-oxides.

IA.6. References

- (1) (a) Tietze, L. F. *Chem. Rev.* **1996**, *96*, 115. (b) Winkler, J. D. *Chem. Rev.* **1996**, *96*, 167. (c) Wang, K. K. *Chem. Rev.* **1996**, *96*, 207. (d) Padwa, A. *Chem. Soc. Rev.* **2009**, *38*, 3072. (e) Ardkhean, R.; Caputo, D. F. J.; Morrow, S. M.; Shi, H.; Xiong, Y.; Anderson, E. A. *Chem. Soc. Rev.* **2016**, *45*, 1557. (f) Blouin, S.; Blond, G.; Donnard, M.; Gulea, M.; Suffert, J. *Synthesis* **2017**, *49*, 1767.
- (2) (a) Nicolaou, K. C.; Edmonds, D. J.; Bulger, P. G. *Angew. Chem. Int. Ed.* **2006**, *45*, 7134. (b) Eilbracht, P.; Barfacker, L.; Buss, C.; Hollmann, C.; Kitsos-Rzychon, B. E.; Kranemann, C. L.; Rische, T.; Roggenbuck, R.; Schmidt, A. *Chem. Rev.* **1999**, *99*, 3329. (c) Wasilke, J. C.; Obrey, S. J.; Baker, R. T.; Bazan, G. C. *Chem. Rev.* **2005**, *105*, 1001. (d) Pellissier, H. *Chem. Rev.* **2013**, *113*, 442. (e) Tietze, L. F.; Modi, A. *Med. Res. Rev.* **2000**, *20*, 304. (f) Koeller, K. M.; Wong, C.-H. *Chem. Rev.* **2000**, *100*, 4465. (g) Climent, M. J.; Corma, A.; Iborra, S. *Chem. Rev.* **2011**, *111*, 1072. (h) Cardoso, A. L.; Pinho e Melo, T. M. V. D. *Eur. J. Org. Chem.* **2012**, 6479.

- (i) Clavier, H.; Pellissier, H. *Adv. Synth. Catal.* **2012**, *354*, 3347. (j) Pellissier, H. *Chem. Rev.* **2013**, *113*, 442.
- (3) (a) Armstrong, R. W.; Beau, J.-M.; Cheon, S. H.; Christ, W. J.; Fujioka, H.; Ham, W.-H.; Hawkins, L. D.; Jin, H.; Kang, S. H.; Kishi, Y.; Martinelli, M. J.; McWhorter, W. W.; Mizuno, M. J.; Nakata, M.; Stutz, A. E.; Talamas, F. X.; Taniguchi, M.; Tino, J. A.; Ueda, K.; Uenishi, J.-i.; White, J. B.; Yonaga, M. *J. Am. Chem. Soc.* **1989**, *111*, 7530. (b) Suh, E. M.; Kishi, Y. *J. Am. Chem. Soc.* **1994**, *116*, 11205. (c) Kishi, Y. *Pure Appl. Chem.* **1993**, *65*, 771.
- (4) (a) Trost, B. M. *Science* **1991**, *254*, 1471. (b) Ramachary, D. B.; Jain, S. *Org. Biomol. Chem.* **2011**, *9*, 1277. (c) L. F. Tietze, *Domino Reactions in Organic Synthesis* (Wiley-VCH, **2006**). (d) Corey, E. J.; Czakó, B.; Kürti, L. *Molecules and Medicine* (John Wiley, **2007**). (e) Hudlicky, T.; Reed, J. W. *The Way of Synthesis: Evolution of Design and Methods for Natural Products* (Wiley-VCH, **2007**).
- (5) (a) Skoda-Földes, R.; Kollár, L. *Chem. Rev.* **2003**, *103*, 4095. (b) Yoder, R. A.; Johnston, J. N. *Chem. Rev.* **2005**, *105*, 473.
- (6) (a) Johnson, W. S.; Gravestock, M. B.; McCarry, B. E. *J. Am. Chem. Soc.* **1971**, *93*, 4332. (b) Johnson, W. S. *Angew. Chem. Int. Ed.* **1976**, *88*, 33.
- (7) Heathcock, C. H. *Angew. Chem. Int. Ed.* **1992**, *31*, 665.
- (8) Heathcock, C. H.; Kath, J. C.; Ruggeri, R. B. *J. Org. Chem.* **1995**, *60*, 1120.
- (9) Lynen, F. *Pure Appl. Chem.* **1967**, *14*, 137.
- (10) (a) Corey, E. J.; Russey, W. E.; Ortiz de Montellano, P. R. *J. Am. Chem. Soc.* **1966**, *88*, 4750. (b) Corey, E. J.; Virgil, S. C. *J. Am. Chem. Soc.* **1991**, *113*, 4025. (c) Corey, E. J.; Virgil, S. C.; Sarshar, S. *J. Am. Chem. Soc.* **1991**, *113*, 8171. (d) Corey, E. J.; Virgil, S. C.; Liu, D. R.; Sarshar, S. *J. Am. Chem. Soc.* **1992**, *114*, 1524.
- (11) (a) Robinson, R. *J. Chem. Soc.* **1917**, *111*, 762. (b) Robinson, R. *J. Chem. Soc.* **1917**, *111*, 876. (c) Schöpf, C.; Lehmann, G.; Arnold, W. *Angew. Chem. Int. Ed.* **1937**, *50*, 779.
- (12) Tramontini, M. *Synthesis* **1973**, 703.
- (13) (a) Stork, G.; Burgstahler, A. W. *J. Am. Chem. Soc.* **1955**, *77*, 5068. (b) Eschenmoser, A.; Ruzicka, L.; Jeger, O.; Arigoni, D. *Helv. Chim. Acta* **1955**, *38*, 1890. (c) Stadler, P. A.; Eschenmoser, A.; Schinz, H.; Stork, G. *Helv. Chim. Acta* **1957**, *40*, 2191.

- (14) (a) Seebach, D. *Angew. Chem. Int.* **1920**, *29*, 1320. (b) Cornforth, J. W. *Aust. J. Chem.* **1993**, *46*, 157. (c) Yan, L.-J.; Wang, Y.-C. *ChemistrySelect* **2016**, *1*, 6948. (d) Zhang, B.; Studer, A. *Chem. Soc. Rev.* **2015**, *44*, 3505. (e) Maes, B. W. in *Microwave-Assisted Synthesis of Heterocycles* (ed. Eycken, E.; Kappe, C. O.) Springer, Berlin, Heidelberg, **2006**, *1*, 155. (f) Khoury, H. K.; Dömling, A. in *Synthesis of Heterocycles via Multicomponent Reaction* (ed. Orru, R. V. A.; Ruijter, E.) Springer, Berlin, Heidelberg, **2010**, *23*, 85.
- (15) (a) Wender, P. A.; Miller, B. L. *Nature* **2009**, *460*, 197. (b) P. A.; Wender, B. L. Miller, in *Connectivity Analysis and Multibond-forming Processes in Organic Synthesis: Theory and Applications* (ed. Hudlicky, T.) 27–66 (JAI Press, **1993**).
- (16) (a) Manoj, B. G.; Bonifácio, D. B. Luque, V.; R.; Branco, P. S.; Varma, R. S. *Chem. Soc. Rev.* **2013**, *42*, 5522. (b) Heravi, M. M.; Zadsirjan, V.; Kamjou, K. *Curr. Org. Chem.* **2015**, *19*, 813. (c) Simon, M. O.; Li, C.-J. *Chem. Soc. Rev.* **2012**, *41*, 1415. (d) Dunn, P. J. *Chem. Soc. Rev.* **2012**, *41*, 1452. (e) Gao, S.; Liu, H.; Wu, Z.; Yao, H.; Lin, A. *Green Chem.* **2017**, *19*, 1861. (f) Eghbali, N.; Li, C.-J. *Green Chem.* **2007**, *9*, 213. (g) Yang, Y.; Zhang, S.; Tang, L.; Hu, Y.; Zha, Z.; Wang, Z. *Green Chem.* **2016**, *18*, 2609. (h) Xiao, J.; Wen, H.; Wang, L.; Xu, L.; Hao, Z.; Shao, C.-L.; Wang, C.-Y. *Green Chem.* **2016**, *18*, 1032. (i) Sarkar, A.; Santra, S.; Kundu, S. K.; Hajra, A.; Zyryanov, G. V.; Chupakhin, O. N.; Charushinb, V. N.; Majee, A. *Green Chem.* **2016**, *18*, 4475. (j) Chen, X. Y.; Zhang, X.; Wan, J.-P. *Org. Biomol. Chem.* **2022**, *20*, 2356. (k) Pawlowski, R.; Stanek, F.; Stodulski, M. *Molecules* **2019**, *24*, 1533.
- (17) (a) Singh, S. V.; Singh, K. *Carcinogenesis* **2012**, *33*, 1833. (b) Zubía, E.; Ortega, M. J.; Hernández-Guerrero, C. J.; Carballo, J. L. *J. Nat. Prod.* **2008**, *71*, 608. (c) Fimognari, C.; Nüsse, M.; Cesari, R.; Iori, R.; Cantelli-Forti, G.; Hrelia, P. *Carcinogenesis* **2002**, *23*, 581.
- (18) Edman, P. *Arch. Biochem.* **1949**, *22*, 475.
- (19) (a) Ozaki, S. *Chem. Rev.* **1972**, *72*, 457. (b) Sharma, S. *Sulfur Rep.* **1989**, *8*, 327. (c) Mukerjee, A. K.; Ashare, R. *Chem. Rev.* **1991**, *91*, 1. (d) Avalos, M.; Bablano, R.; Cintas, P.; Jimenez, J. L.; Palacios, J. C. *Heterocycles* **1992**, *33*, 973. (e) Nedolya, N. A.; Trofimov, B. A.; Senning, A. *Sulfur Rep.* **1996**, *17*, 183. (f) Trofimov, B. A. *J. Heterocycl. Chem.* **1999**, *36*, 1469. (g) Sommen, G. *Synlett* **2004**, *7*, 1323.

- (20) (a) Zhong, B.; Al-Awar, R. S.; Shih, C.; Grimes, Jr., J. H.; Vieth, M.; Hamdouchi, C. *Tetrahedron* **2006**, *47*, 2161; and references therein. (b) Wei, T. B.; Lin, Q.; Zhang, Y. M.; Wei, W. *Synth. Commun.* **2004**, *34*, 181.
- (21) Bedane, K. G.; Singh, G. S. *ARKIVOC* **2015**, *6*, 206.
- (22) Takamizawa, A.; Hirai, K.; Matsui, K. *Bull. Chem. Soc. Jpn.* **1963**, *36*, 1214.
- (23) (a) Koch, R.; Wentrup, C. *J. Chem. Soc. Perkin Trans. 2* **2000**, 1846. (b) Koch, R.; Wentrup, C. *J. Org. Chem.* **2013**, *78*, 1802.
- (24) Insuasty, H.; Estrada, M.; Cortes, E.; Quiroga, J.; Insuasty, B.; Rodrigo Abonía, R.; Noguera, M.; Coboc, J. *Tetrahedron Lett.* **2006**, *47*, 5441.
- (25) Hemdan, M. M.; Fahmy, A. F.; Ali, N. F.; Hegazi, E.; Abd-Elhaleem, A. *Chin. J. Chem.* **2008**, *26*, 388.
- (26) Afon'kin, A. A.; Kostrikin, M. L.; Shumeiko, A. E.; Popov, A. F. *Russ. J. Org. Chem.* **2011**, *47*, 731.
- (27) Khalilzadeh, M. A.; Yavari, I.; Hossaini, Z.; Sadeghifar, H. *Monatsh Chem.* **2009**, *140*, 467.
- (28) Manaka, A.; Ishii, T.; Takahashi, K.; Sato, M. *Tetrahedron Lett.* **2005**, *46*, 419.
- (29) Ranjan, A.; Deore, A. S.; Yerande, S. G.; Dethe, D. H. *Eur. J. Org. Chem.* **2017**, 4130.
- (30) Singh, C. B.; Murru, S.; Kavala, V.; Patel, B. K. *Org. Lett.* **2006**, *8*, 5397.
- (31) Zeng, R.-S.; Zou, J.-P.; Zhi, S.-J.; Chen, J.; Shen, Q. *Org. Lett.* **2003**, *5*, 1657.
- (32) Saini, K. M.; Saunthwal, R. K.; Kumar, S.; Verma, A. K. *J. Org. Chem.* **2019**, *84*, 2689.
- (33) Saini, K. M.; Saunthwal, R. K.; Kumar, S.; Verma, A. K. *Org. Biomol. Chem.* **2019**, *17*, 2657.
- (34) L'abbe, G.; Sannen, I.; Dehaen, W. *J. Chem. Soc. Perkin Trans. 1* **1993**, 27.
- (35) Modi, A.; Sau, P.; Patel, B. K. *Org. Lett.* **2017**, *19*, 6128.
- (36) Tolpygin, I. E.; Shepelenko, E. N.; Borodkin, G. S.; Dubonosov, A. D.; Bren', V. A.; Minkin, V. I. *Chem. of Heterocycl. Compds.* **2010**, *46*, 542.
- (37) Ranjan, A.; Yerande, R.; Wakchaure, P. B.; Yerande, S. G.; Dethe, D. H. *Org. Lett.* **2014**, *16*, 5788.
- (38) El-Sharkawi, K. A.; El-Sehrawi, H. M.; Ibrahim, R. A. *Int. J. Org. Chem.* **2012**, *2*, 126.
- (39) Saeed, A.; Batool, M. *Med. Chem. Res.* **2007**, *16*, 143.

- (40) Elmoghayar, M. R. H.; Elghandour, A. H. H. *Monatsh Chem.* **1986**, *117*, 201.
- (41) (a) Kutschy, P.; Ficery, V.; Dzurilla, M. *Chem. Pap.* **1994**, *48*, 39. (b) Kutschy, P.; Ficery, V.; Dzurilla, M. *Chem. Abstr.* **1994**, *121*, 108634.
- (42) Palsuledesai, C. C.; Murru, S.; Sahoo, S. K.; Patel, B. K. *Org. Lett.* **2009**, *11*, 3382.
- (43) Modi, A.; Ali, W.; Patel, B. K. *Org. Lett.* **2017**, *19*, 432.
- (44) Xun, X.; Zhao, M.; Xue, J.; Hu, T.; Zhang, M.; Li, G.; Hong, L. *Org. Lett.* **2019**, *21*, 8266.





CHAPTER IB

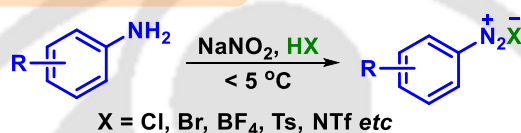
IB. An Outline of Metal-Free Cascade Reactions of Arenediazonium Salts**IB.1. Introduction**

Diazonium salts, epitomize a group of organic compounds with the general formula $R-N\equiv N^+X^-$, in which R is a carbon-based residue (mostly aryl or alkyl) and X is a halide or more often a non-nucleophilic organic or inorganic anion. Arenediazonium salts were discovered as a new class of chemicals in 1858 by the German chemist Johann Peter Griess.¹ Since their first discovery, the chemistry of arene diazonium salts has seen a vivid upsurge in synthetic applications. As compared to their aryl analogous, alkyl diazonium salts show low stability which poses severe limitations on their isolation and restricts their application in organic synthesis. This dramatic increase is reflected in seminal publications and several prominent named reactions associated with arene diazonium salts since the 19th century. Their implication within the arsenal of synthetic organic chemistry is exemplified by the fact that many name reactions are part of the standard chemistry textbook knowledge today.²

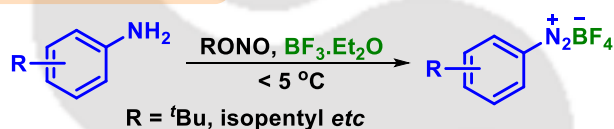
In the literature, the method of forming diazonium salts is termed as ‘diazotation’, ‘diazonation’, or ‘diazotization’. Conventionally, diazonium salts are prepared by the reaction of inexpensive and abundantly available primary aromatic amines with nitrous acid (generated *in situ* from $NaNO_2$ and a strong acid). The diazotization is carried out at low temperature (0 ° to 10 °C) in an aqueous solution, or non-aqueous media with high yields (Scheme IB.1.1a). Owing to their, intrinsic instability and explosive nature, these salts are generally synthesized *in situ*. For example, arenediazonium chlorides, which were frequently used in the early years, are unstable and highly sensitive to shock and sometimes can be explosive above 0 °C. In a recent article, Fairlamb *et al.*³ have nicely summarized the “*Need for Caution in the Preparation of Aryl Diazonium Tetrafluoroborates.*” Hence, substantial efforts have been given to increase the bench stability and shelf life of arenediazonium salts. By screening different counterions, it was observed that

counteranions with low nucleophilicity *viz.*, tetrafluoroborate, hexafluorophosphate, tosylate, and disulfonimide are best anions in stabilizing the arenediazonium cations. These diazonium salts can be isolated and stored at low temperatures. Moreover, the combination of sodium nitrite and strong acid is another obstacle that has restricted their synthetic application because of the formation of undesirable side products and poor functional group tolerance. In this perspective, organic nitrites (RONO₂) in the presence of BF₃.Et₂O has emerged as a mild and easy-to-handle synthetic route for the preparation of diazonium salts (Scheme IB.1.1b). Another substitute for arenediazonium salt is aryl triazene which can be easily generated by the reaction of arenediazonium salts with secondary amines.⁴

(a) **Classical approach:**



(b) **Modern approach:**

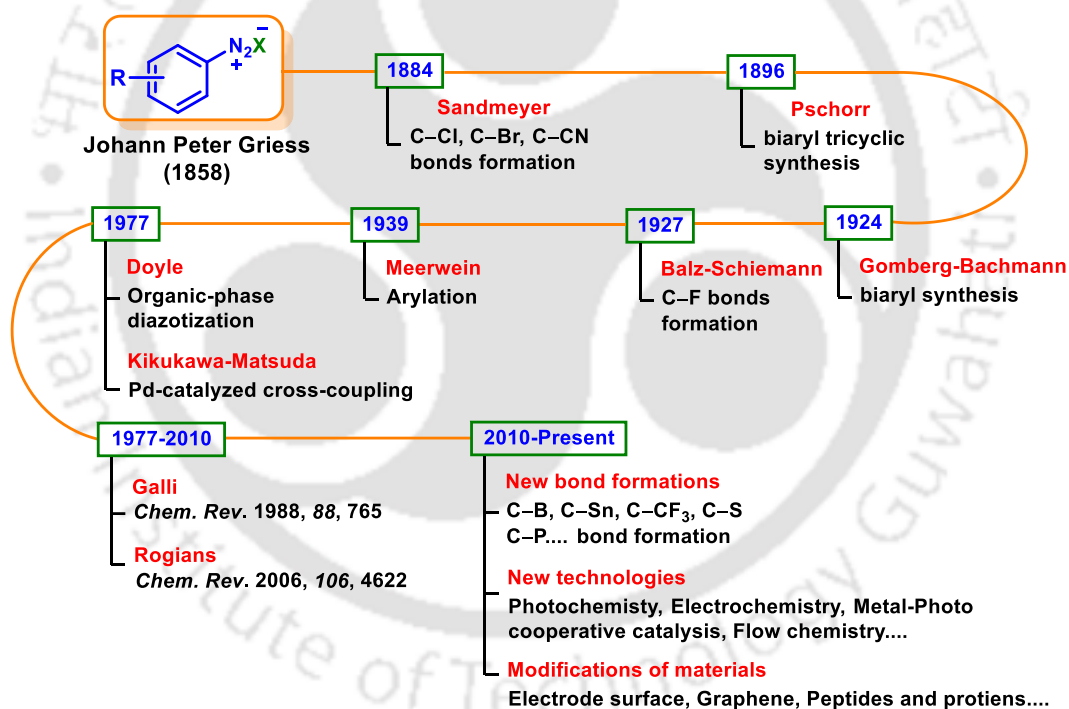


Scheme IB.1.1. Preparation of arenediazonium salts.

IB.2. Historical Background

Over the past 150 years, the chemistry of diazonium salts has evolved and shaped the art of organic synthesis and still attracts great attention for their distinct properties and reactivities (Scheme IB.2.1). In 1884, Sandmeyer disclosed that by treatment with Cu (I) halides, benzenediazonium salt can be easily converted to aryl halides.⁵ At the end of the 19th century, Pschorr pioneered a copper-catalyzed synthesis of phenanthrenes from biphenyldiazonium salts. The proposed mechanism shows the formation of the aryl radical by single-electron transfer (SET) from the copper(I) followed by radical substitution of the suspended aryl group.⁶ In 1924, Gomberg and Bachmann extended Pschorr's work to an intermolecular biaryl synthesis through the insertion of the aryl radical into benzene.⁷ Only three years later, Balz and Schiemann achieved an important breakthrough where they described the thermal (or photolytic) decomposition of arenediazonium tetrafluoroborates to aromatic fluorides, which cannot be accessed by the Sandmeyer reaction.⁸ In 1939, Meerwein and co-workers reported an extensive study on Cu(II)-catalyzed reaction of

areediazonium salts with α,β -unsaturated carbonyl compounds. The reaction was later known as Meerwein arylation, in which the aryl group adds across the double bond.⁹ In 1977, Mike P. Doyle developed a novel system for diazotization that could be performed in the organic phase with organic nitrites in the absence of strong aqueous acids. Thus, extending the diazotization for water-incompatible substrates.¹⁰ In 1977, Kikukawa and Matsuda established the transition-metal-catalyzed cross-coupling of areediazonium salts which opened new avenues for further advancement in cross-coupling chemistry using aryl diazonium salts as an alternative to aryl halides.¹¹ In the late 19th century, when methods for aromatic functionalization were virtually restricted, the chemistry of diazonium salts heralded a new era in aromatic substitution and cross-coupling chemistry for the construction of C–C and C–heteroatom bond formation. However, since then, the field of aryl diazonium chemistry has been dormant for a long time (Scheme IB.2.1).



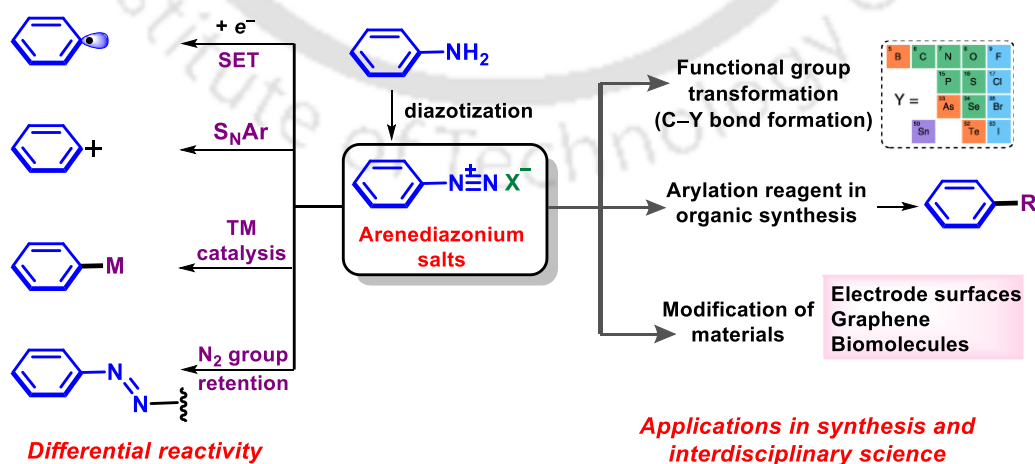
Scheme IB.2.1. Chronological evolution of areediazonium salts chemistry.

IB.3. Reactivity and Modern Applications

With the introduction of new technologies such as photochemistry, electrochemistry, flow chemistry, and metal-photo cooperative catalysis, aryl diazonium chemistry has witnessed a renaissance in the past decade.¹² The reactions of areediazonium salts (Figure IB.3.1) can be categorized into four classes:

- Transformations via aryl radical (thermal or electro/photochemical)
- Transformations via aryl cation
- Transition-metal-catalyzed processes
- Transformations with retention of the dinitrogen group

The first three reactions, transformation via aryl radical (thermal or electro/photochemical transformations), aryl cations, and transition-metal-catalyzed processes are based on the intrinsic electrophilicity of diazonium salts with N_2 as an excellent leaving group. Since the leaving group (N_2) is thermodynamically very stable, these reactions are energetically favored. The transformation via aryl radical involves a single electron transfer (SET) mechanism mediated by low-valent metal salts such as Cu(I), Fe(II), Ti(III), organic donors (amines, thiols), excited photocatalysts, and in electrochemical cells. The resultant aryl radical intermediates are very reactive toward transition metals, weak π -bond systems such as alkenes, alkynes, arenes, and nonbonding electrons at heavier heteroatoms (S, Se, P, etc.) and solvent molecules. In the absence of a suitable reducing agent and thermal treatment, arenediazonium salts form highly energetic aryl cation which swiftly reacts even with poor nucleophiles. Owing to its ability to serve as aryl halide surrogates, diazonium salts have been widely employed in transition-metal-catalyzed cross-coupling reactions for C–C and C–heteroatom bond formation. In the presence of nucleophiles such as phenols, anilines, sulfonium ylide, active methylene compounds, *etc.* the diazo group of arene diazonium ion serves as a nitrogen electrophile, yielding products with the retention dinitrogen (Figure IB.3.1).¹³



Scheme IB.3.1. Differential reactivity and applications of arene diazonium salts.

The mesomeric stabilization extends the stability of arenediazonium salts which can be easily handled under ambient conditions and consequently entertain rich chemistry of aromatic *ipso*-substitution, *N*-terminal addition reactions, and cycloadditions. Among all these reactions, C–H arylation using aryl diazonium salts is the most extensively studied transformation followed by other functional group conversions and nitrogen retaining transformations.

The broad utility and rich legacy of diazonium chemistry originate from the inexpensive aniline precursors and the availability of diverse diazotization conditions. Although diazonium chemistry is contemplated as classic chemistry, it remains a hot topic of research and new developments have been emerging constantly from both industry and academia. With the merger of new technologies, aryl diazonium chemistry has afforded new tools for the construction of aromatic C–C and C–Y (Y = B, P, S, Sn, Se, etc.) bonds. Additionally, arenediazonium salts have found synthetic applications in the synthesis of complex carbocycles and nitrogen-containing heterocyclic compounds. These novel synthetic applications are further implemented in designing and synthesizing medicinally active agents and modification of bulk materials *viz.* electrode surfaces and graphenes (Scheme IB.3.1). Biomolecules, particularly peptides and proteins can now also be swiftly altered by arenediazonium reagents. Moreover, starting from easily available aniline derivatives, transformations via the retention of the N₂ group of arenediazonium salts have enabled industrial applications in the syntheses of functional molecules, such as haloarenes, azo dyes, and nanomaterials. In addition, diazonium salts are also extremely valuable in the dye and pigment industries for the preparation of azo compounds.¹⁴

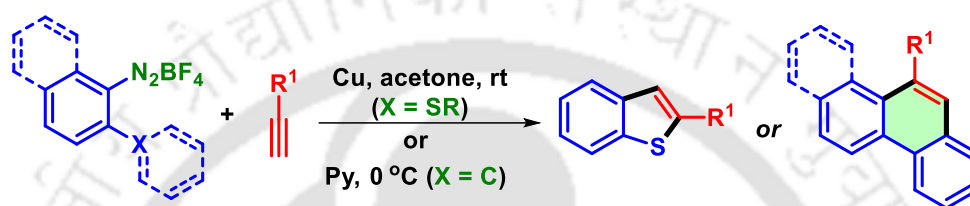
Since the work delineated in this dissertation solely belongs to metal-free cascade reactions of arene diazonium salts for C–C and C–heteroatom formations using traditional and modern approaches, the description pertaining to these is only discussed here.

IB.4. Representative Examples of Transition Metal-Free Cascade Reactions of Arenediazonium Salts

IB.4.1. C–C bonds formation

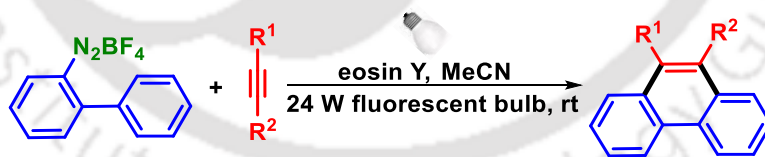
Aryl diazonium salts are susceptible to undergo homolytic dediazonation to provide aryl radicals, and the *in situ* generated aryl radicals can be trapped by other reactive species

to form the desired products. Among many different approaches to aryl radicals, the photo-induced reduction of aryl diazonium salts through electron transfer is particularly attractive. The condensed (hetero)aryl ring systems can be generated via homolytic annulation reactions between suitable *ortho*-substituted arenediazonium salts and alkynes via radical addition–cyclization sequences. Such annulation reactions were first demonstrated by Zanardi's group in 1984 with *ortho*-methylthio or *o*-phenyl arenediazonium salts and terminal alkynes to produce 2-arylbenzothiophenes and condensed polycyclic aromatic hydrocarbons (PAHs) respectively (Scheme IB.4.1.1).¹⁵



Scheme IB.4.1.1. Radical annulation of *o*-substituted arenediazonium salts.

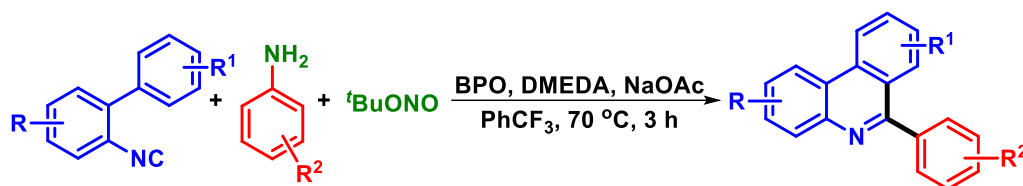
In 2012, Zhou's group extended Zanardi's work to a metal-free synthesis of phenanthrenes derivatives by reacting biaryldiazonium salts and alkynes in presence of eosin Y as a catalyst. This visible light-induced strategy provided a diversity of 9-substituted or 9,10-disubstituted phenanthrenes via a cascade radical addition and cyclization sequence. Both terminal and internal alkynes were suitable for this protocol (Scheme IB.4.1.2).¹⁶



Scheme IB.4.1.2. Synthesis of 9-substituted or 9,10-disubstituted phenanthrenes.

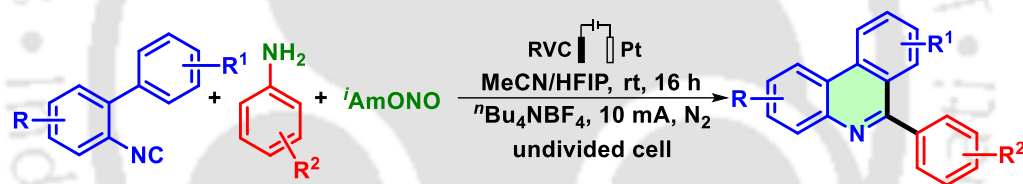
A transition-metal-free process for the synthesis of diversely substituted phenanthridine derivatives was accomplished by Zhu and co-workers using 2-isocyanobiphenyls with arylamines. The arylamines are *in situ* diazotized by ^tBuONO. The arylative cyclization proceeds through key biphenyl imidoyl radical intermediates formed by the addition of aryl radicals to 2-isocyanobiphenyls in a homolytic aromatic substitution (HAS) manner. Mechanistic studies revealed another competitive pathway that involves a single electron transfer of biphenyl imidoyl radical to the corresponding nitrilium

intermediate followed by electrophilic aromatic substitution (S_EAr) along with previously reported HAS (Scheme IB.4.1.3).¹⁷



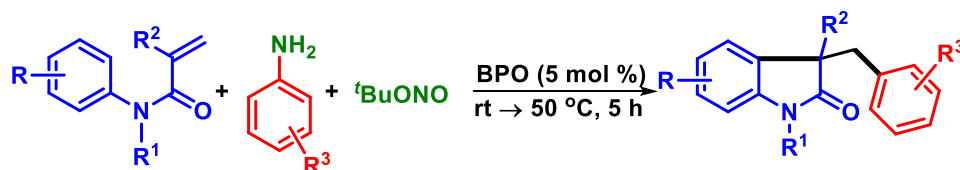
Scheme IB.4.1.3. Synthesis of phenanthridine derivatives.

Recently, Sharma *et al.* reported an electrochemical synthesis of 6-aryl phenanthridines by reacting 2-isocyanobiphenyls with arylamines. The arylamines are *in situ* diazotized by *iso*-amyl nitrite (*i*AmONO). The cathodic reduction of *in situ* generated diazonium ions forms aryl radicals which on coupling with 2-isocyanobiphenyls generates imidoyl radicals. The intramolecular cyclization of imidoyl radicals generates a series of phenanthridines in good to excellent yields (Scheme IB.4.1.4).¹⁸



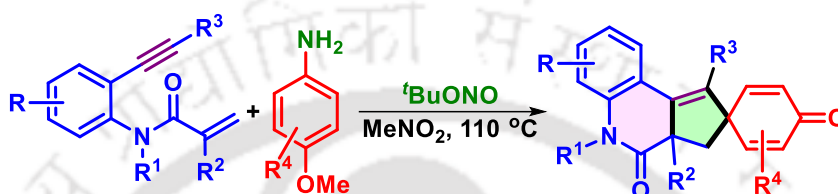
Scheme IB.4.1.4. Electrochemical synthesis of phenanthridines.

A metal-free Meerwein carbonylation of alkenes was developed by Tang's group for the synthesis of 3-benzyl-3-alkyloxindoles using *N*-arylacrylamides, benzoyl peroxide, *tert*-butyl nitrite, and an array of anilines. The anilines are *in situ* diazotized by *tert*-butyl nitrite. This protocol proceeds through radical mediated tandem Meerwein arylation/C–H cyclization process and avoids the use of a transition-metal catalyst and elevated temperatures. The pharmaceutically important 3-benzyl-3-alkyloxindole scaffold was obtained in moderate to good yields using diversely substituted *N*-arylacrylamides and anilines (Scheme IB.4.1.5).¹⁹



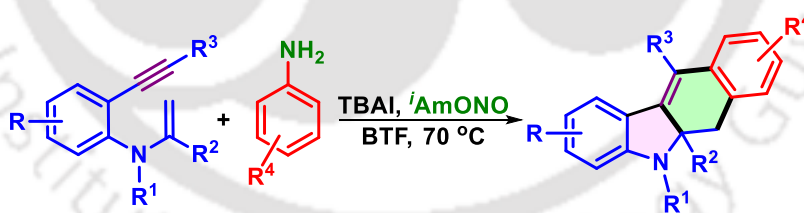
Scheme IB.4.1.5. Synthesis of 3-benzyl-3-alkyloxindoles.

In 2014, Jiang group disclosed the C-center radical-triggered cascade bicyclization of *N*-tethered 1,7-enynes with *in situ* diazotized 4-methoxyanilines to synthesize spirocyclohexadienone containing cyclopenta[*c*]quinolin-4-ones. This radical deaminative *ipso*-cyclization of 4-methoxyanilines generates three new C–C bonds without additional oxidant via 6-*exo-dig* cyclization/5-*exo-trigipso*-cyclization. The reaction features bond-forming/annulation efficiency, broad substrate scope, and high functional group tolerance under metal-free conditions (Scheme IB.4.1.6).²⁰



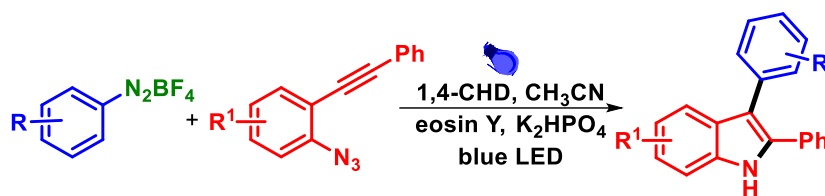
Scheme IB.4.1.6. Synthesis of cyclopenta[*c*]quinolin-4-ones.

In 2016, Studer's group developed a radical cascade cyclization strategy of 1,6-enynes with arylamines in the presence of *tert*-butyl ammonium iodide (TBAI) and benzo trifluoride (BTF) as a solvent. Herein, *i*AmONO helps in the *in situ* diazotizations of anilines and one-electron reduction whereas, TBAI acts as a chain initiator. The unique metal-free protocol provided access to a broad range of substituted polycyclic compounds in moderate to good yields (Scheme IB.4.1.7).²¹



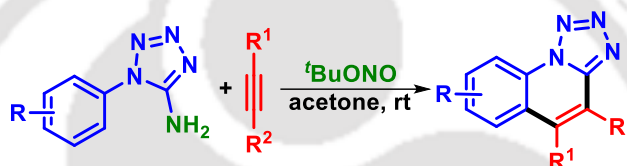
Scheme IB.4.1.7. Synthesis of cyclopenta[*c*]quinolin-4-ones.

In 2017, Cheng group reported a visible-light mediated cyclization of *o*-azidoarylalkynes and aryl diazonium salts. The procedure provides a metal-free approach for the synthesis of unsymmetrical 2,3-diaryl-substituted indoles at room temperature from readily available starting materials. These reactions exhibit excellent substrate scope and predictable regioselectivity (Scheme IB.4.1.8).²²



Scheme IB.4.1.8. Photocatalytic synthesis of 2,3-disubstituted indoles.

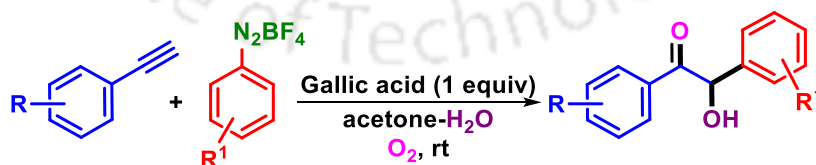
In 2019, Wu and co-workers reported a method for the synthesis of tetrazolo[1,5-*a*]quinolines via radical cyclization of tetrazole amines with alkynes. The tetrazolo[1,5-*a*]quinoline derivatives were obtained in good to moderate yields in a shorter reaction time, with high regioselectivities and a wide-range of functional group tolerance. The TBN and water play important roles in generating the aryl radicals from the *in situ* formed tetrazolatediazonium salts (Scheme IB.4.1.9).²³



Scheme IB.4.1.9. Metal-free synthesis of tetrazolo[1,5-*a*]quinolines.

IB.4.2. C–O bonds formation

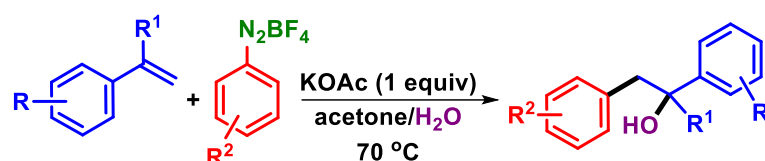
An organo-promoted synthesis of unprotected α -hydroxy ketones is achieved by Alcaide and co-workers using terminal alkynes and arenediazonium salts under mild aerobic conditions. This transformation involves the generation of an aryl radical from arenediazonium salts which on reaction with the alkyne generates a new radical species able to react with water and oxygen to afford the α -hydroxyketones in good to excellent yields (Scheme IB.4.2.1).²⁴



Scheme IB.4.2.1. Metal-free synthesis of α -hydroxyketones.

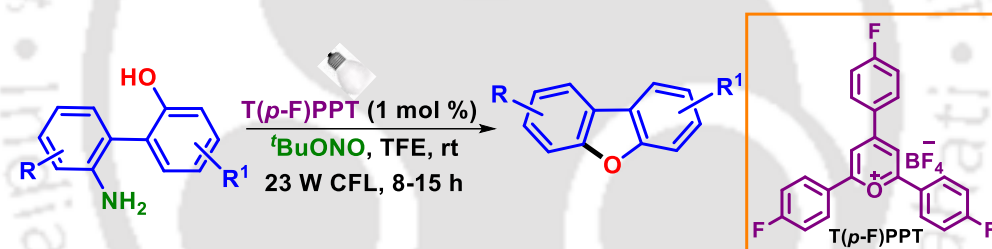
In 2016, Heinrich *et al.* reported a base-mediated radical carbohydroxylation of unactivated terminal alkenes with aryldiazonium salts under mild thermal conditions. In alcoholic solvents, the strategy could be extended to carboetherification as well as to a two-

step, metal-free Meerwein arylation leading to stilbenes. Herein diazonium ion itself acts as an oxidant to propagate the radical chain (Scheme IB.4.2.2).²⁵



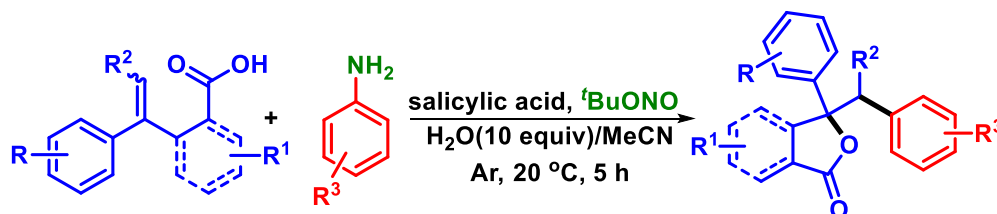
Scheme IB.4.2.2. Metal-free carbohydroxylation of styrenes.

An efficient visible-light-induced synthesis of dibenzofurans is developed by Cho's group using *in situ* diazotized 2-(2'-aminoaryl)phenols. Herein, *t*BuONO helps in the *in situ* diazotization whereas, 2,4,6-tris(4-fluorophenyl)pyrylium tetrafluoroborate (T(*p*-F)PPT) acts as an organic photosensitizer under visible-light irradiation. The high excited oxidizing potential of T(*p*-F)PPT is responsible for the formation of the oxyradical intermediate that leads to various functionalized dibenzofuran derivatives. The method can be scaled up to a gram scale (Scheme IB.4.2.3).²⁶



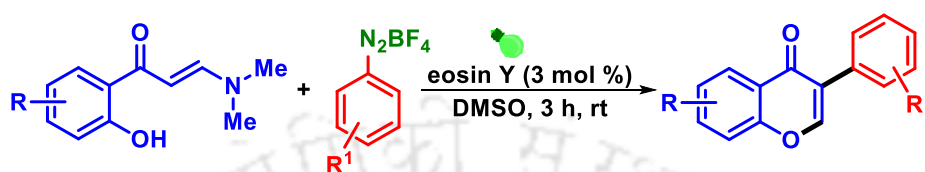
Scheme IB.4.2.3. Metal-free synthesis of dibenzofurans.

In 2019, Gonzalez-Gomez's group reported a metal-free arylation-lactonization sequence of γ -alkenoic acids with *in situ* generated diazonium salts from bench-stable anilines. In the presence of salicylic acid (10 mol %) and H₂O (10 equiv), the reaction is completed in less than 5 h without thermal/photochemical activation, giving diversely functionalized γ,γ -disubstituted butyrolactones (Scheme IB.4.2.4).²⁷



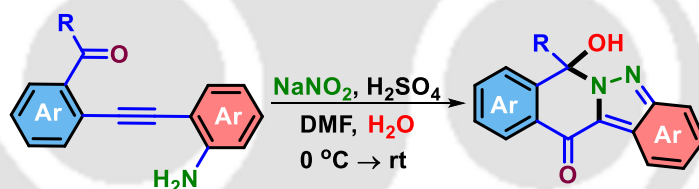
Scheme IB.4.2.4. Metal-free synthesis of γ,γ -disubstituted butyrolactones.

In 2020, Mkrtchyan and Iaroshenko developed the visible-light-mediated synthesis of isoflavones through arylation of *ortho*-hydroxyarylenaminones using arenediazonium salts in presence of eosin Y as a photocatalyst. The photo-Meerwein arylation provided absolute C-3 selectivity with high functional group tolerance and good to moderate yields. The photogenerated aryl radicals initiate the radical chain step (Scheme IB.4.2.5).²⁸



Scheme IB.4.2.5. Synthesis of C3-substituted isoflavones.

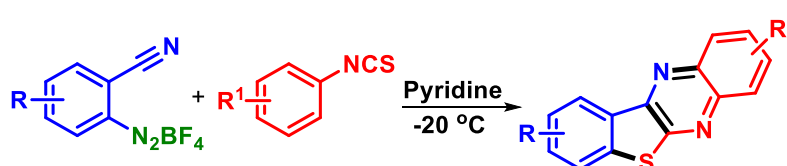
Qiu and Xu's group achieved transition-metal-free, acid-mediated bicyclization of diaryl alkynes with the *in situ* generated diazonium salts as the "N" source leading to the synthesis of a range of polycyclic 2*H*-indazoles in good to excellent yields. The notable features of this bicyclization process are mild reaction conditions, no column chromatography, and good functional group compatibility with high bond-formation efficiency (Scheme IB.4.2.6).²⁹



Scheme IB.4.2.6. Synthesis of polycyclic 2*H*-indazoles.

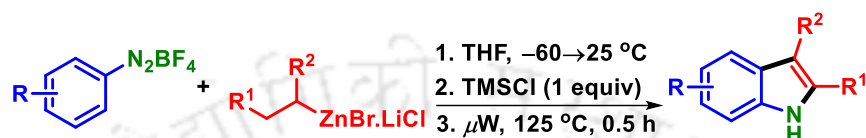
IB.4.3. C–N bonds formation

In 1997, Zanardi's group reported a synthesis of benzothienoquinoxalines via a [3 + 2] radical cascade annulation reaction using *o*-cyano arenediazonium salts and aryl isothiocyanates. The benzothienoquinoxalines were obtained in good to moderate yields (Scheme IB.4.3.1).³⁰



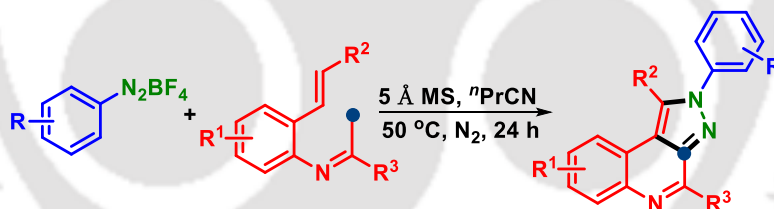
Scheme IB.4.3.1. Synthesis of benzothienoquinoxalines.

In 2010, Knochel and co-workers reported Fischer indole synthesis by reacting primary and secondary alkyl zinc reagents with an array of arenediazonium salts under microwave irradiation. The reaction proceeds via the Japp-Klingemann reaction followed by [3,3]-sigmatropic shift and subsequent aromatization. This organometallic version of the Fischer indole synthesis tolerates a broad range of functional groups and shows absolute regioselectivity with good to moderate yields (Scheme IB.4.3.2).³¹



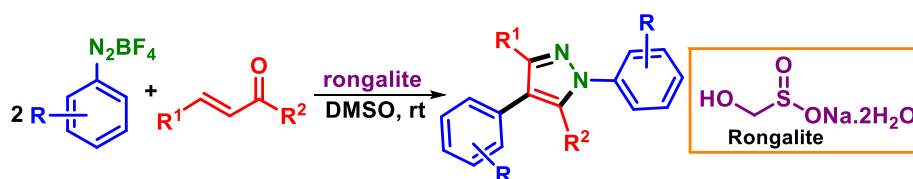
Scheme IB.4.3.2. Synthesis of 2,3-disubstituted indoles.

A practical and straightforward dehydrogenative [2 + 2 + 1] heteroannulation was accomplished by Song and Li's group for the synthesis of pyrazolo[3,4-*c*]quinolines by reacting *N*-(*o*-alkenylaryl)imines with aryldiazonium salts. Herein, the methyl group (a sp³-hybrid C-atom) of *N*-(*o*-alkenylaryl)imines serves as one carbon synthon and 5 Å MS are used as a solid base to trigger the reaction. The dehydrogenative strategy is simple to operate with high functional group tolerance (Scheme IB.4.3.3).³²



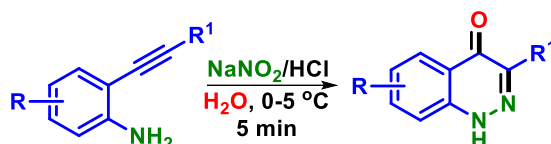
Scheme IB.4.3.3. Synthesis of pyrazolo[3,4-*c*]quinolines.

In 2019, Wu *et al.* reported arenediazonium salts as a dual synthon in the synthesis of substituted pyrazoles from α,β -unsaturated aldehydes or ketones under metal- and oxidant-free conditions. The three-component radical annulation reaction is promoted by rongalite, an industrial product as a radical initiator and reducing reagent. Herein, arenediazonium salts served as the precursor of both the aryl and aryl hydrazine units (Scheme IB.4.3.4).³³



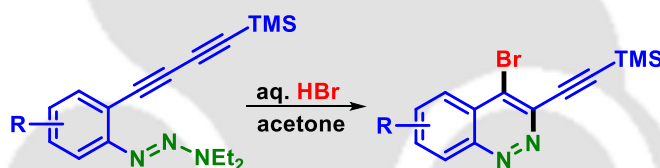
Scheme IB.4.3.4. Rongalite-mediated synthesis of pyrazoles.

A one-pot Richter cyclization was achieved by Ranu and co-workers for the synthesis of 3-aryl/alkyl-4(1*H*)-cinnolones by *in situ* diazotizing the 2-aryl/alkylethynyl aniline with sodium nitrite and dilute hydrochloric acid. The reaction was carried out in aqueous media within a short period of time (Scheme IB.4.3.5).³⁴



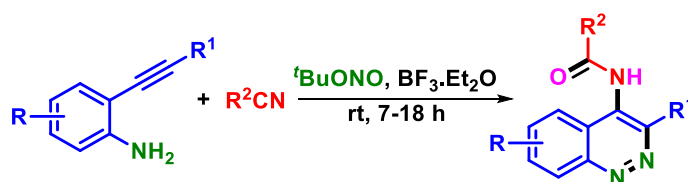
Scheme IB.4.3.5. Synthesis of 3-aryl/alkyl-4(1*H*)-cinnolones.

In 2011, Popik and Balova *et al.* disclosed a short and efficient acid-mediated Richter cyclization for the synthesis of cinnoline-fused cyclic enediynes. Moreover, the preliminary studies of its cycloaromatization and nuclease activity were also explored. Herein, *o*-(1,3-butadiynyl)phenyltriazenes were used as masked arenediazonium precursors (Scheme IB.4.3.6).³⁵



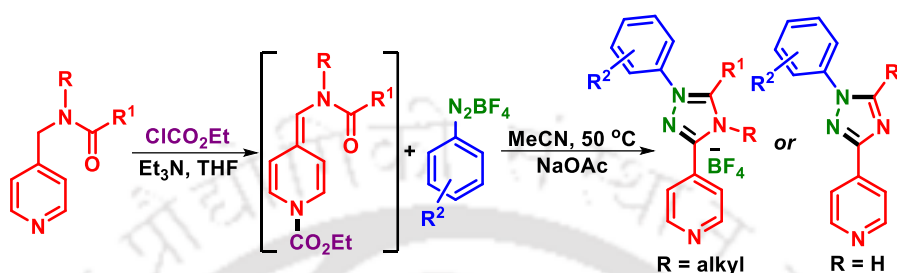
Scheme IB.4.3.6. Synthesis of cinnoline-fused cyclic enediynes.

In 2016, Wang and co-workers reported a Lewis acid-promoted one-pot strategy for the synthesis of 4-amido-cinnoline derivatives by treating 2-alkynylanilines with nitriles in the presence of ^tBuONO and BF₃·Et₂O. Moisture present in the reaction is the source of carbonyl oxygen. This cascade cyclization proceeds smoothly at ambient temperature providing diversely substituted 4-amido-cinnolines in moderate to good yields. Salient features of the method include the construction of two new C–N bonds in a single reaction, mild reaction conditions, metal-free, and excellent functional group tolerance (Scheme IB.4.3.7).³⁶



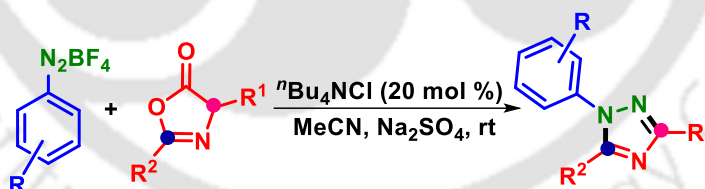
Scheme IB.4.3.7. Synthesis of 4-amido-cinnolines.

A transition metal-free, base-mediated [3 + 2] cyclocondensation reaction for the synthesis of substituted 1,2,4-triazolium salts or neutral 1,2,4-triazoles was reported by the Pigge group in 2016. Initially, *N*-acylated 4-(aminomethyl)pyridines are dearomatized to alkyldiene dihydropyridines (anhydrobases) which on reaction with arenediazonium salts offers a general route to pyridyl-substituted 1,2,4-triazoles (Scheme IB.4.3.8).³⁷



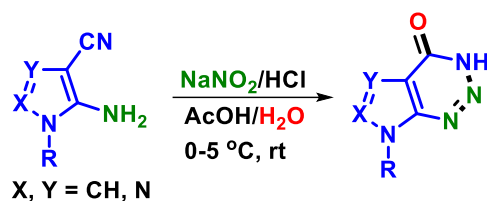
Scheme IB.4.3.8. Synthesis of pyridyl-substituted 1,2,4-triazoles.

An efficient and practical cycloaddition/decarboxylation strategy for the synthesis of trisubstituted 1,2,4-triazoles was reported by Chen and co-workers. In this metal-free process, the reaction between azlactones and arenediazonium salts provided 1,3,5-trisubstituted 1,2,4-triazoles in moderate to good yields with a wide range of substrate scope. In this methodology, arenediazonium salts act as two nitrogen units rather than the sources of aryl radicals, which provide an alternative class of *N*-source for the synthesis of bioactive 1,2,4-triazoles (Scheme IB.4.3.9).³⁸



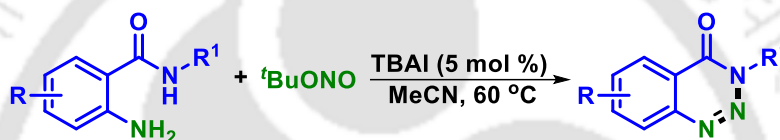
Scheme IB.4.3.9. Synthesis of 1,3,5-trisubstituted 1,2,4-triazoles.

In 2008, Moyano *et al.* developed a facile and effective one-pot multicomponent synthesis of pyrazolo[3,4-*d*][1,2,3]triazin-4-ones and imidazo[4,5-*d*][1,2,3]triazin-4-ones by *in situ* diazotizing easily accessible aminopyrazoles and aminoimidazoles with aqueous NaNO₂ in a mixture of HCl/AcOH (3:1), respectively. A broad range of functional groups is well tolerated in this transformation (Scheme IB.4.3.10).³⁹



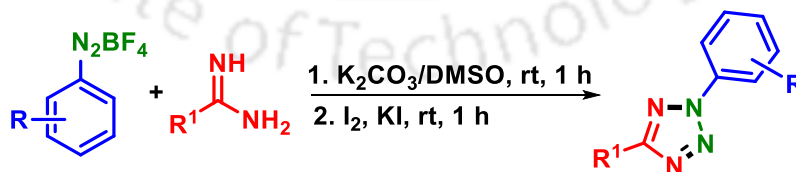
Scheme IB.4.3.10. Synthesis of triazine derivatives.

Yan and Liu's group developed a mild and efficient TBAI-catalyzed synthesis of 1,2,3-benzotriazine-4-(3*H*)-ones from 2-aminobenzamides and ^tBuONO. The diazotization of 2-aminobenzamides was conducted in the absence of strong acid. Herein, ^tBuONO acts as *N*-synthon. Various functional groups were tolerated under present reaction conditions to afford 1,2,3-benzotriazine-4-(3*H*)-ones in good to excellent yields (Scheme IB.4.3.11).⁴⁰



Scheme IB.4.3.11. Synthesis of 1,2,3-benzotriazine-4-(3*H*)-ones.

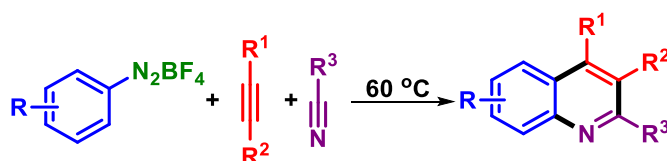
In 2015, Liu *et al.* disclosed a one-pot sequential process for the synthesis of 2,5-disubstituted tetrazoles using aryldiazonium salts and amidines. The reaction between aryldiazonium salts and amidines generates imino-triazenes under basic conditions. Further treatment of imino-triazenes with KI/I₂, provided a diverse array of 2,5-difunctionalized tetrazoles via oxidative N–N bond formation. Notable features of the present protocol are atom efficiency, easy-to-handle reaction conditions, and broad functional group tolerance with excellent yields (Scheme IB.4.3.12).⁴¹



Scheme IB.4.3.12. Synthesis of 2,5-disubstituted tetrazoles.

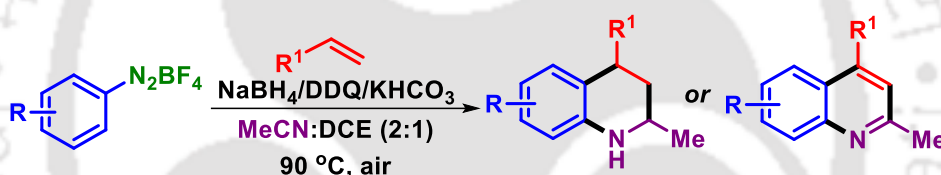
Yu's group reported a three-component cascade annulation of readily available aryl diazonium salts, nitriles, and alkynes to give an efficient and rapid synthesis of multiply substituted quinolones. The methodology is catalyst- and additive-free. Various aryl

diazonium salts, nitriles, and alkynes can participate in this transformation which shows a broad substrate scope, and giving up to 83% yield (Scheme IB.4.3.12).⁴²



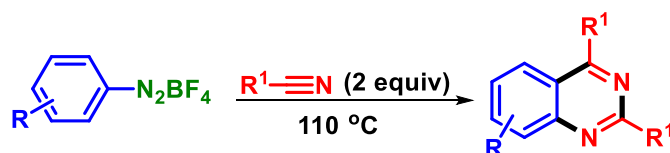
Scheme IB.4.3.12. Metal-free synthesis of multi-substituted quinolines.

In 2018, Lee *et al.* documented a similar metal-free, one-pot synthesis of diversely substituted (tetrahydro)quinolines through a three-component assembly reaction of arenediazonium salts, nitriles, and styrenes. The titled compound could be further transformed into quinolines and tetrahydroquinolines depending on the reaction conditions. The advantages of this protocol include its simplicity, metal-free and mild conditions, readily available starting materials, and good functional group tolerance (Scheme IB.4.3.13).⁴³



Scheme IB.4.3.13. Metal-free synthesis of multi-substituted quinolones.

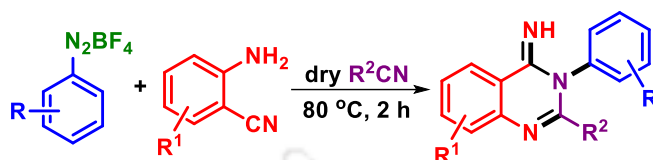
Liu's group described a [2 + 2 + 2] modular synthesis of multi-substituted quinazolines by the direct reaction of aryldiazonium salts with two equivalents of nitriles. In the proposed mechanism, the reaction of aryldiazonium salt with a nitrile provided the initial formation of a reactive nitrilium ion, which is attacked by another molecule of nitrile followed by electrophilic cyclization to deliver the desired product. The notable features of the present methodology are flexibility in the substitution patterns, readily available substrates, short reaction time, metal-free, and gram-scale synthesis (Scheme IB.4.3.14).⁴⁴



Scheme IB.4.3.14. Metal-free synthesis of quinazolines.

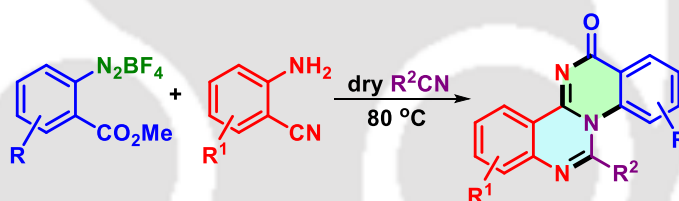
A transition metal-free, three-component synthesis of diversely substituted quinazolin-4(3*H*)-imines has been accomplished by the Liu group using aryldiazonium

salts, aryl/alkyl nitriles, and 2-cyanoanilines. Initially, the reaction of aryl/alkyl nitriles and aryldiazonium salts generates a reactive *N*-arylnitrilium intermediate, which undergoes a nucleophilic cascade reaction with 2-cyanoanilines to afford quinazolin-4(3*H*)-imines in good to excellent yields (Scheme IB.4.3.15).⁴⁵



Scheme IB.4.3.14. Metal-free synthesis of quinazolin-4(3*H*)-imines.

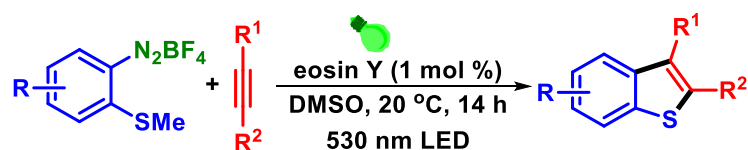
Later in 2018, the Liu group extended their work on arenediazonium salts and alkyl/aryl nitrile to synthesize quinazolino[3,4-*a*]quinazolin-13-ones under metal and base-free conditions. The direct reaction of *o*-(methoxycarbonyl)benzenediazonium salts, nitriles, and 2-cyanoanilines proceeds via amination/tandem cyclization/amidation to afford the desired quinazolino[3,4-*a*]quinazolin-13-ones scaffolds in good to excellent yields (Scheme IB.4.3.16).⁴⁶



Scheme IB.4.3.14. Metal-free synthesis of quinazolino[3,4-*a*]quinazolin-13-ones.

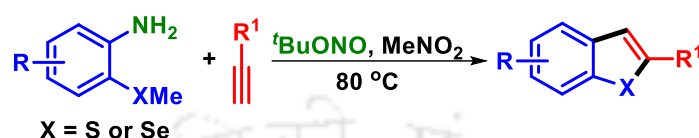
IB.4.4. C–S bonds formation

In 2012, Köing group reported the visible-light-mediated regioselective synthesis of substituted benzothiophenes by reacting *o*-methylthio-arenediazonium salts with alkynes and eosin Y as the photoredox catalyst. The radical annulation process can tolerate various substituted diazonium salts and different alkynes (Scheme IB.4.4.1).⁴⁷



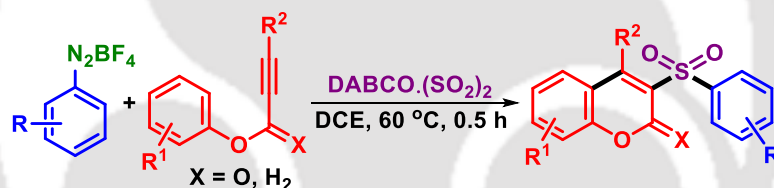
Scheme IB.4.4.1. Synthesis of substituted benzothiophenes.

Later Zhang group extended the above photocatalytic synthesis and developed an intermolecular radical cascade reaction of *o*-methylthio-arylamines or *o*-methylselanyl-arylamines and terminal alkynes in the presence of *tert*-butyl nitrite. The methodology has complete regioselectivity and the benzothiophenes or benzoselenophenes are obtained in moderate to good yields (Scheme IB.4.4.2).⁴⁸



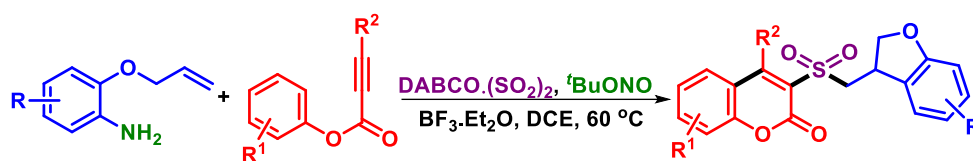
Scheme IB.4.4.2. *tert*-Butyl nitrite mediated synthesis of benzothiophenes.

In 2012, Wu group disclosed a catalyst-free approach for the synthesis of 3-sulfonated coumarins by reacting aryldiazonium tetrafluoroborates, DABCO·(SO₂)₂, and aryl propiolates under thermal conditions. The reaction proceeds via radical addition, spirocyclization followed by 1,2-migration of esters. Herein, DABCO·(SO₂)₂ acts as a SO₂ surrogate (Scheme IB.4.4.3).⁴⁹



Scheme IB.4.4.3. Synthesis of 3-sulfonated coumarins.

A *tert*-butyl nitrite mediated radical cyclization and rearrangement process has been achieved by Wu *et al.* for the synthesis of 3-((2,3-dihydrobenzofuran-3-yl)methyl)sulfonyl coumarins by reacting 2-(allyloxy)anilines, DABCO-bis(sulfur dioxide), and aryl propiolates in presence of BF₃·Et₂O. The process involves the generation of 2-(allyloxy)aryl radical followed by intramolecular addition to a double bond to afford an alkyl radical intermediate. The alkyl radical further reacts with SO₂ to produce an alkylsulfonyl radical which on reaction with aryl propiolates would provide sulfonyl-bridged dihydrobenzofuran and coumarin derivatives (Scheme IB.4.4.4).⁵⁰



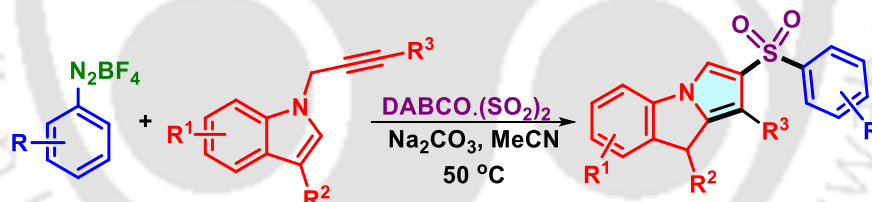
Scheme IB.4.4.4. Synthesis of sulfonyl-bridged dihydrobenzofuran and coumarins.

In 2018, Wu group reported a metal and base-free three-component reaction of 1-(2-allylaryl)thioureas, DABCO-bis(sulfur dioxide), and aryldiazonium salts at room temperature. The sulfonated [3,1]-benzothiazepines were obtained in good yields via thiosulfonylation of alkenes with the insertion of SO₂. The reaction of diazonium salts and DABSO generates aryl sulfonyl radicals which on reaction with thioureas affords the benzothiazepine scaffolds (Scheme IB.4.4.5).⁵¹



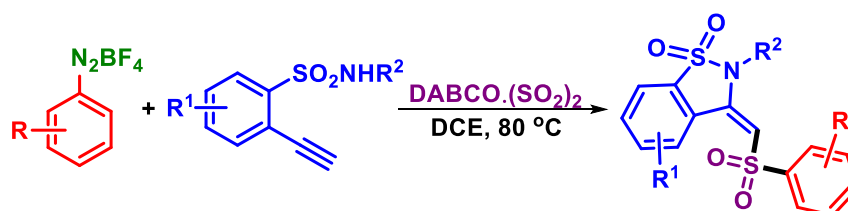
Scheme IB.4.4.5. Synthesis of sulfonated [3,1]-benzothiazepines.

A base-mediated, metal-free, three-component reaction of aryldiazonium salts, DABCO-bis(sulfur dioxide), and 1-(prop-2-yn-1-yl)indoles has been accomplished by Wu *et al.* The arylsulfonyl radical initiates the transformation under mild conditions, giving rise to sulfonated 9H-pyrrolo[1,2-*a*]indoles in moderate to good yields (Scheme IB.4.4.6).⁵²



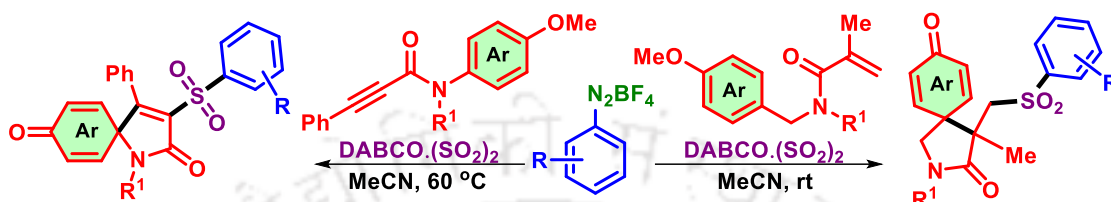
Scheme IB.4.4.6. Synthesis of sulfonated 9H-pyrrolo[1,2-*a*]indoles.

Wu *et al.* extended their work on arenediazonium salts and DABCO-bis(sulfur dioxide) by synthesizing 3-sulfonated-2,3-dihydrobenzo[*d*]isothiazole 1,1-dioxides from 2-ethynylbenzenesulfonamides. The *in situ* generated arylsulfonyl radical initiates the radical chain reaction. The DABCO released from DABCO-bis(sulfur dioxide) acts as the carrier for single electron transfer, as well as a base to afford the corresponding sulfonated benzosultams (Scheme IB.4.4.7).⁵³



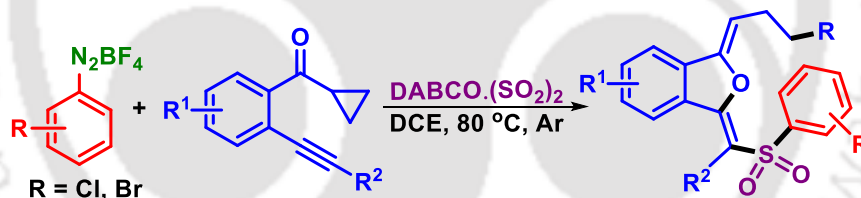
Scheme IB.4.4.7. Synthesis of sulfonated benzosultams.

In 2019, Volla *et al.* established a suitable method for the synthesis of azaspiro[4,5]-decanes and azaspiro[4,5]-trienones by reacting *N*-benzylacrylamides or *N*-arylpropiolamides respectively. The radical cascade spirocyclization proceeds under metal-free conditions and involves *in situ* generations of arylsulfonyl radicals from DABSO and arenediazonium salts (Scheme IB.4.4.8).⁵⁴



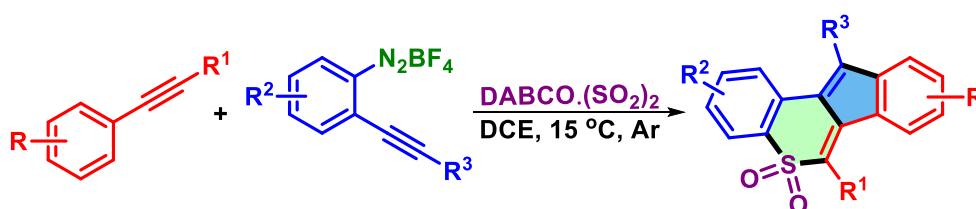
Scheme IB.4.4.8. Synthesis of azaspiro[4,5]-decanes and azaspiro[4,5]-trienones.

A novel radical-induced annulation/1,8-halosulfonylation of β -alkynyl ketones was realized by the Jiang group in 2019 by reacting haloaryl diazonium tetrafluoroborates and DABCO.bis(sulfur dioxide) under thermal conditions. The multicomponent pathway afforded the sulfone-containing 1,3-dimethylene-substituted (*Z,Z*)-isobenzofurans as single stereoisomers in good to excellent yields (Scheme IB.4.4.9).⁵⁵



Scheme IB.4.4.9. Synthesis of 1,3-dimethylene-substituted (*Z,Z*)-isobenzofurans.

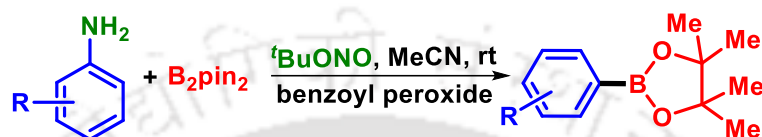
In the same year, Jiang and co-workers accomplished a regioselective synthesis of polycyclic sulfones through radical-triggered cascade bicyclization of 2-alkynyl aryl diazonium tetrafluoroborates, DABCO·(SO₂)₂, and internal alkynes. This oxidant- and catalyst-free process is initiated by an *in situ* generated arylsulfonyl radical from arenediazonium salts and DABSO. The indeno[1,2-*c*]thiochromene 5,5-dioxides were obtained in good yields via 6-*exo-dig*/5-*endo-trig* bicyclization (Scheme IB.4.4.10).⁵⁶



Scheme IB.4.4.10. Synthesis of indeno[1,2-*c*]thiochromene 5,5-dioxides.

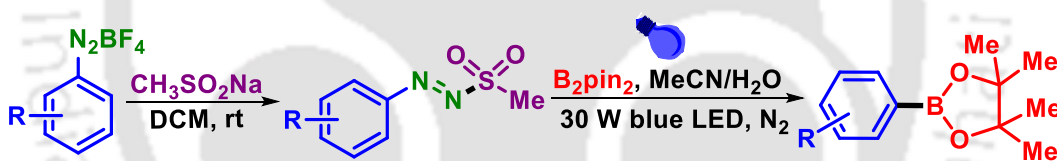
IB.4.5. C–Y bonds formation (Y = B, Se, Te, Sn, P)

In 2010, Wang and co-workers reported a metal-free borylation of arylamines via *in situ* diazotization using *tert*-butyl nitrite. The salient features of the present protocol are inexpensive and readily available starting materials, and no possibility of metal contamination of borylated products which can be used in Pd-catalyzed Suzuki–Miyaura couplings without further purification (Scheme IB.4.5.1).⁵⁷



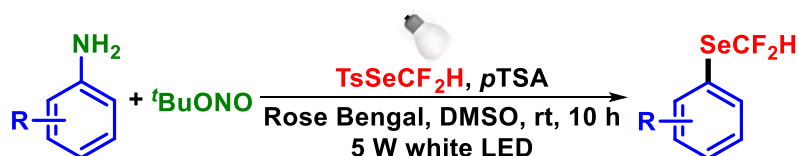
Scheme IB.4.5.1. Synthesis of pinacol boronates.

Wang *et al.* illustrated a visible light-induced borylation from arylazo sulfones under photocatalyst-free and additive-free conditions. The starting precursor arylazo sulfones can be easily synthesized by reacting arenediazonium salts with sodium methanesulfinate at room temperature (Scheme IB.4.5.2).⁵⁸



Scheme IB.4.5.2. Synthesis of pinacol boronates.

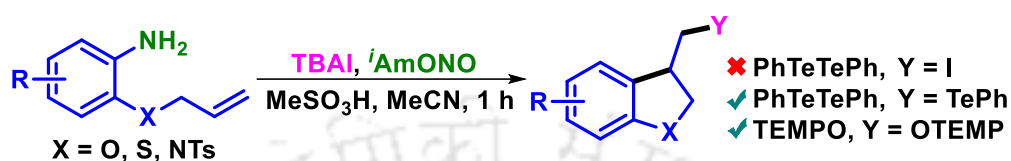
In 2020, Lu and Zhao's group reported a visible-light photocatalytic difluoromethylselenolation of *in situ* generated arenediazonium salts using Se-(difluoromethyl) 4-methylbenzenesulfonoselenoate (readily accessible and shelf-stable). Herein, Rose Bengal serves as a photocatalyst (Scheme IB.4.5.3).⁵⁹



Scheme IB.4.5.3. Difluoromethylselenolation of aryl amines.

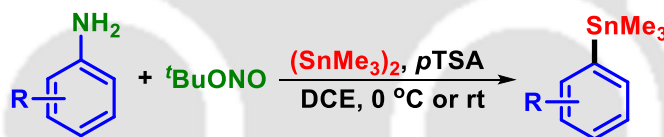
In 2014, Studer and co-workers disclosed a TBAI promoted carbiodination, carbotelluration, and carboaminoxylation strategy of *in situ* generated arenediazonium

salts. The aryl radicals undergo 5-*exo* and 6-*exo* cyclization to form cyclized alkyl radicals which are trapped by iodide ions after a single electron transfer. When the reaction is carried out in the presence of TEMPO and PhTeTePh, the corresponding carboaminoxylated and phenyltellurated cyclized products are obtained (Scheme IB.4.5.4).⁶⁰



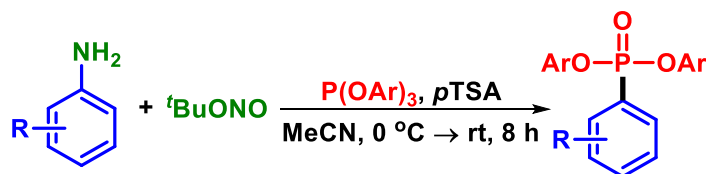
Scheme IB.4.5.4. Metal free functionalizations of aryl amines.

Wang and Zhang's group accomplished the synthesis of aryl trimethylstannane derivatives using *in situ* diazotized arylanilines. In this Sandmeyer type transformation, 1,1,1,2,2,2-hexamethyldistannane (SnMe_3)₂ is used as precursor for $-\text{SnMe}_3$. The salient features of this reaction are mild conditions, broad substrate scope, and moderate to good yields in most cases (Scheme IB.4.5.5).⁶¹



Scheme IB.4.5.5. Metal-free stannylation of aryl amines.

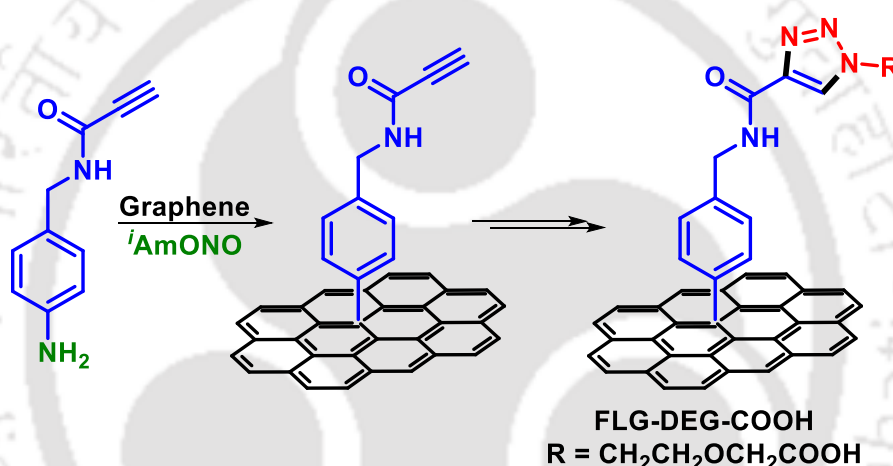
In 2016, Wang group developed a metal-free phosphorylation process based on a Sandmeyer-type transformation with *in situ* diazotized arylanilines. This phosphorylation strategy proceeds under mild reaction conditions without the exclusion of moisture or air, tolerates a wide range of functional groups, and affords the phosphorylation products in moderate to good yields (Scheme IB.4.5.6).⁶²



Scheme IB.4.5.6. Metal-free phosphorylation of aryl amines.

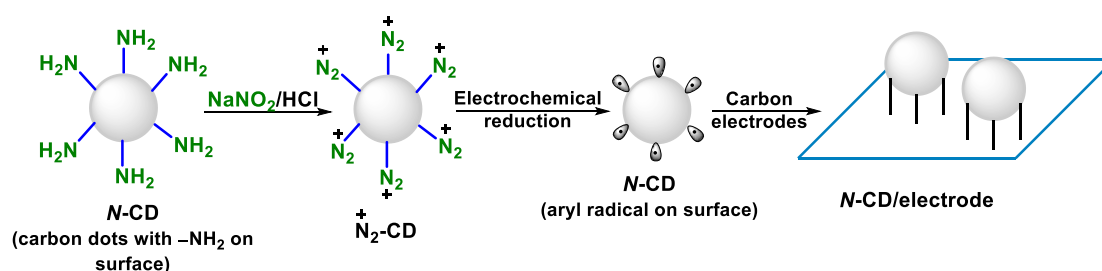
IB.5. Arenediazonium Salts: An Archetype for Modification of Functional Materials and Molecules

In well-known graphene modifications, both the presynthesized and the *in situ* generated arenediazonium salts are employed to access the aryl group functionality. In 2020, Assali *et al.* synthesized an array of covalently functionalized graphene materials with functional groups $-\text{OH}$, $-\text{NH}_2$, or $-\text{COOH}$ through the direct diazonium functionalization of few-layergraphene (FLG). The modified FLG-DEG-COOH has the highest reduction in glutathione activity. The chemical functionalization of graphene might be a step toward the foundation of an active class of antimicrobial agents (Scheme IB.5.1).⁶³



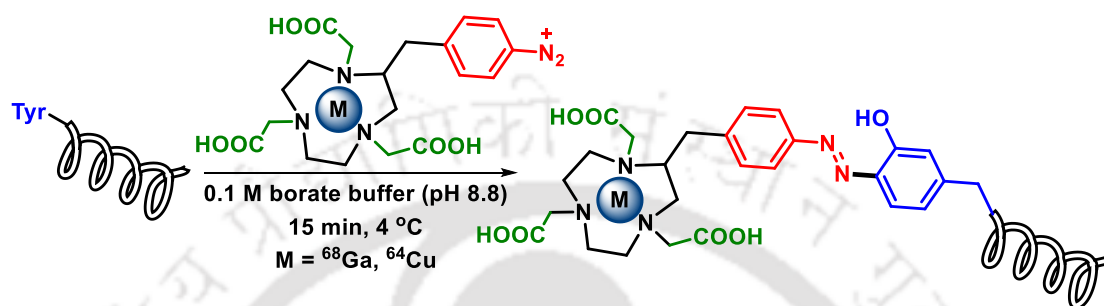
Scheme IB.5.1. Functionalization of the few-layergraphenes.

In 2020, Lorenzo's group developed the electrochemical protocol for electrografting of diazotized *N*-doped carbon nanodots (*N*-CD) onto the surface of carbon electrodes. The final nano-hybrid surface displays a higher electrical conductivity, compared with the unmodified surface, and an effective and insistent electrocatalytic effect on the oxidation of $[\text{Ru}(\text{bpy})_3]^{2+}$ (Scheme IB.5.2).⁶⁴



Scheme IB.5.2. Diazotized *N*-CD electrografting on carbon electrodes.

Tyrosine is an attractive targeted site for chemo- and site-selective protein modification. In 2019, Wuest *et al.* achieved a site-selective azo coupling between tyrosine and aryl diazonium salts. In this method, ^{64}Cu - and ^{68}Ga -labeled 1,4,7-triazacyclononane-1,4,7-triacetic acid-diazonium salts are used as a building block. The described method epitomizes an advanced and useful bioconjugation approach for selective targeting of tyrosine residues in peptides and proteins (Scheme IB.5.3).⁶⁵



Scheme IB.5.3. Chemo-selective bioconjugation of tyrosine residues.

IB.6. References

- (1) Grieffs, P. *Justus Liebigs Ann. Chem.* **1858**, 106, 123.
- (2) (a) Flood, D. T. *Org. Synth.* **1943**, 2, 295. (b) Mo, F.; Dong, G.; Zhang, Y.; Wang, J. *Org. Biomol. Chem.* **2013**, 11, 1582. (c) He, L.; Qiu, G.; Gao, Y.; Wu, J. *Org. Biomol. Chem.* **2014**, 12, 6965. (d) Trusova, M. E.; Kutonova, K. V.; Kurtukov, V. V.; Filimonov, V. D.; Postnikov, P. S. *Resource-Efficient Technologies* **2016**, 2, 36. (e) Mo, F.; Qiu, D.; Zhang, Y.; Wang, J. *Acc. Chem. Res.* **2018**, 51, 496. (f) Hodgson, H. H. *Chem. Rev.* **1947**, 40, 251. (g) Galli, C. *Chem. Rev.* **1988**, 88, 765. (h) Roglans, A.; Pla-Quintana, A.; Moreno-Mañas, M. *Chem. Rev.* **2006**, 106, 4622. (i) Felpin, F.-X.; NassarHardy, L.; Le Callonnec F.; Fouquet, E. *Tetrahedron*, **2011**, 67, 2815. (j) Taylor, J. G.; Moro, A. V. Correia, C. R. D. *Eur. J. Org. Chem.*, **2011**, 1403. (k) Edmison, M. T. *Chem. Rev.* **1957**, 57, 77.
- (3) D. F.; James, Fairlamb, I. J. S. *Org. Lett.* **2020**, 22, 7057.
- (4) (a) Koziakov, D.; Wu, G.; Jacobi von Wangelin, A. *Org. Biomol. Chem.* **2018**, 16, 4942. (b) Oger, N.; d'Halluin, M.; Grogne, E. L.; Felpin, F.-X. *Org. Process Res. Dev.* **2014**, 18, 1786. (c) Filimonov, V. D.; Trusova, M.; Postnikov, P.; Krasnokutskaya, E. A.; Lee, Y. M.; Hwang, H. Y.; Kim, H.; Chi, K.-W. *Org. Lett.* **2008**, 10, 3961. (d) Barbero, M.; Crisma, M.; Degani, I.; Fochi, R.; Perracino, P.; *Synthesis*, **1998**, 1171. (e) Schotten, C.; Leprevost, S. K.; Yong, L. M.; Hughes, C.

- E.; Harris, K. D. M.; Browne, D. L. *Org. Process Res. Dev.* **2020**, *24*, 2336. (f) Kosynkin, D. V.; Tour, J. M. *Org. Lett.* **2001**, *3*, 993. (g) Andrus, M. B.; Song, C. *Org. Lett.* **2001**, *3*, 3761.
- (5) (a) Sandmeyer, T. *Ber. Dtsch. Chem. Ges.* **1884**, *17*, 1633. (b) Sandmeyer, T. *Ber. Dtsch. Chem. Ges.* **1884**, *17*, 2650.
- (6) Pschorr, R. *Ber. Dtsch. Chem. Ges.* **1896**, *29*, 496.
- (7) Gomberg, M.; Bachmann, W. E. *J. Am. Chem. Soc.* **1924**, *46*, 2339.
- (8) Balz, G.; Schiemann, G. *Ber. Dtsch. Chem. Ges. B* **1927**, *60*, 1186.
- (9) Meerwein, H.; Büchner, E.; van Emster, K. *J. Prakt. Chem.* **1939**, *152*, 237.
- (10) (a) Doyle, M. P.; Dellaria, J. F.; Siegfried, B.; Bishop, S. W. *J. Org. Chem.* **1977**, *42*, 3494. (b) Doyle, M. P.; Siegfried, B.; Dellaria, J. F. *J. Org. Chem.* **1977**, *42*, 2426.
- (11) (a) Kikukawa, K.; Matsuda, T. *Chem. Lett.* **1977**, *6*, 159. (b) Kikukawa, K.; Nagira, K.; Terao, N.; Wada, F.; Matsuda, T. *Bull. Chem. Soc. Jpn.* **1979**, *52*, 2609.
- (12) (a) Oger, N.; Le Grogneac, E.; Felpin, F.-X. *Org. Chem. Front.* **2015**, *2*, 590. (b) Chen, J.; Xie, X.; Liu, J.; Yu, Z.; Su, W. *React. Chem. Eng.*, **2022**, *7*, 1247. (c) Zhang, X.; Mei, Y.; Li, Y.; Hu, J.; Huang, D.; Bi, Y. *Asian J. Org. Chem.* **2021**, *10*, 453. (d) Babu, S. S.; Muthuraja, P.; Yadav, P.; Gopinath, P. *Adv. Synth. Catal.* **2021**, *363*, 1782. (e) Garlets, Z. J.; Nguyen, J. D.; Stephenson, C. R. *J. Isr. J. Chem.* **2014**, *54*, 351. (f) Ghosh, I.; Marzo, L.; Das, A.; Shaikh, R.; König, B. *Acc. Chem. Res.* **2016**, *49*, 1566. (g) Srivastava, V.; Singh, P. P. *RSC Adv.* **2017**, *7*, 31377. (g) Hopkinson, M. N.; Tlahuext-Aca, A.; Glorius, F. *Acc. Chem. Res.* **2016**, *49*, 2261.
- (13) (a) Mo, F.; Qiu, D.; Zhang, L.; Wang, J. *Chem. Rev.* **2021**, *121*, 5741. (b) Felpin, F.-X.; Sengupta, S. *Chem. Soc. Rev.* **2019**, *48*, 1150. (c) Liu, J.; Jiang, J.; Zheng, L.; Liu, Z.-Q. *Adv. Synth. Catal.* **2020**, *362*, 4876. (d) Koziakov, D.; Majek, M.; von Wangelin A. *J. Org. Biomol. Chem.* **2016**, *14*, 11347. (e) Swain, C. G.; Sheats, J. E.; Harbison, K. G. *J. Am. Chem. Soc.* **1975**, *97*, 783. (f) Clayden, J.; Greeves, N.; Warren, S.; Wothers, P. *Organic Chemistry*, Oxford University Press, **2001**, p. 598. (g) García Martínez, A.; de la Moya Cerero, S.; Barcina, J. O.; Jiménez, F. M.; Maroto, B. L. *Eur. J. Org. Chem.* **2013**, 6098. (h) Andrieux, C. P.; Pinson, J. *J. Am. Chem. Soc.* **2003**, *125*, 14801.
- (14) (a) Brown, D. G.; Boström, J. *J. Med. Chem.* **2016**, *59*, 4443. (b) Mennen, S. M.; Alhambra, C.; Allen, C. L.; Barberis, M.; Berritt, S.; Brandt, T. A.; Campbell, A.

- D.; Castañón, J.; Cherney, A. H.; Christensen, M.; Damon, David B.; de Diego, J. E.; García-Cerrada, S.; García-Losad, P.; Haro, R.; Janey, J.; Leitch, D. C.; Li, L.; Liu, F.; Lobben, P. C.; MacMillan, D. W. C.; Magano, J.; McInturff, E.; Monfette, S.; Post, R. J.; Schultz, D.; Sitter, B. J.; Stevens, J. M.; Strambeanu, I. I.; Twilton, J.; Wang, K.; Zajac, Matthew A. *Org. Process Res. Dev.* **2019**, *23*, 1213. (b) Paulus, G. L.; Wang, Q. H.; Strano, M. S. *Acc. Chem. Res.* **2013**, *46*, 160. (c) Sengupta, S.; Chandrasekaran, S. *Org. Biomol. Chem.* **2019**, *17*, 8308. (d) Belmont, J. A.; Bureau, C.; Chehimi, M. M.; GamDerouich, S.; Pinson, J. *Aryl Diazonium Salts: New Coupling Agents in Polymer and Surface Science*, Wiley-VCH, Weinheim, Germany, **2012**, 334. (e) Mohamed, A. A.; Salmi, Z.; Dahoumane, S. A.; Mekki, A.; Carbonnier, B.; Chehimi, M. M. *Adv. Colloid Interface Sci.* **2015**, *225*, 16. (f) Cao, C.; Zhang, Y.; Jiang, C.; Qian, M.; Liu, G. *ACS Appl. Mater. Interfaces* **2017**, *9*, 5031. (g) Zollinger, H. *Color Chemistry. Syntheses, Properties, and Applications of Organic Dyes and Pigments*, Wiley-VCH, Zürich, 3rd revised edn, **2003**. (h) Hunger, K.; Herbst, W. Pigments, Organic, in Ullmann's Encyclopedia of Industrial Chemistry, Wiley-VCH, Weinheim, **2012**.
- (15) (a) Leardini, R.; Pedulli, G. F.; Tundo, A.; Zanardi, G. *J. Chem. Soc., Chem. Commun.* **1985**, 1390. (b) Leardini, R.; Nanni, D.; Tundo, A.; Zanardi, G. *Synthesis* **1988**, 333.
- (16) Xiao, T.; Dong, X.; Tang, Y.; Zhou, L. *Adv. Synth. Catal.* **2012**, *354*, 3195.
- (17) Xia, Z.; Huang, J.; He, Y.; Zhao, J.; Lei, J.; Zhu, Q. *Org. Lett.* **2014**, *16*, 2546.
- (18) Malviya, B. K.; Singh, K.; Jaiswal, P. K.; Karnatak, M.; Verma, V. P.; Badsara, S. S.; Sharma, S. *New J. Chem.* **2021**, *45*, 6367.
- (19) Tang, S.; Zhou, D.; Wang, Y.-C. *Eur. J. Org. Chem.* **2014**, 3656.
- (20) Li, J.; Zhang, W.-W.; Wei, X.-J.; Liu, F.; Hao, W.-J.; Wang, S.-L.; Li, G.; Tu, S.-J.; Jiang, B. *J. Org. Chem.* **2017**, *82*, 6621.
- (21) Xuan, J.; Gonzalez-Abradelo, D.; Strassert, C. A.; Daniliuc, C.-G. Studer, A. *Eur. J. Org. Chem.* **2016**, 4961.
- (22) Jin, C.; Su, L.; Ma, D.; Cheng, M. *New J. Chem.* **2017**, *41*, 14053.
- (23) Liu, T.; Jia, Y.-G.; Wu, L. *Org. Biomol. Chem.* **2019**, *17*, 261.
- (24) Alcaide, B.; Almendros, P.; Fernández, I.; Herrera, F.; Luna, A. *Chem. Eur. J.* **2017**, *23*, 17227.
- (25) Kindt, S.; Wicht, K.; Heinrich, M. R. *Angew. Chem. Int. Ed.* **2016**, *55*, 8744.

- (26) Cho, J. Y.; Roh, G.-B.; Cho, E. J. *J. Org. Chem.* **2018**, *83*, 805.
- (27) Felipe-Blanco, D.; Gonzalez-Gomez, J. C. *Eur. J. Org. Chem.* **2019**, 7735.
- (28) Mkrtchyan, S.; Iaroshenko, V. O. *Chem. Commun.* **2020**, *56*, 2606.
- (29) Zhang, C.; Chang, S.; Dong, S.; Qiu, L.; Xu, X. *J. Org. Chem.* **2018**, *83*, 9125.
- (30) (a) Leardini, R.; Nanni, D.; Pareschi, P.; Tundo, A.; Zanardi, G. *J. Org. Chem.* **1997**, *62*, 8394. (b) Benati, L.; Leardini, R.; Minozzi, M.; Nanni, D.; Spagnolo, P.; Zanardi, G. *J. Org. Chem.* **2000**, *65*, 8669. (c) Benati, L.; Calestani, G.; Leardini, R.; Minozzi, M.; Nanni, D.; Spagnolo, P.; Strazzari, S.; Zanardi, G.; *J. Org. Chem.* **2003**, *68*, 3454.
- (31) (a) Haag, B. A.; Zhang, Z.-G.; Li, J.-S.; Knochel, P. *Angew. Chem. Int. Ed.* **2010**, *49*, 9513. (b) Zhang, Z.-G.; Haag, B. A.; Li, J.-S.; Knochel, P. *Synthesis* **2011**, 23.
- (32) Deng, G.-B.; Li, H.-B.; Yang, X.-H.; Song, R.-J.; Hu, M.; Li, J.-H. *Org. Lett.* **2016**, *18*, 2012.
- (33) Wang, M.; Tang, B.-C.; Xiang, J.-C.; Chen, X.-L.; Ma, J.-T.; Wu, Y.-D.; Wu, A.-X. *Org. Lett.* **2019**, *21*, 8934.
- (34) Dey, R.; Ranu, B. C. *Tetrahedron* **2011**, *67*, 8918.
- (35) (a) Vinogradova, O. V.; Balova, I. A.; Popik, V. V. *J. Org. Chem.* **2011**, *76*, 6937. (b) Vinogradova, O. V.; Sorokoumov, V. N.; Balova, I. A. *Tetrahedron Lett.* **2009**, *50*, 6358.
- (36) Senadi, G. C.; Gore, B. S.; Hu, W.-P.; Wang, J.-J. *Org. Lett.* **2016**, *18*, 2890.
- (37) Joshi, M. S.; Pigge, F. C. *Org. Lett.* **2016**, *18*, 5916.
- (38) Yu, X.-Y.; Xiao, W.-J.; Chen, J.-R. *Eur. J. Org. Chem.* **2019**, 6994.
- (39) (a) Colomer, J. P.; Moyano, E. L. *Tetrahedron Lett.* **2011**, *52*, 1561. (b) Moyano, E. L.; Colomer, J. P.; Yranzo, G. I. *Eur. J. Org. Chem.* **2008**, 3377.
- (40) Yan, Y.; Li, H.; Niu, B.; Zhu, C.; Chen, T.; Liu, Y. *Tetrahedron Lett.* **2016**, *57*, 4170.
- (41) Ramanathan, M.; Wang, Y.-H.; Liu, S.-T. *Org. Lett.* **2015**, *17*, 5886.
- (42) Wang, H.; Xu, Q.; Shen, S.; Yu, S. *J. Org. Chem.* **2017**, *82*, 770.
- (43) Youn, S. W.; H. Yoo, J.; Lee, E. M.; Lee, S. Y. *Adv. Synth. Catal.* **2018**, *360*, 278.
- (44) Ramanathan, M.; Liu, S.-T. *J. Org. Chem.* **2017**, *82*, 8290.
- (45) Ramanathan, M.; Liu, Y.-H.; Peng, S.-M.; Liu, S.-T. *Org. Lett.* **2017**, *19*, 5840.
- (46) Ramanathan, M.; Liu, S.-T. *J. Org. Chem.* **2018**, *83*, 22, 14138.
- (47) Hari, D. P.; Hering, T.; König, B. *Org. Lett.* **2012**, *14*, 5334.

- (48) Zang, H.; Sun, J.-G.; Dong, X.; Li, P.; Zhang, B. *Adv. Synth. Catal.* **2016**, *358*, 1746.
- (49) Zheng, D.; Yu, J.; Wu, J. *Angew. Chem. Int. Ed.* **2016**, *55*, 11925.
- (50) Wang, X.; Liu, T.; Zheng, D.; Zhong, Q.; Wu, J. *Org. Chem. Front.* **2017**, *4*, 2455.
- (51) He, F.-S.; Wu, Y.; Zhang, J.; Xia, H.; Wu, J. *Org. Chem. Front.* **2018**, *5*, 2940.
- (52) Chen, H.; Liu, M.; Qiu, G.; Wu, J. *Adv. Synth. Catal.* **2019**, *361*, 146.
- (53) Zhou, K.; Xia, H.; Wu, J. *Org. Chem. Front.* **2017**, *4*, 1121.
- (54) Nair, A. M.; Halder, I.; Khan, S.; Volla, C. M. R. *Adv. Synth. Catal.* **2020**, *362*, 224.
- (55) Huang, M.-H.; Shi, H.-N.; Zhu, C.-F.; He, C.-L.; Hao, W.-J.; Tu, S.-J.; Jiang, B. *Adv. Synth. Catal.* **2019**, *361*, 5340.
- (56) Qin, X.-Y.; He, L.; Li, J.; Hao, W.-J.; Tu, S.-J.; Jiang, B. *Chem. Commun.* **2019**, *55*, 3227.
- (57) Mo, F.; Jiang, Y.; Qiu, D.; Zhang, Y.; Wang, J. *Angew. Chem. Int. Ed.* **2010**, *49*, 1846.
- (58) Xu, Y.; Yang, X.; Fang, H. *J. Org. Chem.* **2018**, *83*, 12831.
- (59) Lu, K.; Li, Q.; Xi, X.; Zhou, T.; Zhao, X. *J. Org. Chem.* **2020**, *85*, 122.
- (60) Hartmann, M.; Studer, A. *Angew. Chem. Int. Ed.* **2014**, *53*, 8180.
- (61) Qiu, D.; Meng, H.; Jin, L.; Wang, S.; Tang, S.; Wang, X.; Mo, F.; Zhang, Y.; Wang, J. *Angew. Chem. Int. Ed.* **2013**, *52*, 11581.
- (62) Wang, S.; Qiu, D.; Mo, F.; Zhang, Y.; Wang, J. *J. Org. Chem.* **2016**, *81*, 11603.
- (63) Assali, M.; Almasri, M.; Kittana, N.; Alsouqi, D. *ACS Biomater. Sci. Eng.* **2020**, *6*, 112.
- (64) Gutiérrez-Sánchez, C.; Mediavilla, M.; Guerrero-Esteban, T.; Revenga-Parra, M.; Pariente, F.; Lorenzo, E. *Carbon* **2020**, *159*, 303.
- (65) Leier, S.; Richter, S.; Bergmann, R.; Wuest, M.; Wuest, F. *ACS Omega* **2019**, *4*, 22101.

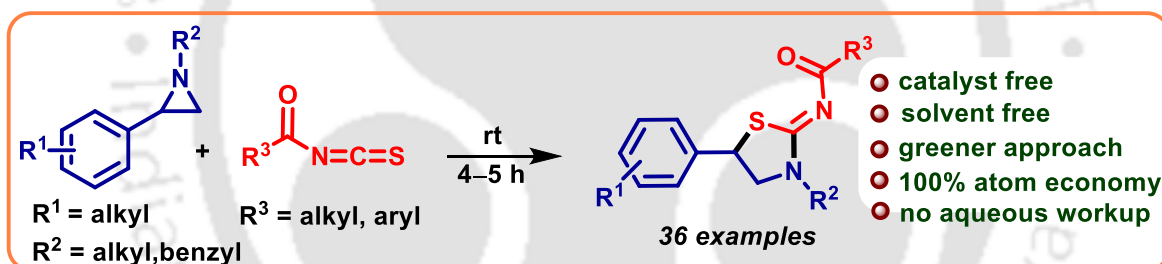
CHAPTER II

ACS
Sustainable
Chemistry & Engineering

March 2018 | Volume 6 | Number 3

pubs.acs.org/acscce

Catalyst and Solvent Free Domino Ring Opening Cyclization: A Greener and Atom Economic Route to 2-Iminothiazolidines



Abstract: A catalyst-free regioselective synthesis of 2-iminothiazolidines has been achieved by reacting unactivated aziridines with aroyl isothiocyanates at ambient temperature in 100% atom economy via a domino ring opening cyclization. The present protocol operates under solvent free conditions as well as in the absence of any catalyst making it a greener and ecofriendly approach.



CHAPTER II

II. Catalyst and Solvent Free Domino Ring Opening Cyclization: A Greener and Atom Economic Route to 2-Iminothiazolidines

II.1. Introduction

In the modern era of synthetic organic chemistry, domino reactions with 100% atom economy have demonstrated a remarkable impact on the synthesis of complex and biologically active natural products.¹ Usually, the synthesis of any target organic compound involves a stepwise formation of individual bonds requiring workup at each step followed by isolation of the intermediate. However, a cascade reaction is a well-orchestrated sequence of individual reactions that enables the one-pot construction of several bonds without workup and isolation of any of the intermediates. The practicality of any cascade reaction is correlated to the bond-forming efficacy, increase in structural complexity, and its suitability for a general application. Bond forming efficacy is the number of bonds that are formed in one sequence.¹

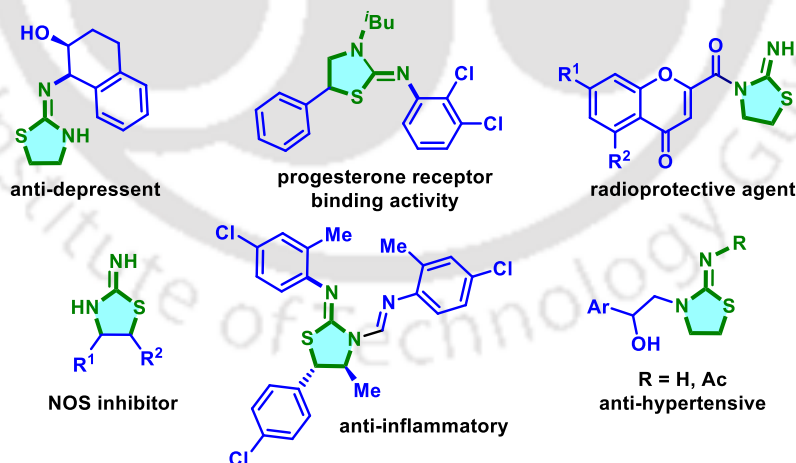


Figure II.1.1. Representative examples of bioactive 2-iminothiazolidines.

Among cascade reactions, a [3 + 2] cycloaddition of aziridines with heterocumulenes provides a promising approach for the synthesis of five-membered heterocycles.² Among these, iminothiazolidines are important structural scaffolds found in many biologically

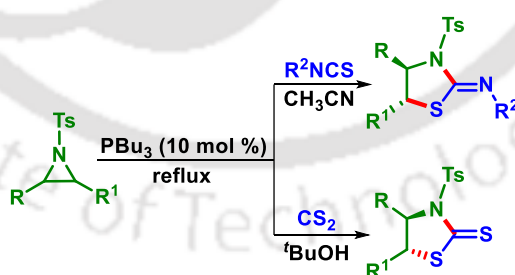
active compounds possessing a wide range of activity such as anti-inflammatory,³ anti-depressant⁴, and anti-Alzheimer.⁵ They also act as nitric oxide synthase (NOS) inhibitor⁶ and find applications as a γ -radio-protective agent.⁷ These moieties have also been used as organo-catalyst in many reactions.⁸ Some of the biologically active compounds possessing 2-iminothiazolidine are depicted in Figure II.1.1.

The synthesis of such compounds is therefore, an important issue for chemists. Consequently, large efforts have been devoted to the development of efficient 2-iminothiazolidines syntheses. But one of the most promising routes is the domino ring-opening cyclization (DROC) of aziridines with isothiocyanates employing various catalytic systems, either metals or Lewis acids, or organo-catalysts.^{2h-j} The following section describes the synthesis of 2-iminothiazolidines.

II.2. Differential Strategies Towards the Synthesis of 2-Iminothiazolidines

II.2.1. Synthesis of 2-iminothiazolidines via ring-opening cyclization (DROC) of aziridines

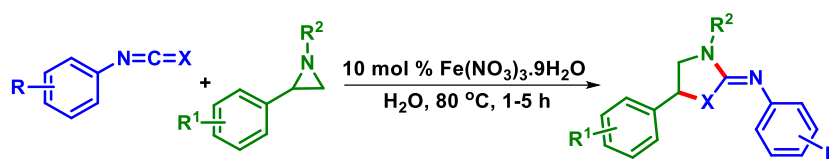
Hou *et al.* disclosed an organophosphine-catalyzed domino ring opening cyclization of aziridine with aryl isothiocyanates and carbon disulfide affording 1,3-thiazolidine derivatives. Herein, Bu_3P acts as a catalyst. The ^{31}P NMR analysis of a 1:1 mixture of CS_2 and Bu_3P suggested the formation of a zwitterionic species (Scheme II.2.1.1).⁹



Scheme II.2.1.1. Organocatalyzed synthesis of 2-iminothiazolidines.

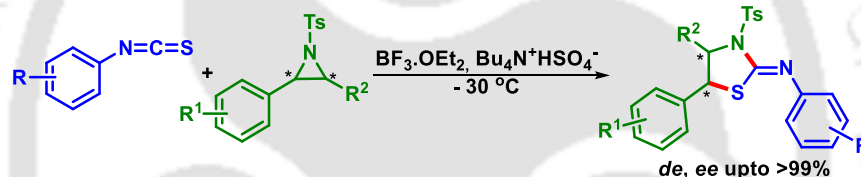
In 2013, Punniyamurthy group accomplished a Fe(III)-catalyzed “on-water” synthesis of 2-iminothiazolidines using activated aziridine and aryl isothiocyanates as coupling partners. Mechanistic investigation revealed that on the water-oil interface, the reaction is going via a concerted path. The binding of Fe(III) species to the N-atom of

aziridine creates a partial positive charge and makes it susceptible to the nucleophilic attack of isothiocyanate (Scheme II.2.1.2).¹⁰



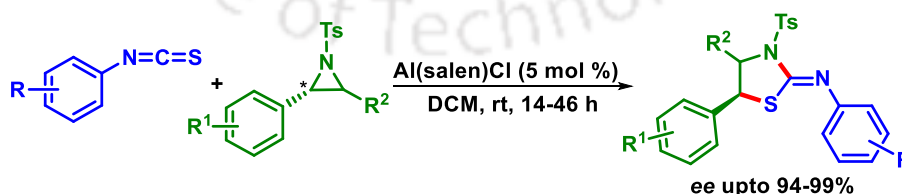
Scheme II.2.1.2. *Fe(II)-catalyzed synthesis of 2-iminothiazolidines.*

A Lewis acid-catalyzed stereospecific synthesis of 2-iminothiazolidines was illustrated by Ghorai and co-workers using activated aziridines with aryl/alkyl isothiocyanates. The synthesized 2-iminothiazolidines were obtained in good yields with excellent diastereo- and enantiospecificity (de, ee up to >99%). Herein, $\text{BF}_3 \cdot \text{Et}_2\text{O}$ is used as a catalyst and tetrabutylammonium hydrogen sulfate (TBAHS) as an additive to reduce the degree of partial racemization of chiral aziridines (Scheme II.2.1.3).¹¹



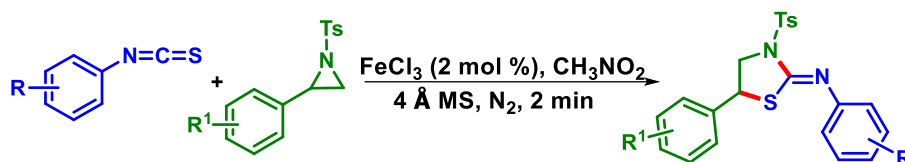
Scheme II.2.1.3. *Lewis acid catalyzed synthesis of 2-iminothiazolidines.*

In 2016, Punniyamurthy and co-workers disclosed another enantiospecific [3 + 2] cycloaddition of unactivated chiral aziridines with isothiocyanates using $\text{Al}(\text{salen})\text{Cl}$ as the catalyst. The salient features of this methodology are safe and mild reaction conditions, inexpensive $\text{Al}(\text{salen})\text{Cl}$ as the catalyst, broad substrate scope, high yield with excellent enantiomeric purities and 100% atom economy (Scheme II.2.1.4).¹²



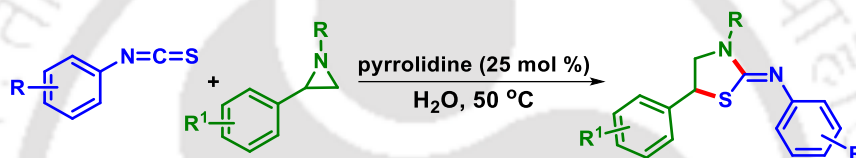
Scheme II.2.1.4. *Al-catalyzed synthesis of 2-iminothiazolidines.*

A quick Lewis acid catalyzed domino ring-opening cyclization of aziridine and aryl isothiocyanate was reported by the Zheng group. The cycloaddition reaction was accomplished in two minutes using FeCl_3 as a catalyst (Scheme II.2.1.5).¹³



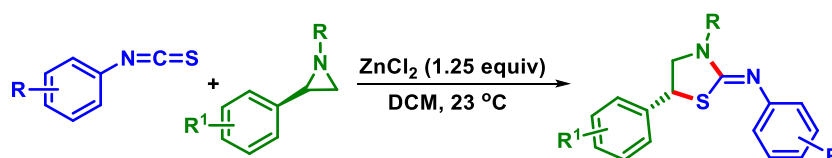
Scheme II.2.1.5. *Fe(III)-catalyzed synthesis of 2-iminothiazolidines.*

In 2014, Punniyamurthy *et al.* disclosed a pyrrolidine catalyzed [3 + 2] cycloaddition of isothiocyanates, isoselenocyanates and carbon disulfide with aziridines. The “on-water” reaction proceeds at a moderate temperature with broad substrate scope and excellent yields. The pyrrolidine reacts with heterocumulenes to form an urea-like intermediate. This intermediate is the actual nucleophile that reacts with aziridine in a S_N^2 manner to afford thiazolidine derivatives (Scheme II.2.1.6).¹⁴



Scheme II.2.1.6. *Base-catalyzed synthesis of 2-iminothiazolidines.*

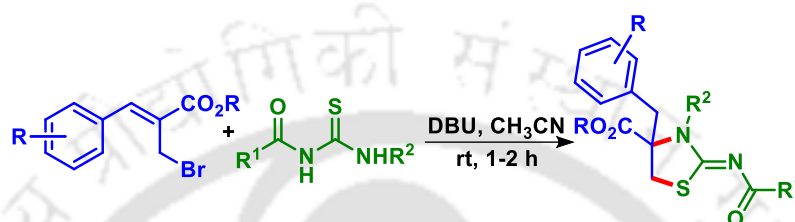
A Zn(II)-catalyzed stereoselective [3 + 2] cycloaddition of aziridines with alkyl and aryl isothiocyanates and carbodiimides is presented by the Stoltz group in 2014. The coordination of Zn(II) species to *N*-sulfonyl aziridines releases the strain energy which promotes this ring expansion of aziridines to imino-imidazolidines and enantioenriched iminothiazolidines. In this process, electron-rich aryl substituted aziridines show better reactivity while *N*-substituted aziridines with more electron-withdrawing groups take shorter reaction times. The inversion at the benzylic position confirms that the reaction is proceeding via a S_N^2 pathway (Scheme II.2.1.7).¹⁵



Scheme II.2.1.7. *Zn(II)-promoted synthesis of 2-iminothiazolidines.*

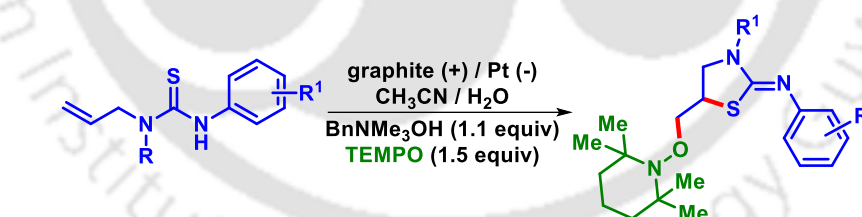
II.2.2. Synthesis of 2-iminothiazolidines using thiourea derivatives

In 2015, Sá *et al.* demonstrated an efficient protocol for the synthesis of 2-iminothiazolidines using substituted thioureas and allylic bromides having electron-withdrawing groups (derived from the Morita–Baylis–Hillman reaction). This base-mediated [3 + 2] annulation involves nucleophilic displacement, followed by intramolecular anti-Michael addition of the preformed allylic isothiureas (Scheme II.2.2.1).¹⁶



Scheme II.2.2.1. Base-mediated [3 + 2] annulation of allylic bromide and thioureas.

The electrochemical synthesis of biologically important thiazolidine-2-imines was disclosed by Ahmed group using thiourea-tethered terminal alkenes. The oxysulfurization strategy was developed in flow electro-microreactor technology where only electricity is used to generate radical intermediates. The salient features of this protocol are mild, metal-free, and electrolyte-free conditions which tolerate a broad range of substrates (Scheme II.2.2.2).¹⁷

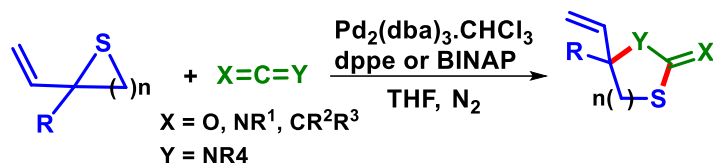


Scheme II.2.2.2. Electrosynthesis of 2-iminothiazolidines.

II.2.3. Synthesis of 2-iminothiazolidines via ring-opening cyclization (DROC) of thiiranes

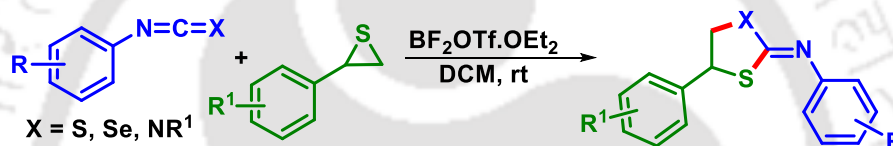
In 2001, Alper and co-workers reported the first Pd(II)-catalyzed enantioselective ring expansion of 2-vinylthiiranes with various heterocumulenes. This regioselective ring-expansion provided substituted thiazolidine, oxathiolane, and dithiolane derivatives in good to moderate yields using carbodiimides, isocyanates, ketenimines, diphenylketene,

and isothiocyanates as starting precursor. The nature of the heterocumulene dictates the enantiomeric excess of this cyclization reaction (Scheme II.2.3.1).¹⁸



Scheme II.2.3.1. *Pd(II)-catalyzed ring expansion of thiiranes.*

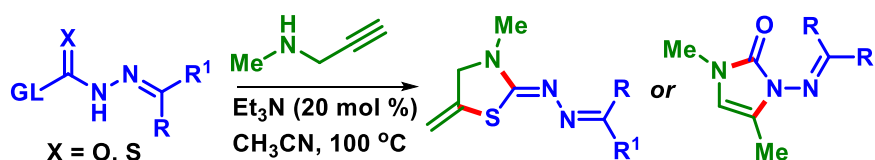
A Lewis acid catalyzed synthesis of 2-imino-dithiolane/-thiaselenolane/-thiazolidine frameworks has been developed by the Punniyamurthy group via [3 + 2]-cycloaddition of 2-aryl/alkylthiiranes with isothiocyanates, isoselenocyanates, and carbodiimides. Herein, $\text{BF}_2\text{OTf}\cdot\text{OEt}_2$ acts as a catalyst. The reaction proceeds at room temperature with good selectivity and a broad range of substrate scope (Scheme II.2.3.2).¹⁹



Scheme II.2.3.2. *Lewis acid-catalyzed ring expansion of thiiranes.*

II.2.4. Synthesis of 2-iminothiazolidines using propargylamines

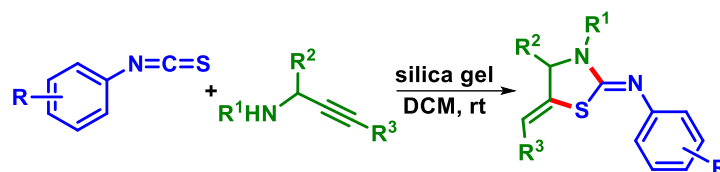
Beauchemin and co-workers reported a base-catalyzed diversity-oriented synthesis of amino-imidazolones and thiazolidines by reacting masked *N*-isocyanate and *N*-isothiocyanate with secondary propargylic and allylic systems. The reactions of propargylic amines with masked *N*-isocyanates gave the direct synthesis of imidazolones scaffolds. While, in the case of masked *N*-isothiocyanates, cyclization ensued through the attack of the *S*-atom followed by little to no isomerization to yield alkene-substituted thiazolidines (Scheme II.2.4.1).²⁰



Scheme II.2.4.1. *Base-catalyzed synthesis of 2-iminothiazolidines.*

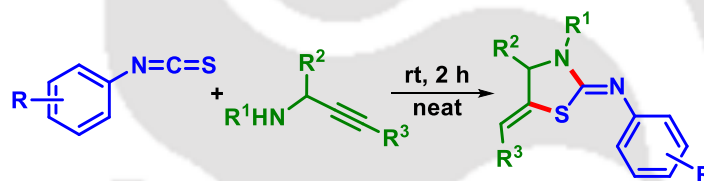
A metal-free synthesis of vinylidene substituted 2-iminothiazolidines is illustrated by the Lovely's group using propargylamines and isothiocyanates. In this reaction, silica gel

is used to promote the thioacylation followed by intramolecular hydrosulfenylation of propargylamines (Scheme II.2.4.2).²¹



Scheme II.2.4.2. Silica gel mediated synthesis of 2-iminothiazolidines.

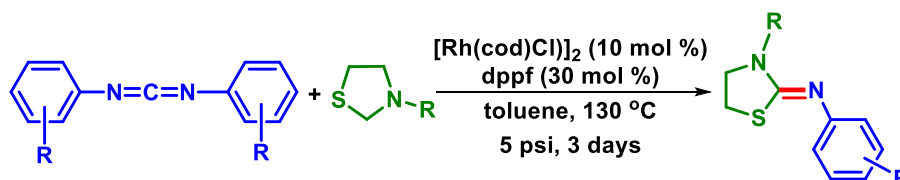
In 2017, Dethé *et al.* disclosed a metal-free thiol-yne coupling for the synthesis of thiazolidin-2-ylideneamine using propargylamine and isothiocyanate as coupling partners. The *in situ* generated propargylthiourea undergoes 5-*exo-dig* cyclization to give thiazolidin-2-ylideneamine under a neat condition. The present protocol provided a wide variety of thiazolidin-2-ylideneamine derivatives under metal-free, solvent-free conditions with no requirement of additional additives (Scheme II.2.4.3).²²



Scheme II.2.4.3. Synthesis of 2-iminothiazolidines via thiol-yne coupling.

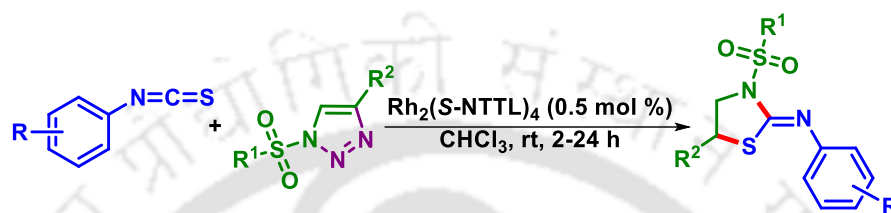
II.2.5. Miscellaneous approach for the synthesis of 2-iminothiazolidines

In 2004, Alper and co-workers disclosed a Rh(II)-catalyzed regioselective synthesis of thiazolidinimine derivatives using readily available thiazolidines and carbodiimides. The reaction ensues oxidative addition of the Rh complex to the thiazolidine followed by regiospecific insertion of carbodiimides via one of the two C–N bonds and the imine elimination process. The reported catalyst system is tolerant to a variety of thiazolidines and carbodiimides derivatives (Scheme II.2.5.1).²³



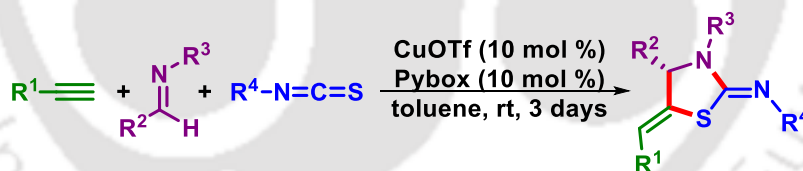
Scheme II.2.5.1. Rh(II)-catalyzed synthesis of 2-iminothiazolidines.

A Rh(II)-catalyzed denitrogenative approach has been developed by Fokin *et al.* for the synthesis of 2-iminothiazolidines via readily available 1-mesyl-1,2,3-triazoles and aryl isothiocyanates. This formal [3 + 2] cycloaddition reaction features triazole–diazoimine equilibrium which results in the formation of metal-stabilized highly reactive azavinyl metal-carbenes. These carbenes further react with heterocumulenes isocyanates, and isothiocyanates resulting in a wide variety of imidazolones and thiazoles (Scheme II.2.5.2).²⁴



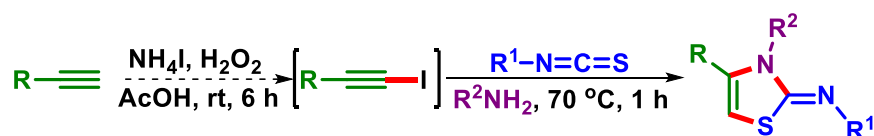
Scheme II.2.5.2. *Rh(II)-catalyzed synthesis of 2-iminothiazolidines.*

A chiral copper–pybox complex catalyzed synthesis of 2-iminothiazolidines is demonstrated by Dethe's group. In this multi-component reaction, imines, terminal alkynes, and aryl isothiocyanates undergo a regioselective intramolecular 5-*exo-dig* hydrothiolation reaction to give enantiopure thiazolidine-2-imines (60–99% *ee*) (Scheme II.2.5.3).²⁵



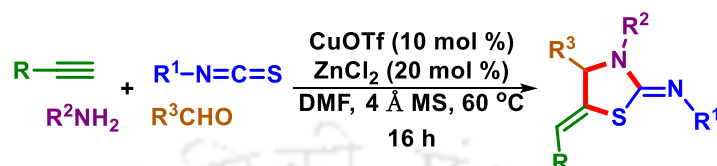
Scheme II.2.5.3. *Cu(I)-catalyzed synthesis of 2-iminothiazolidines.*

In 2016, Meshram's group developed an efficient multicomponent domino protocol for the synthesis of 2-iminothiazolidines using readily available aryl acetylenes, amines, and phenyl isothiocyanates. In this one-pot telescopic reaction, aryl acetylenes are initially converted to iodoalkynes using ammonium iodide and hydrogen peroxide followed by the addition of amines, and phenyl isothiocyanates (Scheme II.2.5.4).²⁶



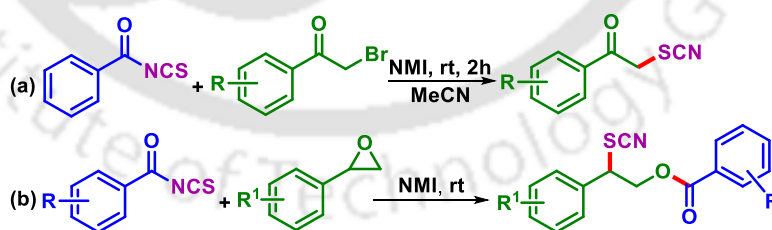
Scheme II.2.5.4. *Multicomponent synthesis of 2-iminothiazolidines.*

In 2018, Shehzadi and co-workers developed a $\text{Cu}^{\text{I}}/\text{Zn}^{\text{II}}$ dual catalytic system for the synthesis of thiazolidine-2-imines using aldehydes, amines, alkynes, and isothiocyanates as reacting partners. This one-pot four-component synthesis avoids the use of preformed propargylamines and imines and ensues via an intramolecular 5-*exo-dig* hydrothiolation of *in situ* generated propargyl thiourea (Scheme II.2.5.5).²⁷



Scheme II.2.5.5. $\text{Cu}^{\text{I}}/\text{Zn}^{\text{II}}$ -catalyzed synthesis of 2-iminothiazolidines.

The above literature precedents reveal that a plethora of reactions is present for the synthesis of 2-iminothiazolidines. Nevertheless, many of these methods suffer from certain drawbacks such as prolonged reaction time, use of organic solvents and harsh reaction conditions, or expensive catalytic systems. In this context, the development of a greener and atom economic approach for the synthesis of thiazolidine is deemed worthy of investigation. Due to their unique structural feature aroyl isothiocyanate can serve either as an electrophile ($\text{ArCO}-$) or an ambident nucleophile ($-\text{SCN}$).²⁸ In our previous reports, we have demonstrated the utility of aroyl isothiocyanates as a nucleophile with α -bromoketone (Scheme II.2.5.6a) while both as an electrophile and a nucleophile with oxirane through a concomitant transfer of thiocyanate as the nucleophile and the aroyl moiety as an electrophile (Scheme II.2.5.6b).^{28c,d}



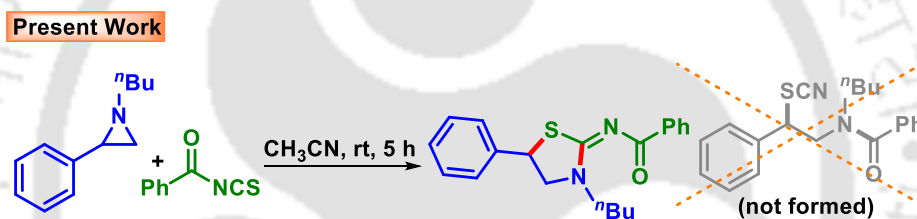
Scheme II.2.5.6. Differential reactivity of isothiocyanates.

Thus, it will be interesting to see the outcome of the reaction, if aziridine is used instead of oxirane. Will it form thiazolidine moiety via a [3 + 2] cycloaddition similar to aryl isothiocyanates¹⁰⁻¹⁴ or undergo a double group transfer similar to oxirane?^{28d} Both the possibilities exist for aziridine since it is susceptible to undergo double group transfer in a nucleophile less-nucleophilic substitution fashion or undergo a [3 + 2] cycloaddition with

heterocumulene (N=C=S) of aroyl isothiocyanate leading to 2-iminothiazolidines. In our previous double group transfer process, a *tert*-amine such as *N*-methyl imidazole (NMI) was used as the organo-catalyst for the simultaneous double group transfer reaction involving an oxirane (Scheme 1a).^{28d} However, in the present strategy one of the starting materials (aziridine) itself is a *tert*-amine, so it might act similar to NMI and serve as a substrate cum organo-catalyst which means non-requirements of the extra catalyst.

II.3. Present Work

To synchronize our hypothesis, a reaction was performed between benzoyl isothiocyanates (1 equiv) (a) and 1-butyl-2-phenylaziridine (1 equiv) (**1**) in acetonitrile (2 mL). A new product was isolated in 77% yield under the catalyst-free condition (Scheme II.3.1).



Scheme II.3.1. Catalyst and solvent-free synthesis of 2-iminothiazolidines.

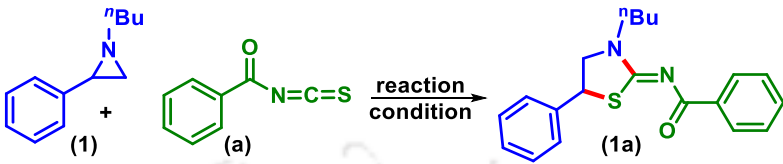
The IR spectra of the isolated product did not show any peak in the range of 2175–2140 cm^{-1} ($-\text{SCN}$) and peak around 1680 cm^{-1} (*tert* amide), suggesting the absence of $-\text{SCN}$ as well as amide ($\text{R}_2\text{N}-\text{COPh}$) functionality. However, a peak at 1626 cm^{-1} suggests the presence of a carbonyl group in the resultant product. Further, ^1H and $^{13}\text{C}\{^1\text{H}\}$ NMR (absence of a peak in the range 105–115 ppm in $^{13}\text{C}\{^1\text{H}\}$ NMR for $-\text{SCN}$) revealed the structure of the product to be 2-iminothiazolidine. Finally, a single X-ray crystallographic diffraction study of one of the derivatives re-established its structure to be 2-iminothiazolidine (*N*-3-isobutyl-5-phenylthiazolidin-2-ylidene)-4-methylbenzamide (**6b**). The formation of the 2-iminothiazolidine reveals that [3 + 2] cycloaddition reaction is more favorable than double group transfer (Scheme II.3.1).

Optimizations of Reaction Conditions:

Intrigued by this catalyst-free protocol for the synthesis of 2-iminothiazolidine, further optimizations were carried out to maximize the product yield. For this, 1-butyl-2-

phenyl aziridine (**1**) and benzoyl isothiocyanate (**a**) were chosen as the model substrates. The only parameter that could be varied is the solvent, so different polar and non-polar solvents were screened to enhance the product yield.

Table II.3.1. Optimization of the reaction conditions^{a,b}



Entry	Solvent	Temp °C	Yield (%) ^b
1	Acetonitrile	rt	77
2	Acetone	rt	74
3	EtOAc	rt	69
4	DCM	rt	79
5	Toluene	rt	78
6	H ₂ O	rt	83
7	-	rt	88

^aReaction condition: **1** (0.20 mmol), **a** (0.20 mmol), solvent (2 mL), 5 h.
^bYield of isolated product.

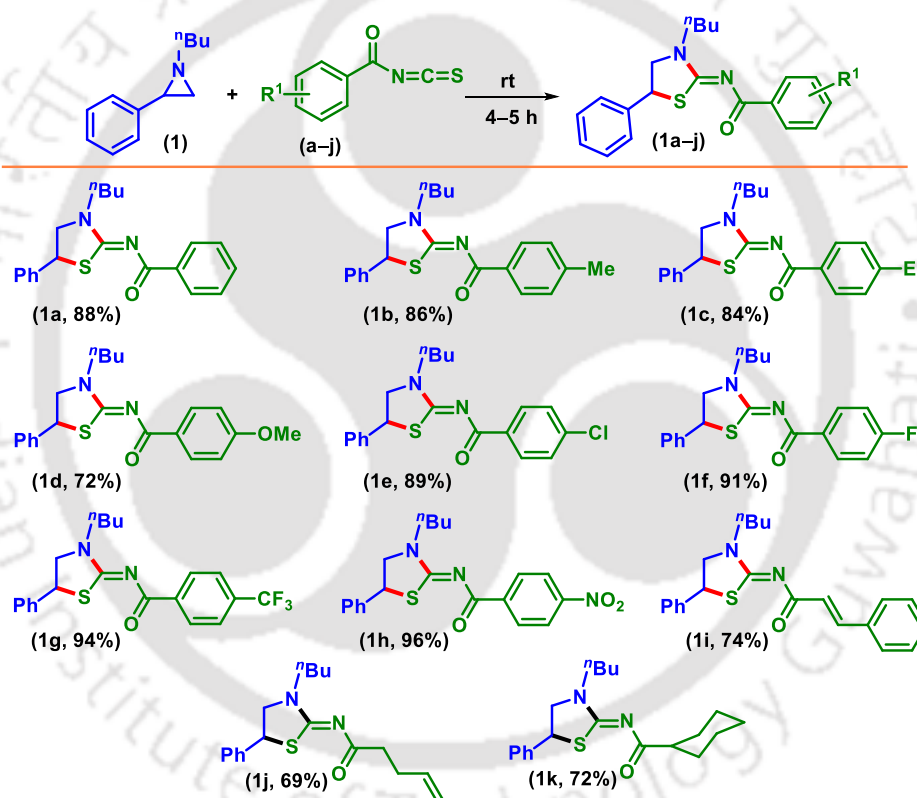
When the reaction was performed in acetone rather than CH₃CN (Table II.3.1, entry 2) a comparable yield (74%) of the product was obtained. Whereas the use of EtOAc (Table II.3.1, entry 3) gave a lesser yield (69%) of the desired product. Similarly, dichloromethane (DCM) and toluene (Table II.3.1, entry 4 and 5) were found to be equally effective (79% and 78%) to that of CH₃CN when the reaction was performed in these solvents. Since water is the most benign solvent, reactions carried out in the water are gaining much attention nowadays.²⁹ So, the reaction was carried out in aqueous media. Gratifyingly, the maximum isolated yield of 83% was obtained when water was used as the solvent (Table II.3.1, entry 6). To our delight, when the reaction was carried out under a neat condition since all the reagents are liquid at room temperature, a further improvement in the isolated yield of the product (**1a**, 88%) was observed (Table II.3.1, entry 7) making the process even more eco-friendly and greener from the synthetic and environmental point of view.

Substrate Scope for 2-Iminothiazolidine Synthesis:

Having established a solvent-free optimized reaction condition, this protocol was subsequently applied for [3 + 2] cycloaddition of various *N*-alkyl-2-phenyl aziridines and aroyl isothiocyanates as shown in Scheme II.3.2. At first, the scope of different aroyl

isothiocyanate (**a–j**) was tested with 1-butyl-2-phenyl aziridine (**1**). As can be seen from Scheme II.3.2, a range of aroyl isothiocyanates bearing electron-donating as well as electron-withdrawing groups reacted efficiently with (**1**) to afford their desired products (**1a–1j**) in good to excellent yields. Aroyl isothiocyanates bearing electron-donating (EDG) substituents such as *p*-Me (**b**), *p*-Et (**c**), and *p*-OMe (**d**) afforded their corresponding products (**1b**, 86%), (**1c**, 84%) and (**1d**, 72%). When electron-donating substituents were present on the phenyl ring of the aroyl isothiocyanate, relatively inferior yields of the corresponding product were obtained.

Scheme II.3.2. Scope of 2-iminothiazolidines with different isothiocyanate^{a,b}



^aReaction condition: **1** (0.50 mmol), **a–j** (0.50 mmol), 4–5 h, under air. ^bIsolated pure product.

The lower yield of the products (**1b–1d**) obtained from aroyl isothiocyanates (**b–d**) might be due to the inductive (+I) and resonance (+R) effect of the substituents. Electron-donating substituent having (+I) and (+R) effect might decrease the electrophilicity of sp carbon of heterocumulene (NCS). On the other hand, excellent yields of the 2-iminothiazolidines were obtained when moderately [*p*-Cl (**e**) (**1e**, 89%) and *p*-F (**f**) (**1f**, 91%)] and strongly [*p*-CF₃ (**g**) (**1g**, 94%) and *p*-NO₂ (**h**) (**1h**, 96%)] electron-withdrawing

groups (EWG) were present on the aroyl isothiocyanates (Scheme II.3.2). Apart from aromatic, aliphatic isothiocyanates such as cinnamoyl (**i**), 1-pentenoyl isothiocyanate (**j**) and cyclohexoyl isothiocyanates (**k**) also underwent reaction efficiently with 1-butyl-2-phenyl aziridine (**1**) affording their corresponding 2-iminothiazolidine (**1i**), (**1j**) and (**1k**) in 74%, 69% and 72% yields respectively (Scheme II.3.2).

Next, the scope of the present protocol was extended by reacting a variety of aziridines (**2–12**) with different aroyl isothiocyanates and the results are summarized in Scheme II.3.3. Aziridines bearing electron-donating and electron-withdrawing substituents in the phenyl ring (**2–4**) underwent efficient reaction with benzoyl isothiocyanate (**a**) giving their corresponding 2-iminothiazolidines (**2a–4a**) in good yields (81–91%). Herein, the electronic effect of substituents present on the phenyl ring of the aziridine is opposite to that of the aroyl isothiocyanates. Aziridine bearing moderately electron-donating substituent *p*-Me (**2**), gave its corresponding product (**2a**) in 91% yield, while aziridine substituted with electron-withdrawing groups such as *p*-Cl (**3**) and *p*-F (**4**) afforded their expected product (**3a**) and (**4a**) in 86% and 81% yields respectively. After reviewing the scope for aroyl isothiocyanates and phenyl substituted aziridines the effect of substituents at the nitrogen atom of aziridine was evaluated (Scheme II.3.3).

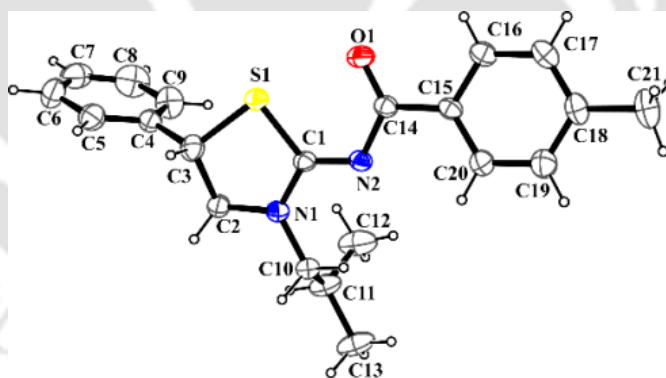
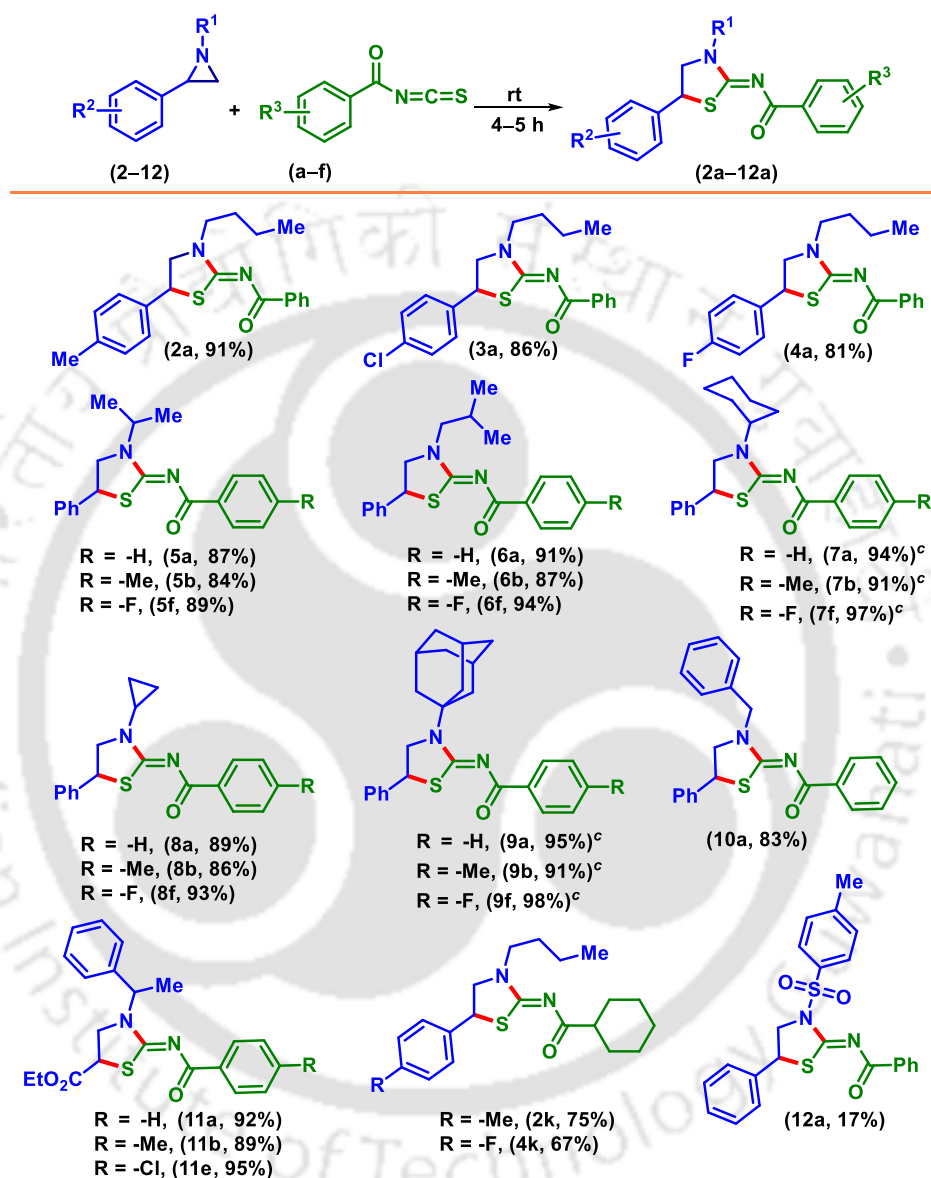


Figure II.3.1. ORTEP view of (**6b**).

Fascinatingly, the present [3 + 2] cycloaddition strategy can tolerate structurally discrete substituents (R^1 , R^2 , R^3) with steric bulk and different electronic properties, which provides a straightforward and practical pathway for forming a richly decorated 2-iminothiazolidine in excellent yields (Scheme II.3.3). Aziridines having substituents at the nitrogen atom such as isopropyl (**5**), *sec*-butyl (**6**), cyclohexyl (**7**), cyclopropyl (**8**), adamantyl (**9**), benzyl (**10**) underwent smooth reaction with different aroyl isothiocyanates (**a–f**) to provide their respective products (**5a–10a**) in good to excellent yields (83%–98%)

(Scheme II.3.3). The structure of the product (**6b**) has been unambiguously established by single crystal X-ray crystallography (Figure II.3.1).

Scheme II.3.3. Scope of 2-iminothiazolidines with different aziridines^{a,b,c}



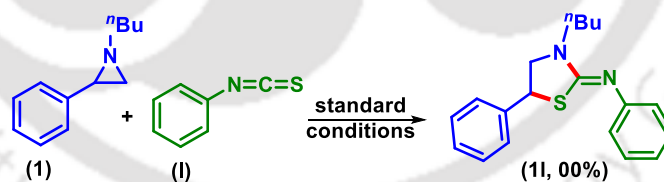
^aReaction condition: **2-12** (0.50 mmol), **a-f** (0.50 mmol), 4-5 h. ^bIsolated pure product.

^cNo column chromatography required.

To extend the scope of the present domino ring opening cyclization leading to the synthesis of 2-iminothiazolidine, other aliphatic aziridines such as ethyl 1-(1-phenylethyl)aziridine-2-carboxylate (**11**) was reacted with various aroyl isothiocyanates (**a**), (**b**) and (**e**) (Scheme II.3.3). Herein also, their corresponding products (**11a**, 92%) (**11b**, 89%) and (**11e**, 95%) were isolated in excellent regioselectivity. Similarly, aliphatic isothiocyanates such as cyclohexoyl isothiocyanates (**k**) reacted smoothly with aziridines

(2) and (4) to afford their corresponding product (2k) and (4k) in 75% and 67% respectively. After successfully synthesizing a library of 2-iminothiazolidines from un-activated aziridines, we desired to explore the strategy of activated aziridines to see the efficacy of domino ring opening cyclization. A reaction was performed between an activated 2-phenyl-1-tosylaziridine (12) and benzoyl isothiocyanate (a) under the standard reaction condition. Unfortunately, the reaction of activated aziridine (12) was not equally productive to that of un-activated aziridines (1–11) affording the corresponding [3+2] cycloaddition product *N*-(5-phenyl-3-tosylthiazolidin-2-ylidene)benzamide (12a) in a mere yield of 17%. Formation of the product (12a) in poor yield might be due to the unavailability of aziridine lone pair towards nucleophilic attack at the thiocyanate carbon for triggering subsequent ring opening via the attack of thiolate onto the aziridine (Scheme II.3.3).

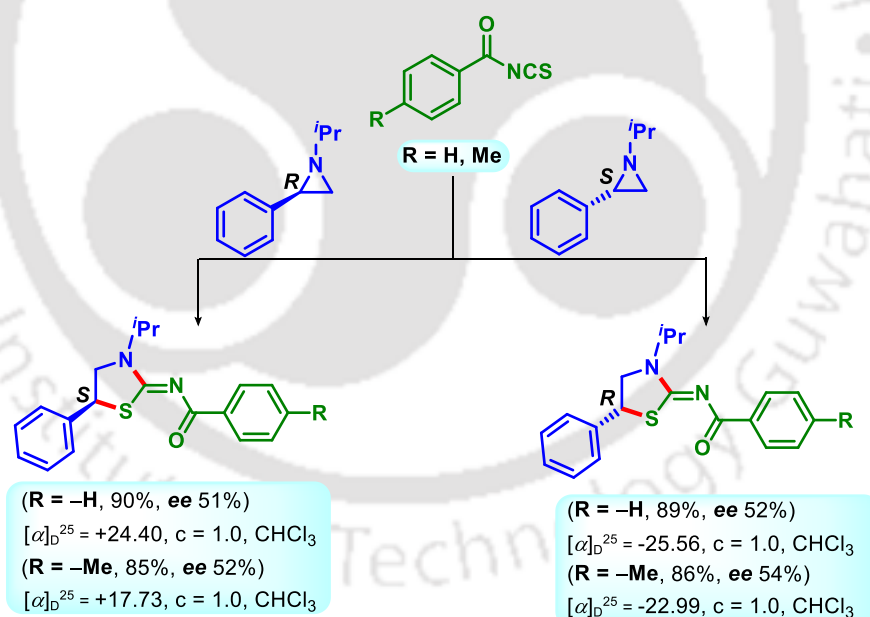
A similar [3 + 2] cycloaddition of aziridines with aryl isothiocyanates for the synthesis of 2-iminothiazolidines requires metal or organo-catalysts.¹⁰⁻¹⁴ Thus we were curious to see whether the present solvent and catalyst-free strategy could also be equally effective towards [3 + 2] cycloaddition with aryl isothiocyanate (ArNCS), so a reaction was carried out between aziridine (1) and PhNCS (I). Unlike aroyl isothiocyanates (ArCO–NCS) a complete failure of the reaction in the case of PhNCS (I) suggests that the former is perhaps catalyst-free protocol because of the ambident nature of aroyl isothiocyanate (Scheme II.3.4).¹⁰⁻¹⁴



Scheme II.3.4. Demonstration of ambident nature of aroyl isothiocyanate.

To check whether the reaction is proceeding via a S_N^1 or S_N^2 type mechanism, a reaction was carried out between enantiomerically pure aziridine (*S*)-1-isopropyl-2-phenylaziridine (13) $\{[\alpha_D] = +68.18, c = 1.0, CHCl_3\}$ and benzoyl isothiocyanate (a). The corresponding 2-iminothiazolidine (13a) thus obtained (89%) was found to be optically active $\{[\alpha_D] = -25.56, c = 1.0, CHCl_3\}$ suggesting a S_N^2 type path for domino ring opening cyclization (Scheme II.3.5). Similarly, the opposite isomer (*R*)-1-isopropyl-2-phenylaziridine (14) $\{[\alpha_D] = -71.40, c = 1.0, CHCl_3\}$ when reacted with (a) gave an optically active 2-iminothiazolidine (14a) (90%) $\{[\alpha_D] = +24.40, c = 1.0, CHCl_3\}$. While,

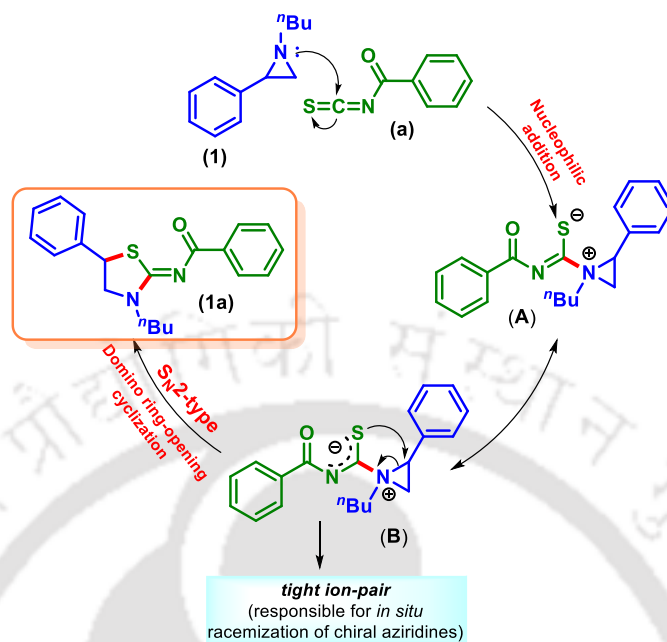
aroyl isothiocyanates (**b**) when reacted with chiral aziridines (**13**) and (**14**) gave their corresponding products (**13b**, 86%) and (**14b**, 85%) and were found to be optically active with specific rotation $\{[\alpha]_D = -22.99, c = 1.0, \text{CHCl}_3\}$ and $\{[\alpha]_D = +17.73, c = 1.0, \text{CHCl}_3\}$ respectively (Scheme II.3.5). This observation reconfirms the S_N^2 path and nucleophilic attack is at the benzylic position of the aziridine. Having established the catalyst-free phenomenon of the present protocol, we also envisaged that chiral aziridines (**13**) and (**14**) should serve as a chiral substrate thereby giving a high enantiomeric excess of the products (**13a**) and (**14a**). Unfortunately, the products (**13a**, ee 52%) and (**14a**, ee 51%) were found to have poor enantioselectivity as confirmed by their HPLC analysis. Similarly, its other derivatives (**13b**, ee 52%) and (**14a**, ee 52%) also show similar enantioselectivity. The formation of opposite enantiomers with low enantioselectivity for the substrates (**13**) and (**14**) may be due to the presence of a tight ion pair present in the dipolar intermediate (**A**). Since no other reagent is present in the reaction medium that can stabilize (**A**) which is responsible for the partial *in situ* racemization of chiral substrates (**13**) and (**14**), (Scheme II.3.5).³⁰



Scheme II.3.5. Synthesis of chiral 2-iminothiazolidines.

Based on the earlier reports and our experimental findings, a plausible reaction mechanism has been proposed as shown in Scheme II.3.6.¹⁰⁻¹⁴ Because of the nucleophilicity of aziridine its lone pair first attacks at the sp carbon of heterocumulene NCS forming a thiourea intermediate (**A**). This negative charge on sulphur then attacks the

benzylic site of aziridine associated with concurrent ring opening giving the 2-iminothiazolidine moiety (Scheme II.3.6).



Scheme II.3.6. Plausible mechanism for the synthesis of 2-iminothiazolidines.

In summary, we have established an elegant catalyst-free domino ring opening cyclization approach for the synthesis of 2-iminothiazolidine. This methodology allows the useful synthesis of many valuable 2-iminothiazolidine via catalyst and solvent-free approach. In this protocol, C–N and C–S bonds are assembled at the same time and have the merits of wide-ranging substrate scope, a greener approach and shorter reaction time.

II.4. Experimental Section

II.4.1. General Information: All the compounds were commercial grade and used without further purification. Organic extracts were dried over anhydrous sodium sulfate. Solvents were removed in a rotary evaporator under reduced pressure. Silica gel (60–120 mesh size) was used for the column chromatography. Reactions were monitored by TLC on silica gel 60 F₂₅₄ (0.25 mm). NMR spectra were recorded in CDCl₃ with tetramethylsilane as an internal standard for proton NMR (400 and 600 MHz) CDCl₃ solvent as an internal standard for ¹³C{¹H} NMR (100 and 150 MHz). HRMS spectra were recorded using ESI mode (Q-TOF MS Analyzer). IR spectra were recorded in KBr or neat.

II.4.2. Crystallographic Description

CCDC Number for Compound 6b: CCDC-1579291 contains the supplementary crystallographic data for this paper. These data can be obtained free of charge from The Cambridge Crystallographic Data Centre via www.ccdc.cam.ac.uk/data_request/cif.

Crystallographic Description of *N*-(3-Isobutyl-5-phenylthiazolidin-2-ylidene)-4-methylbenzamide (6b): C₂₁H₂₄N₂OS, crystal dimensions 0.35 x 0.32 x 0.29mm, $M_r = 352.48$, orthorhombic, space group P 21 21 21, $a = 5.6334(5)$, $b = 17.0832(16)$, $c = 20.6455(19)$ Å, $\alpha = 90^\circ$, $\beta = 90^\circ$, $\gamma = 90^\circ$, $V = 1986.9(3)$ Å³, $Z = 4$, $\rho_{\text{calcd}} = 1.178$ g/cm³, $\mu = 0.173$ mm⁻¹, $F(000) = 752.0$, reflection collected / unique = 3413 / 2406, refinement method = full-matrix least-squares on F^2 , final R indices [$I > 2\sigma(I)$]: $R_1 = 0.0697$, $wR_2 = 0.1508$, R indices (all data): $R_1 = 0.1041$, $wR_2 = 0.1275$, goodness of fit = 0.821.

II.4.3. General Procedure for the Synthesis of *N*-(3-Butyl-5-phenylthiazolidin-2-ylidene)benzamide (1a): 1-Butyl-2-phenylaziridine (**1**) (0.50 mmol, 87.5 mg) and benzoyl isothiocyanate (**a**) (0.50 mmol, 81.5 mg) were combined in a 5 mL oven-dried round bottom flask equipped with a magnetic needle. The flask was then covered with a glass stopper and stirred at room temperature for 5 h. The progress of the reaction was monitored by TLC. After completion of the reaction, the crude product so obtained was then purified by silica gel column chromatography (No column chromatography was required for compounds **7a–7f** and **9a–9f**) using EtOAc / hexane (0.7 : 9.3) as eluent to give the product (**1a**) (149 mg, 88%).

II.4.4. General Procedure for the Synthesis of Aroyl Isothiocyanate (a-k): Benzoyl chloride (5 mmol), KSCN (1.5 equiv), and CH₃CN (15 ml) were taken in a 25 ml oven-dried round bottom flask. Then it was fitted with a condenser and the resultant reaction mixture was stirred in a pre-heated oil bath maintained at 85 °C. The progress of the reaction was monitored by TLC. After completion (color changes from white to yellow) the reaction mixture was cooled to room temperature. The reaction mixture was evaporated under reduced pressure to remove CH₃CN. Then it was admixed with ethyl acetate (30 mL) and washed successively with a saturated solution of sodium bicarbonate (2 x 5 mL) and brine solution (2 x 5 mL). The organic layer was dried over anhydrous sodium sulfate and the solvent was evaporated in a vacuum. The crude product thus obtained was purified using

column chromatography with hexane as eluent to afford the desired benzoyl isothiocyanate in quantitative yield.

II.5. References

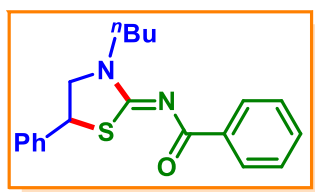
- (1) (a) Tietze, L. F. *Chem. Rev.* **1996**, *96*, 115. (b) Winkler, J. D. *Chem. Rev.* **1996**, *96*, 167. (c) Wang, K. K. *Chem. Rev.* **1996**, *96*, 207. (d) Padwa, A. *Chem. Soc. Rev.* **2009**, *38*, 3072. (e) Ardkhean, R.; Caputo, D. F. J.; Morrow, S. M.; Shi, H.; Xiong, Y.; Anderson, E. A. *Chem. Soc. Rev.* **2016**, *45*, 1557. (f) Blouin, S.; Blond, G.; Donnard, M.; Gulea, M.; Suffert, J. *Synthesis* **2017**, *49*, 1767. (g) Eilbracht, P.; Barfacker, L.; Buss, C.; Hollmann, C.; Kitsos-Rzychon, B. E.; Kranemann, C. L.; Rische, T.; Roggenbuck, R.; Schmidt, A. *Chem. Rev.* **1999**, *99*, 3329. (h) Wasilke, J. C.; Obrey, S. J.; Baker, R. T.; Bazan, G. C. *Chem. Rev.* **2005**, *105*, 1001. (i) Pellissier, H. *Chem. Rev.* **2013**, *113*, 442. (j) Tietze, L. F.; Modi, A. *Med. Res. Rev.* **2000**, *20*, 304. (k) Koeller, K. M.; Wong, C.-H. *Chem. Rev.* **2000**, *100*, 4465. (l) Climent, M. J.; Corma, A.; Iborra, S. *Chem. Rev.* **2011**, *111*, 1072. (m) Cardoso, A. L.; Pinho e Melo, T. M. V. D. *Eur. J. Org. Chem.* **2012**, 6479. (n) Clavier, H.; Pellissier, H. *Adv. Synth. Catal.* **2012**, *354*, 3347. (o) Pellissier, H. *Chem. Rev.* **2013**, *113*, 442. (p) Wender, P. A.; Miller, B. L. *Nature* **2009**, *460*, 197.
- (2) (a) Butler, C. D.; Inman, A. G.; Alper, H. *J. Org. Chem.* **2000**, *65*, 5887. (b) Trost, B. M.; Fandrick, D. R. *J. Am. Chem. Soc.* **2003**, *125*, 11836. (c) Okano, A.; Oishi, S.; Tanaka, T.; Fujii, N.; Ohno, H. *J. Org. Chem.* **2010**, *75*, 3396. (d) Munegumi, T.; Azumaya, I.; Kato, T.; Masu, H.; Saito, S. *Org. Lett.* **2006**, *8*, 379. (e) Singh, G. S.; D'hooghe, M.; Kimpe, N. D. *Chem. Rev.* **2007**, *107*, 2080. (f) Stankovic', S.; D'hooghe, M.; Catak, S.; Eum, H.; Waroquier, M.; Speybroeck, V. V.; Kimpe, N. D.; Ha, H.-J. *Chem. Soc. Rev.* **2012**, *41*, 643. (g) Kaicharla, T.; Jacob, A.; Gonnade, R. G.; Biju, A. T. *Chem. Commun.* **2017**, *53*, 8219. (h) Wu, J.-Y.; Luo, Z.-B.; Dai, L.-X.; Hou, X.-L. *J. Org. Chem.* **2008**, *73*, 9137. (i) Goldberg, A. F. G.; O'Connor, N. R.; Craig II, R. A.; Stoltz, B. M. *Org. Lett.* **2012**, *14*, 5314. (j) Jeong, T.; Han, S.; Mishra, N. K.; Sharma, S.; Lee, S.-Y.; Oh, J. S.; Kwak, J. H.; Jung, Y. H.; Kim, I. S. *J. Org. Chem.* **2015**, *80*, 7243. (k) Han, S.; Mishra, N. K.; Sharma, S.; Park, J.; Choi, M.; Lee, S.-Y.; Oh, J. S.; Jung, Y. H.; Kim, I. S. *J. Org. Chem.* **2015**, *80*, 8026. (l) Jeong, T.; Lee, S. H.; Mishra, N. K.; De, U.; Park, J.; Dey, P.; Kwak, J. H.; Jung, Y. H.; Kim, H. S.; Kim, I. S. *Adv. Synth. Catal.* **2017**, *359*, 2329.

- (3) Takagi, M.; Ishimitsu, K.; Nishibe, T. *U.S. Patent 6762200*, **2004**.
- (4) Shukla, U. K.; Singh, R.; Khanna, J. M.; Saxena, A. K.; Singh, H. K.; Sur, R. N.; Dhawan, B. N.; Anand, N. *Collect. Czech. Chem. Commun.* **1992**, *57*, 415.
- (5) Zubova, O. V.; Fedoseev, V. M.; Silaev, A. B. *Chem. Abstr.* **1964**, *61*, 50560.
- (6) Ueda, S.; Terauchi, H.; Yano, A.; Matsumoto, M.; Kubo, T.; Kyoya, Y.; Suzuki, K.; Ido, M.; Kawasaki, M. *Bioorg. Med. Chem.* **2004**, *12*, 4101.
- (7) Hosseinimehr, S. J.; Shafiee, A.; Mozdarani, H.; Akhlagpour, S.; Froughizadeh, M. *J. Radiat. Res.* **2002**, *43*, 293.
- (8) (a) Birman, V. B.; Li, X. *Org. Lett.* **2006**, *8*, 1351. (b) Birman, V. B.; Jiang, H.; Li, X.; Guo, L.; E. Uffman, W. *J. Am. Chem. Soc.* **2006**, *128*, 6536. (c) Serra, M. E. S.; Costa, D.; Murtinho, D.; Tavares, N. C. T.; Pinho e Melo, T. M. V. D. *Tetrahedron* **2016**, *72*, 5923. (d) Bivona, L. A.; Giacalone, F.; Vaccaro, L.; Aprile, C.; Gruttadauria, M. *ChemCatChem.* **2015**, *7*, 2526. (e) Braga, A. L.; Silveira, C. C.; de Bolster, M. W.G.; Schrekker, H. S.; Wessjohann, L. A.; Schneider, P. H. *J. Mol. Catal. A Chem.* **2005**, *239*, 235.
- (9) Wu, J.-Y.; Luo, Z.-B.; Dai, L.-X.; Hou, X.-L. *J. Org. Chem.* **2008**, *73*, 9137.
- (10) Sengoden, M.; Punniyamurthy, T. *Angew. Chem. Int. Ed.* **2013**, *52*, 572.
- (11) Bhattacharyya, A.; Kavitha, C. V.; Ghorai, M. K. *J. Org. Chem.* **2016**, *81*, 6433.
- (12) Sengoden, M.; Irie, R.; Punniyamurthy, T. *J. Org. Chem.* **2016**, *81*, 11508.
- (13) Gao, L.; Fu, K.; Zheng, G. *RSC Adv.* **2016**, *6*, 47192.
- (14) Sengoden, M.; Vijay, M.; Balakumara, E.; Punniyamurthy, T. *RSC Adv.* **2014**, *4*, 54149.
- (15) Craig II, R. A.; O'Connor, N. R. A.; Goldberg, F. G.; Stoltz, B. M. *Chem. Eur. J.* **2014**, *20*, 4806.
- (16) Ferreira, M.; Sá, M. M. *Adv. Synth. Catal.* **2015**, *357*, 829.
- (17) Islam, M.; Kariuki, B. M.; Shafiq, Z.; Wirth, T.; Ahmed, N. *Eur. J. Org. Chem.* **2019**, 1371.
- (18) Larksarp, C.; Sellier, O.; Alper, H. *J. Org. Chem.* **2001**, *66*, 3502.
- (19) Satheesh, V.; Kumar, S. V.; Vijay, M.; Barik, D.; Punniyamurthy, T. *Asian J. Org. Chem.* **2018**, *7*, 1583.
- (20) Vincent-Rocan, J.-F.; Derasp, J. S.; Beauchemin, A. M. *Chem. Commun.* **2015**, *51*, 16405.
- (21) Singh, R. P.; Gout, D.; Lovely, C. J. *Eur. J. Org. Chem.* **2019**, 1726.

- (22) Ranjan, A.; Deore, A. S.; Yerande, S. G.; Dethe, D. H. *Eur. J. Org. Chem.* **2017**, 4130.
- (23) Zhou, H.-B.; Dong, C.; Alper, H. *Chem. Eur. J.* **2004**, *10*, 6058.
- (24) Chuprakov, S.; Kwok, S. W.; Fokin, V. V. *J. Am. Chem. Soc.* **2013**, *135*, 4652.
- (25) Ranjan, A.; Mandal, A.; Yerande, S. G.; Dethe, D. H. *Chem. Commun.* **2015**, *51*, 14215.
- (26) Kumar, G. S.; Kumar, A. S.; Meshram, H. M. *Synlett* **2016**, *27*, 399.
- (27) Shehzadia, S. A.; Khan, I.; Saeed, A.; Larik, F. A.; Channar, P. A.; Hassan, M.; Raza, H.; Abbas, Q.; Seo, S.-Y. *Bioorg. Chem.* **2019**, *84*, 518.
- (28) (a) Singh, C. B.; Murru, S.; Kavala V.; Patel, B. K. *Org. Lett.* **2006**, *8*, 5397. (b) Castanheiro, T.; Suffert, J.; Donnard, M.; Gulea, M. *Chem. Soc. Rev.* **2016**, *45*, 494 and references cited therein. (c) Palsuledesai, C. C.; Murru, S.; Sahoo, S. K.; Patel, B. K. *Org. Lett.* **2009**, *11*, 3382. (d) Modi, A.; Ali, W.; Patel, B. K. *Org. Lett.* **2017**, *19*, 432.
- (29) (a) Manoj, B. G.; Bonifácio, D. B. Luque, V.; R.; Branco, P. S.; Varma, R. S. *Chem. Soc. Rev.* **2013**, *42*, 5522. (b) Heravi, M. M.; Zadsirjan, V.; Kamjou, K. *Curr. Org. Chem.* **2015**, *19*, 813. (c) Simon, M. O.; Li, C.-J. *Chem. Soc. Rev.* **2012**, *41*, 1415. (d) Dunn, P. J. *Chem. Soc. Rev.* **2012**, *41*, 1452. (e) Gao, S.; Liu, H.; Wu, Z.; Yao, H.; Lin, A. *Green Chem.* **2017**, *19*, 1861. (f) Eghbali, N.; Li, C.-J. *Green Chem.* **2007**, *9*, 213. (g) Yang, Y.; Zhang, S.; Tang, L.; Hu, Y.; Zha, Z.; Wang, Z. *Green Chem.* **2016**, *18*, 2609. (h) Xiao, J.; Wen, H.; Wang, L.; Xu, L.; Hao, Z.; Shao, C.-L.; Wang, C.-Y. *Green Chem.* **2016**, *18*, 1032. (i) Sarkar, A.; Santra, S.; Kundu, S. K.; Hajra, A.; Zyryanov, G. V.; Chupakhin, O. N.; Charushinb, V. N.; Majee, A. *Green Chem.* **2016**, *18*, 4475.
- (30) Ghorai, M. K.; Shukla, D.; Bhattacharyya, A. *J. Org. Chem.* **2012**, *77*, 374.

II.6. Spectral data of product

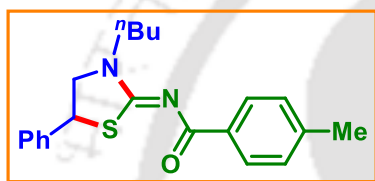
N-(3-Butyl-5-phenylthiazolidin-2-ylidene)benzamide (1a)



Yellowish solid (149 mg, 88%); mp: 80–82 °C. ¹H NMR (600 MHz, CDCl₃): δ (ppm) 0.99 (t, 3H, *J* = 7.8 Hz), 1.42 (m, 2H), 1.69 (m, 2H), 3.71 (dd, 1H, *J* = 7.2, 3.0 Hz), 3.82 (t, 2H, *J* = 7.8 Hz), 4.01 (dd, 1H, *J* = 8.4, 2.4 Hz), 4.71 (t, 1H, *J* = 7.8 Hz), 7.30 (t, 1H, *J* = 7.2 Hz), 7.34 (t, 2H, *J* =

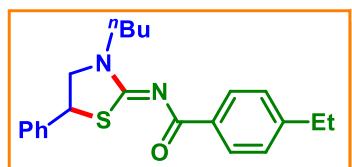
7.8 Hz), 7.39 (d, 2H, $J = 7.8$ Hz), 7.43 (t, 2H, $J = 7.8$ Hz), 7.50 (t, 1H, $J = 7.2$ Hz), 8.30 (d, 2H, $J = 7.8$ Hz); $^{13}\text{C}\{^1\text{H}\}$ NMR (100 MHz, CDCl_3): δ (ppm) 13.9, 20.2, 29.4, 46.8, 47.6, 57.3, 127.5, 128.1, 128.3, 129.1, 129.7, 132.0, 137.0, 139.5, 171.0, 175.9; IR (KBr): 3063, 2958, 2859, 1626, 1614, 1539, 1405, 1333, 1289 cm^{-1} ; HRMS (ESI): calcd. for $\text{C}_{20}\text{H}_{23}\text{N}_2\text{OS}^+$ [$\text{M} + \text{H}^+$] 339.1526; found 339.1531.

***N*-(3-Butyl-5-phenylthiazolidin-2-ylidene)-4-methylbenzamide (1b)**



White solid (151 mg, 86%); mp: 100–102 °C. ^1H NMR (600 MHz, CDCl_3): δ (ppm) 0.99 (t, 3H, $J = 7.2$ Hz), 1.42 (m, 2H), 1.69 (m, 2H), 2.41 (s, 3H), 3.69 (dd, 1H, $J = 7.8$, 3.0 Hz), 3.81 (t, 2H, $J = 7.2$ Hz), 4.00 (dd, 1H, $J = 8.4$, 2.4 Hz), 4.71 (t, 1H, $J = 7.8$ Hz), 7.23 (d, 2H, $J = 8.4$ Hz), 7.34 (t, 3H, $J = 7.2$ Hz), 7.40 (d, 2H, $J = 7.8$ Hz), 8.19 (d, 2H, $J = 7.8$ Hz); $^{13}\text{C}\{^1\text{H}\}$ NMR (100 MHz, CDCl_3): δ (ppm) 14.0, 20.3, 21.8, 29.4, 46.8, 47.6, 57.3, 127.6, 128.3, 128.9, 129.1, 129.8, 134.3, 139.6, 142.4, 170.8, 176.0; IR (KBr): 2957, 2925, 2856, 1611, 1538, 1407, 1247, 1169, 1017 cm^{-1} ; HRMS (ESI): calcd. for $\text{C}_{21}\text{H}_{25}\text{N}_2\text{OS}^+$ [$\text{M} + \text{H}^+$] 353.1682; found 353.1687.

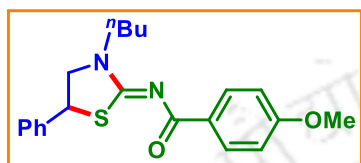
***N*-(3-Butyl-5-phenylthiazolidin-2-ylidene)-4-ethylbenzamide (1c)**



Yellowish solid (154 mg, 84%); mp: 76–78 °C. ^1H NMR (600 MHz, CDCl_3): δ (ppm) 0.98 (t, 3H, $J = 7.8$ Hz), 1.25 (t, 3H, $J = 7.2$ Hz), 1.41 (m, 2H), 1.67 (m, 2H), 2.69 (q, 2H, $J = 7.8$ Hz), 3.68 (dd, 1H, $J = 7.2$, 3.6 Hz), 3.80 (t, 2H, $J = 7.8$ Hz), 3.98 (dd, 1H, $J = 8.4$, 3.0 Hz), 4.69 (t, 1H, $J = 7.8$ Hz), 7.26 (t, 2H, $J = 8.4$ Hz), 7.29 (d, 1H, $J = 7.2$ Hz), 7.33 (t, 2H, $J = 7.8$ Hz), 7.38 (d, 2H, $J = 7.2$ Hz), 8.21 (d, 2H, $J = 7.8$ Hz); $^{13}\text{C}\{^1\text{H}\}$ NMR (100 MHz, CDCl_3): δ (ppm) 13.9, 15.5, 20.2, 29.0, 29.3, 46.7, 47.5, 57.2, 127.5, 127.6, 128.2, 129.0, 129.9, 134.5, 139.5, 148.5, 170.6, 175.9; IR (KBr): 3026, 2962, 2930, 1619, 1537, 1403,

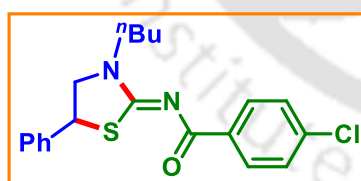
1288, 1170, 1016 cm^{-1} ; HRMS (ESI): calcd. for $\text{C}_{22}\text{H}_{27}\text{N}_2\text{OS}^+$ [$\text{M} + \text{H}^+$] 367.1839; found 367.1835.

N-(3-Butyl-5-phenylthiazolidin-2-ylidene)-4-methoxybenzamide (1d)

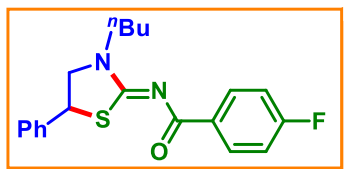


Yellow solid (132 mg, 72%); mp: 88–90 °C. ^1H NMR (600 MHz, CDCl_3): δ (ppm) 0.98 (t, 3H, $J = 7.8$ Hz), 1.41 (d, 2H, $J = 7.8$ Hz), 1.68 (m, 2H), 3.68 (dd, 1H, $J = 7.2, 3.6$ Hz), 3.80 (t, 2H, $J = 7.2$ Hz), 3.85 (s, 3H), 3.98 (dd, 1H, $J = 8.4, 2.4$ Hz), 4.69 (t, 1H, $J = 7.8$ Hz), 6.92 (d, 2H, $J = 9.0$ Hz), 7.29 (t, 1H, $J = 7.2$ Hz), 7.33 (t, 2H, $J = 7.8$ Hz), 7.39 (d, 2H, $J = 7.2$ Hz), 8.26 (d, 2H, $J = 9.0$ Hz); $^{13}\text{C}\{^1\text{H}\}$ NMR (100 MHz, CDCl_3): δ (ppm) 13.9, 20.2, 29.3, 46.7, 47.5, 55.5, 57.2, 113.3, 127.5, 128.2, 129.0, 129.7, 131.7, 139.6, 162.7, 170.4, 175.4; IR (KBr): 2958, 2930, 2858, 1618, 1571, 1538, 1403, 1250, 1160, 1029 cm^{-1} ; HRMS (ESI): calcd. for $\text{C}_{21}\text{H}_{25}\text{N}_2\text{O}_2\text{S}^+$ [$\text{M} + \text{H}^+$] 369.1631; found 369.1640.

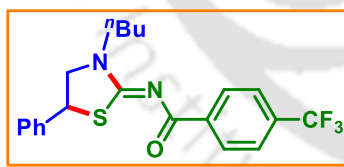
N-(3-Butyl-5-phenylthiazolidin-2-ylidene)-4-chlorobenzamide (1e)



Yellow solid (166 mg, 89%); mp: 107–109 °C. ^1H NMR (600 MHz, CDCl_3): δ (ppm) 0.98 (t, 3H, $J = 7.2$ Hz), 1.41 (m, 2H), 1.66–1.71 (m, 2H), 3.72 (dd, 1H, $J = 7.8, 3.6$ Hz), 3.80 (t, 2H, $J = 7.2$ Hz), 4.02 (dd, 1H, $J = 8.4, 1.8$ Hz), 4.72 (t, 1H, $J = 7.8$ Hz), 7.31 (d, 1H, $J = 7.2$ Hz), 7.34 (t, 2H, $J = 7.8$ Hz), 7.39 (d, 4H, $J = 8.4$ Hz), 8.22 (d, 2H, $J = 8.4$ Hz); $^{13}\text{C}\{^1\text{H}\}$ NMR (150 MHz, CDCl_3): δ (ppm) 13.9, 20.2, 29.4, 46.8, 47.6, 57.4, 127.5, 128.3, 128.4, 129.1, 131.2, 135.5, 138.0, 139.3, 171.2, 174.8; IR (KBr): 2962, 2926, 2856, 1623, 1537, 1411, 1322, 1242, 1117, 1062 cm^{-1} ; HRMS (ESI): calcd. for $\text{C}_{20}\text{H}_{22}\text{ClN}_2\text{OS}^+$ [$\text{M} + \text{H}^+$] 373.1136; found 373.1130.

***N*-(3-Butyl-5-phenylthiazolidin-2-ylidene)-4-fluorobenzamide (1f)**

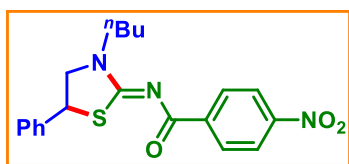
Yellow solid (162 mg, 91%); mp: 94–96 °C. ^1H NMR (400 MHz, CDCl_3): δ (ppm) 0.98 (t, 3H, $J = 7.6$ Hz), 1.38–1.44 (m, 2H), 1.65–1.70 (m, 2H), 3.71 (dd, 1H, $J = 7.6, 3.6$ Hz), 3.80 (t, 2H, $J = 7.2$ Hz), 4.01 (dd, 1H, $J = 8.4, 2.8$ Hz), 4.71 (t, 1H, $J = 8.0$ Hz), 7.08 (t, 2H, $J = 8.8$ Hz), 7.31 (dd, 1H, $J = 8.0, 3.6$ Hz), 7.37 (dd, 4H, $J = 8.0, 4.8$ Hz), 8.30 (dd, 2H, $J = 8.4, 2.8$ Hz); $^{13}\text{C}\{^1\text{H}\}$ NMR (150 MHz, CDCl_3): δ (ppm) 13.9, 20.2, 29.4, 46.8, 47.6, 57.4, 115.0, 115.1, 127.5, 128.4, 129.1, 132.1, 132.2, 133.23, 133.24, 139.4, 164.5, 166.2, 171.1, 174.8; IR (KBr): 3064, 2958, 2929, 2860, 1622, 1537, 1410, 1239, 1146 cm^{-1} ; HRMS (ESI): calcd. for $\text{C}_{20}\text{H}_{22}\text{FN}_2\text{OS}^+$ [$\text{M} + \text{H}^+$] 357.1431; found 357.1435.

***N*-(3-Butyl-5-phenylthiazolidin-2-ylidene)-4-(trifluoromethyl)benzamide (1g)**

White solid (191 mg, 94%); mp: 123–125 °C. ^1H NMR (600 MHz, CDCl_3): δ (ppm) 0.99 (t, 3H, $J = 8.4$ Hz), 1.42 (m, 2H), 1.67–1.72 (m, 2H), 3.75 (dd, 1H, $J = 7.2, 3.6$ Hz), 3.83 (t, 2H, $J = 7.2$ Hz), 4.04 (dd, 1H, $J = 8.4, 3.0$ Hz), 4.75 (t, 1H, $J = 7.8$ Hz), 7.31 (m, 1H), 7.35 (t, 2H, $J = 7.8$ Hz), 7.39 (d, 2H, $J = 7.2$ Hz), 7.69 (d, 2H, $J = 7.8$ Hz), 8.38 (d, 2H, $J = 8.4$ Hz); $^{13}\text{C}\{^1\text{H}\}$ NMR (150 MHz, CDCl_3): δ (ppm) 13.9, 20.2, 29.4, 46.9, 47.7, 57.5, 125.10, 125.12, 125.15, 125.17, 127.5, 128.5, 129.2, 130.0, 133.1, 133.3, 139.3, 140.3, 171.7, 174.6; IR (KBr): 2953, 2925, 2853, 1622, 1536, 1411, 1322, 1290, 1015 cm^{-1} ; HRMS (ESI): calcd. for $\text{C}_{21}\text{H}_{22}\text{F}_3\text{N}_2\text{OS}^+$ [$\text{M} + \text{H}^+$] 407.1399; found 407.1402.

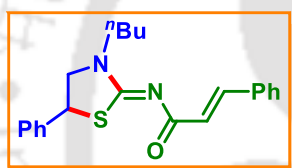
***N*-(3-Butyl-5-phenylthiazolidin-2-ylidene)-4-nitrobenzamide (1h)**

White solid (184 mg, 96%); mp: 171–173 °C. ^1H NMR (600 MHz, CDCl_3): δ (ppm) 0.99 (t, 3H, $J = 7.2$ Hz), 1.40–1.46 (m, 2H), 1.68–1.73 (m, 2H), 3.77 (dd, 1H, $J =$



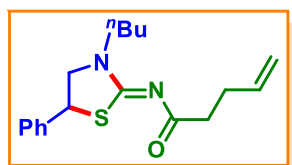
7.8, 3.6 Hz), 3.84 (t, 2H, $J = 7.8$ Hz), 4.07 (dd, 1H, $J = 8.4$, 2.4 Hz), 4.77 (t, 1H, $J = 7.8$ Hz), 7.31 (m, 1H), 7.35 (t, 2H, $J = 7.8$ Hz), 7.39 (d, 2H, $J = 7.2$ Hz), 8.25 (d, 2H, $J = 9.0$ Hz), 8.40 (d, 2H, $J = 9.0$ Hz); $^{13}\text{C}\{^1\text{H}\}$ NMR (100 MHz, CDCl_3): δ (ppm) 13.9, 20.2, 29.4, 46.9, 47.8, 57.6, 123.4, 127.5, 128.6, 129.2, 130.6, 139.1, 142.6, 149.9, 172.1, 173.8; IR (KBr): 2960, 2927, 2852, 1625, 1594, 1537, 1406, 1340, 1245, 1015 cm^{-1} ; HRMS (ESI): calcd. for $\text{C}_{20}\text{H}_{22}\text{N}_3\text{O}_3\text{S}^+$ [$\text{M} + \text{H}^+$] 384.1376; found 384.1380.

N-((*R*)-3-Butyl-5-phenylthiazolidin-2-ylidene)cinnamamide (**1i**)



Yellow gummy (135 mg, 74%). ^1H NMR (400 MHz, CDCl_3): δ (ppm) 0.99 (t, 3H, $J = 7.6$ Hz), 1.41 (m, 2H), 1.63–1.70 (m, 2H), 3.68 (dd, 1H, $J = 7.6$, 3.2 Hz), 3.76 (dd, 2H, $J = 6.8$, 1.2 Hz), 3.98 (dd, 1H, $J = 10.5$, 2.8 Hz), 4.68 (t, 1H, $J = 8.0$ Hz), 6.77 (d, 1H, $J = 16.0$ Hz), 7.30–7.40 (m, 8H), 7.57 (dd, 2H, $J = 7.6$, 1.6 Hz), 7.81 (d, 1H, $J = 15.6$ Hz); $^{13}\text{C}\{^1\text{H}\}$ NMR (100 MHz, CDCl_3): δ (ppm) 13.9, 20.1, 29.3, 46.7, 47.4, 57.2, 126.7, 127.5, 128.1, 128.3, 128.8, 129.0, 129.6, 135.7, 139.4, 142.2, 170.4, 176.4; IR (KBr): 3062, 2957, 2929, 2860, 1638, 1595, 1534, 1403, 1338, 1176 cm^{-1} ; HRMS (ESI): calcd. for $\text{C}_{22}\text{H}_{25}\text{N}_2\text{OS}^+$ [$\text{M} + \text{H}^+$] 365.1682; found 365.1690.

N-(3-Butyl-5-phenylthiazolidin-2-ylidene)pent-4-enamide (**1j**)

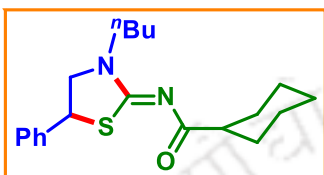


Yellow gummy (109 mg, 69%). ^1H NMR (400 MHz, CDCl_3): δ (ppm) 0.95 (t, 3H, $J = 7.6$ Hz), 1.35 (m, 2H), 1.60 (dt, 2H, $J = 7.2$ Hz), 2.43 (t, 2H, $J = 6.8$ Hz), 2.56 (m, 1H), 3.61–3.68 (m, 3H), 3.93 (dd, 1H, $J = 8.4$, 2.4 Hz), 4.64 (t, 1H, $J = 8.0$ Hz), 4.95–5.08 (m, 3H), 5.86–5.93 (m, 1H), 7.28–7.37 (m, 5H); $^{13}\text{C}\{^1\text{H}\}$ NMR (100 MHz, CDCl_3): δ (ppm) 13.9, 20.2, 29.4, 29.9, 39.5, 46.8, 47.3, 57.2, 114.6, 127.6, 128.4, 129.1, 138.7, 139.5, 169.9, 184.6; IR (KBr): 2966, 2925, 2855, 1635, 1534, 1405,

1019 cm^{-1} ; HRMS (ESI): calcd. for $\text{C}_{18}\text{H}_{25}\text{N}_2\text{OS}^+$ [$\text{M} + \text{H}^+$] 317.1682; found 317.1685.

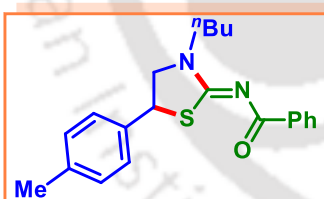
N-(3-Butyl-5-phenylthiazolidin-2-ylidene)cyclohexanecarboxamide (**1k**)

Colorless gummy (124 mg, 72%). ^1H NMR (400 MHz, CDCl_3): δ (ppm) 0.95 (t, 3H, $J = 7.6$ Hz), 1.20-1.40 (m, 7H), 1.63 (m, 3H), 1.76 (m, 2H), 1.95 (m, 2H), 2.37 (m, 1H), 3.65 (m, 3H), 3.90 (dd, 1H, $J = 8.4, 2.4$ Hz), 4.64 (t, 1H, $J = 6.8$ Hz), 7.33 (m, 5H); $^{13}\text{C}\{^1\text{H}\}$ NMR (100 MHz, CDCl_3): δ (ppm) 14.0, 20.1, 26.1, 26.2, 26.4, 29.3, 29.75, 29.85, 46.9, 47.3, 48.2, 57.2, 127.7, 128.3, 129.1, 139.5, 170.0, 187.9; IR (KBr): 2927, 2855, 1631, 1534, 1403, 1245, 912 cm^{-1} ; HRMS (ESI): calcd. for $\text{C}_{20}\text{H}_{29}\text{N}_2\text{OS}^+$ [$\text{M} + \text{H}^+$] 345.1995; found 345.1990.



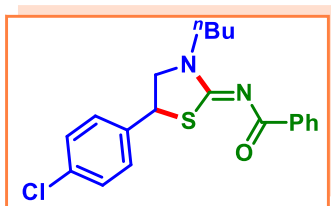
N-(3-Butyl-5-(*p*-tolyl)thiazolidin-2-ylidene)benzamide (**2a**)

Yellow gummy (162 mg, 91%). ^1H NMR (600 MHz, CDCl_3): δ (ppm) 0.99 (t, 3H, $J = 7.2$ Hz), 1.42 (m, 2H), 1.69 (m, 2H), 2.34 (s, 3H), 3.68 (dd, 1H, $J = 7.8, 3.0$ Hz), 3.82 (td, 2H, $J = 7.8$ Hz), 3.98 (dd, 1H, $J = 7.8, 2.4$ Hz), 4.69 (t, 1H, $J = 8.4$ Hz), 7.15 (d, 2H, $J = 8.4$ Hz), 7.29 (t, 2H, $J = 7.8$ Hz), 7.43 (t, 3H, $J = 7.2$ Hz), 8.30 (t, 2H, $J = 8.4$ Hz); $^{13}\text{C}\{^1\text{H}\}$ NMR (100 MHz, CDCl_3): δ (ppm) 13.9, 21.1, 21.2, 29.3, 46.5, 47.5, 57.3, 127.4, 128.0, 129.6, 129.7, 131.8, 136.2, 136.9, 138.0, 171.0, 175.8; IR (KBr): 3022, 2957, 2926, 1626, 1538, 1404, 1248, 1022 cm^{-1} ; HRMS (ESI): calcd. for $\text{C}_{21}\text{H}_{25}\text{N}_2\text{OS}^+$ [$\text{M} + \text{H}^+$] 353.1682; found 353.1680.



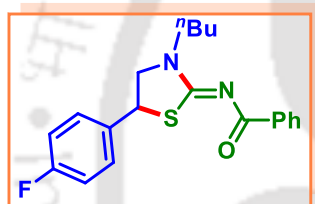
N-(3-Butyl-5-(4-chlorophenyl)thiazolidin-2-ylidene)benzamide (**3a**)

Yellow solid (165 mg, 86%); mp: 104–106 $^{\circ}\text{C}$. ^1H NMR (600 MHz, CDCl_3): δ (ppm) 0.98 (t, 3H, $J = 7.2$ Hz), 1.38–1.44 (m, 2H), 1.65–1.70 (m, 2H), 3.65 (dd, 1H, $J = 7.2, 3.6$ Hz), 3.81 (t, 2H, $J = 7.8$ Hz), 4.00 (dd, 1H, $J = 9.6,$



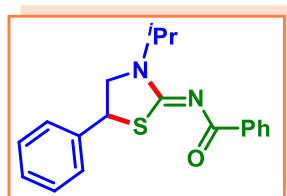
1.2 Hz), 4.67 (t, 1H, $J = 7.8$ Hz), 7.31 (m, 4H), 7.43 (t, 2H, $J = 7.2$ Hz), 7.50 (t, 1H, $J = 7.2$ Hz), 8.28 (d, 2H, $J = 7.2$ Hz); $^{13}\text{C}\{^1\text{H}\}$ NMR (100 MHz, CDCl_3): δ (ppm) 13.9, 20.3, 29.4, 46.1, 47.7, 57.2, 128.2, 128.9, 129.3, 129.8, 132.0, 134.1, 136.8, 138.2, 170.7, 176.0; IR (KBr): 2959, 2929, 2865, 1618, 1538, 1405, 1247, 1092 cm^{-1} ; HRMS (ESI): calcd. for $\text{C}_{21}\text{H}_{22}\text{ClN}_2\text{OS}^+$ [$\text{M} + \text{H}^+$] 385.1136; found 385.1140.

***N*-(3-Butyl-5-(4-fluorophenyl)thiazolidin-2-ylidene)benzamide (4a)**



Creamy solid (149 mg, 81%); mp: 91–93 °C. ^1H NMR (600 MHz, CDCl_3): δ (ppm) 0.98 (t, 3H, $J = 7.2$ Hz), 1.40 (m, 2H), 1.67 (m, 2H), 3.65 (dd, 1H, $J = 7.8, 3.6$ Hz), 3.80 (t, 2H, $J = 7.8$ Hz), 3.99 (dd, 1H, $J = 8.4, 2.4$ Hz), 4.69 (t, 1H, $J = 7.8$ Hz), 7.01 (t, 2H, $J = 8.4$ Hz), 7.35 (dd, 2H, $J = 8.4, 3.0$ Hz), 7.42 (t, 2H, $J = 7.8$ Hz), 7.49 (t, 1H, $J = 7.2$ Hz), 8.28 (d, 2H, $J = 7.2$ Hz); $^{13}\text{C}\{^1\text{H}\}$ NMR (100 MHz, CDCl_3): δ (ppm) 13.9, 20.2, 29.4, 46.0, 47.6, 57.4, 115.9, 116.1, 128.2, 129.2, 129.3, 129.8, 132.0, 135.35, 135.38, 136.8, 161.3, 163.8, 170.8, 176.0; IR (KBr): 2958, 2925, 2855, 1626, 1536, 1510, 1405, 1229, 1159 cm^{-1} ; HRMS (ESI): calcd. for $\text{C}_{21}\text{H}_{22}\text{FN}_2\text{OS}^+$ [$\text{M} + \text{H}^+$] 369.1431; found 369.1440.

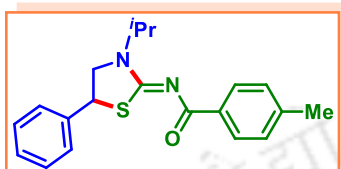
***N*-(3-Isopropyl-5-phenylthiazolidin-2-ylidene)benzamide (5a)**



White solid (141 mg, 87%); mp: 117–119 °C. ^1H NMR (400 MHz, CDCl_3): δ (ppm) 1.21 (d, 3H, $J = 6.8$ Hz), 1.26 (d, 3H, $J = 6.8$ Hz), 3.58 (dd, 1H, $J = 7.6, 3.6$ Hz), 3.91 (dd, 1H, $J = 8.4, 2.4$ Hz), 4.59 (t, 1H, $J = 8.0$ Hz), 5.09 (dt, 1H, $J = 6.8$ Hz), 7.22–7.29 (m, 3H), 7.32–7.37 (m, 4H), 7.42 (m, 1H), 8.22 (t, 2H, $J = 8.4$ Hz); $^{13}\text{C}\{^1\text{H}\}$ NMR (100 MHz, CDCl_3): δ (ppm) 19.7, 20.0, 46.5, 48.4, 52.1, 127.5, 128.1, 128.3, 129.1, 129.8, 131.9, 137.0, 139.5, 170.7, 176.0; IR (KBr): 2955, 2924, 2854, 1626, 1516, 1462,

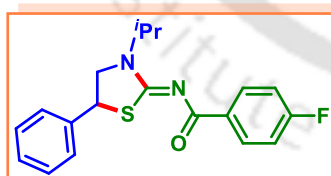
1404, 1327, 1243, 1059 cm^{-1} ; HRMS (ESI): calcd. for $\text{C}_{19}\text{H}_{21}\text{N}_2\text{OS}^+$ [$\text{M} + \text{H}^+$] 325.1369; found 325.1375.

***N*-(3-Isopropyl-5-phenylthiazolidin-2-ylidene)-4-methylbenzamide (5b)**



White solid (142 mg, 84%); mp: 119–121 °C. ^1H NMR (400 MHz, CDCl_3): δ (ppm) 1.26 (d, 3H, $J = 6.8$ Hz), 1.31 (d, 3H, $J = 6.8$ Hz), 2.39 (s, 3H), 3.62 (dd, 1H, $J = 7.6, 3.2$ Hz), 3.95 (dd, 1H, $J = 8.4, 2.4$ Hz), 4.64 (t, 1H, $J = 8.0$ Hz), 5.14 (m, 1H), 7.22 (d, 2H, $J = 8.0$ Hz), 7.31 (m, 3H), 7.39 (d, 2H, $J = 6.8$ Hz), 8.19 (d, 2H, $J = 8.4$ Hz); $^{13}\text{C}\{^1\text{H}\}$ NMR (100 MHz, CDCl_3): δ (ppm) 19.6, 20.0, 21.8, 46.8, 48.3, 52.1, 127.5, 128.3, 128.8, 129.1, 129.8, 134.3, 139.6, 142.3, 170.4, 176.0; IR (KBr): 3028, 2974, 2924, 2854, 1621, 1522, 1461, 1408, 1328, 1170, 947 cm^{-1} ; HRMS (ESI): calcd. for $\text{C}_{20}\text{H}_{23}\text{N}_2\text{OS}^+$ [$\text{M} + \text{H}^+$] 339.1526; found 339.1530.

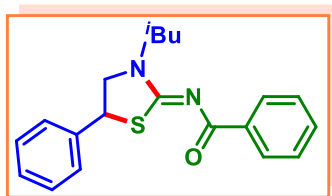
4-Fluoro-*N*-(3-isopropyl-5-phenylthiazolidin-2-ylidene)benzamide (5f)



Yellow solid (152 mg, 89%); mp: 163–165 °C. ^1H NMR (500 MHz, CDCl_3): δ (ppm) 1.30 (dd, 6H, $J = 8.5, 8.5$ Hz), 3.66 (dd, 1H, $J = 9.5, 4.5$ Hz), 3.98 (dd, 1H, $J = 10.0, 3.5$ Hz), 4.67 (t, 1H, $J = 9.5$ Hz), 5.13 (dt, 1H, $J = 9.0$ Hz), 7.08 (t, 2H, $J = 11.0$ Hz), 7.29–7.41 (m, 5H), 8.30 (dd, 2H, $J = 11.0, 4.5$ Hz); $^{13}\text{C}\{^1\text{H}\}$ NMR (150 MHz, CDCl_3): δ (ppm) 19.7, 20.1, 46.6, 48.5, 52.2, 115.0, 115.1, 127.5, 128.4, 129.1, 132.14, 132.22, 133.29, 133.31, 139.5, 164.5, 166.2, 170.8, 174.9; IR (KBr): 3028, 2974, 2924, 2854, 1621, 1522, 1461, 1408, 1328, 1170, 947 cm^{-1} ; HRMS (ESI): calcd. for $\text{C}_{19}\text{H}_{20}\text{FN}_2\text{OS}^+$ [$\text{M} + \text{H}^+$] 343.1275; found 343.1280.

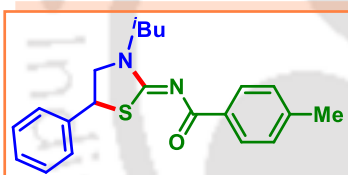
***N*-(3-Isobutyl-5-phenylthiazolidin-2-ylidene)benzamide (6a)**

Yellow gummy (154 mg, 91%). ^1H NMR (600 MHz, CDCl_3): δ (ppm) 1.00 (t, 6H, $J = 6.6$ Hz), 2.15 (dt, 1H, $J =$



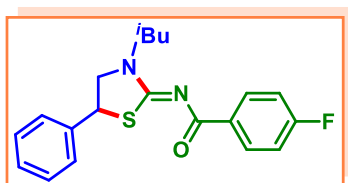
7.2 Hz), 3.58 (dd, 1H, $J = 7.2, 6.0$ Hz), 3.66–3.73 (m, 2H), 4.02 (dd, 1H, $J = 8.4, 2.4$ Hz), 4.73 (t, 1H, $J = 7.8$ Hz), 7.31 (d, 1H, $J = 7.2$ Hz), 7.34 (d, 2H, $J = 7.8$ Hz), 7.40 (s, 2H), 7.44 (d, 2H, $J = 7.2$ Hz), 7.50 (t, 1H, $J = 7.2$ Hz), 8.28 (t, 2H, $J = 7.8$ Hz); $^{13}\text{C}\{^1\text{H}\}$ NMR (100 MHz, CDCl_3): δ (ppm) 20.39, 20.40, 27.4, 46.8, 55.2, 58.0, 127.5, 128.1, 128.2, 129.0, 129.6, 131.8, 136.9, 139.2, 171.4, 175.8; IR (KBr): 3061, 2959, 2870, 1626, 1536, 1405, 1284, 1000 cm^{-1} ; HRMS (ESI): calcd. for $\text{C}_{20}\text{H}_{23}\text{N}_2\text{OS}^+$ [$\text{M} + \text{H}^+$] 339.1526; found 339.1530.

***N*-(3-Isobutyl-5-phenylthiazolidin-2-ylidene)-4-methylbenzamide (6b)**



Yellow solid (153 mg, 87%); mp: 107–109 °C. ^1H NMR (400 MHz, CDCl_3): δ (ppm) 0.99 (dd, 6H, $J = 6.8, 2.4$ Hz), 2.14 (dt, 1H, $J = 6.8$ Hz), 2.40 (s, 3H), 3.56 (dd, 1H, $J = 7.2, 6.0$ Hz), 3.64–3.72 (m, 2H), 4.00 (dd, 1H, $J = 8.4, 2.4$ Hz), 4.72 (t, 1H, $J = 8.0$ Hz), 7.24 (t, 2H, $J = 8.0$ Hz), 7.27–7.34 (m, 3H), 7.40 (d, 2H, $J = 7.2$ Hz), 8.17 (d, 2H, $J = 8.0$ Hz); $^{13}\text{C}\{^1\text{H}\}$ NMR (100 MHz, CDCl_3): δ (ppm) 20.54, 20.55, 21.8, 27.5, 47.0, 55.4, 58.2, 127.7, 128.4, 128.9, 129.1, 129.9, 134.4, 139.4, 142.4, 171.3, 176.0; IR (KBr): 2956, 2923, 2846, 1622, 1536, 1408, 1284, 1170, 1001 cm^{-1} ; HRMS (ESI): calcd. for $\text{C}_{21}\text{H}_{25}\text{N}_2\text{OS}^+$ [$\text{M} + \text{H}^+$] 353.1682; found 353.1690.

4-Fluoro-*N*-(3-isobutyl-5-phenylthiazolidin-2-ylidene)benzamide (6f)

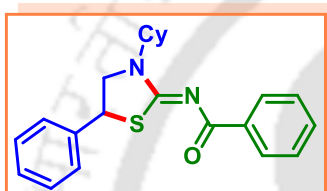


Yellow solid (167 mg, 94%); mp: 148–150 °C. ^1H NMR (400 MHz, CDCl_3): δ (ppm) 0.99 (dd, 6H, $J = 6.8, 2.8$ Hz), 2.10–2.17 (m, 1H), 3.56 (dd, 1H, $J = 7.6, 6.0$ Hz), 3.63–3.74 (m, 2H), 4.02 (dd, 1H, $J = 8.4, 2.8$ Hz), 4.73 (t, 1H, $J = 8.0$ Hz), 7.09 (t, 2H, $J = 8.8$ Hz), 7.30–7.37 (m, 3H), 7.40 (t, 2H, $J = 6.8$ Hz), 8.28 (dd, 2H, $J = 8.8$ Hz); $^{13}\text{C}\{^1\text{H}\}$ NMR (150 MHz, CDCl_3): δ (ppm) 20.5, 27.4,

46.9, 55.3, 58.1, 115.0, 115.1, 127.6, 128.4, 129.1, 132.07, 132.13, 133.2, 133.3, 139.2, 164.5, 166.2, 171.5, 174.8; IR (KBr): 3063, 2956, 2870, 1622, 1534, 1428, 1408, 1305, 1192, 1000 cm^{-1} ; HRMS (ESI): calcd. for $\text{C}_{20}\text{H}_{22}\text{FN}_2\text{OS}^+$ $[\text{M} + \text{H}^+]$ 357.1431; found 357.1440.

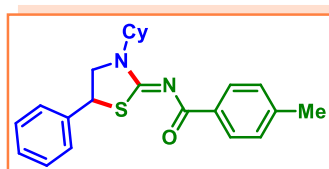
N-(3-Cyclohexyl-5-phenylthiazolidin-2-ylidene)benzamide (7a)

Pale yellow solid (171 mg, 94%); mp: 130–132 °C. ^1H NMR (600 MHz, CDCl_3): δ (ppm) 1.13 (m, 1H), 1.43–152 (m, 4H), 1.73 (d, 1H, $J = 13.2$ Hz), 1.87 (m, 2H), 1.95 (dd, 2H, $J = 12.0, 2.4$ Hz), 3.69 (dd, 1H, $J = 7.2, 3.6$ Hz), 4.01 (dd, 1H, $J = 7.8, 3.0$ Hz), 4.65 (t, 1H, $J = 7.2$ Hz), 4.73 (m, 1H), 7.29 (m, 1H), 7.34 (t, 2H, $J = 7.8$ Hz), 7.39 (d, 2H, $J = 7.2$ Hz), 7.44 (t, 2H, $J = 7.2$ Hz), 7.50 (t, 1H, $J = 7.2$ Hz), 8.28 (d, 2H, $J = 8.4$ Hz); $^{13}\text{C}\{^1\text{H}\}$ NMR (100 MHz, CDCl_3): δ (ppm) 24.4, 24.6, 24.7, 29.0, 29.3, 45.3, 52.2, 55.7, 126.3, 127.0, 127.1, 127.9, 128.6, 130.8, 135.7, 138.6, 169.4, 174.5; IR (KBr): 2927, 2854, 1625, 1519, 1406, 1280, 1018 cm^{-1} ; HRMS (ESI): calcd. for $\text{C}_{22}\text{H}_{25}\text{N}_2\text{OS}^+$ $[\text{M} + \text{H}^+]$ 365.1682; found 365.1685.



N-(3-Cyclohexyl-5-phenylthiazolidin-2-ylidene)-4-methylbenzamide (7b)

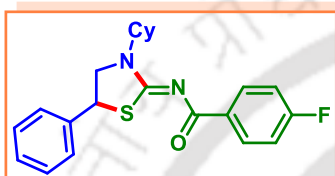
Pale yellow solid (172 mg, 91%); mp: 109–111 °C. ^1H NMR (600 MHz, CDCl_3): δ (ppm) 1.11 (m, 1H), 1.40–1.48 (m, 4H), 1.71 (d, 1H, $J = 7.2$ Hz), 1.85 (m, 2H), 1.92 (t, 2H, $J = 12.0$ Hz), 2.39 (s, 3H), 3.65 (dd, 1H, $J = 7.2, 4.2$ Hz), 3.96 (dd, 1H, $J = 8.4, 3.0$ Hz), 4.60 (t, 1H, $J = 7.8$ Hz), 4.69 (m, 1H), 7.22 (d, 2H, $J = 7.8$ Hz), 7.26 (d, 1H, $J = 7.2$ Hz), 7.31 (t, 2H, $J = 6.6$ Hz), 7.36 (d, 2H, $J = 7.2$ Hz), 8.18 (d, 2H, $J = 7.8$ Hz); $^{13}\text{C}\{^1\text{H}\}$ NMR (100 MHz, CDCl_3): δ (ppm) 21.7, 25.5, 25.76, 25.83, 30.1, 30.4, 46.4, 53.1, 56.6, 127.4, 128.2, 128.8, 129.0, 129.7, 134.3, 139.8, 142.2, 170.3, 175.8; IR (KBr): 3024, 2931, 2855, 1620, 1522, 1409, 1169, 1010 cm^{-1} ; HRMS (ESI):



calcd. for $C_{23}H_{27}N_2OS^+$ [$M + H^+$] 379.1839; found 379.1845.

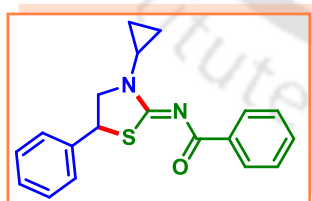
***N*-(3-Cyclohexyl-5-phenylthiazolidin-2-ylidene)-4-fluorobenzamide (7f)**

Yellow solid (185 mg, 97%); mp: 132–134 °C. 1H NMR (600 MHz, $CDCl_3$): δ (ppm) 1.09–1.16 (m, 1H), 1.42–1.50 (m, 4H), 1.72 (d, 1H, $J = 13.2$ Hz), 1.89 (d, 4H, $J = 9.6$ Hz), 3.68 (dd, 1H, $J = 6.6, 4.2$ Hz), 3.99 (dd, 1H, $J = 8.4, 2.4$ Hz), 4.63 (t, 1H, $J = 7.8$ Hz), 4.68 (m, 1H), 7.09 (t, 2H, $J = 9.0$ Hz), 7.28 (d, 1H, $J = 7.2$ Hz), 7.32 (t, 2H, $J = 7.8$ Hz), 7.36 (d, 2H, $J = 7.2$ Hz), 8.29 (dd, 2H, $J = 9.0, 3.0$ Hz); $^{13}C\{^1H\}$ NMR (150 MHz, $CDCl_3$): δ (ppm) 25.4, 25.68, 25.74, 30.0, 30.3, 46.4, 53.1, 56.7, 114.8, 115.0, 127.3, 128.2, 128.9, 131.9, 132.0, 133.19, 133.21, 139.6, 164.3, 166.0, 170.5, 174.6; IR (KBr): 2929, 2855, 1623, 1519, 1407, 1364, 1320, 1224, 1144, 1014 cm^{-1} ; HRMS (ESI): calcd. for $C_{22}H_{24}FN_2OS^+$ [$M + H^+$] 383.1588; found 383.1590.



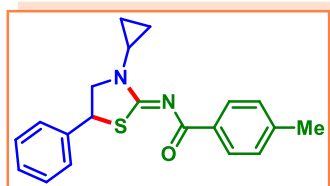
***N*-(3-Cyclopropyl-5-phenylthiazolidin-2-ylidene)-4-fluorobenzamide (8a)**

Brown solid (143 mg, 89%); mp: 90–92 °C. 1H NMR (400 MHz, $CDCl_3$): δ (ppm) 0.95 (m, 4H), 3.00 (m, 1H), 3.65 (td, 1H, $J = 9.2$ Hz), 3.94 (td, 1H, $J = 9.2$ Hz), 4.62 (t, 1H, $J = 7.6$ Hz), 7.24–7.36 (m, 5H), 7.42 (t, 2H, $J = 7.2$ Hz), 7.49 (dd, 1H, $J = 8.4, 1.6$ Hz), 8.32 (d, 2H, $J = 7.2$ Hz); $^{13}C\{^1H\}$ NMR (100 MHz, $CDCl_3$): δ (ppm) 6.8, 7.1, 29.9, 46.7, 57.8, 127.5, 128.1, 128.3, 129.0, 129.8, 132.1, 136.7, 139.1, 172.6, 176.1; IR (KBr): 3062, 2924, 2853, 1627, 1521, 1402, 1329, 1220, 1024 cm^{-1} ; HRMS (ESI): calcd. for $C_{19}H_{19}N_2OS^+$ [$M + H^+$] 323.1213; found 323.1215.



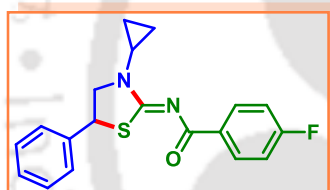
***N*-(3-Cyclopropyl-5-phenylthiazolidin-2-ylidene)-4-methylbenzamide (8b)**

Yellow solid (144 mg, 86%); mp: 117–119 °C. 1H NMR (400 MHz, $CDCl_3$): δ (ppm) 0.87–0.99 (m, 4H), 2.38 (s,



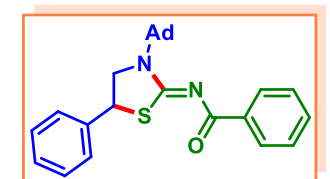
3H), 2.98 (m, 1H), 3.63 (dd, 1H, $J = 8.0, 3.2$ Hz), 3.92 (dd, 1H, $J = 8.0, 2.8$ Hz), 4.61 (t, 1H, $J = 7.6$ Hz), 7.22 (t, 3H, $J = 8.0$ Hz), 7.33 (m, 4H), 8.20 (d, 2H, $J = 8.0$ Hz); $^{13}\text{C}\{^1\text{H}\}$ NMR (100 MHz, CDCl_3): δ (ppm) 6.8, 7.2, 21.8, 29.9, 46.6, 57.8, 127.5, 128.3, 128.9, 129.0, 130.0, 134.1, 139.2, 142.5, 172.3, 176.1; IR (KBr): 3027, 2923, 2853, 1622, 1523, 1401, 1330, 1169, 1019 cm^{-1} ; HRMS (ESI): calcd. for $\text{C}_{20}\text{H}_{21}\text{N}_2\text{OS}^+$ [$\text{M} + \text{H}^+$] 337.1369; found 337.1365.

***N*-(3-Cyclopropyl-5-phenylthiazolidin-2-ylidene)-4-fluorobenzamide (8f)**



Yellow solid (158 mg, 93%); mp: 122–124 °C. ^1H NMR (400 MHz, CDCl_3): δ (ppm) 0.90–1.02 (m, 4H), 2.97–3.03 (m, 1H), 3.68 (dd, 1H, $J = 7.6, 3.2$ Hz), 3.97 (dd, 1H, $J = 8.0, 2.8$ Hz), 4.65 (t, 1H, $J = 8.0$ Hz), 7.09 (dd, 3H, $J = 8.8, 2.0$ Hz), 7.31–7.36 (m, 4H), 8.33 (dd, 2H, $J = 9.2, 3.2$ Hz); $^{13}\text{C}\{^1\text{H}\}$ NMR (100 MHz, CDCl_3): δ (ppm) 6.8, 7.2, 30.0, 46.7, 57.9, 115.0, 115.2, 127.5, 128.4, 129.1, 132.2, 132.3, 133.10, 133.13, 139.0, 164.2, 166.7, 172.8, 175.0; IR (KBr): 3002, 2923, 2848, 1623, 1523, 1409, 1331, 1223, 1146, 1028 cm^{-1} ; HRMS (ESI): calcd. for $\text{C}_{19}\text{H}_{18}\text{FN}_2\text{OS}^+$ [$\text{M} + \text{H}^+$] 341.1118; found 341.1120.

***N*-(3-(Adamantan-1-yl)-5-phenylthiazolidin-2-ylidene)benzamide (9a)**

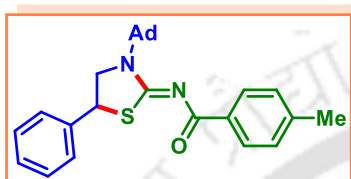


Creamy solid (198 mg, 95%); mp: 160–162 °C. ^1H NMR (400 MHz, CDCl_3): δ (ppm) 1.77 (q, 6H, $J = 12.4$ Hz), 2.20 (s, 3H), 2.47 (t, 6H, $J = 14.4$ Hz), 3.83 (dd, 1H, $J = 7.6, 3.2$ Hz), 4.15 (dd, 1H, $J = 7.6, 3.2$ Hz), 4.53 (t, 1H, $J = 8.0$ Hz), 7.26–7.36 (m, 3H), 7.41–7.52 (m, 5H), 8.29 (dd, 2H, $J = 8.8, 1.6$ Hz); $^{13}\text{C}\{^1\text{H}\}$ NMR (100 MHz, CDCl_3): δ (ppm) 30.1, 36.4, 39.8, 45.4, 54.9, 60.9, 127.4, 128.05, 128.10, 128.9, 129.5, 131.7, 137.3, 139.6, 170.2, 174.8; IR (KBr): 3067, 2908, 2851, 1625, 1506, 1451,

1387, 1227, 1156, 1054 cm^{-1} ; HRMS (ESI): calcd. for $\text{C}_{26}\text{H}_{29}\text{N}_2\text{OS}^+$ [$\text{M} + \text{H}^+$] 417.1995; found 417.1202.

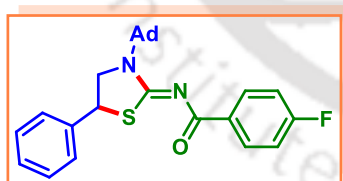
***N*-(3-(Adamantan-1-yl)-5-phenylthiazolidin-2-ylidene)-4-methylbenzamide (9b)**

Yellow solid (196 mg, 91%); mp: 123–125 °C. ^1H NMR (600 MHz, CDCl_3): δ (ppm) 1.75 (q, 6H, $J = 12.0$ Hz), 2.18 (s, 3H), 2.39 (s, 3H), 2.45 (q, 6H, $J = 12.0$ Hz), 3.80 (dd, 1H, $J = 7.8, 3.0$ Hz), 4.12 (dd, 1H, $J = 7.8, 3.0$ Hz), 4.51 (t, 1H, $J = 7.8$ Hz), 7.26 (dd, 3H, $J = 7.8, 7.2$ Hz), 7.32 (t, 2H, $J = 7.8$ Hz), 7.40 (d, 2H, $J = 7.8$ Hz), 8.16 (d, 2H, $J = 8.4$ Hz); $^{13}\text{C}\{^1\text{H}\}$ NMR (150 MHz, CDCl_3): δ (ppm) 21.7, 30.1, 36.4, 39.9, 45.5, 54.9, 60.9, 127.4, 127.6, 128.1, 128.9, 129.3, 129.6, 134.6, 139.6, 170.0, 174.9; IR (KBr): 2909, 2852, 1649, 1497, 1384, 1225, 1050, 1019 cm^{-1} ; HRMS (ESI): calcd. for $\text{C}_{27}\text{H}_{31}\text{N}_2\text{OS}^+$ [$\text{M} + \text{H}^+$] 431.2152; found 431.2160.



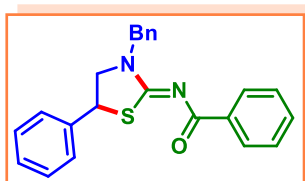
***N*-(3-(Adamantan-1-yl)-5-phenylthiazolidin-2-ylidene)-4-fluorobenzamide (9f)**

Yellow solid (212 mg, 98%); mp: 146–148 °C. ^1H NMR (600 MHz, CDCl_3): δ (ppm) 1.76 (m, 6H), 2.20 (s, 3H), 2.46 (q, 6H, $J = 11.4$ Hz), 3.84 (dd, 1H, $J = 7.2, 3.6$ Hz), 4.15 (dd, 1H, $J = 7.8, 3.0$ Hz), 4.54 (t, 1H, $J = 7.2$ Hz), 7.10 (m, 2H), 7.30 (dd, 1H, $J = 7.2, 4.2$ Hz), 7.34 (m, 2H), 7.41 (t, 2H, $J = 7.2$ Hz), 8.27 (dd, 2H, $J = 9.0, 3.0$ Hz); $^{13}\text{C}\{^1\text{H}\}$ NMR (100 MHz, CDCl_3): δ (ppm) 30.1, 36.4, 39.9, 45.5, 55.0, 61.1, 115.01, 115.2, 127.4, 128.2, 129.0, 131.8, 131.9, 133.58, 133.61, 139.5, 164.3, 166.0, 170.4, 173.9; IR (KBr): 2920, 2853, 1624, 1510, 1385, 1226, 1018 cm^{-1} ; HRMS (ESI): calcd. for $\text{C}_{26}\text{H}_{28}\text{FN}_2\text{OS}^+$ [$\text{M} + \text{H}^+$] 435.1901; found 435.1906.



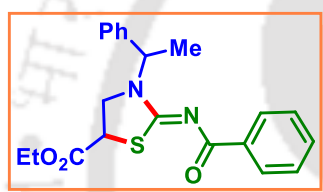
***N*-(3-Benzyl-5-phenylthiazolidin-2-ylidene)benzamide (10a)**

Pale yellow solid (154 mg, 83%); mp: 94–96 °C. ^1H NMR (600 MHz, CDCl_3): δ (ppm) 3.63 (dd, 1H, $J = 7.8, 3.6$ Hz),



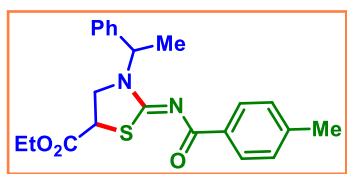
3.92 (dd, 1H, $J = 8.4, 3.6$ Hz), 4.72 (t, 1H, $J = 8.4$ Hz), 5.07 (dd, 2H, $J = 14.4, 13.8$ Hz), 7.32 (m, 5H), 7.39 (m, 5H), 7.47 (t, 2H, $J = 7.8$ Hz), 7.54 (t, 1H, $J = 7.2$ Hz), 8.38 (d, 2H, $J = 7.2$ Hz); $^{13}\text{C}\{^1\text{H}\}$ NMR (100 MHz, CDCl_3): δ (ppm) 46.7, 51.4, 56.5, 127.6, 128.2, 128.26, 128.32, 128.6, 129.05, 129.07, 129.9, 132.1, 135.8, 136.8, 139.2, 171.6, 176.1; IR (KBr): 3062, 2623, 2853, 1626, 1533, 1403, 1325, 1248, 1161 cm^{-1} ; HRMS (ESI): calcd. for $\text{C}_{23}\text{H}_{21}\text{N}_2\text{OS}^+$ [$\text{M} + \text{H}^+$] 373.1369; found 373.1362.

5-Ethyl 2-(benzoylimino)-3-(1-phenylethyl)thiazolidine-5-carboxylate (11a)



Yellow gummy (176 mg, 92%). ^1H NMR (400 MHz, CDCl_3): δ (ppm) 1.26 (t, 3H, $J = 6.8$ Hz), 1.75 (d, 3H, $J = 7.2$ Hz), 3.27 (m, 1H), 3.98 (m, 2H), 4.18 (q, 2H, $J = 7.2$ Hz), 6.33 (q, 1H, $J = 6.8$ Hz), 7.31 (d, 1H, $J = 6.8$ Hz), 7.38 (m, 4H), 7.44 (d, 2H, $J = 7.6$ Hz), 7.49 (d, 1H, $J = 7.2$ Hz), 8.32 (t, 2H, $J = 7.2$ Hz); $^{13}\text{C}\{^1\text{H}\}$ NMR (150 MHz, CDCl_3): δ (ppm) 14.1, 15.7, 42.2, 45.9, 54.5, 62.2, 127.4, 128.1, 128.2, 128.9, 129.8, 132.1, 136.3, 138.7, 169.4, 170.5, 176.0; IR (KBr): 2980, 2931, 1734, 1616, 1405, 1326, 1256, 1199, 1021 cm^{-1} ; HRMS (ESI): calcd. for $\text{C}_{21}\text{H}_{23}\text{N}_2\text{O}_3\text{S}^+$ [$\text{M} + \text{H}^+$] 383.1424; found 383.1430.

5-Ethyl 2-((4-methylbenzoyl)imino)-3-(1-phenylethyl)thiazolidine-5-carboxylate (11b)

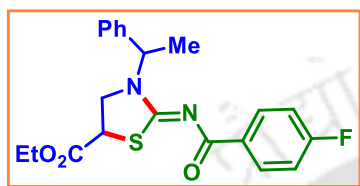


Yellow gummy (176 mg, 89%). ^1H NMR (600 MHz, CDCl_3): δ (ppm) 1.26 (t, 3H, $J = 7.2$ Hz), 1.74 (d, 3H, $J = 7.2$ Hz), 2.39 (s, 3H), 3.25 (dd, 1H, $J = 7.2, 6.6$ Hz), 3.97 (m, 2H), 4.18 (m, 2H), 6.32 (q, 1H, $J = 7.2$ Hz), 7.22 (d, 2H, $J = 7.8$ Hz), 7.29 (t, 1H, $J = 7.2$ Hz), 7.35 (d, 2H, $J = 7.8$ Hz), 7.38 (d, 2H, $J = 7.2$ Hz), 8.20 (d, 2H, $J = 7.2$ Hz); $^{13}\text{C}\{^1\text{H}\}$ NMR (150 MHz, CDCl_3): δ (ppm) 14.1, 15.7, 21.7, 42.2, 45.8, 54.4, 62.2, 127.4, 128.1, 128.9, 129.9, 133.7, 138.8, 142.6, 169.2, 170.5, 176.0; IR (KBr): 2980,

2927, 1734, 1613, 1529, 1407, 1324, 1199, 1019 cm^{-1} ;
HRMS (ESI): calcd. for $\text{C}_{22}\text{H}_{25}\text{N}_2\text{O}_3\text{S}^+$ [$\text{M} + \text{H}^+$]
397.1580; found 397.1584.

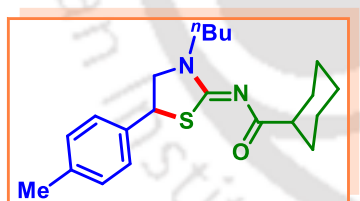
5-Ethyl 2-((4-chlorobenzoyl)imino)-3-(1-phenylethyl)thiazolidine-5-carboxylate (11e)

Yellow gummy (197 mg, 95%). ^1H NMR (400 MHz, CDCl_3): δ (ppm) 1.28 (t, 3H, $J = 7.6$ Hz), 1.75 (d, 3H, $J = 7.2$ Hz), 3.29 (m, 1H), 3.97–4.02 (m, 2H), 4.20 (q, 2H, $J = 7.2$ Hz), 6.29 (q, 1H, $J = 6.8$ Hz), 7.36 (m, 7H), 8.23 (d, 2H, $J = 8.8$ Hz); $^{13}\text{C}\{^1\text{H}\}$ NMR (150 MHz, CDCl_3): δ (ppm) 14.2, 15.8, 42.3, 46.1, 54.6, 62.4, 127.4, 128.3, 128.4, 129.0, 131.3, 135.0, 138.3, 138.7, 169.8, 170.5, 175.2; IR (KBr): 3063, 2980, 2934, 1735, 1617, 1528, 1405, 1325, 1198, 1013 cm^{-1} ; HRMS (ESI): calcd. for $\text{C}_{21}\text{H}_{22}\text{ClN}_2\text{O}_3\text{S}^+$ [$\text{M} + \text{H}^+$] 417.1034; found 417.1040.



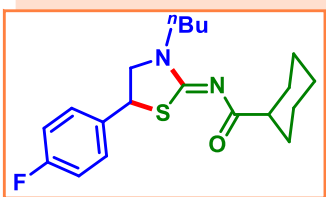
***N*-(3-Butyl-5-(*p*-tolyl)thiazolidin-2-ylidene)cyclohexanecarboxamide (2k)**

Colorless gummy (134 mg, 74%). ^1H NMR (400 MHz, CDCl_3): δ (ppm) 0.96 (t, 3H, $J = 7.2$ Hz), 1.28 (m, 7H), 1.61 (m, 3H), 1.76 (m, 2H), 1.96 (d, 2H, $J = 12.6$), 2.33 (s, 3H), 2.38 (m, 1H), 3.60 (dd, 1H, $J = 8.4, 2.8$ Hz), 3.67 (td, 2H, $J = 7.2$ Hz), 3.88 (dd, 1H, $J = 8.0, 1.2$ Hz), 4.62 (t, 1H, $J = 8.0$ Hz), 7.14 (d, 2H, $J = 8.0$ Hz), 7.25 (d, 2H, $J = 8.0$ Hz); $^{13}\text{C}\{^1\text{H}\}$ NMR (100 MHz, CDCl_3): δ (ppm) 14.0, 20.2, 21.3, 26.1, 26.2, 29.4, 29.8, 29.9, 46.7, 47.3, 48.2, 57.2, 127.6, 129.8, 136.3, 138.1, 170.1, 188.0; IR (KBr): 2929, 2856, 1735, 1634, 1526, 1449, 1165, 1128 cm^{-1} ; HRMS (ESI): calcd. for $\text{C}_{21}\text{H}_{31}\text{N}_2\text{OS}^+$ [$\text{M} + \text{H}^+$] 359.2152; found 359.2150.



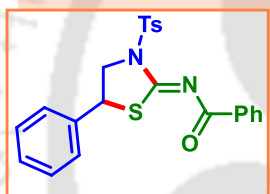
***N*-(3-Butyl-5-(4-fluorophenyl)thiazolidin-2-ylidene)cyclohexanecarboxamide (4k)**

Colorless gummy (121 mg, 67%). ^1H NMR (400 MHz, CDCl_3): δ (ppm) 0.95 (t, 3H, $J = 7.2$ Hz), 1.29 (m, 7H), 1.61 (m, 3H), 1.76 (m, 2H), 1.95 (m, 2H), 2.37 (m, 1H),



3.56 (dd, 1H, $J = 7.6, 3.6$ Hz), 3.66 (t, 2H, $J = 7.2$ Hz), 3.89 (dd, 1H, $J = 8.4, 2.4$ Hz), 4.61 (t, 1H, $J = 8.0$ Hz), 7.01 (t, 2H, $J = 8.4$ Hz), 7.33 (dd, 2H, $J = 5.6, 3.2$ Hz); $^{13}\text{C}\{^1\text{H}\}$ NMR (100 MHz, CDCl_3): δ (ppm) 13.9, 20.1, 26.07, 26.11, 26.3, 29.3, 29.7, 29.8, 46.1, 47.3, 48.2, 57.2, 115.9, 116.1, 129.25, 129.33, 135.37, 135.41, 161.3, 163.8, 169.7, 188.0; IR (KBr): 2929, 2856, 1734, 1626, 1535, 1453, 1230, 1163, 1017 cm^{-1} ; HRMS (ESI): calcd. for $\text{C}_{20}\text{H}_{28}\text{FN}_2\text{OS}^+$ [$\text{M} + \text{H}^+$] 363.1901; found 363.1905.

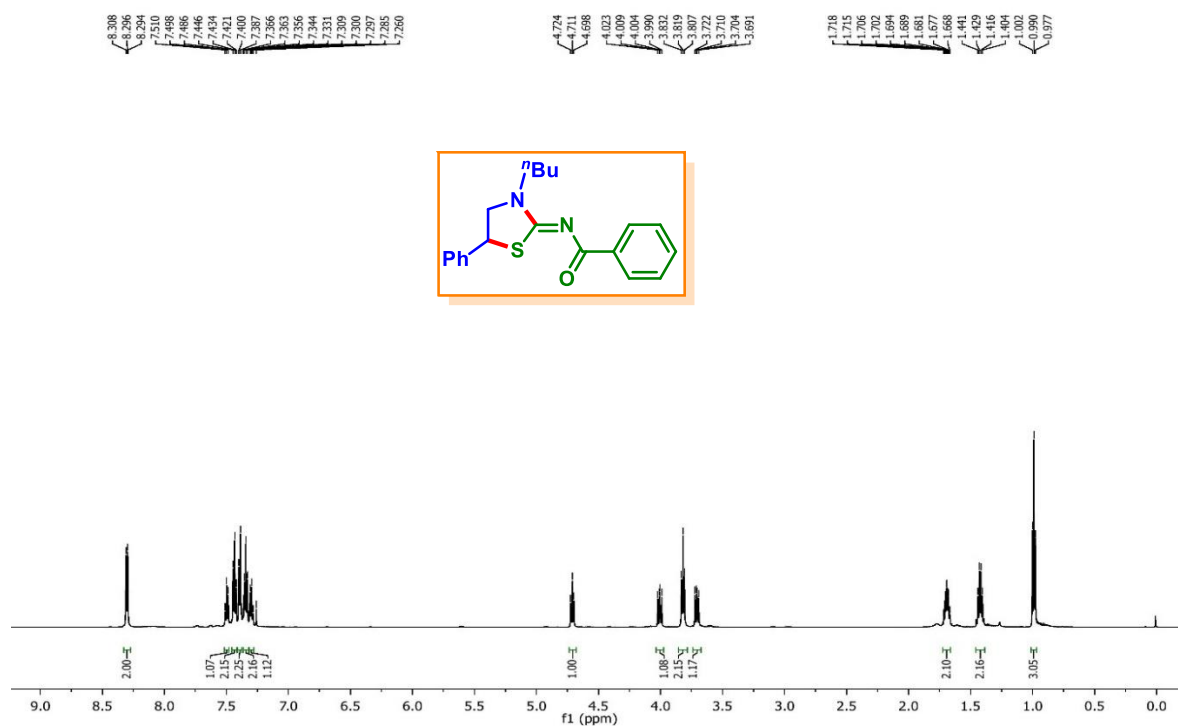
***N*-(5-Phenyl-3-tosylthiazolidin-2-ylidene)benzamide (12a)**



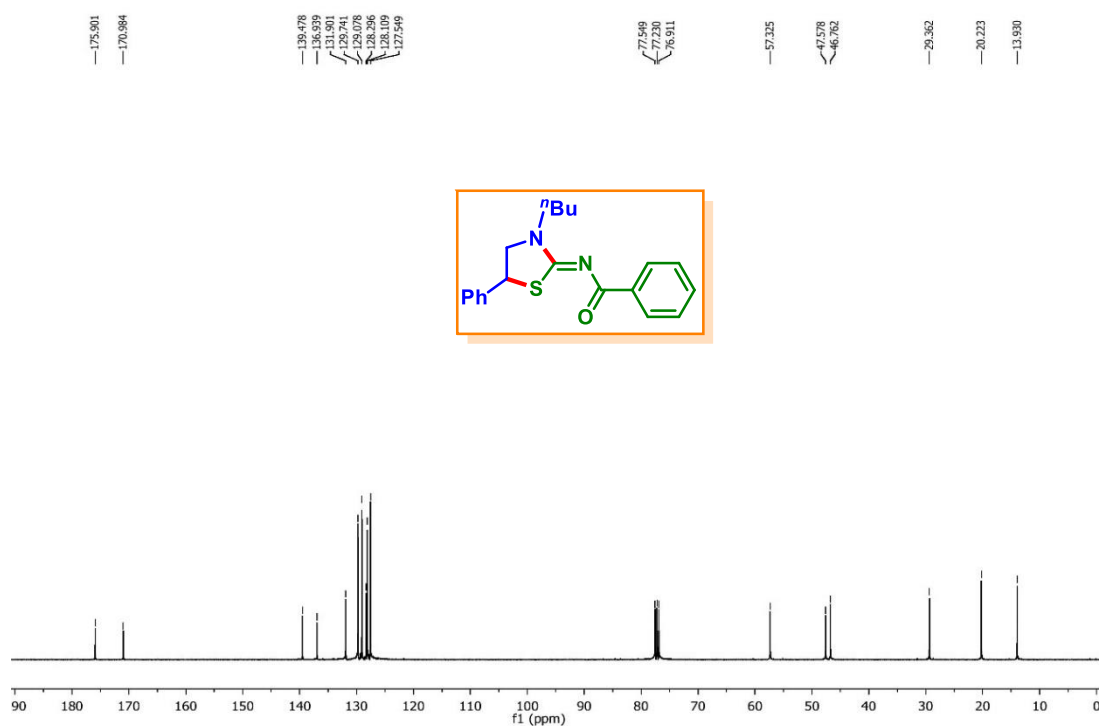
Yellow solid (37 mg, 17%); mp: 115–117 °C. ^1H NMR (400 MHz, CDCl_3): δ (ppm) 2.40 (s, 3H), 4.16 (dd, 1H, $J = 8.8, 2.0$ Hz), 4.65 (dd, 1H, $J = 7.2, 3.2$ Hz), 4.79 (dd, 1H, $J = 7.2, 1.2$ Hz), 7.27 (d, 2H, $J = 8.0$ Hz), 7.37 (m, 5H), 7.49 (m, 3H), 7.97 (dd, 2H, $J = 6.8, 4.8$ Hz), 8.27 (dd, 2H, $J = 8.4, 1.6$ Hz); $^{13}\text{C}\{^1\text{H}\}$ NMR (150 MHz, CDCl_3): δ (ppm) 21.9, 46.8, 55.8, 127.8, 128.7, 128.8, 129.0, 129.4, 129.8, 130.5, 133.3, 134.7, 135.3, 136.8, 145.8, 168.0, 176.0; IR (KBr): 2923, 2854, 1640, 1561, 1451, 1170, 1087 cm^{-1} ; HRMS (ESI): calcd. for $\text{C}_{23}\text{H}_{21}\text{N}_2\text{O}_3\text{S}_2^+$ [$\text{M} + \text{H}^+$] 437.0988; found 437.0990.

II.7. Representative Spectra

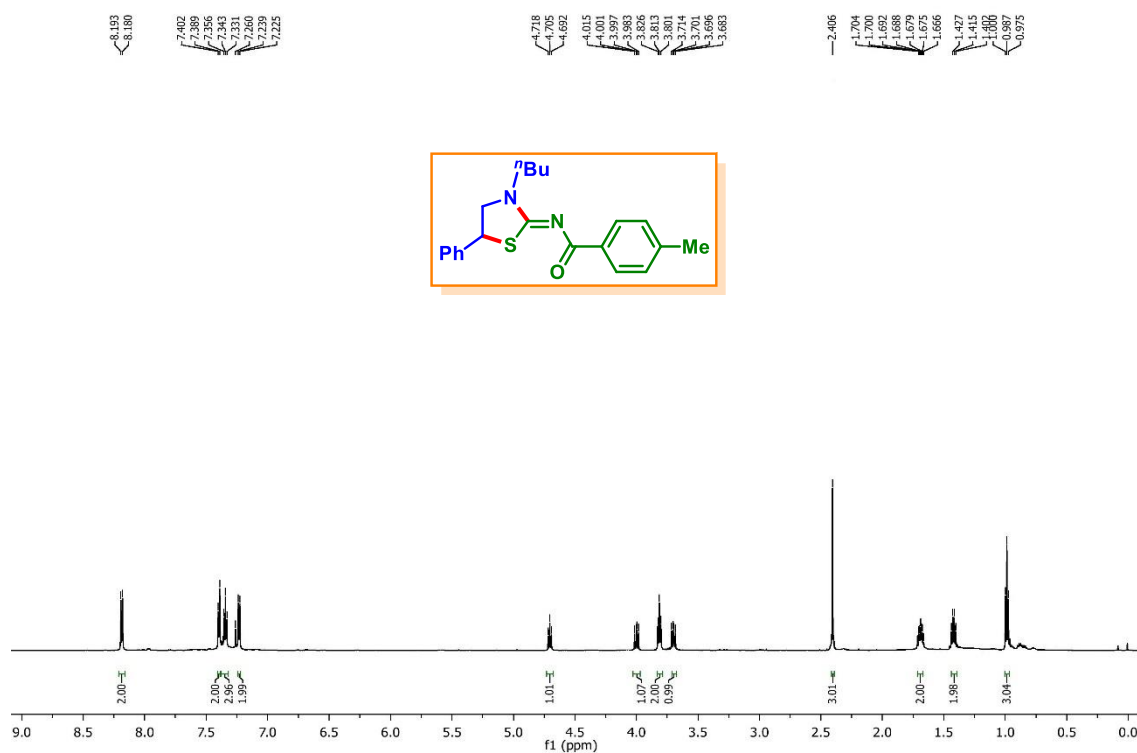
N-(3-Butyl-5-phenylthiazolidin-2-ylidene)benzamide (1a): ^1H NMR (600 MHz, CDCl_3)



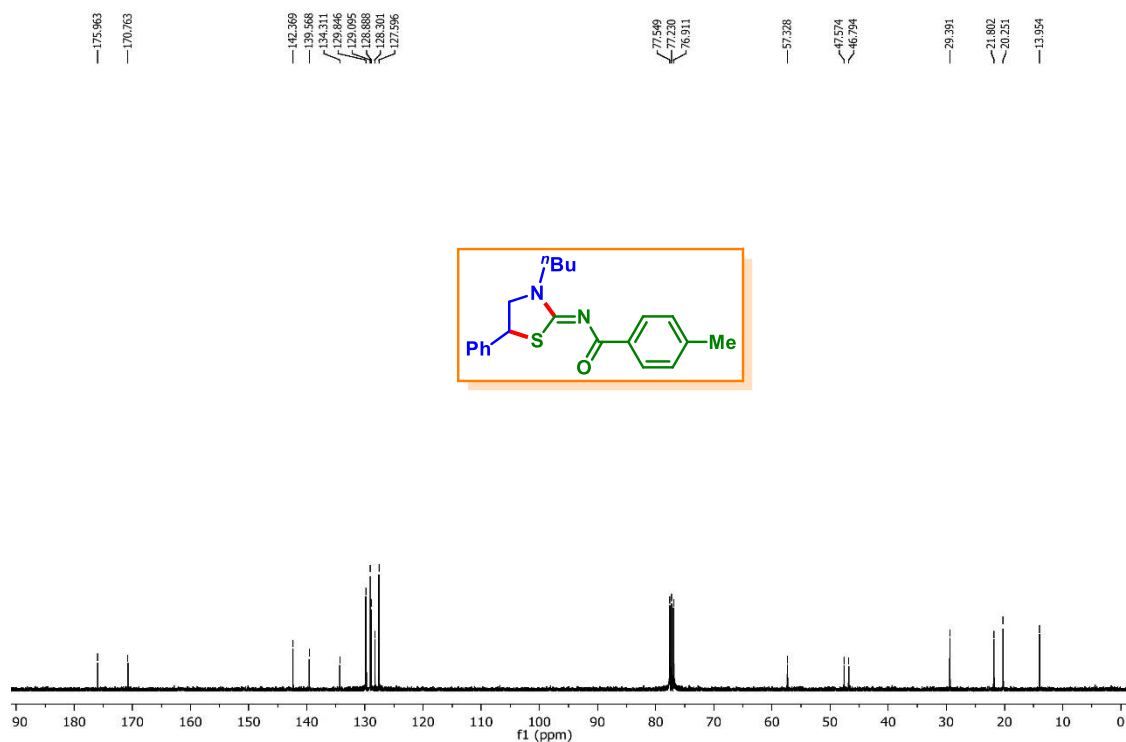
N-(3-Butyl-5-phenylthiazolidin-2-ylidene)benzamide (1a): $^{13}\text{C}\{^1\text{H}\}$ NMR (100 MHz, CDCl_3)



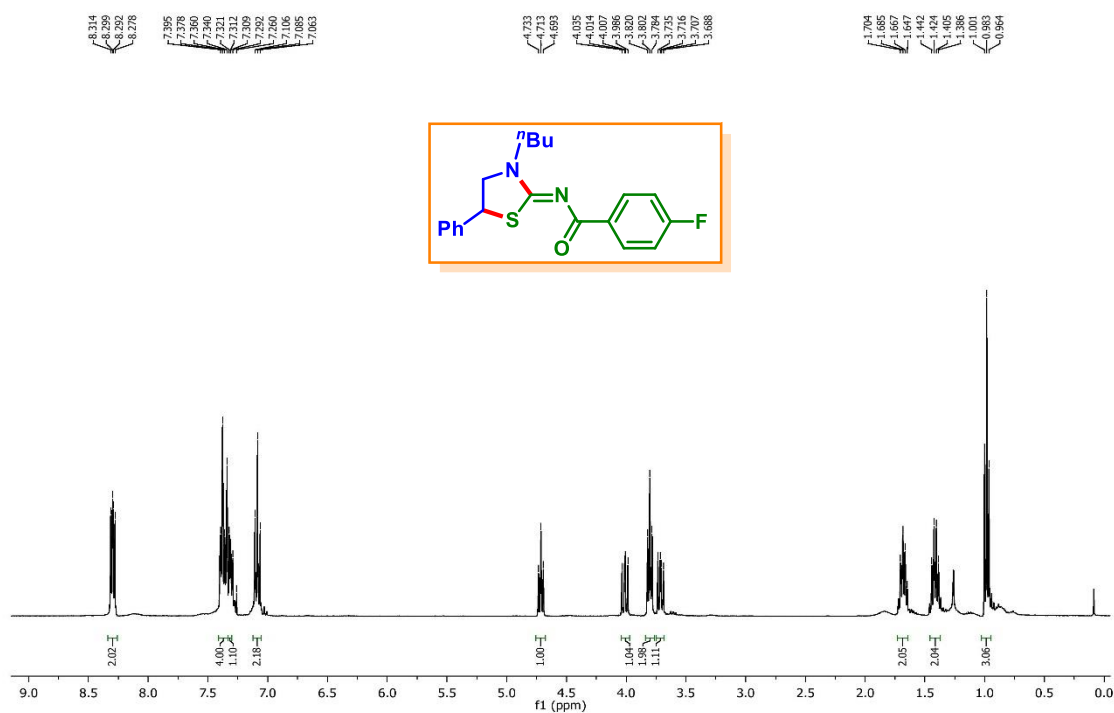
***N*-(3-Butyl-5-phenylthiazolidin-2-ylidene)-4-methylbenzamide (1b):** ^1H NMR (600 MHz, CDCl_3)



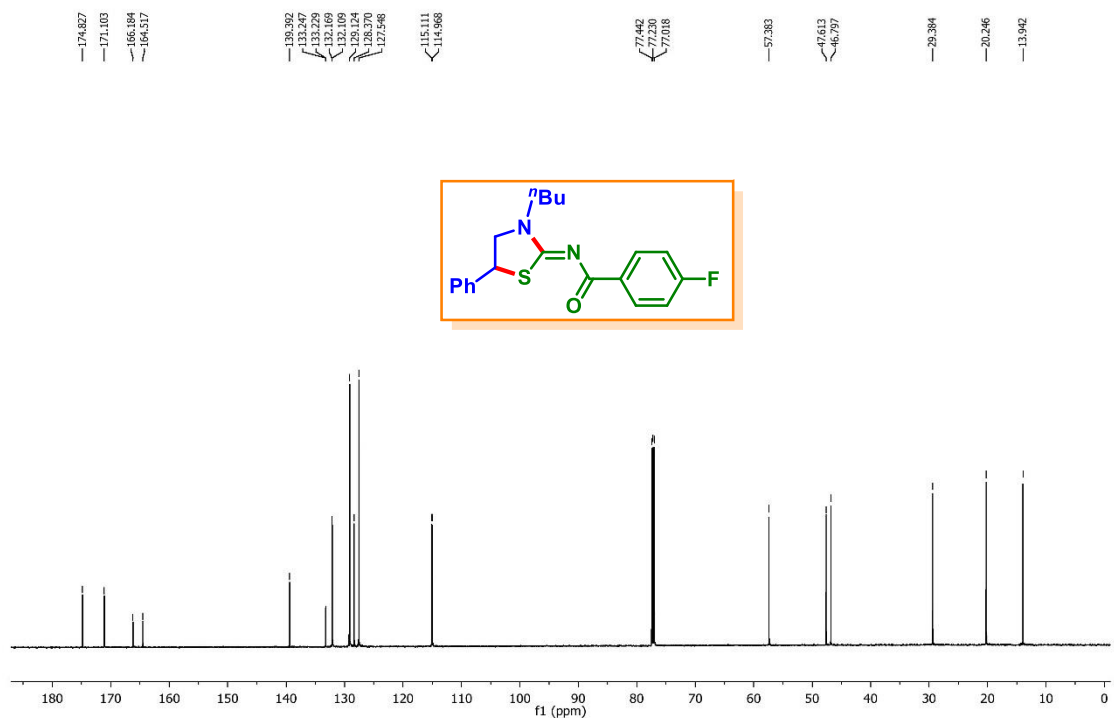
***N*-(3-Butyl-5-phenylthiazolidin-2-ylidene)-4-methylbenzamide (1b):** $^{13}\text{C}\{^1\text{H}\}$ NMR (100 MHz, CDCl_3)



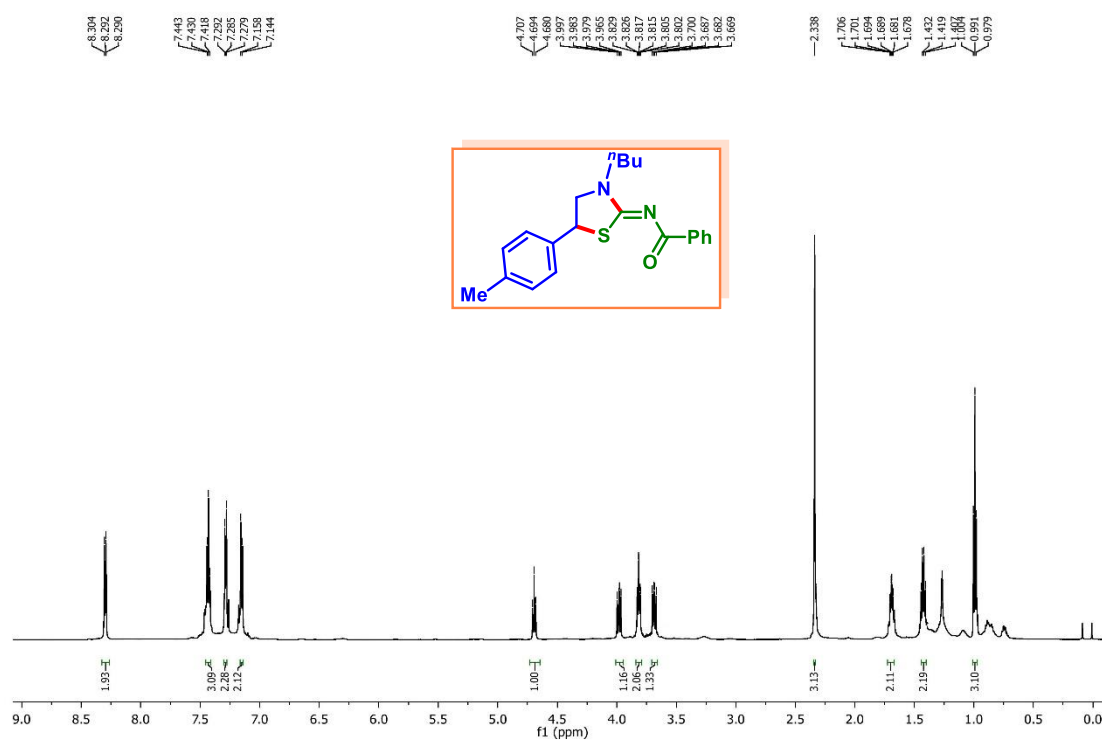
***N*-(3-Butyl-5-phenylthiazolidin-2-ylidene)-4-fluorobenzamide (1f):** ^1H NMR (400 MHz, CDCl_3)



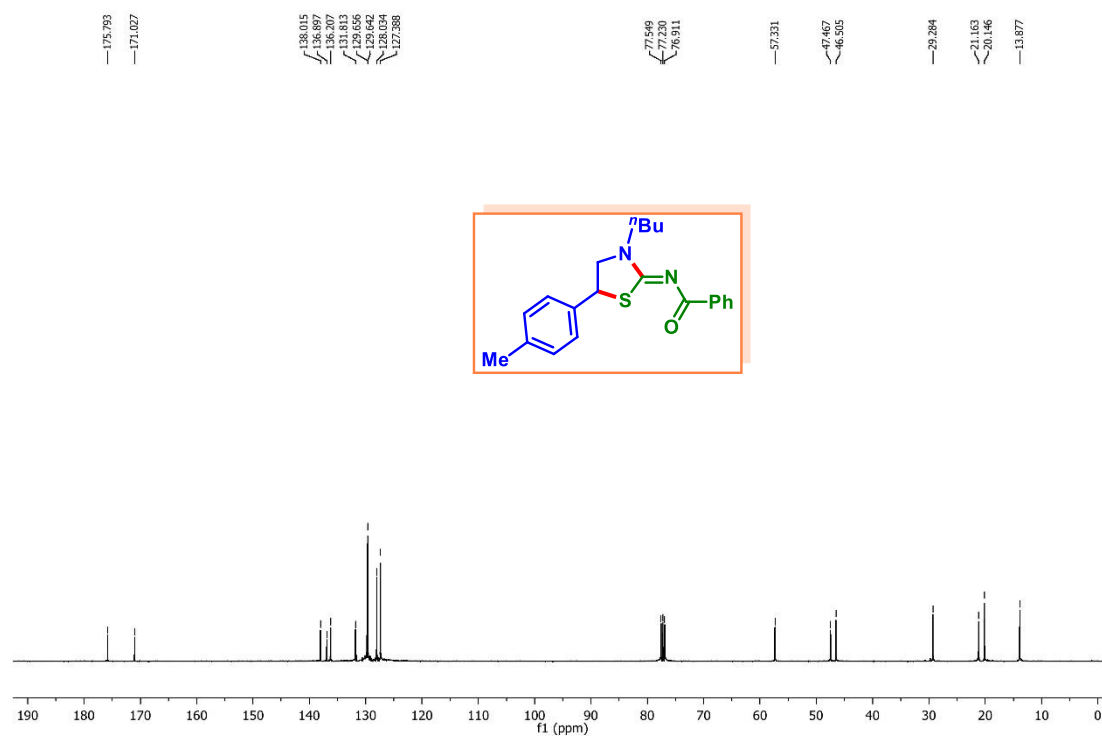
***N*-(3-Butyl-5-phenylthiazolidin-2-ylidene)-4-fluorobenzamide (1f):** $^{13}\text{C}\{^1\text{H}\}$ NMR (150 MHz, CDCl_3)



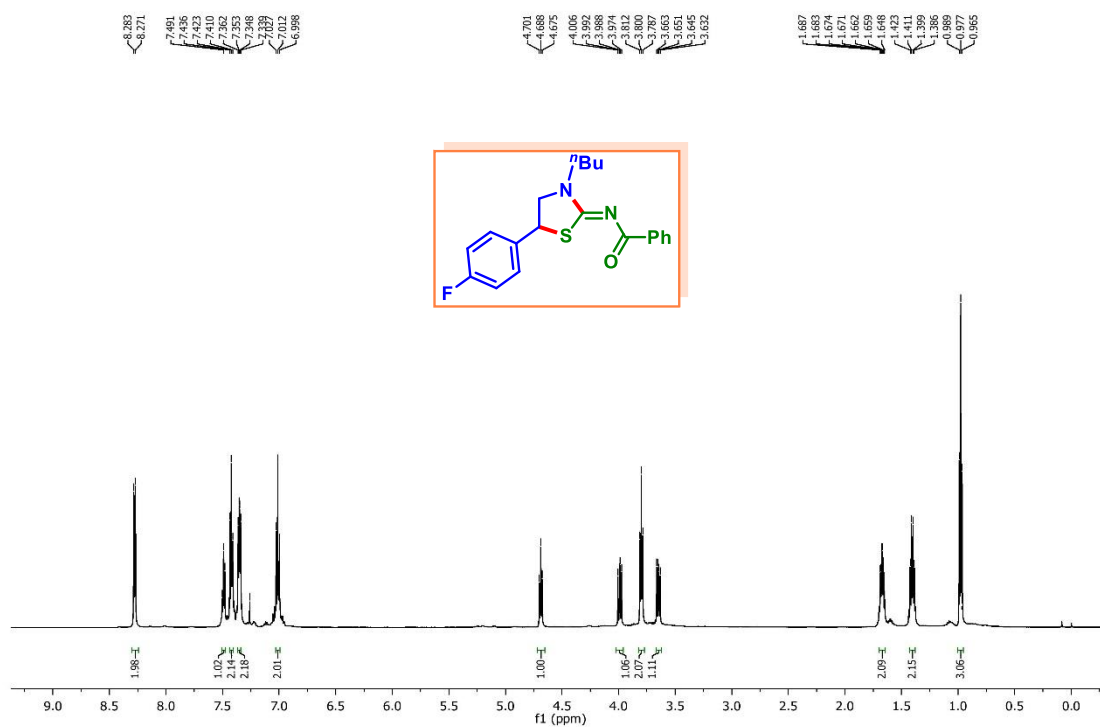
***N*-(3-Butyl-5-(*p*-tolyl)thiazolidin-2-ylidene)benzamide (2a):** ^1H NMR (600 MHz, CDCl_3)



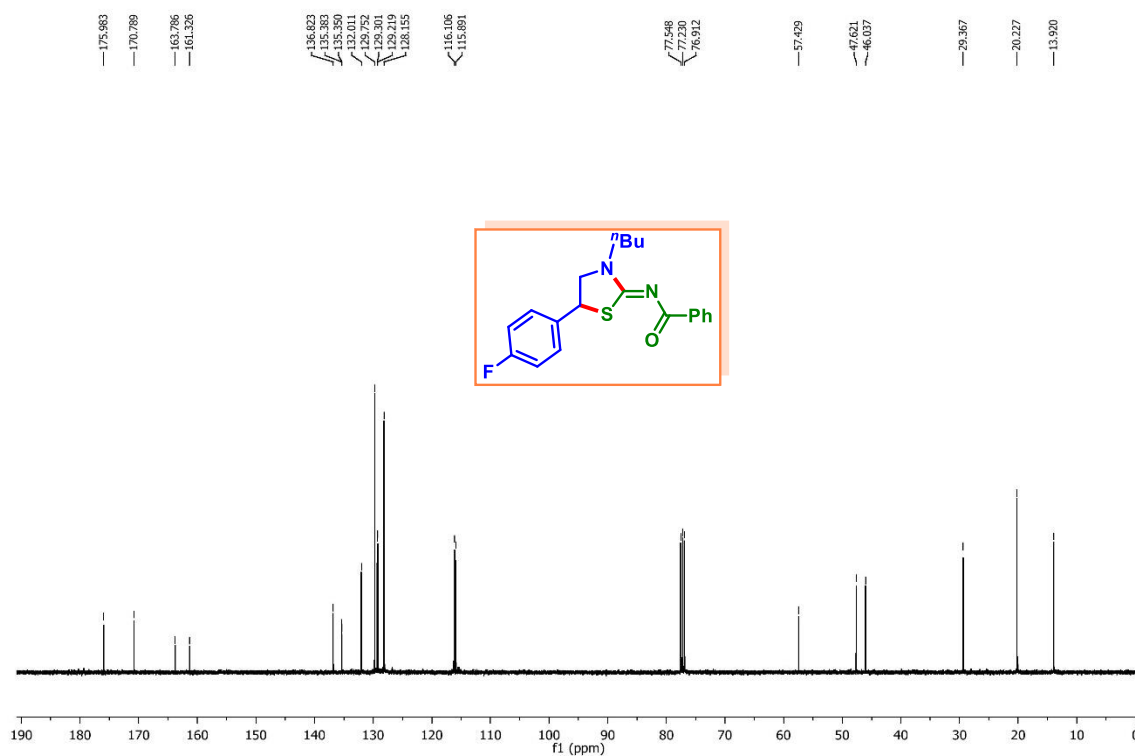
***N*-(3-Butyl-5-(*p*-tolyl)thiazolidin-2-ylidene)benzamide (2a):** $^{13}\text{C}\{^1\text{H}\}$ NMR (100 MHz, CDCl_3)



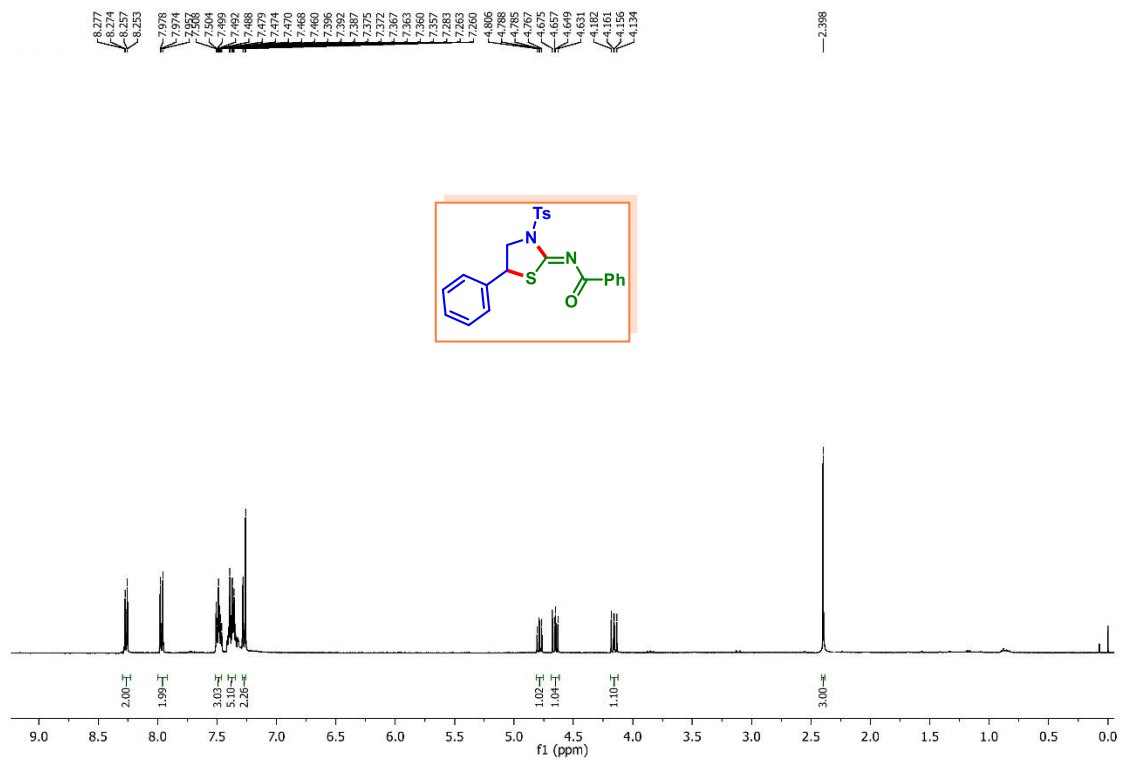
***N*-(3-Butyl-5-(4-fluorophenyl)thiazolidin-2-ylidene)benzamide (4a):** ^1H NMR (600 MHz, CDCl_3)



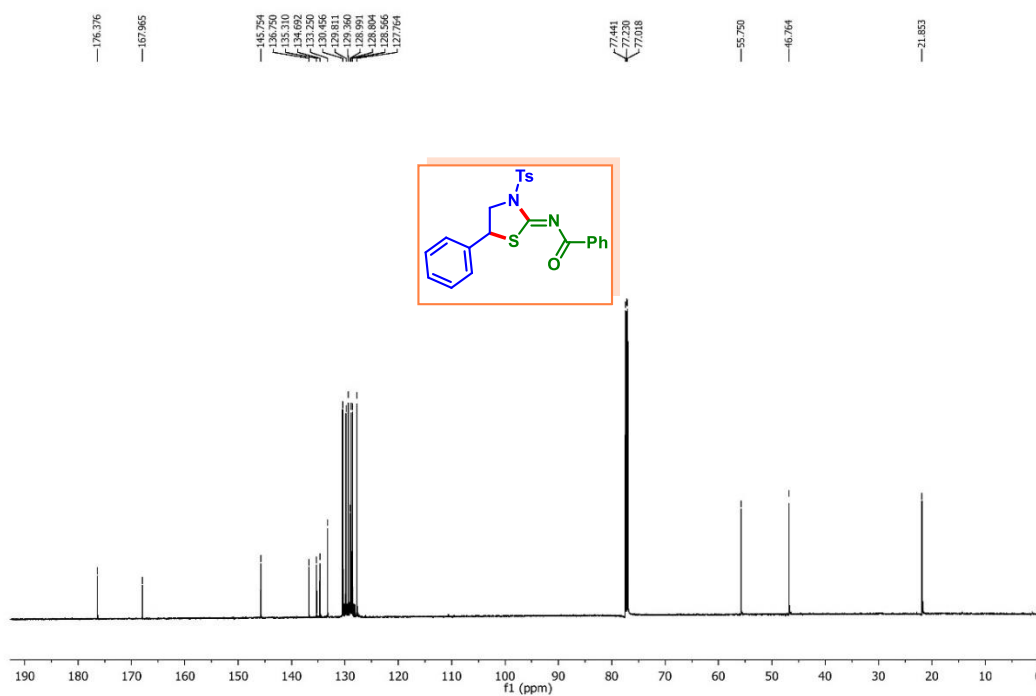
***N*-(3-Butyl-5-(4-fluorophenyl)thiazolidin-2-ylidene)benzamide (4a):** $^{13}\text{C}\{^1\text{H}\}$ NMR (100 MHz, CDCl_3)



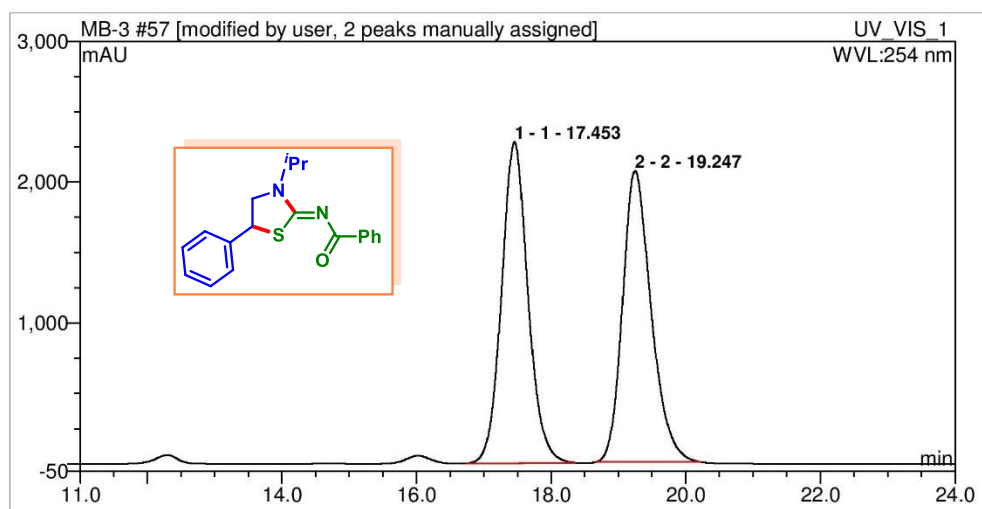
***N*-(5-Phenyl-3-tosylthiazolidin-2-ylidene)benzamide (12a):** ^1H NMR (400 MHz, CDCl_3)



***N*-(5-Phenyl-3-tosylthiazolidin-2-ylidene)benzamide (12a):** $^{13}\text{C}\{^1\text{H}\}$ NMR (150 MHz, CDCl_3)

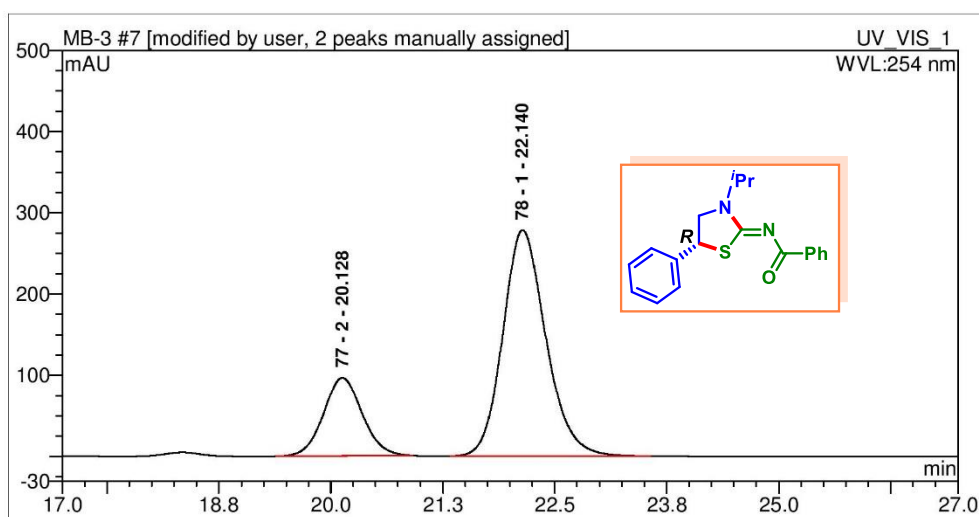


II.7.1. HPLC Chromatogram of the Products



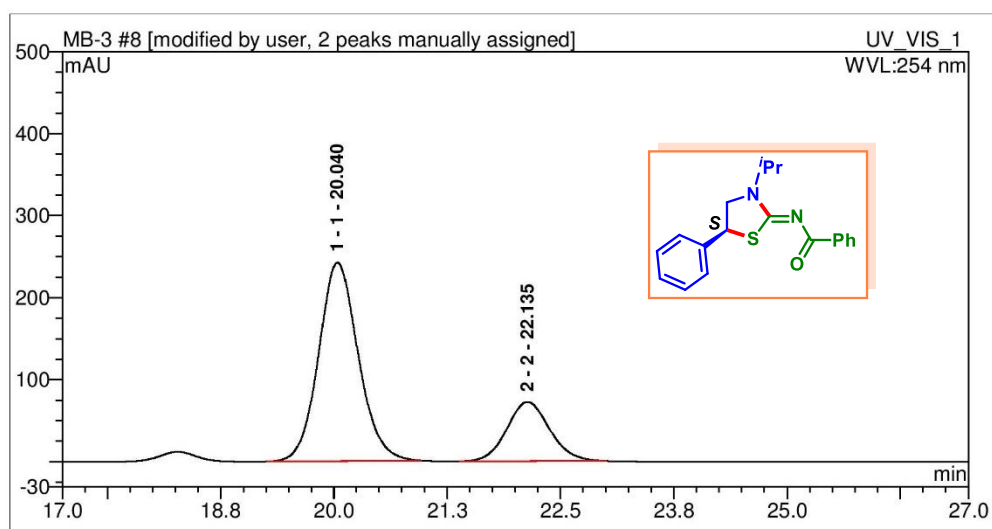
No.	Peak Name	Ret.Time (detected) min	Area mAU*min	Rel.Area(ident.) %	Height mAU	Amount
1	1	17.45	1035.896	50.36516843	2278.187	n.a.
2	2	19.25	1020.875	49.63483157	2066.156	n.a.

HPLC analysis: Chiralpak IA Column, *n*-hexane/*i*-PrOH = 92/8, flow rate 1.0 mL/min, λ = 254 nm



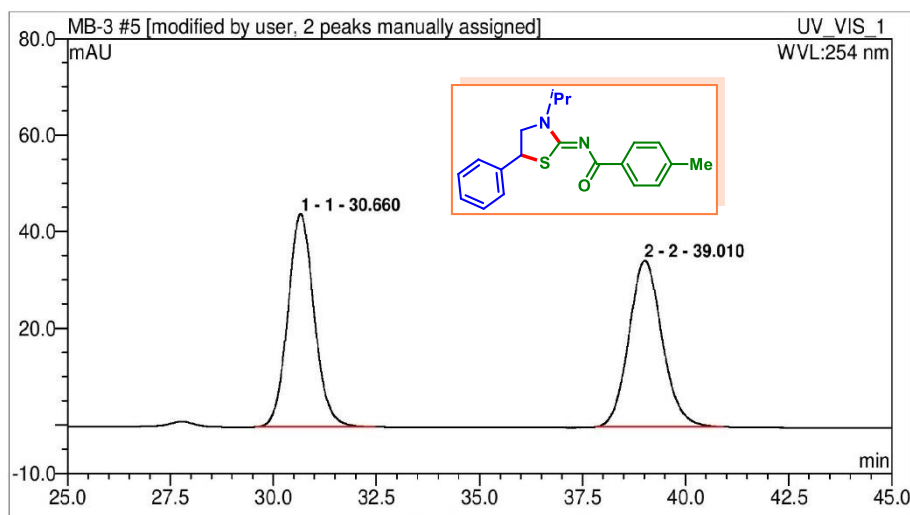
No.	Peak Name	Ret.Time (detected) min	Area mAU*min	Rel.Area(ident.) %	Height mAU	Amount
77	2	20.13	48.36232	23.77931845	96.01792	n.a.
78	1	22.14	155.017	76.2205629	278.057	n.a.

HPLC analysis: ee = 52%, Chiralpak IA Column, *n*-hexane/*i*-PrOH = 92/8, flow rate 1.0 mL/min, λ = 254 nm (t_{major} = 22.14 min, t_{minor} = 20.13 min).



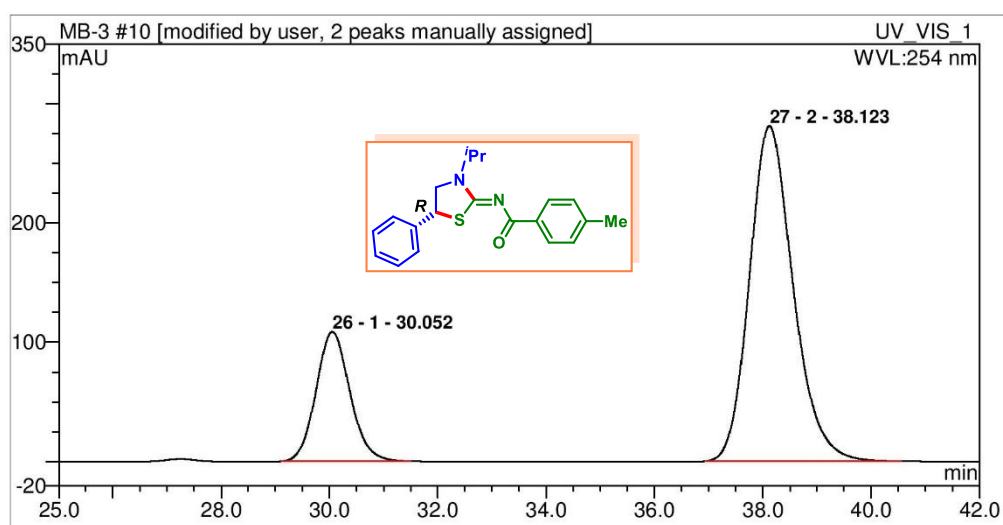
No.	Peak Name	Ret.Time (detected) min	Area mAU*min	Rel.Area(ident.) %	Height mAU	Amount
1	1	20.04	122.8046	75.64384711	242.0144	n.a.
2	2	22.14	39.541	24.35615289	72.242	n.a.

HPLC analysis: ee = 51%, Chiralpak IA Column, *n*-hexane/*i*-PrOH = 92/8, flow rate 1.0 mL/min, λ = 254 nm (t_{major} = 20.04 min, t_{minor} = 22.14 min).



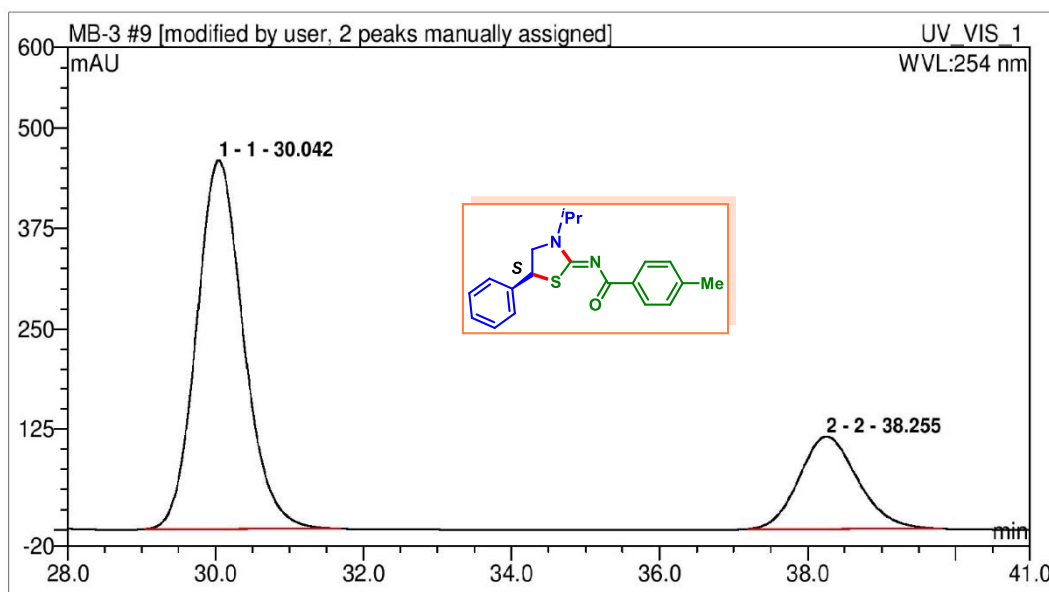
No.	Peak Name	Ret.Time (detected) min	Area mAU*min	Rel.Area(ident.) %	Height mAU	Amount
1	1	30.66	32.66863	50.36630267	44.031	n.a.
2	2	39.01	32.193	49.63369733	34.349	n.a.

HPLC analysis: Chiralpak IA Column, *n*-hexane/*i*-PrOH = 92/8, flow rate 1.0 mL/min, λ = 254 nm



No.	Peak Name	Ret.Time (detected) min	Area mAU*min	Rel.Area(ident.) %	Height mAU	Amount
26	1	30.05	78.73413	23.07012848	108.3308	n.a.
27	2	38.12	262.548	76.92987152	280.769	n.a.

HPLC analysis: ee = 54%, Chiralpak IA Column, *n*-hexane/*i*-PrOH = 92/8, flow rate 1.0 mL/min, λ = 254 nm (t_{major} = 38.12 min, t_{minor} = 30.05 min).



No.	Peak Name	Ret.Time (detected) min	Area mAU*min	Rel.Area(ident.) %	Height mAU	Amount
1	1	30.04	336.8516	76.19016306	459.0593	n.a.
2	2	38.26	105.268	23.80983694	114.868	n.a.

HPLC analysis: ee = 52%, Chiralpak IA Column, *n*-hexane/*i*-PrOH = 92/8, flow rate 1.0 mL/min, λ = 254 nm (t_{major} = 30.04 min, t_{minor} = 38.26 min).



CHAPTER III

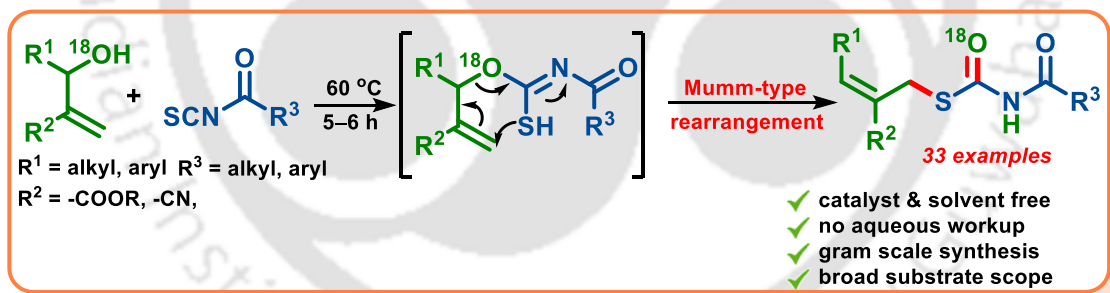
Volume 16 | Number 42 | 14 November 2018 | Pages 7763–7986

Organic & Biomolecular Chemistry

rsc.li/obc



Catalyst and Solvent Free Domino Ring Opening Cyclization: A Greener and Atom Economic Route to 2-Iminothiazolidines



Abstract: A catalyst and solvent free synthesis of *S*-allyl benzoylcarbamothioates has been achieved from the in situ generated benzoylcarbonimidothioates obtained by reacting MBH alcohols with aroyl isothiocyanates. An intramolecular thia-Michael addition of the in situ generated adduct triggers a Mumm-type rearrangement leading to a stereoselective synthesis of highly functionalised *S*-allyl benzoylcarbamothioates.



CHAPTER III

III. A Cascade Synthesis of *S*-allyl Benzoylcarbamothioates via Mumm-type Rearrangement

III.1. Introduction

The progress of cascade synthetic methods, where structural divergence is selectively congregated at the molecular level from multifunctional small molecules in one pot, has been established as one of the key epitomes of modern organic chemistry. Toward this endeavor, cascade processes have found wide applications because they successfully implement the goal and principle of sustainability.¹

Among the sulfur-based compounds, *S*-aryl carbamothioates (*S*-alkyl thiourethanes) are the crucial unit that is widespread in many biologically active molecules such as herbicides, thiobencarb and orbencarb (Figure III.1.1).² A considerably large number of methodologies have been developed to construct the *S*-aryl thiocarbamate core structure and the emphasis of research has been on the reactions of amines with thiols and phosgene or with carbonyl sulfide,³ the reactions of dialkylamines with carbon monoxide and sulfur,⁴ and metal-catalyzed thiolation of acyl compounds.⁵

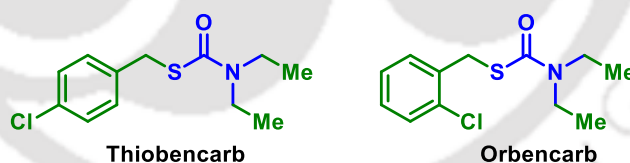
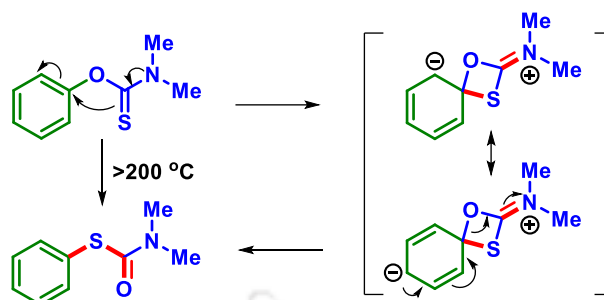


Figure III.1.1. Representative examples of bioactive *S*-aryl carbamothioates.

The quintessential strategy for their synthesis is **Newman–Kwart rearrangement** (NKR) which involves thermal rearrangement ($O_{Ar} \rightarrow S_{Ar}$) of aromatic thiocarbamates. The generally accepted mechanism for the NKR involves nucleophilic attack of the *S*-atom of the thiocarbamate moiety to the *ipso*-position of the aromatic ring, resulting in a four-membered ring transition state. However, the rearrangement proceeds at very high temperatures (>200 °C), making it unpractical for substrates containing thermally sensitive functional groups (Scheme III.1.1).⁶ Thus, constant efforts were given towards the

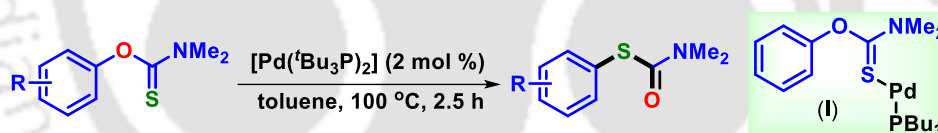
modifications of NKR reaction. The following section describes the synthesis of *S*-aryl carbamothioates.



Scheme III.1.1. The Newmann-Kwart rearrangement.

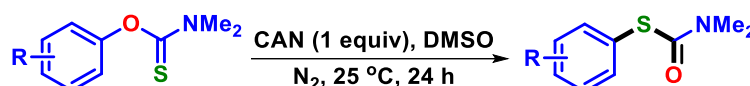
III.2. Ideas Toward the Synthesis of *S*-Aryl Carbamothioates

Lloyd-Jones and co-workers reported a $[\text{Pd}(\text{tBu}_3\text{P})_2]$ catalyzed Newmann-Kwart rearrangement of *S*-aryl carbamothioates at 100 °C. Substrates having electron-withdrawing groups show better reactivity than electron-donating substituents. Mechanistic studies and theoretical calculations suggest that a *S*-coordinated monophosphine–palladium complex (I), initiates the oxidative addition followed by tautomerization and reductive elimination sequence (Scheme III.2.1).⁷



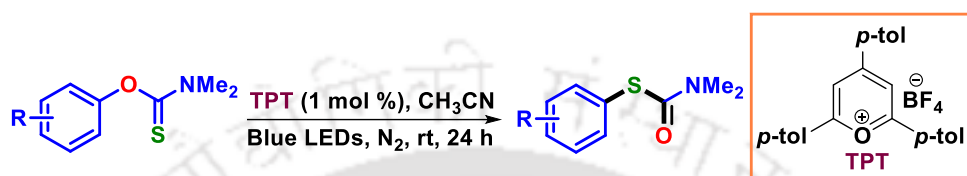
Scheme III.2.1. Pd(II) catalyzed synthesis of *S*-aryl carbamothioates.

In 2018, Pittelkow *et al.* reported a ceric ammonium nitrate (CAN) mediated Newman-Kwart rearrangement of *O*-thiocarbamate. Substrates having electron-donating substituents gave clean conversion and almost quantitative yield. Computational studies support an intramolecular SET mechanism and formation of thiyl radical cation (Scheme III.2.2).⁸



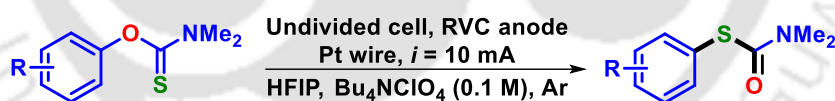
Scheme III.2.2. CAN-mediated synthesis of *S*-aryl carbamothioates.

Nicewicz *et al.* disclosed a photoredox-mediated Newman-Kwart rearrangement using 2,4,6-tri(*p*-tolyl)pyrylium tetrafluoroborate (TPT) as a catalyst. Unlike the thermal NKR route, this process takes place at ambient temperature and is more compatible with electron-rich substituents. Cyclic voltammetry studies show that oxidation of the thiocarbonyl moiety to thiyl radical cation is likely involved in the rearrangement (Scheme III.2.3).⁹



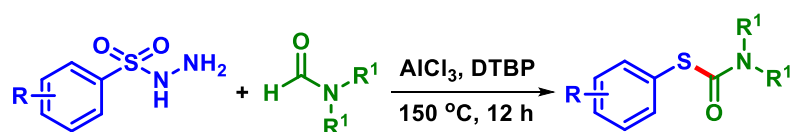
Scheme III.2.3. Photoredox-mediated NKR reaction.

An electrochemical method for the rearrangement of *O*-aryl thiocarbamates to the equivalent *S*-aryl thiocarbamates is illustrated by the Francke group. The salient features of this mild approach are ambient temperature, requires only catalytic amounts of both electric charge and metal, and additive free. When the reaction was performed in a flow reactor instead of a batch process, a quantitative yield was obtained without any supporting electrolyte. Compared to the thermal NKR approach, this methodology favors electron-rich substituents (Scheme III.2.4).¹⁰



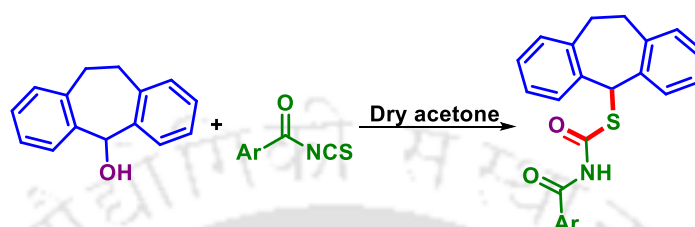
Scheme III.2.4. Electrochemical approach for NKR reaction.

In 2015, Mao and Zhang's group demonstrated an AlCl_3 -promoted thiolation of formamide C–H bonds with arylsulfonyl hydrazides as thiol surrogates. In this strategy, di-*tert*-butyl peroxide (DTBP) is used as an oxidant (Scheme III.2.5).^{5b}



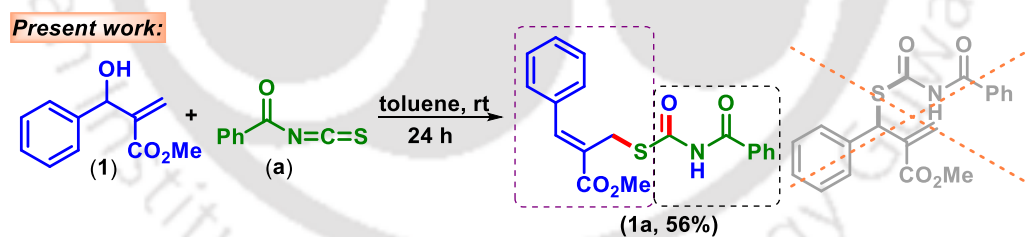
Scheme III.2.5. AlCl_3 -promoted thiolation of formamides.

Căproiu and Dumitrascu *et al.* disclosed an unexpected *S*-thiocarbamate synthesis via a benzylic Newman-Kwart rearrangement using 5-dibenzosuberol and aroyl isothiocyanates. The structures of these new derivatives were confirmed by elemental analysis, spectroscopic methods (IR, ^1H NMR, $^{13}\text{C}\{^1\text{H}\}$ NMR), and X-ray crystallography (Scheme III.2.6).¹¹



Scheme III.2.6. Synthesis of *S*-thiocarbamate.

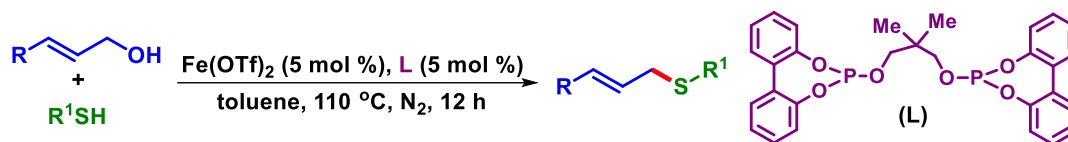
Taking cues from the reactivity of aroyl isothiocyanate, we articulated that this could be the precursor to afford *S*-thiocarbamates upon reaction with Morita-Baylis-Hillman (MBH) alcohol. Thus, a reaction was carried out between methyl 2-(hydroxy(phenyl)methyl) acrylate (**1**) and benzoyl isothiocyanate (**a**) in toluene (2 mL) at room temperature. Instead of a *S*-thiocarbamate, a new allyl thioether (**1a**) containing two important moieties *viz.* imide and 2-methylthioacrylate, was isolated in 56% yield possibly via a Mumm type of rearrangement (Scheme III.2.7).



Scheme III.2.7. Synthesis of *S*-allyl benzoylcarbamothioates.

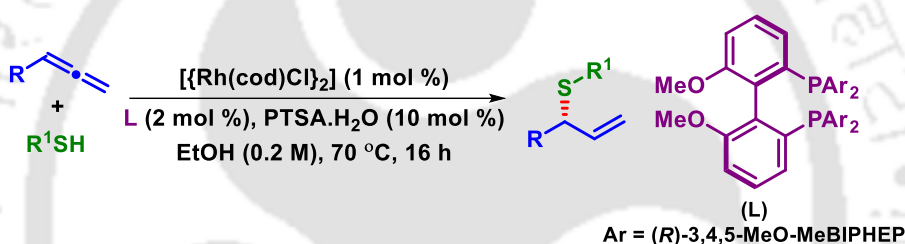
Despite the remarkable progress made to date, the construction of allylic thioethers via metal-free C–S bond forming reactions is still lacking. Several strategies, including transition metal-catalyzed substitution reaction, thiocarbonylation, insertion reaction, and transition metal-catalyzed or organocatalyzed Michael additions, have been well recognized over the years to construct C–S bonds.¹² Below are some of the examples for the synthesis of *S*-allyl thioethers.

Zhang's group reported a Fe(II) catalyzed cross-coupling reaction of allylic alcohols and thiols using a diphosphite ligand (**L**). A variety of thiols and alcohols were compatible with this strategy yielding their corresponding product in high yield and selectivity (Scheme III.2.8).¹³



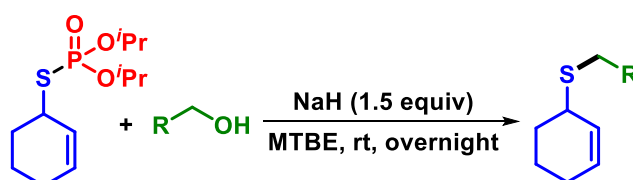
Scheme III.2.8. Fe(II)-catalyzed synthesis of S-allyl thioethers.

In 2015, Breit group reported an atom-economic, Rh(I) catalyzed highly regio- and enantioselective hydrothiolation of terminal allenes. Upon further oxidation with *m*-CPBA, a variety of allylic sulfones were prepared in enantiomerically pure form (Scheme III.2.9).¹⁴



Scheme III.2.9. Asymmetric hydrothiolation with terminal allenes.

In 2010, Wu *et al.* disclosed a base-mediated synthesis of allylic thioethers by reacting phosphorothioate esters and alcohols in methyl *tert*-butyl ether (MTBE) as a solvent. This one-step reaction proceeds via the addition of an exogenous alkoxide to the corresponding allylic phosphorothioate ester. This stereospecific process delivers the enantioenriched thioethers in good yields and avoids the use of malodorous sulfur compounds such as thioacetic acid or thiols (Scheme III.2.10).¹⁵



Scheme III.2.10. Base-mediated synthesis of S-allyl thioethers.

Imides are significant structural motifs found in various natural products and pharmaceutical agents.^{16a,b} Figure III.2.1 shows selected examples of biological active imide moiety *viz.*, Diacetazolol (Dermagan),^{16c} tetraacetythylenediamine (TAED)^{16d} and the anxiolytic drug Aniracetam (Ampamet).^{16c} Such imides motif also appears in certain natural products such as fumaramidmycin,^{16e,f} coniothyriomycin^{16g}, and unnatural compound SB-253514.^{16h} They also appear as precursors in a variety of reactions, such as condensation, alkylation, acylation, and cycloaddition.¹⁷

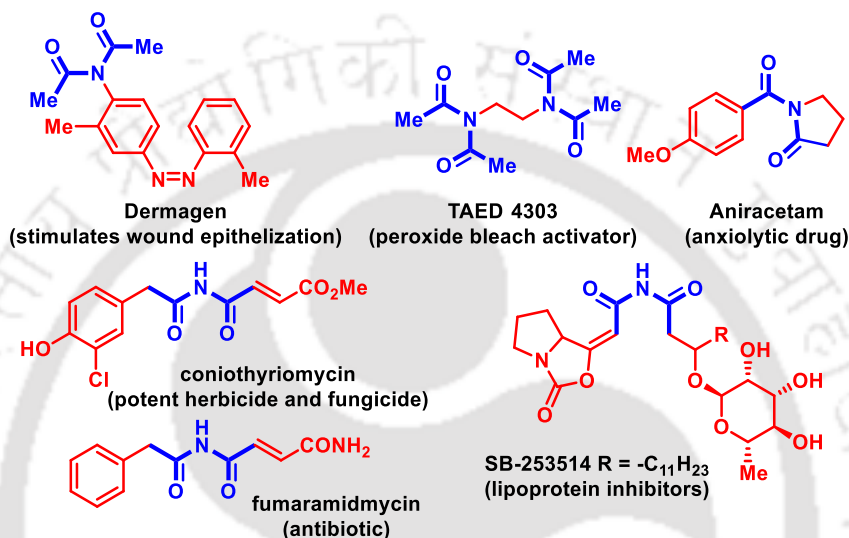
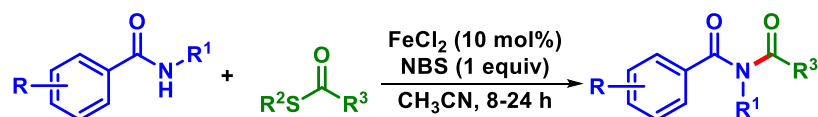


Figure III.2.1. Examples of biologically active imides.

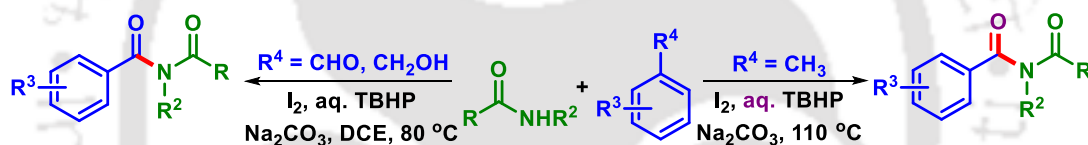
The classical methodology for the synthesis of imides relies on the condensation of amides with carboxylic acids and their derivatives. *N*-Acylation of amides using aldehydes as the acyl source is one of the important synthetic tools in the construction of imides. There are limited precedents for the synthesis of imides based on metal-catalyzed cross-coupling strategies such as, (i) Rh(II)-catalyzed sulfamidation of aldehydes,^{18a-c} (ii) Fe/Cu catalyzed coupling of aldehydes and thioesters with carboxamides,^{18d-g} (iii) oxidation of *N*-alkylbenzamides,^{18h-j} and (iv) ceric ammonium nitrate (CAN)-promoted oxidation of 4,5-diphenyloxazoles.^{18k} Though the above-mentioned protocols describe elegant methods for the construction of imide motifs but the limitation is, that it is applicable for the derivatization of sulfonamides or carboxamides only.¹⁹ Despite several procedures available for their synthesis, the use of designer substrates, poor yields, cumbersome multi-stepped processes, and inadequate product diversity are some of the limitations. Below are some of the examples for the synthesis of imides.

Fu and Jiang's group reported an efficient Fe(II) chloride/*N*-bromosuccinimide (NBS)-mediated synthesis of imides and acylsulfonamides using thioesters and carboxamides/sulfonamide as coupling partners. This process requires no additional ligands or additives (Scheme III.2.11).²⁰



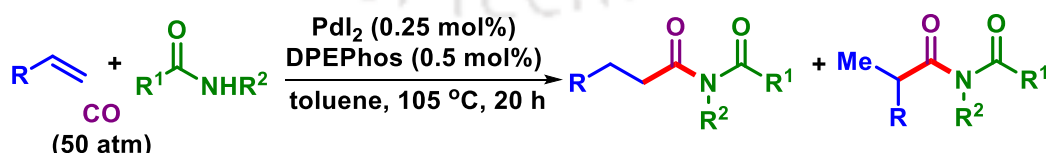
Scheme III.2.11. *FeCl₂/NBS-mediated couplings of carboxamides with thioesters.*

Singh's group disclosed a TBHP-mediated direct coupling of NH-amides with methylarenes using iodine as a catalyst. This method also works with benzyl alcohols and benzaldehydes which yields the corresponding imides in good to moderate yields. Mechanistic investigation suggests a radical pathway. Further, the ¹⁸O-labeled experiment confirmed water to be the source of *O*-atom in imides (Scheme III.2.12).²¹



Scheme III.2.12. *TBHP-mediated synthesis of imides.*

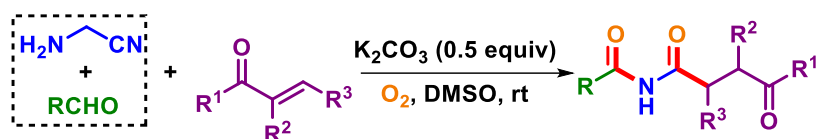
A Pd(II) catalyzed synthesis of imides using olefins, NH-amides, and carbon monoxide has been reported by Beller *et al.* via hydroamidocarbonylation. The imides were synthesized in good yield and good regioselectivity. The synthetic potential of this methodology was demonstrated by synthesizing the anxiolytic drug Aniracetam (Scheme III.2.13).²²



Scheme III.2.13. *Pd(II)-catalyzed synthesis of imides.*

In 2014, Pan and Liu's group described a base promoted synthesis of imides by reacting α -(alkylideneamino)nitriles with molecular oxygen. A wide variety of imides were

synthesized in good to moderate yield with a wide range of functional group tolerance (Scheme III.2.14).²³



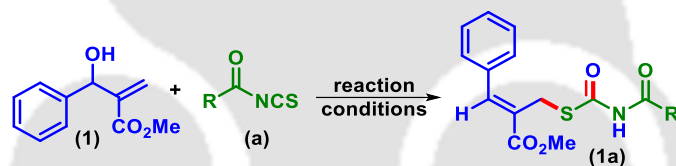
Scheme III.2.14. Base promoted synthesis of imides.

III.3. Present Work

Optimizations of Reaction Conditions:

In pursuit to accomplish an appropriate reaction condition for this unparalleled transformation, other reaction parameters such as solvents and temperature were screened using methyl 2-(hydroxy(phenyl)methyl) acrylate (**1**) and benzoyl isothiocyanate (**a**) as the reacting partners.

Table III.3.1. Optimization of the reaction conditions^{a,b}



Entry	Solvent	Temp. (°C)	Time	Yield ^b (%)
1	Toluene	rt	24 h	56
2	1,4-Dioxane	rt	24 h	35
3	DCE	rt	24 h	59
4	DCM	rt	24 h	43
5	Chlorobenzene	rt	24 h	60
6	DMF	rt	24 h	39
7	DMSO	rt	24 h	12
8	CH ₃ CN	rt	24 h	9
9	H ₂ O	rt	24 h	64
10	-	rt	24 h	70
11	-	50	9 h	83
12	-	60	5 h	96
13	-	80	5 h	91

^aReaction conditions: (**1**) (0.2 mmol), (**a**) (0.2 mmol), solvent (2 mL), under air.

^bIsolated yield.

Initially, different non-polar solvents such as 1,4-dioxane, DCE, DCM, and chlorobenzene were tested. When the reaction was carried out in 1,4-dioxane instead of toluene (Table III.3.1, entry 2) the yield dropped to 35%, whereas the use of 1,2-

dichloroethane (DCE) (Table III.3.1, entry 3) gave a comparable yield (59%). When the reaction was performed in DCM and chlorobenzene the product was isolated in 43% and 60% yields respectively (Table III.3.1, entry 4 and 5). Further, the use of polar solvents such as DMF (39%), DMSO (12%), and acetonitrile (9%) (Table III.3.1, entries 6-8) was found to be inferior to that of chlorobenzene (Table III.3.1, entry 5). This reaction in water gave a 64% yield of the product (**1a**) (Table III.3.1, entry 9) which, however, was associated with several other side products. In our previous reports, the maximum yield of products was obtained under a solvent-free condition using aroyl isothiocyanates.²⁴ Thus, a reaction under a neat condition was attempted at room temperature. To our delight, an improved yield (70%) of the product (**1a**) was obtained (Table III.3.1, entry 10). Interestingly, performing a neat reaction at elevated temperatures of 50 °C and 60 °C, not only improved the yield but also shortened the reaction time giving 83% and 96% of the product in 9 h and 5 h respectively (Table III.3.1, entry 11 and 12). However, no further improvement in the yield or reduction in reaction time was observed when the reaction was performed at 80 °C (Table III.3.1, entry 13).

Substrate Scope for the Synthesis of *S*-Allyl Benzoylcarbamothioates:

Encouraged by this catalyst and solvent-free synthesis, various aroyl isothiocyanates (**a–k**) were reacted with MBH alcohol (**1**) to enhance the scope and generality of this rearrangement reaction (Scheme III.3.1). As can be seen from Scheme III.3.1, differently functionalized aroyl isothiocyanates bearing electron neutral –H (**a**), electron-donating (**b–d**) as well as electron-withdrawing groups reacted smoothly with (**1**) affording their desired products (**1a–1k**) in good to excellent yields. Benzoyl isothiocyanate (**a**) when reacted with (**1**) gave the product (**1a**) in 96% yield. The structure of the product (**1a**) has been unambiguously established by single crystal X-ray crystallography (Figure III.3.1).

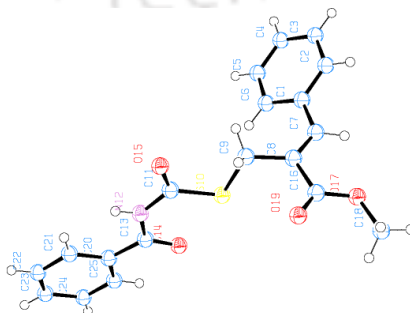
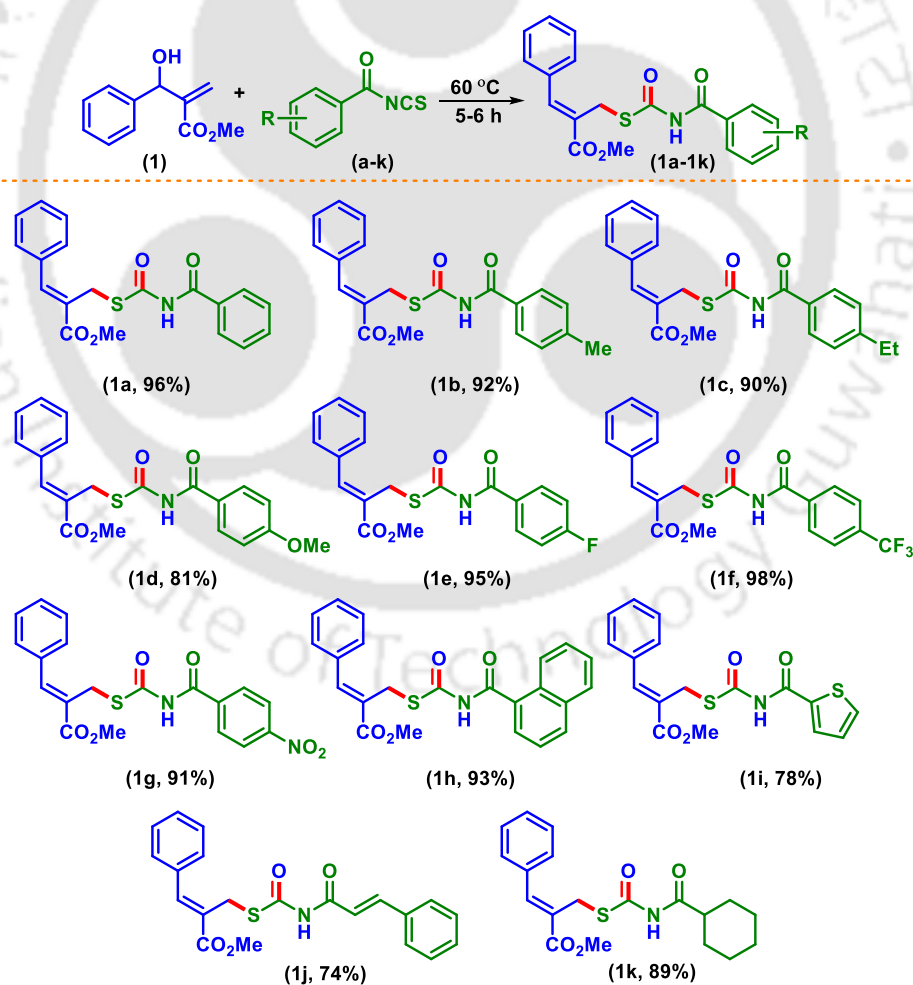


Figure III.3.1 ORTEP view of (**1a**) with 50% thermal ellipsoid probability.

Aroyl isothiocyanates bearing electron-donating (EDG) substituents *viz.* *p*-Me (**b**), *p*-Et (**c**), and *p*-OMe (**d**) when reacted with (**1**) provided their corresponding products (**1b**, 92%), (**1c**, 90%) and (**1d**, 81%) in good yields. This protocol was also equally successful for aroyl isothiocyanates bearing moderately {*p*-F (**e**)} and strongly {*p*-CF₃ (**f**), and *p*-NO₂ (**g**)} electron-withdrawing groups (EWG) giving their respective products (**1e**, 95%), (**1f**, 98%), (**1g**, 91%) in excellent yields (Scheme III.3.1). 2-Naphthoyl isothiocyanate (**h**) reacted effectively with (**1**) giving its product (**1h**, 93%) in good yield. Heteroaromatic isothiocyanates such as thiophenoyl (**i**) also reacted competently with (**1**) affording its *S*-allyl benzoylcarbamothioate (**1i**) in 78% yield. In addition, aliphatic isothiocyanates such as cinnamoyl (**j**) and cyclohexoyl (**k**) furnished their rearranged products (**1j**, 74%) and (**1k**, 89%) in slightly lesser yields.

Scheme III.3.1. Substrate scope for the synthesis of *S*-allyl benzoyl carbamothioates^{a,b}

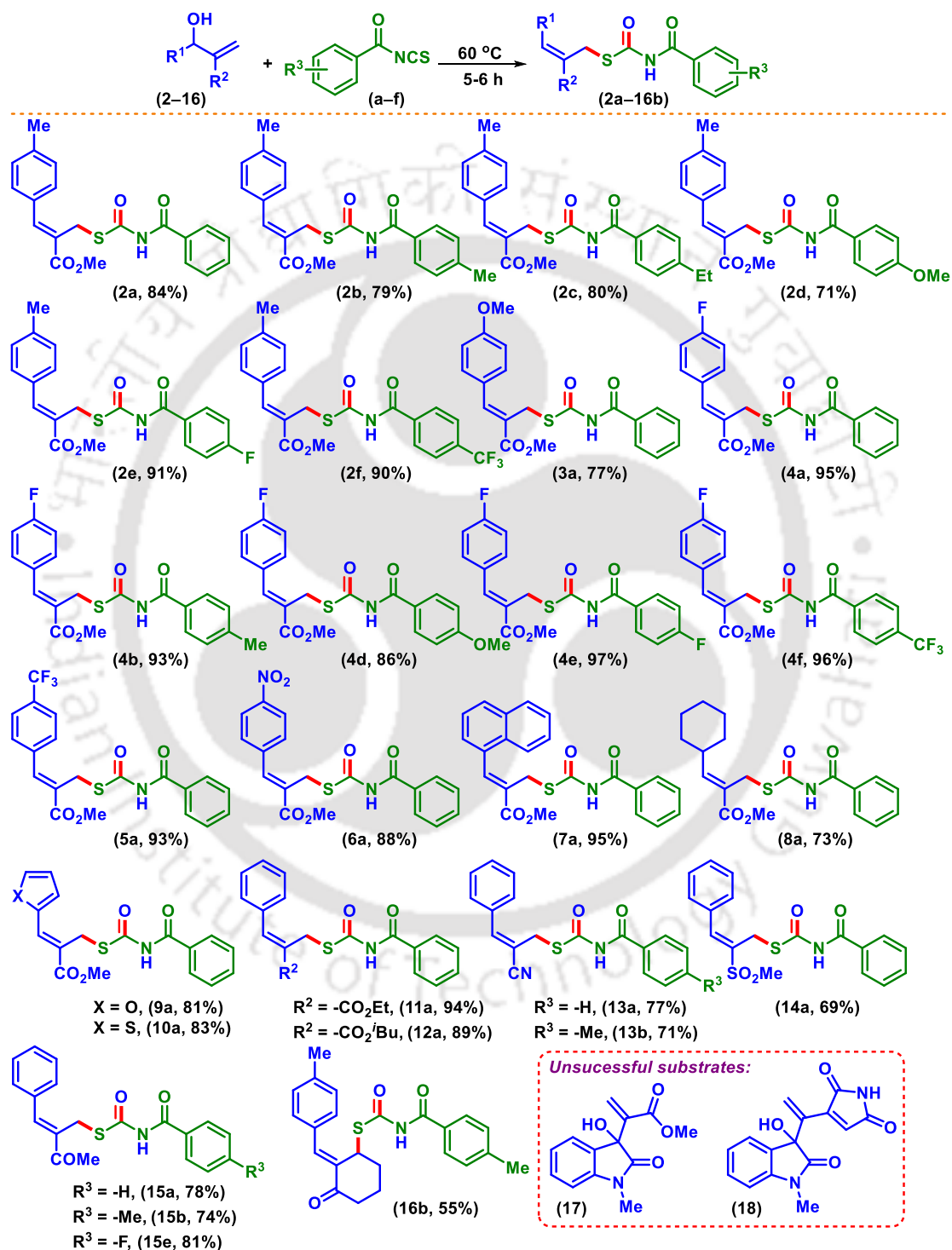


^aReaction conditions: (**1**) (0.5 mmol), (**a-k**) (0.5 mmol), under air at 60 °C for 5–6 h. ^bYield of the isolated pure product.

The substrate scope and generality of this protocol were further investigated by treating other Morita-Baylis-Hilman (MBH) alcohols (**2–16**) with various aroyl isothiocyanates (**a–f**) and the results are summarized in Scheme III.3.2. The MBH alcohol (**2**) reacted with a variety of aroyl isothiocyanates (**a–f**) bearing electron-neutral (**a**), electron-donating {*p*-Me (**b**), *p*-OMe (**c**), *p*-Et (**d**)} and electron-withdrawing {*p*-F (**e**), *p*-CF₃ (**f**)} groups affording their anticipated *S*-allyl benzoylcarbamothioates (**2a**, 84%), (**2b**, 79%), (**2c**, 80%), (**2d**, 71%), (**2e**, 91%), (**2f**, 90%) in good to excellent yields (Scheme III.3.2). A *p*-OMe substituted MBH alcohol (**3**) upon reaction with benzoyl isothiocyanate (**a**) giving the desired product (**3a**) in 77% yield. However, *p*-F (**4**) substituted MBH alcohol when reacted with different aroyl isothiocyanates (**a–f**) afforded their rearranged products (**4a**, 95%), (**4b**, 93%), (**4d**, 86%), (**4e**, 97%) and (**4f**, 96%) in excellent yields (Scheme III.3.2). When the phenyl ring R¹ of MBH alcohol is substituted with strongly electron-withdrawing groups such as *p*-CF₃ (**5**) and *p*-NO₂ (**6**) their respective products (**5a**, 93%) and (**6a**, 88%) were obtained in good yields. A naphthyl substituted MBH alcohol (**7**) when reacted with benzoyl isothiocyanate (**a**) afforded the product (**7a**) in 95% yield. Aliphatic MBH alcohol such as methyl 2-(cyclohexyl(hydroxy)methyl)acrylate (**8**) produced its rearranged product (**8a**) but in a relatively lower yield (73%). Moderate yields of products (**9a**, 81%) and (**10a**, 83%) were obtained when furan (**9**) and thiophene (**10**) containing MBH alcohols were reacted with benzoyl isothiocyanate (**a**) under the optimized reaction condition. After successfully demonstrating the present strategy for R² as methyl ester (–CO₂Me), other esters such as –CO₂Et (**11**) and –CO₂^{*i*}Bu (**12**) were also screened and their corresponding products (**11a**, 94%), (**12a**, 89%) were obtained in good yields (Scheme III.3.2). However, when R² as an ester was replaced by a –CN group (**13**) and reacted with aroyl isothiocyanates (**a**) and (**b**) their rearranged products (**13a**, 77%) and (**13b**, 71%) were obtained in moderate yields. The feasibility of the present strategy was further surveyed by replacing R² with –SO₂Me (**14**) and –COMe (**15**) and reacting with different aroyl isothiocyanates. To our delight their corresponding products (**14a**, 69%) and {(**15a**, 78%), (**15b**, 74%) and (**15e**, 81%) } were obtained in good to moderate yields. When cyclohex-2-en-1-one (**16**) derived MBH alcohol was reacted with 4-methylbenzoyl isothiocyanate (**b**) afforded its anticipated product (**16b**) in 55% yield. The reaction was not productive at all when isatin-derived MBH alcohols (**17** and **18**) were reacted with benzoyl isothiocyanate (**a**) (Scheme III.3.2). This might be due to the steric hindrance of MBH alcohols that

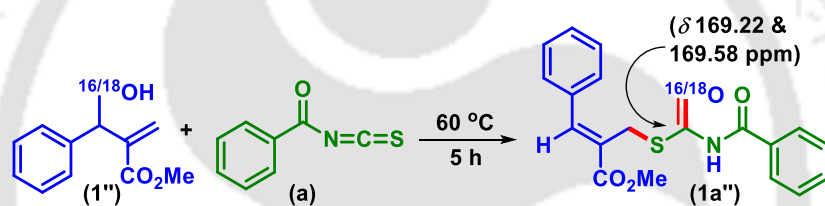
prevents the nucleophilic addition at the sp^2 carbon of $-N=C=S$. Unlike aroyl isothiocyanates, both starting materials remain unconsumed even after 24 h.

Scheme III.3.2. Scope of S-allyl benzoylcarbamothioate with different acrylates^{a,b}



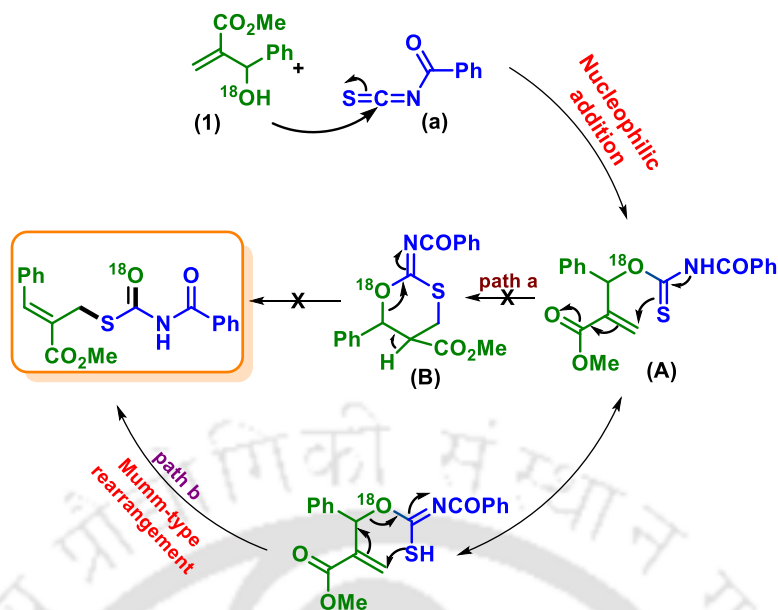
^aReaction conditions: **2-16** (0.5 mmol), **a-f** (0.5 mmol), under air at 60 °C for 5-6 h. ^bYield of the isolated pure product.

The configuration of the double bond of the *S*-allyl benzoylcarbamothioate was confirmed by the 1D NOE experiment. It was appealing to note that *Z*-isomer is obtained exclusively. To demonstrate the scalability of the present methodology a reaction was carried out with methyl 2-(hydroxy(phenyl)methyl) acrylate (**1**) (5 mmol, 963 mg) and benzoyl isothiocyanate (**a**) (5 mmol, 815 mg) under the standard optimized reaction condition giving 87% yield of the product (**1a**). Further, systematic investigations were carried out to depict a plausible mechanism for this transformation. A reaction was carried out with a preformed ^{18}O -labeled MBH alcohol²⁵ and benzoyl isothiocyanate (**a**) under the optimized condition. An ^{18}O -labeled *S*-allyl benzoylcarbamothioate (**1a''**) was obtained as confirmed by HRMS analysis. Further, $^{13}\text{C}\{^1\text{H}\}$ NMR analysis of **1a''** shows two signals (δ 169.622 and 169.658 ppm) due to both labeled and unlabeled carbonyl group of carbamothioate. This observation suggests that the carbonyl oxygen is originating from the $-\text{OH}$ of MBH alcohol (Scheme III.3.3).



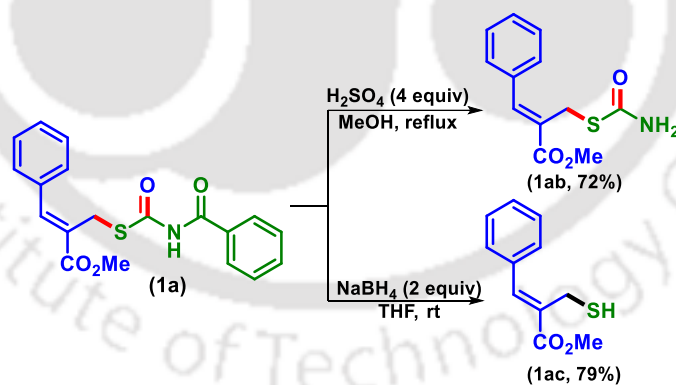
Scheme III.3.3. ^{18}O Labeling experiment.

Two possible paths can account for this migration (Scheme III.3.4). The first possible route is the generation of a benzoylcarbonimidothioate intermediate (**A**) after nucleophilic addition of MBH alcohol (**1**) with benzoyl isothiocyanate (**a**) which undergo thia-Michael addition to form a cyclic intermediate 1,3-oxathiane (**B**). The intermediate (**B**) opens up to give an *S*-allyl benzoylcarbamothioate (**1a**) (Scheme III.3.4, path a). However, a careful examination of ^1H NMR of the reaction mixture obtained by reacting (**1**) and (**a**) at different time intervals rules out the possible formation of any cyclic intermediate (**B**). The other possibility is that the intermediate (**A**) undergoes a thia-Michael addition with concurrent Mumm-type of rearrangement (Scheme III.3.4, path b). The Mumm rearrangement is a significant part of the Ugi reaction that involves 1,3 acyl migration of an acyl imidate to an imide.²⁶ The above labeling experiment supports the occurrence of Mumm-type rearrangement (Scheme III.3.4).²⁵



Scheme III.3.4. Plausible reaction mechanism.

To demonstrate the applicability of our protocol, the *S*-allyl benzoylcarbamothioate (**1a**) was subjected to a few useful organic transformations (Scheme III.3.5). Acid hydrolysis of (**1a**) was carried out which furnished (**1ab**) by cleavage of the imide bond. When (**1a**) was treated with NaBH_4 , selective cleavage of the C–S bond takes place giving (**1ac**) in moderate yield.



Scheme III.3.5. Synthetic transformations of **1a**.

In summary, we have developed an elegant approach for the synthesis of *S*-allyl benzoylcarbamothioate via Mumm-type rearrangement. This methodology allows the useful synthesis of many valuable *S*-allyl benzoylcarbamothioate under mild conditions and avoids the use of costly and harmful materials or cumbersome multi-stepped processes. The ^{18}O labeling experiments support the proposed mechanistic pathway. In this protocol, C–O

and C–S bonds are assembled simultaneously and have the merits of a wide range of substrate scope, neat condition, and simple purification.

III.4. Experimental Section

III.4.1. General Information: All the compounds were commercial grade and used without further purification. HPLC-grade solvents were purchased from commercial sources. Organic extracts were dried over anhydrous sodium sulfate. Solvents were removed in a rotary evaporator under reduced pressure. Silica gel (60–120 mesh size) was used for the column chromatography. Reactions were monitored by TLC on silica gel 60 F₂₅₄ (0.25 mm). All NMR spectra were recorded in DMSO with tetramethylsilane (TMS) as an internal standard for ¹H NMR (400 and 600 MHz) and CDCl₃ solvent as an internal standard for ¹³C{¹H} NMR (100 and 150 MHz). NMR. Both ¹H and ¹³C{¹H} NMR spectra were referenced to the residual DMSO (δ 2.50 and 39.50 ppm). HRMS spectra were recorded using ESI mode (Q-TOF MS Analyzer). IR spectra were recorded in KBr or neat in FT-IR spectra.

III.4.2. Crystallographic Description

CCDC Number for Compound 1a: CCDC-1844331 contains the supplementary crystallographic data for this paper. These data can be obtained free of charge from The Cambridge Crystallographic Data Centre via www.ccdc.cam.ac.uk/data_request/cif.

Crystallographic Description of Z-Methyl-2-(((benzoylcarbamoyl)thio)methyl)-3-phenylacrylate (1a): C₂₁H₂₁NO₄S, crystal dimensions 0.35 x 0.32 x 0.29 mm, $M_r = 383.45$, triclinic, space group P $\bar{1}$ $\bar{1}$ $\bar{1}$, $a = 5.2634(5)$, $b = 12.909(2)$, $c = 14.964(2)$ Å, $\alpha = 73.896(14)^\circ$, $\beta = 89.385(10)^\circ$, $\gamma = 80.113(11)^\circ$, $V = 961.6(2)$ Å³, $Z = 2$, $\rho_{\text{calcd}} = 1.324$ g/cm³, $\mu = 0.195$ mm⁻¹, $F(000) = 404.0$, reflection collected / unique = 3376 / 2129, refinement method = full-matrix least-squares on F^2 , final R indices [$I > 2\sigma(I)$]: $R_1 = 0.1253$, $wR_2 = 0.1960$, R indices (all data): $R_1 = 0.0786$, $wR_2 = 0.1430$, goodness of fit = 1.134.

III.4.3. General Procedure for the Synthesis of (Z)-methyl 2-(((benzoylcarbamoyl)thio)methyl)-3-phenylacrylate (1a): Methyl 2-(hydroxy(phenyl)methyl)acrylate (**1**) (0.5 mmol, 87.5 mg) and benzoyl isothiocyanate (**a**) (0.5 mmol, 81.5 mg) were combined in an 5 mL oven-dried round bottom flask equipped

with a magnetic needle. The reaction mixture was then stirred at 60 °C for 6 h. The progress of the reaction was monitored by TLC. After completion of the reaction, (indicated by the formation of white solid) the crude product so obtained was then purified by silica gel column chromatography using EtOAc and hexane (20:80) as eluent to remove all the side product and the final product (**1a**) was obtained using 100% DCM as eluent (170 mg, 96%). The identity and purity of the product were confirmed by spectroscopic analysis.

III.4.4. General Procedure for the Synthesis of Aroyl Isothiocyanate (a-k): Benzoyl chloride (5 mmol), KSCN (1.5 equiv) and CH₃CN (15 mL) were taken in a 25 ml oven-dried round bottom flask. Then it was fitted with a condenser and the resultant reaction mixture was stirred in a pre-heated oil bath maintained at 85 °C. The progress of the reaction was monitored by TLC. After completion (color changes from white to yellow) the reaction mixture was cooled to room temperature. The reaction mixture was evaporated under reduced pressure to remove CH₃CN. Then it was admixed with ethyl acetate (30 mL) and washed successively with a saturated solution of sodium bicarbonate (2 x 5 mL) and brine solution (2 x 5 mL). The organic layer was dried over anhydrous sodium sulfate and the solvent was evaporated in a vacuum. The crude product thus obtained was purified using column chromatography with hexane as eluent to afford the desired benzoyl isothiocyanate in quantitative yield.

III.4.5. General Procedure for the Synthesis of Methyl 2-(hydroxy(phenyl)methyl)acrylate (1-18): The synthesis of all the MBH alcohols (**1-18**, **15**,²⁷ **16**²⁸) was according to the following reported procedure. Benzaldehyde (5 mmol), methyl acrylate (2.5 equiv), and DABCO (1.0 equiv) were taken in a 25 mL oven-dried round bottom flask and sealed with a rubber septum. The resultant reaction mixture was stirred at room temperature under solvent-free conditions for 7-14 days. After completion, the reaction mixture was admixed with ethyl acetate (30 mL) and washed successively with a saturated solution of sodium bicarbonate (2 x 5 mL) and brine solution (2 x 5 mL). The organic layer was dried over anhydrous sodium sulfate and the solvent was evaporated in vacuum. The crude product thus obtained was purified using column chromatography with hexane and EtOAc as eluent to afford the desired MBH alcohols in quantitative yield.

III.4.6. General Procedure for Synthesis of Methyl 2-((carbamoylthio)methyl)-3-phenylacrylate (1ab): Z-Methyl 2-(((benzoylcarbamoyl)thio)methyl)-3-phenylacrylate (**1**) (0.14 mmol, 49.7 mg), MeOH (1 mL) and conc. H₂SO₄ (0.56 mmol, 54.92 mg) were

combined in a 5 mL oven-dried round bottom flask equipped with a magnetic needle. The reaction mixture was then refluxed overnight. After completion of the reaction, the mixture was diluted with EtOAc (10 mL), washed with saturated NaHCO₃ solution (1x10 mL), and finally washed with saturated NaCl solution (1x10 mL), dried over anhydrous sodium sulfate (Na₂SO₄), and evaporated under reduced pressure., the crude product thus obtained was then purified by silica gel column chromatography using EtOAc and hexane (19:81) as **1ab** (25.30 mg, 72%).

III.4.7. General Procedure for Synthesis of Methyl 2-(mercaptomethyl)-3-phenylacrylate (1ac): Z-Methyl 2-(((benzoylcarbamoyl)thio)methyl)-3-phenylacrylate (**1**) (0.14 mmol, 49.7 mg), MeOH (1 mL) and sodium borohydride (0.28 mmol, 10.59 mg) and THF (1 mL) were combined in an 5 mL oven-dried round bottom flask equipped with a magnetic needle. The reaction mixture was then stirred overnight. After completion of the reaction, the mixture was diluted with EtOAc (10 mL), washed with saturated NaHCO₃ solution (1x10 mL), and finally washed with saturated NaCl solution (1x10 mL), dried over anhydrous sodium sulfate (Na₂SO₄), and evaporated under reduced pressure., the crude product thus obtained was then purified by silica gel column chromatography using EtOAc and hexane (10:90) as **1ac** (23 mg, 79%)..

III.4.8. NOE Experiment

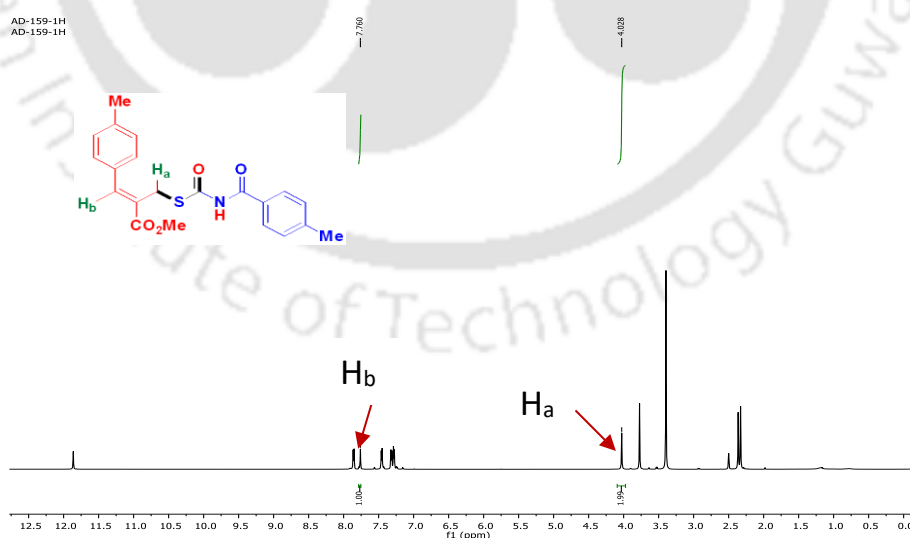


Figure III.4.8.1. ¹H NMR spectra of **2b** (DMSO-*d*₆, 400 MHz).

The relative stereochemistry in the product (**1a–13b**) was determined by the 1D NOE experiment of (**2b**) as the representative example. When proton H_a was irradiated in the

compound (**2b**), no peak enhancement for H_b along with very weak peak enhancement of the proton of the phenyl ring of MBH alcohol was observed (Figure III.4.8.2.). On the other hand, when proton H_b was irradiated, no peak enhancement for the proton H_a was observed as expected (Figure III.4.8.3.). All these NOE observations ultimately suggest that the relative stereochemistry of the product (**2b**) as *Z*-Methyl 2-((((4-methylbenzoyl)carbamoyl)thio)methyl)-3-(*p*-tolyl)acrylate. The spatial interactions of the protons are shown in the figures given below.

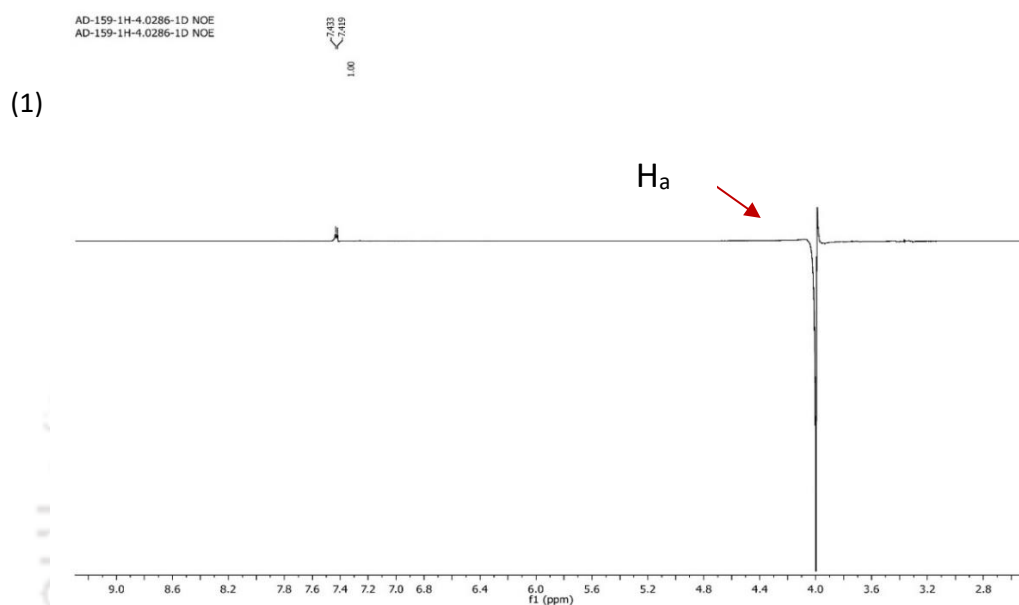


Figure III.4.8.2. Irradiation of H_a.

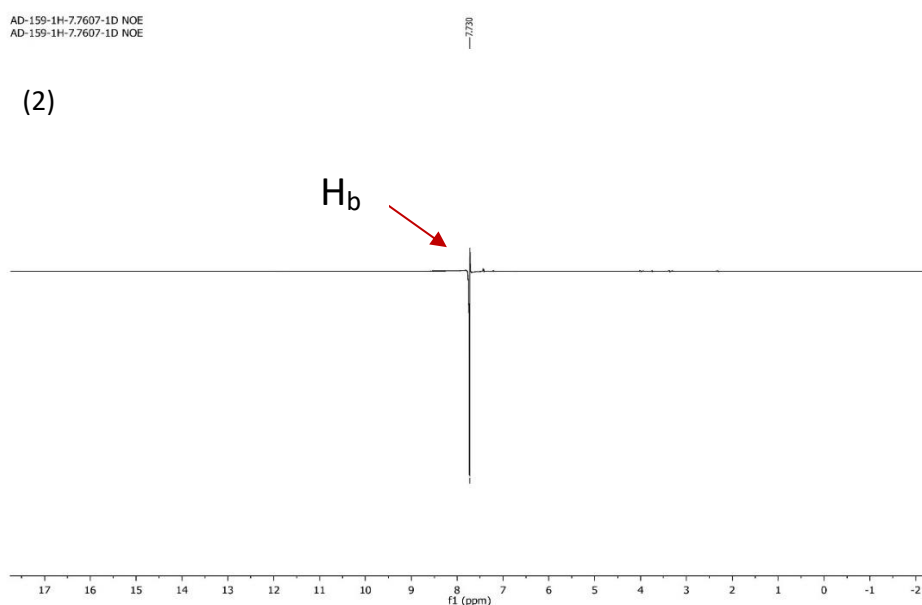


Figure III.4.8.3. Irradiation of H_b.

III.4.9. Mechanistic Investigation

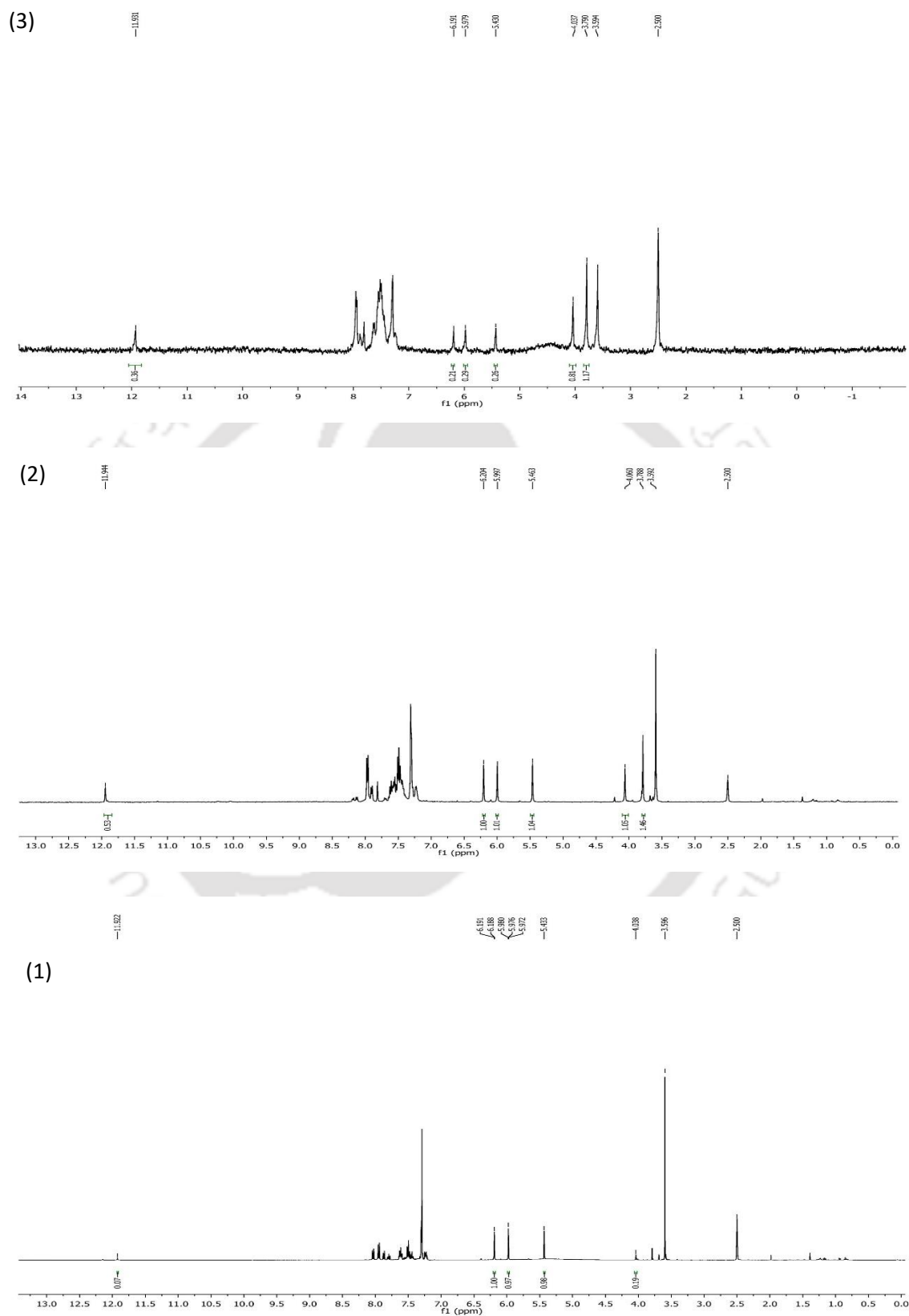


Figure III.4.9.1. ¹H NMR analysis of reaction mixture at (1) 10 min (2) 30 min (3) 1 h.

¹H NMR study for the detection of reaction intermediates: To detect the intermediate species in the reaction mixture for this transformation ¹H NMR spectroscopy was performed. In this study **1a** was taken as a representative example. A 5 mL oven-dried flask was charged with methyl 2-(hydroxy(phenyl)methyl)acrylate (**1**) (0.5 mmol, 87.5 mg) and benzoyl isothiocyanate (**a**) (0.5 mmol, 81.5 mg). Then the reaction mixture was stirred in a pre-heated oil bath at 60 °C. After 10, 20 and 60 min of reaction, small aliquots were withdrawn from the reaction mixture. The crude product thus obtained were used for ¹H NMR study in DMSO-*d*₆ with tetramethylsilane as the internal standard for ¹H NMR (400 MHz). In the ¹H NMR spectra, both starting material and product were observed (Figure III.4.9.1). There was no indication for the formation of cyclic intermediate 1,3-oxathiane. This suggests that the reaction is going through a concerted path.

III.4.10. ¹⁸O Labelling Experiment

Experimental Procedure for the Formation of labeled MBH alcohol (1''**):** To a solution of MBH alcohol (2.5 mmol) in DCM (4 mL) was added Boc₂O (2.55 mmol) in DCM (4 mL) dropwise in an ice bath. The mixture was stirred for 30 min, and DMAP (0.25 mmol) was added in one portion. The reaction was monitored with TLC. Then the mixture was diluted with DCM (20 mL), washed with 4 N HCl (1x10 mL) and saturated NaHCO₃ aqueous (1x10 mL), and finally washed with saturated NaCl aqueous (1x10 mL), dried over anhydrous sodium sulfate (Na₂SO₄), and evaporated under reduced pressure. The crude product so obtained was then purified by silica gel column chromatography using EtOAc and hexane (10:90) as eluent.

The MBH carbonate (**1'**) (58.4 mg, 0.2 mmol, 1.0 equiv), H₂O¹⁸ (8.0 μL, 0.4 mmol, 2.0 equiv), were dissolved in DMF (700 μL) and stirred at room temperature for 10 min, then DABCO (2.24 mg, 0.02 mmol, 0.1 equiv) was added. The reaction mixture was further stirred at room temperature and progress was monitored by TLC. After 4 hours and complete consumption of **1'**, the reaction mixture was directly loaded onto a short silica gel column, followed by gradient elution with EtOAc and hexane (15:85). Removal of the solvent in *vacuo* affords product **1''** (18.1 mg) as pale-yellow oil in 88% yield.

Experimental Procedure for the Formation of labeled S-allyl benzoylcarbamothioate (1a''**):** Labeled methyl 2-(hydroxy(phenyl)methyl)acrylate (**1''**) (0.10 mmol, 19.4 mg) and benzoyl isothiocyanate (**a**) (0.10 mmol, 16.3 mg) were combined in a 5 mL oven-dried round bottom flask equipped with a magnetic needle. The reaction mixture was then stirred

at 60 °C for 6 h. The crude mixture thus obtained was used for the $^{13}\text{C}\{^1\text{H}\}$ NMR study in $\text{DMSO-}d_6$ with tetramethylsilane as the internal standard for $^{13}\text{C}\{^1\text{H}\}$ NMR (150 MHz). The formation of labeled *S*-allyl benzoylcarbamothioate (**1a''**) was confirmed by spectroscopic and HRMS analysis (Figures III.4.10.1 and III.4.10.2).

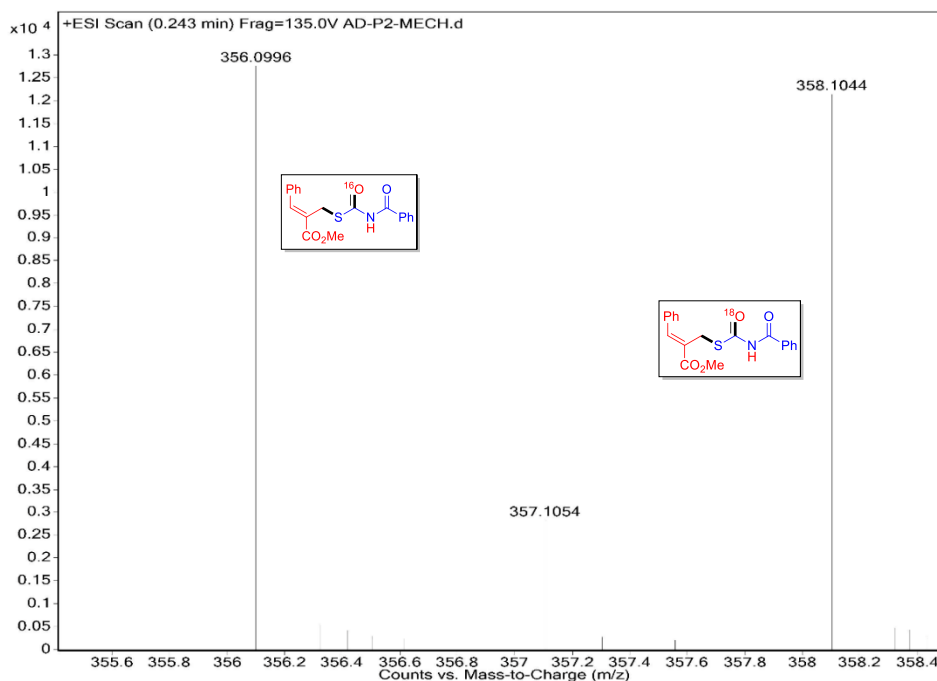


Figure III.4.10.1. HRMS spectrum of ^{18}O labeled **1a''**.

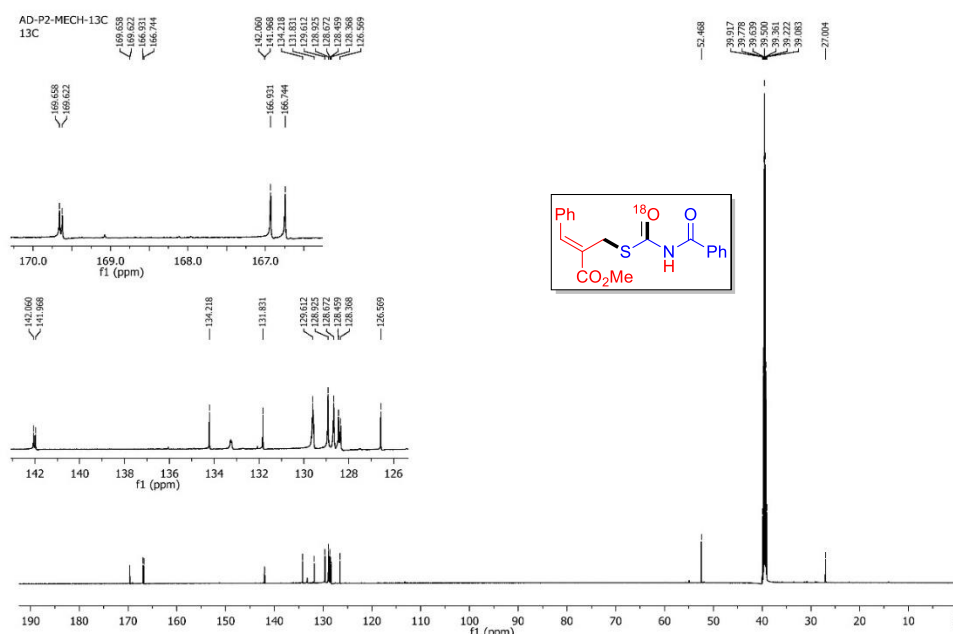


Figure III.4.10.2. $^{13}\text{C}\{^1\text{H}\}$ NMR spectrum of ^{18}O labeled **1a''** ($\text{DMSO-}d_6$, 150 MHz).

III.5. References

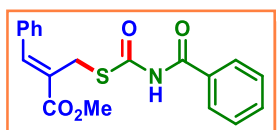
- (1) (a) Padwa, A. *Chem. Soc. Rev.* **2009**, 38, 3072. (b) Ardkhean, R.; Caputo, D. F. J.; Morrow, S. M.; Shi, H.; Xiong, Y.; Anderson, E. A. *Chem. Soc. Rev.* **2016**, 45, 1557. (c) Blouin, S.; Blond, G.; Donnard, M.; Gulea, M.; Suffert, J. *Synthesis*, **2017**, 49, 1767. (d) Pellissier, H. *Chem. Rev.* **2013**, 113, 442. (e) Climent, M. J.; Corma, A.; Iborra, S. *Chem. Rev.* **2011**, 111, 1072.
- (2) Mizuno, T.; Iwai, T.; Ito, T. *Tetrahedron* **2004**, 60, 2869.
- (3) (a) Tilles, H. *J. Am. Chem. Soc.* **1959**, 81, 714. (b) Chin-Hsien, W. *Synthesis* **1981**, 622. (c) Wynne, J. H.; Jensen, S.D.; Snow, A.W. *J. Org. Chem.* **2003**, 68, 3733.
- (4) (a) Mizuno, T.; Nishiguchi, I.; Okushi, T.; Hirashima, T. *Tetrahedron Lett.* **1991**, 32, 6867. (b) Mizuno, T.; Nishiguchi, I.; Hirashima, T. *Tetrahedron* **1993**, 49, 2403.
- (5) (a) Yuan, Y.-Q.; Guo, S.-R.; Xiang, J.-N. *Synlett* **2013**, 24, 443. (b) Chen, J.; Mao, J.; He, Y.; Shi, D.; Zou, B.; Zhang, G. *Tetrahedron* **2015**, 71, 9496.
- (6) (a) Lloyd-Jones, G. C.; Moseley, J. D.; Renny, J. S. *Synthesis* **2008**, 5, 661. (b) Zonta, C.; De Lucchi, O.; Volpicelli, R.; Cotarca, L. In *Sulfur-Mediated Rearrangements II*; Schaumann, E., Ed.; Springer: Berlin/Heidelberg, **2006**; Vol. 275, pp 131.
- (7) Harvey, J. N.; Jover, J.; Lloyd-Jones, G. C.; Moseley, J. D.; Murray, P.; Renny, J. S. *Angew. Chem. Int. Ed.* **2009**, 48, 7612.
- (8) Pedersen, S. K.; Ulfkjær, A.; Newman, M. N.; Yogarasa, S.; Petersen, A. U.; Sølling, T. I.; Pittelkow, M. *J. Org. Chem.* **2018**, 83, 12000.
- (9) Perkowski, A. J.; Cruz, C. L.; Nicewicz, D. A. *J. Am. Chem. Soc.* **2015**, 137, 15684.
- (10) Broese, T.; Roesel, A. F.; Prudlik, A.; Francke, R. *Org. Lett.* **2018**, 20, 7483.
- (11) Căproiu, M. T.; Dumitrascu, F.; Shova, S.; Chiriță, I. C.; Missir, A. V.; Cioroianu, D.-M. *Tetrahedron Lett.* **2014**, 55, 4011.
- (12) (a) Zhu, P.; He, X.; Chen, X.; You, Y.; Yuan, Y. Weng, Z. *Tetrahedron* **2014**, 70, 672. (b) Singh, P.; Bai, R.; Choudhary, R.; Sharma, M. C. Badsara, S. S. *RSC Adv.* **2017**, 7, 30594. (c) Zhang, L.; Zhu, J.; Ma, J.; Wu, L.; Zhang, W.-H. *Org. Lett.* **2017**, 19, 6308. (d) Xu, Q.-L.; Liu, W.-B.; Dai, L.-X.; You, S.-L. *J. Org. Chem.* **2010**, 75, 4615. (e) Reddy, P. S.; Reddy, M. A.; Sreedhar, B.; Rao, M. V. B. *Synth. Commun.* **2010**, 40, 2075.
- (13) Wang, D.-Y.; Peng, X.-M.; Wang, G.-Z.; Zhang, Y.-J.; Guo, T.; Zhang, P.-K. *Asian J. Org. Chem.* **2018**, 7, 875.

- (14) Pritzius, A. B.; Breit, B. *Angew. Chem. Int. Ed.* **2015**, *127*, 3164.
- (15) Robertson F.; Wu, J. *Org. Lett.* **2010**, *12*, 2668.
- (16) (a) Takeuchi, Y.; Shiragami, T.; Kimura, K.; Suzuki, E.; Shibata, N. *Org. Lett.* **1999**, *1*, 1571. (b) Capitosti, S. M.; Hansen, T. P.; Brown, M. L. *Org. Lett.* **2003**, *5*, 2865. (c) *The Merck Index*, version 12:3, Merck&Co Inc. Whitehouse Station, NJ. USA, **1999** (d) Kim, E.-S.; Park, K. Y.; Heo, J.-M.; Kim, B. J.; Ahn, K. D.; Lee, J.-G. *Ind. Eng. Chem. Res.* **2010**, *49*, 11250. (e) Maruyama, H. B.; Suhara, Y.; Suzuki-Watanabe, J.; Maeshima, Y.; Shimizu, N.; Ogura-Hamada, M.; Fujimoto, H. Takano, K. *J. Antibiot.* **1975**, *28*, 636. (f) Suhara, Y.; Maruyama, H. B.; Kotoh, Y.; Miyasaka, Y.; Yokose, K.; Shirai, H.; Takano, K.; Quitt, P.; Lanz, P. *J. Antibiot.* **1975**, *28*, 648. (g) Krohn, K.; Franke, C.; Jones, P. G.; Aust, H.-J.; Draeger, D.; Schulz, B. *Liebigs Ann. Chem.* **1992**, 789. (h) Pinto, I. L.; Boyd, H. F.; Hickey, D. M. B. *Bioorg. Med. Chem. Lett.* **2000**, *10*, 2015.
- (17) (a) Raheem, I. T.; Goodman, S. N.; Jacobsen, E. N. *J. Am. Chem. Soc.* **2004**, *126*, 706. (b) Vanderwal C. D.; Jacobsen, E. N. *J. Am. Chem. Soc.* **2004**, *126*, 14724. (c) Gandelman, M.; Jacobsen, E. N. *Angew. Chem., Int. Ed.* **2005**, *44*, 2393. (d) Balskus, E. P.; Jacobsen, E. N. *J. Am. Chem. Soc.* **2006**, *128*, 6810. (e) Thompson, S.; McMahan, S. A.; Naismith, J. H.; O'Hagen, D. *Bioorg. Chem.* **2016**, *64*, 37. (f) Feng, C.; Feng, D.; Loh, T.-P. *Chem. Commun.* **2015**, *51*, 342. (g) Wright, A. C.; Haley, C. K.; Lapointe, G.; Stoltz, B. M. *Org. Lett.* **2016**, *18*, 2793.
- (18) (a) Chan, J.; Baucom, K. D.; Murry, J. A. *J. Am. Chem. Soc.* **2007**, *129*, 14106. (b) Wang, L.; Fu, H.; Jiang, Y.; Zhao, Y. *Chem. - Eur. J.* **2008**, *14*, 10722. (c) Wang, J.; Liu, C.; Yuan, J.; Lei, A. *Chem. Commun.* **2014**, *50*, 4736. (d) Yu H.; Zhang, Y. *Eur. J. Org. Chem.* **2015**, 1824. (e) Wang, L.; Fu, H.; Jiang, Y.; Zhao, Y. *Chem. - Eur. J.* **2008**, *14*, 10722. (f) Yu, H.; Chen Y.; Zhang, Y. *Chin. J. Chem.* **2015**, *33*, 531. (g) Nicolaou, K. C.; Mathison, C. J. N. *Angew. Chem. Int. Ed.* **2005**, *44*, 5992. (h) Xu, L.; Zhang, S.; Trudell, M. L. *Chem. Commun.* **2004**, 1668 and references therein. (i) Evans, D. A.; Nagorny, P.; Xu, R. *Org. Lett.* **2006**, *8*, 5669. (j) Zhang, Y.; Pan, L.; Zou, Y.; Xu X.; Liu, Q. *Chem. Commun.* **2014**, *50*, 14334. (k) Yan, X.; Fang, K.; Liu, H.; Xi, C. *Chem. Commun.* **2013**, *49*, 10650.
- (19) (a) Li, H.; Dong, K.; Neumann, H.; Beller, M. *Angew. Chem. Int. Ed.* **2015**, *54*, 10239. (b) Lv, Y.; Li, Y.; Xiong, T.; Lu, Y.; Liu, Q.; Zhang, Q. *Chem. Commun.* **2014**, *50*, 2367. (c) Li, Y.; Zhu, F.; Wang, Z.; Rabeah, J.; Brückner, A.; Wu, X.-F.

- ChemCatChem*. **2017**, *9*, 915. (d) Gálvez, A. O.; Schaack, C. P.; Noda, H.; Bode, J W. *J. Am. Chem. Soc.* **2017**, *139*, 1826.
- (20) Wang, F.; Liu, H.; Fu, H.; Jiang, Y.; Zhao, Y. F. *Adv. Synth. Catal.* **2009**, *351*, 246.
- (21) Aruri, H.; Singh, U.; Kumar, S.; Kushwaha, M.; Gupta, A. P.; Vishwakarma, R. A.; Singh, P. P. *Org. Lett.* **2016**, *18*, 3638.
- (22) Li, H.; Dong, K.; Neumann, H.; Beller, M. *Angew. Chem. Int. Ed.* **2015**, *127*, 10377.
- (23) Zhang, Y.; Pan, L.; Zou, Y.; Xu, X.; Liu, Q. *Chem. Commun.* **2014**, *50*, 14334.
- (24) (a) Palsuledesai, C. C.; Murru, S.; Sahoo, S. K.; Patel, B. K. *Org. Lett.* **2009**, *11*, 3382. (b) Modi, A.; Ali, W.; Patel, B. K. *Org. Lett.* **2017**, *19*, 432. (c) Dahiya, A.; Ali, W.; Patel, B. K. *ACS Sustainable Chem. Eng.* **2018**, *6*, 4272.
- (25) (a) Zhu, B.; Yan, L.; Pan, Y.; Lee, R.; Liu, H.; Han, Z.; Huang, K.-W.; Tan, C.-H.; Jiang, Z. *J. Org. Chem.* **2011**, *76*, 6894.
- (26) (a) Mercalli, V.; Nyadanu, A.; Cordier, M.; Tron, G. C.; Grimaud, L.; Kaim, L. E. *Chem. Commun.* **2017**, *53*, 2118. (b) Chen, J.; Shao, Y.; Ma, L.; Ma, M.; Wan, X. *Org. Biomol. Chem.* **2016**, *14*, 10723. (c) Liang, H.-W.; Yang, Z.; Jiang, K.; Ye, Y.; Wei, Y. *Angew. Chem. Int. Ed.* **2018**, *57*, 5720. (d) Chandgude, A. L.; Dömling, A. *Org. Lett.* **2017**, *19*, 1228. (e) Harayama, H.; Nagahama, T.; Kozera, T.; Kimura, M.; Fugami, K.; Tanaka, S.; Tamaru, Y. *Bull. Chem. Soc. Jpn.* **1997**, *70*, 445. (f) Sakamoto, M.; Yoshiaki, M.; Takahashi, M.; Fujitaa, T.; Watanabe, S. *J. Chem. Soc., Perkin Trans. 1* **1995**, 373.
- (27) Chandrasekhar, S.; Narsihmulu, C.; Saritha, B.; Sultana, S. S. *Tetrahedron Lett.* **2004**, *45*, 5865.
- (28) Aggarwal V. K.; Mereu, A. *Chem. Commun.* **1999**, 2311.

III.6. Spectral data of product

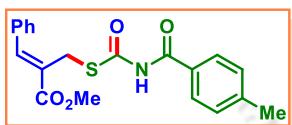
Z-Methyl-2-(((benzoylcarbamoyl)thio)methyl)-3-phenylacrylate (1a):



White solid (96%, 170.4 mg); m.p. 173–175 °C; ^1H NMR (400 MHz, DMSO- d_6): δ (ppm) 3.79 (s, 3H), 4.05 (s, 2H), 7.48 (m, 7H), 7.63 (t, 1H, $J = 7.6$ Hz), 7.80 (s, 1H), 7.95 (d, 2H, $J = 7.6$ Hz), 11.92 (s, 1H); $^{13}\text{C}\{^1\text{H}\}$ NMR (100 MHz, DMSO- d_6): δ (ppm) 27.0, 52.4, 126.6, 128.4, 128.6, 128.9, 129.5, 129.6, 131.8, 133.2, 134.2, 142.0, 166.7, 166.9, 169.6; IR (KBr): 3443,

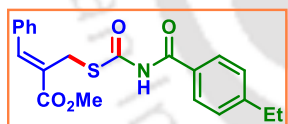
2953, 2923, 2853, 1714, 1696, 1633, 1434, 1261, 1217 cm^{-1} ;
 HRMS (ESI): calcd. for $\text{C}_{19}\text{H}_{18}\text{NO}_4\text{S}^+$ [$\text{M} + \text{H}^+$] 356.0951;
 found 356.0954.

Z-Methyl 2-(((4-methylbenzoyl)carbamoyl)thio)methyl)-3-phenylacrylate (1b):



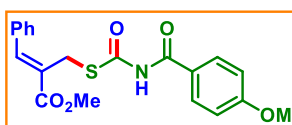
White solid (92%, 169.7 mg); m.p. 199–201 $^{\circ}\text{C}$; ^1H NMR (400 MHz, $\text{DMSO}-d_6$): δ (ppm) 2.36 (s, 3H), 3.79 (s, 3H), 4.03 (s, 2H), 7.32 (d, 2H, $J = 8.0$ Hz), 7.42 (t, 1H, $J = 6.8$ Hz), 7.48 (t, 2H, $J = 7.6$ Hz), 7.56 (d, 2H, $J = 7.2$ Hz), 7.80 (s, 1H), 7.86 (d, 2H, $J = 8.0$ Hz), 11.84 (s, 1H); $^{13}\text{C}\{^1\text{H}\}$ NMR (100 MHz, $\text{DMSO}-d_6$): δ (ppm) 21.1, 26.9, 52.4, 126.6, 128.4, 128.8, 128.9, 129.1, 129.46, 129.54, 134.2, 141.9, 143.6, 166.4, 166.9, 169.6; IR (KBr): 3459, 2957, 2856, 1711, 1694, 1615, 1436, 1381 cm^{-1} ; HRMS (ESI): calcd. for $\text{C}_{20}\text{H}_{20}\text{NO}_4\text{S}^+$ [$\text{M} + \text{H}^+$] 370.1108; found 370.1114.

Z-Methyl 2-(((4-ethylbenzoyl)carbamoyl)thio)methyl)-3-phenylacrylate (1c):



White solid (90%, 172.3 mg); m.p. 170–172 $^{\circ}\text{C}$; ^1H NMR (400 MHz, $\text{DMSO}-d_6$): δ (ppm) 1.18 (t, 3H, $J = 7.6$ Hz), 2.66 (q, 2H, $J = 7.6$ Hz), 3.79 (s, 3H), 4.03 (s, 2H), 7.35 (d, 2H, $J = 8.0$ Hz), 7.42 (m, 1H), 7.48 (t, 2H, $J = 7.6$ Hz), 7.55 (d, 2H, $J = 7.6$ Hz), 7.80 (s, 1H), 7.88 (d, 2H, $J = 8.4$ Hz), 11.84 (s, 1H); $^{13}\text{C}\{^1\text{H}\}$ NMR (100 MHz, $\text{DMSO}-d_6$): δ (ppm) 15.2, 27.0, 28.2, 52.4, 126.6, 128.0, 128.6, 128.9, 129.2, 129.5, 129.6, 134.2, 141.9, 149.0, 166.5, 166.9, 169.6; IR (KBr): 3448, 2967, 2923, 2853, 1715, 1636, 1578, 1384, 1262 cm^{-1} ; HRMS (ESI): calcd. for $\text{C}_{21}\text{H}_{22}\text{NO}_4\text{S}^+$ [$\text{M} + \text{H}^+$] 384.1264; found 384.1267.

Z-Methyl 2-(((4-methoxybenzoyl)carbamoyl)thio)methyl)-3-phenylacrylate (1d):

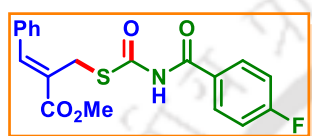


White solid (81%, 155.9 mg); m.p. 181–183 $^{\circ}\text{C}$; ^1H NMR (400 MHz, $\text{DMSO}-d_6$): δ (ppm) 3.79 (s, 3H), 3.83 (s, 3H), 4.02 (s, 2H), 7.05 (d, 2H, $J = 8.8$ Hz), 7.43 (m, 1H), 7.48 (t, 2H, $J = 7.6$ Hz), 7.56 (d, 2H, $J = 7.6$ Hz), 7.80 (s, 1H), 7.96 (d, 2H, $J = 8.8$ Hz), 11.77 (s, 1H); $^{13}\text{C}\{^1\text{H}\}$ NMR (100 MHz, $\text{DMSO}-d_6$): δ

(ppm) 26.9, 52.4, 55.6, 113.9, 123.7, 126.7, 128.8, 129.47, 129.54, 130.6, 134.2, 141.8, 163.2, 165.8, 166.9, 169.7; IR (KBr): 3449, 3004, 2924, 2849, 1690, 1630, 1607, 1469, 1249 cm^{-1} ; HRMS (ESI): calcd. for $\text{C}_{20}\text{H}_{20}\text{NO}_5\text{S}^+$ [$\text{M} + \text{H}^+$] 386.1057; found 386.1067.

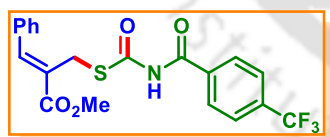
Z-Methyl 2-(((4-fluorobenzoyl)carbamoyl)thio)methyl)-3-phenylacrylate (1e):

White solid (95%, 177.1 mg); m.p. 190–192 °C; ^1H NMR (400 MHz, $\text{DMSO}-d_6$): δ (ppm) 3.79 (s, 3H), 4.03 (s, 2H), 7.35 (t, 2H, $J = 8.8$ Hz), 7.46 (m, 3H), 7.55 (d, 2H, $J = 7.2$ Hz), 7.80 (s, 1H), 8.02 (t, 2H, $J = 7.6$ Hz), 11.94 (s, 1H); $^{13}\text{C}\{^1\text{H}\}$ NMR (100 MHz, $\text{DMSO}-d_6$): δ (ppm) 27.0, 52.4, 115.7 (d, $J = 21.9$ Hz), 126.6, 128.4 (d, $J = 2.7$ Hz), 128.9, 129.6, 131.4 (d, $J = 9.5$ Hz), 134.2, 142.0, 163.8, 165.6, 166.3, 166.9, 169.6; ^{19}F NMR ($\text{DMSO}-d_6$ + Hexafluorobenzene): δ (ppm) -108.34 (s); IR (KBr): 3438, 3277, 2950, 2855, 1710, 1693, 1639, 1511, 1260 cm^{-1} ; HRMS (ESI): calcd. for $\text{C}_{19}\text{H}_{17}\text{FNO}_4\text{S}^+$ [$\text{M} + \text{H}^+$] 374.0857; found 374.0864.



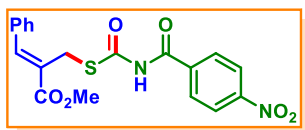
Z-Methyl 3-phenyl-2-(((4-(trifluoromethyl)benzoyl)carbamoyl)thio)methyl)acrylate (1f):

White solid (98%, 207.2 mg); m.p. 195–197 °C; ^1H NMR (400 MHz, $\text{DMSO}-d_6$): δ (ppm) 3.79 (s, 3H), 4.05 (s, 2H), 7.47 (m, 3H), 7.56 (d, 2H, $J = 7.2$ Hz), 7.81 (s, 1H), 7.90 (d, 2H, $J = 8.0$ Hz), 8.12 (d, 2H, $J = 8.0$ Hz), 12.13 (s, 1H); $^{13}\text{C}\{^1\text{H}\}$ NMR (100 MHz, $\text{DMSO}-d_6$): δ (ppm) 27.0, 52.4, 122.4, 125.5 (q, $J = 3.6$ Hz), 126.5, 128.4, 128.9, 129.3, 129.5, 129.6, 134.2, 135.8, 142.1, 165.8, 166.9, 169.5; ^{19}F NMR ($\text{DMSO}-d_6$ + Hexafluorobenzene): δ (ppm) -64.35 (s); IR (KBr): 3432, 2957, 2853, 1720, 1627, 1523, 1444, 1326 cm^{-1} ; HRMS (ESI): calcd. for $\text{C}_{20}\text{H}_{17}\text{F}_3\text{NO}_4\text{S}^+$ [$\text{M} + \text{H}^+$] 424.0825; found 424.0827.



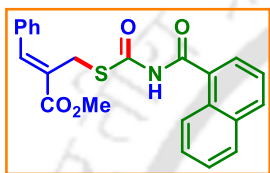
Z-Methyl 2-(((4-nitrobenzoyl)carbamoyl)thio)methyl)-3-phenylacrylate (1g):

Pale yellow solid (91%, 182.1 mg); m.p. 144–146 °C; ^1H NMR (400 MHz, $\text{DMSO}-d_6$): δ (ppm) 3.68 (s, 3H), 6.06 (s, 1H), 6.41 (s, 1H), 6.59 (s, 1H), 7.38 (m, 5H), 8.08 (d, 2H, $J = 6.0$ Hz), 8.31



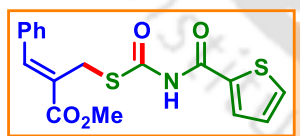
(d, 2H, $J = 6.0$ Hz), 11.48 (s, 1H); $^{13}\text{C}\{^1\text{H}\}$ NMR (100 MHz, DMSO- d_6): δ (ppm) 52.1, 73.9, 123.4, 126.6, 127.5, 128.6, 128.6, 129.8, 137.1, 138.8, 138.9, 149.6, 150.2, 164.79, 164.83; IR (KBr): 3448, 2957, 2924, 2854, 1759, 1713, 1635, 1526, 1349, 1263, 1196 cm^{-1} ; HRMS (ESI): calcd. for $\text{C}_{19}\text{H}_{17}\text{N}_2\text{O}_6\text{S}^+$ [$\text{M} + \text{H}^+$] 401.0802; found 401.0806.

Z-Methyl 2-(((1-naphthoyl)carbamoyl)thio)methyl)-3-phenylacrylate (1h):



White solid (93%, 188.3 mg); m.p. 124–126 °C; ^1H NMR (400 MHz, DMSO- d_6): δ (ppm) 3.82 (s, 3H), 4.14 (s, 2H), 7.48 (m, 3H), 7.62 (m, 5H), 7.82 (d, 1H, $J = 7.2$ Hz), 7.86 (s, 1H), 8.01 (d, 1H, $J = 7.6$ Hz), 8.11 (d, 1H, $J = 8.4$ Hz), 8.21 (d, 1H, $J = 8.8$ Hz), 12.15 (s, 1H); $^{13}\text{C}\{^1\text{H}\}$ NMR (100 MHz, DMSO- d_6): δ (ppm) 27.0, 52.4, 124.7, 124.8, 126.6, 127.1, 127.6, 128.6, 128.9, 129.5, 129.6, 131.0, 131.8, 133.2, 134.2, 142.1, 166.9, 168.4, 169.1; IR (KBr): 3438, 2951, 2930, 2853, 1715, 1694, 1634, 1469, 1250, 1188, 1075 cm^{-1} ; HRMS (ESI): calcd. for $\text{C}_{23}\text{H}_{20}\text{NO}_4\text{S}^+$ [$\text{M} + \text{H}^+$] 406.1108; found 406.1118.

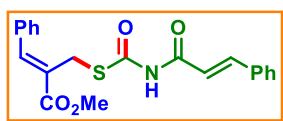
Z-Methyl 3-phenyl-2-(((thiophene-2-carbonyl)carbamoyl)thio)methylacrylate (1i):



Brown solid (78%, 141.2 mg); m.p. 179–181 °C; ^1H NMR (400 MHz, DMSO- d_6): δ (ppm) 3.78 (s, 3H), 4.03 (s, 2H), 7.22 (t, 1H, $J = 8.0$ Hz), 7.45 (m, 3H), 7.54 (d, 2H, $J = 7.2$ Hz), 7.79 (s, 1H), 8.00 (d, 1H, $J = 4.8$ Hz), 8.16 (d, 1H, $J = 3.6$ Hz), 11.99 (s, 1H); $^{13}\text{C}\{^1\text{H}\}$ NMR (100 MHz, DMSO- d_6): δ (ppm) 27.0, 52.4, 126.6, 128.7, 128.9, 129.5, 129.6, 132.1, 134.2, 135.1, 136.8, 142.0, 160.8, 166.9, 169.3; IR (KBr): 3441, 3227, 2922, 1709, 1682, 1633, 1470, 1268 cm^{-1} ; HRMS (ESI): calcd. for $\text{C}_{17}\text{H}_{16}\text{NO}_4\text{S}_2^+$ [$\text{M} + \text{H}^+$] 362.0515; found 362.0521.

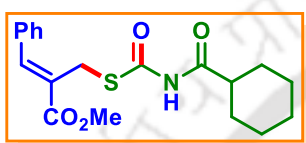
Z-Methyl 2-(((cinnamoyl)carbamoyl)thio)methyl)-3-phenylacrylate (1j):

White solid (74%, 140.9 mg); m.p. 194–196 °C; ^1H NMR (400 MHz, DMSO- d_6): δ (ppm) 3.79 (s, 3H), 4.02 (s, 2H), 6.81 (d, 1H, $J = 16.0$ Hz), 7.46 (m, 6H), 7.54 (d, 2H, $J = 7.2$ Hz), 7.62 (d, 2H, $J = 3.6$ Hz), 7.70 (d, 1H, $J = 16.0$ Hz), 7.80 (s, 1H), 11.65



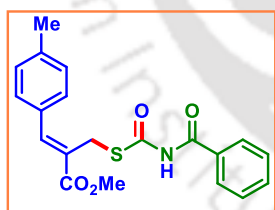
(s, 1H); $^{13}\text{C}\{^1\text{H}\}$ NMR (100 MHz, DMSO- d_6): δ (ppm) 26.8, 52.4, 119.5, 126.5, 128.2, 128.8, 129.1, 129.49, 129.52, 130.7, 134.0, 134.1, 142.0, 144.0, 164.5, 166.8, 168.9; IR (KBr): 3438, 2921, 2851, 1704, 1693, 1634, 1507, 1438, 1195, 1153, 1021 cm^{-1} ; HRMS (ESI): calcd. for $\text{C}_{21}\text{H}_{20}\text{NO}_4\text{S}^+$ $[\text{M} + \text{H}^+]$ 382.1108; found 382.1109.

Z-Methyl 2-(((cyclohexanecarbonyl)carbamoyl)thio)methyl)-3-phenylacrylate (1k):



Pale yellow gummy (89%, 160.7 mg); ^1H NMR (400 MHz, CDCl_3): δ (ppm) 1.24 (m, 4H), 1.44 (m, 2H), 1.76 (m, 2H), 1.88 (d, 2H, $J = 13.2$ Hz), 2.36 (m, 1H), 3.83 (s, 3H), 4.11 (s, 2H), 7.40 (m, 5H), 7.88 (s, 1H), 9.50 (s, 1H); $^{13}\text{C}\{^1\text{H}\}$ NMR (100 MHz, DMSO- d_6): δ (ppm) 25.4, 25.6, 27.7, 28.9, 45.3, 52.5, 126.2, 128.8, 129.4, 129.6, 134.6, 143.6, 167.4, 171.2, 175.8; IR (KBr): 3450, 3063, 2922, 2855, 1715, 1663, 1642, 1448, 1268, 1081 cm^{-1} ; HRMS (ESI): calcd. for $\text{C}_{19}\text{H}_{24}\text{NO}_4\text{S}^+$ $[\text{M} + \text{H}^+]$ 362.1421; found 362.1428.

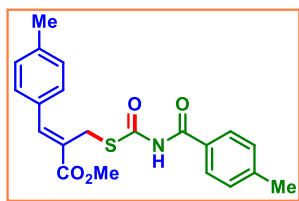
Z-Methyl 2-(((benzoylcarbamoyl)thio)methyl)-3-(*p*-tolyl)acrylate (2a):



White solid (84%, 154.9 mg); m.p. 193–195 °C; ^1H NMR (400 MHz, CDCl_3): δ (ppm) 2.34 (s, 3H), 3.83 (s, 3H), 4.19 (s, 2H), 7.20 (d, 2H, $J = 8.0$ Hz), 7.41 (dd, 4H, $J_1 = 8.4$ Hz, $J_2 = 7.6$ Hz), 7.55 (t, 1H, $J = 7.2$ Hz), 7.89 (s, 1H), 7.95 (d, 2H, $J = 7.6$ Hz), 9.92 (s, 1H); $^{13}\text{C}\{^1\text{H}\}$ NMR (100 MHz, DMSO- d_6): δ (ppm) 20.9, 27.1, 52.3, 125.5, 128.4, 128.6, 129.5, 129.7, 131.3, 131.8, 133.1, 139.4, 142.0, 166.6, 167.0, 169.7; IR (KBr): 3420, 2920, 2853, 1710, 1687, 1638, 1512, 1433, 1258, 1183, 1150 cm^{-1} ; HRMS (ESI): calcd. for $\text{C}_{20}\text{H}_{20}\text{NO}_4\text{S}^+$ $[\text{M} + \text{H}^+]$ 370.1108; found 370.1116.

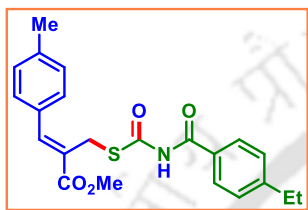
Z-Methyl 2-(((4-methylbenzoyl)carbamoyl)thio)methyl)-3-(*p*-tolyl)acrylate (2b):

White solid (79%, 151.2 mg); m.p. 208–210 °C; ^1H NMR (400 MHz, CDCl_3): δ (ppm) 2.33 (s, 3H), 2.36 (s, 3H), 3.78 (s, 3H), 4.04 (s, 2H), 7.29 (dd, 4H, $J_1 = 8.0$ Hz, $J_2 = 8.4$ Hz), 7.45 (d, 2H, $J = 8.0$ Hz), 7.76 (s, 1H), 7.87 (d, 2H, $J = 8.4$ Hz), 11.84 (s,



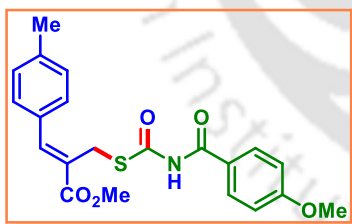
1H); $^{13}\text{C}\{^1\text{H}\}$ NMR (100 MHz, DMSO- d_6): δ (ppm) 20.9, 21.1, 27.0, 52.3, 125.5, 128.4, 128.9, 129.1, 129.5, 129.7, 131.3, 139.5, 142.0, 143.6, 166.4, 167.0, 169.7; IR (KBr): 3447, 2961, 2923, 2855, 1715, 1687, 1639, 1384, 1263 cm^{-1} ; HRMS (ESI): calcd. for $\text{C}_{21}\text{H}_{22}\text{NO}_4\text{S}^+$ [M + H $^+$] 384.1264; found 384.1269.

Z-Methyl 2-(((4-ethylbenzoyl)carbamoyl)thio)methyl)-3-(p-tolyl)acrylate (2c):



White solid (80%, 158.8 mg); m.p. 171–173 °C; ^1H NMR (400 MHz, CDCl_3): δ (ppm) 1.18 (t, 3H, $J = 7.6$ Hz) 2.32(s, 3H), 2.63 (q, 2H, $J = 7.6$ Hz), 3.83 (s, 3H), 4.20 (s, 2H), 7.19 (d, 4H, $J = 7.2$ Hz), 7.40 (d, 2H, $J = 8.0$ Hz), 7.91 (d, 3H, $J = 8.0$ Hz), 10.20 (s, 1H); $^{13}\text{C}\{^1\text{H}\}$ NMR (100 MHz, DMSO- d_6): δ (ppm) 15.2, 21.0, 27.0, 28.2, 52.3, 125.6, 128.0, 128.6, 129.2, 129.5, 129.7, 131.4, 139.5, 142.0, 149.7, 166.5, 167.0, 169.7; IR (KBr): 3442, 2957, 2923, 2853, 1710, 1638, 1576, 1380, 1262, 1020 cm^{-1} ; HRMS (ESI): calcd. for $\text{C}_{22}\text{H}_{24}\text{NO}_4\text{S}^+$ [M + H $^+$] 398.1421; found 398.1430.

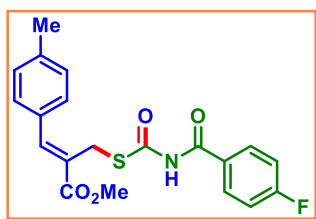
Z-Methyl 2-(((4-methoxybenzoyl)carbamoyl)thio)methyl)-3-(p-tolyl)acrylate (2d):



White solid (71%, 141.6 mg); m.p. 195–197 °C; ^1H NMR (400 MHz, DMSO- d_6): δ (ppm) 2.33 (s, 3H), 3.77 (s, 3H), 3.83 (s, 3H), 4.02 (s, 2H), 7.04 (d, 2H, $J = 9.2$ Hz), 7.28 (d, 2H, $J = 8.0$ Hz), 7.45 (d, 2H, $J = 8.0$ Hz), 7.75 (s, 1H), 7.96 (d, 2H, $J = 8.8$ Hz), 11.76 (s, 1H); $^{13}\text{C}\{^1\text{H}\}$ NMR (100 MHz, DMSO- d_6): δ (ppm) 21.0, 27.0, 52.3, 55.6, 113.9, 123.7, 125.6, 129.5, 129.7, 130.6, 131.4, 139.5, 142.0, 163.2, 165.8, 167.0, 169.8; IR (KBr): 3438, 2954, 2924, 2853, 1719, 1635, 1461, 1384, 1262, 1180, 1020 cm^{-1} ; HRMS (ESI): calcd. for $\text{C}_{21}\text{H}_{22}\text{NO}_5\text{S}^+$ [M + H $^+$] 400.1213; found 400.1217.

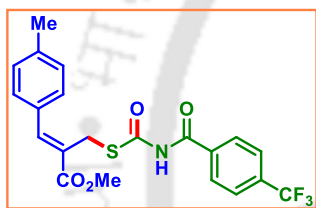
Z-Methyl 2-(((4-fluorobenzoyl)carbamoyl)thio)methyl)-3-(p-tolyl)acrylate (2e):

White solid (91%, 176.1 mg); m.p. 180–182 °C; ^1H NMR (400 MHz, DMSO- d_6): δ (ppm) 2.33 (s, 3H), 3.78 (s, 3H), 4.04(s, 2H), 7.29 (d, 2H, $J = 7.6$ Hz), 7.36 (t, 2H, $J = 8.4$ Hz), 7.46 (d, 2H, $J = 7.6$ Hz), 7.77 (s, 1H), 8.03 (m, 2H), 11.97 (s, 1H);



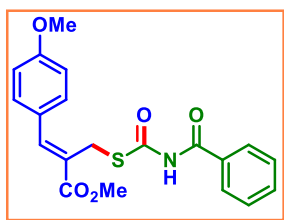
$^{13}\text{C}\{^1\text{H}\}$ NMR (100 MHz, DMSO- d_6): δ (ppm) 20.9, 27.0, 52.3, 115.6 (d, $J = 22.0$ Hz), 125.5, 126.9, 128.34, 128.37, 129.6 (d, $J = 21.7$ Hz), 131.4 (d, $J = 9.2$ Hz), 139.5, 142.0, 163.7, 165.5, 166.2, 167.0, 169.7; ^{19}F NMR (DMSO- d_6 + Hexafluorobenzene): δ (ppm) -110.98 (s); IR (KBr): 3442, 2959, 2924, 2853, 1707, 1634, 1462, 1383, 1259, 1182, 1022 cm^{-1} ; HRMS (ESI): calcd. for $\text{C}_{20}\text{H}_{19}\text{FNO}_4\text{S}^+$ [$\text{M} + \text{H}^+$] 388.1013; found 388.1019.

Z-Methyl 3-(p-tolyl)-2-(((4-(trifluoromethyl)benzoyl)carbamoyl)thio)methyl)acrylate (2f):

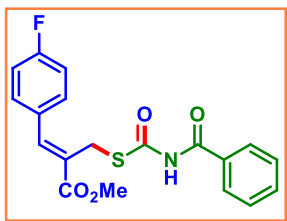


Pale Yellow solid (90%, 196.6 mg); m.p. 172–174 °C; ^1H NMR (400 MHz, DMSO- d_6): δ (ppm) 2.34 (s, 3H), 3.78 (s, 3H), 4.06 (s, 2H), 7.29 (d, 2H, $J = 8.0$ Hz), 7.46 (d, 2H, $J = 8.0$ Hz), 7.77 (s, 1H), 7.90 (d, 2H, $J = 8.4$ Hz), 8.12 (d, 2H, $J = 8.0$ Hz), 12.12 (s, 1H); $^{13}\text{C}\{^1\text{H}\}$ NMR (100 MHz, DMSO- d_6): δ (ppm) 20.9, 27.0, 52.3, 125.1, 125.5 (q, $J = 7.0$ Hz), 129.3, 129.5, 129.7, 131.3, 132.3, 132.7, 135.8, 139.5, 142.1, 165.7, 166.9, 169.5; ^{19}F NMR (DMSO- d_6 + Hexafluorobenzene): δ (ppm) -63.95; IR (KBr): 3441, 2955, 2925, 2854, 1715, 1696, 1633, 1331, 1260, 1129, 1067 cm^{-1} ; HRMS (ESI): calcd. for $\text{C}_{21}\text{H}_{19}\text{F}_3\text{NO}_4\text{S}^+$ [$\text{M} + \text{H}^+$] 438.0981; found 438.0990.

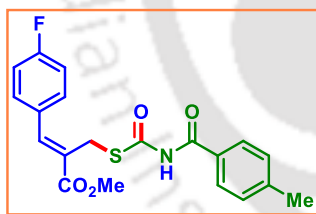
Z-Methyl 2-(((benzoylcarbamoyl)thio)methyl)-3-(4-methoxyphenyl)acrylate (3a):



White solid (77%, 148.2 mg); m.p. 148–150 °C; ^1H NMR (400 MHz, DMSO- d_6): δ (ppm) 3.77 (s, 3H), 3.80 (s, 3H), 4.06 (s, 2H), 7.04 (d, 2H, $J = 8.8$ Hz), 7.54 (m, 4H), 7.64 (t, 1H, $J = 7.2$ Hz), 7.76 (s, 1H), 7.95 (t, 2H, $J = 8.8$ Hz), 11.93 (s, 1H); $^{13}\text{C}\{^1\text{H}\}$ NMR (100 MHz, DMSO- d_6): δ (ppm) 27.2, 52.2, 55.3, 114.4, 123.5, 126.5, 128.4, 128.6, 131.77, 131.84, 133.1, 141.9, 160.4, 166.7, 167.1, 169.8; IR (KBr): 3453, 3003, 2952, 2838, 1719, 1698, 1665, 1511, 1439, 1176, 1031 cm^{-1} ; HRMS (ESI): calcd. for $\text{C}_{20}\text{H}_{20}\text{F}_3\text{NO}_5\text{S}^+$ [$\text{M} + \text{H}^+$] 386.1057; found 386.1058.

Z-Methyl 2-(((benzoylcarbamoyl)thio)methyl)-3-(4-fluorophenyl)acrylate (4a):

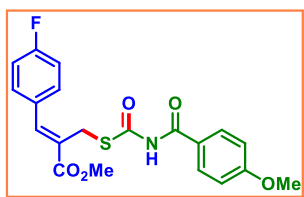
White solid (95%, 177.1 mg); m.p. 164–166 °C; ^1H NMR (400 MHz, $\text{DMSO-}d_6$): δ (ppm) 3.78 (s, 3H), 4.03 (s, 2H), 7.31 (t, 2H, $J = 8.8$ Hz), 7.51 (t, 2H, $J = 7.6$ Hz), 7.62 (dd, 3H, $J_1 = 5.2$ Hz, $J_2 = 2.8$ Hz), 7.78 (s, 1H), 7.95 (d, 2H, $J = 7.6$ Hz), 11.92 (s, 1H); $^{13}\text{C}\{^1\text{H}\}$ NMR (100 MHz, $\text{DMSO-}d_6$): δ (ppm) 26.8, 52.4, 115.9 (d, $J = 21.5$ Hz), 126.5, 128.5 (d, $J = 23.9$ Hz), 130.8 (d, $J = 3.1$ Hz), 131.8, 132.0 (d, $J = 8.5$ Hz), 133.2, 140.8, 161.3, 163.8, 166.7, 166.9, 169.6 ; ^{19}F NMR ($\text{DMSO-}d_6 + \text{Hexafluorobenzene}$): δ (ppm) -113.27 (s); IR (KBr): 3438, 2921, 2851, 1634, 1507, 1438, 1255, 1195, 1153, 1021 cm^{-1} ; HRMS (ESI): calcd. for $\text{C}_{19}\text{H}_{17}\text{FNO}_4\text{S}^+$ [$\text{M} + \text{H}^+$] 374.0857; found 374.0863.

Z-Methyl 3-(4-fluorophenyl)-2-(((4-methylbenzoyl)carbamoyl)thio)methyl)acrylate (4b):

White solid (93%, 179.9 mg); m.p. 193–195 °C; ^1H NMR (400 MHz, $\text{DMSO-}d_6$): δ (ppm) 2.37 (s, 3H), 3.78 (s, 3H), 4.01 (s, 2H), 7.33 (m, 4H), 7.62 (m, 2H), 7.78 (s, 1H), 7.86 (d, 2H, $J = 8.0$ Hz), 11.84 (s, 1H); $^{13}\text{C}\{^1\text{H}\}$ NMR (100 MHz, $\text{DMSO-}d_6$): δ (ppm) 21.1, 26.8, 52.4, 115.9 (d, $J = 21.6$ Hz), 126.51, 126.53, 128.4, 128.9, 129.2, 130.7 (d, $J = 3.2$ Hz), 132.0 (d, $J = 8.6$ Hz), 140.7, 143.6, 163.7, 166.4, 166.8, 169.6; ^{19}F NMR ($\text{DMSO-}d_6 + \text{Hexafluorobenzene}$): δ (ppm) -113.33; IR (KBr): 3452, 2922, 2855, 1639, 1508, 1435, 1384, 1262, 1161 cm^{-1} ; HRMS (ESI): calcd. for $\text{C}_{20}\text{H}_{19}\text{FNO}_4\text{S}^+$ [$\text{M} + \text{H}^+$] 388.1013; found 388.1020.

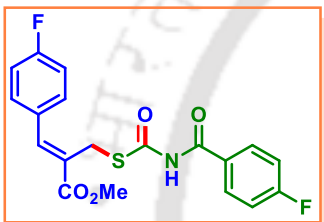
Z-Methyl 3-(4-fluorophenyl)-2-(((4-methoxybenzoyl)carbamoyl)thio)methyl)acrylate (4d):

White solid (86%, 173.3 mg); m.p. 188–190 °C; ^1H NMR (400 MHz, $\text{DMSO-}d_6$): δ (ppm) 3.79 (s, 3H), 3.84 (s, 3H), 4.00 (s, 2H), 7.05 (d, 2H, $J = 8.8$ Hz), 7.33 (t, 2H, $J = 8.4$ Hz), 7.63 (dd, 2H, $J_1 = 5.6$ Hz, $J_2 = 2.8$ Hz), 7.78 (s, 1H), 7.96 (d, 2H, $J = 8.8$ Hz), 11.77 (s, 1H); $^{13}\text{C}\{^1\text{H}\}$ NMR (100 MHz, $\text{DMSO-}d_6$): δ



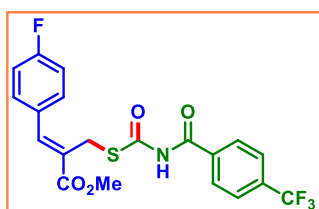
(ppm) 26.8, 52.4, 55.6, 113.9, 115.9 (d, $J = 21.5$ Hz), 123.6, 126.5, 130.6, 130.8(d, $J = 3.1$ Hz), 132.0 (d, $J = 8.6$ Hz), 140.6, 163.2, 165.8, 166.8, 169.6 ; ^{19}F NMR (DMSO- d_6 + Hexafluorobenzene): δ (ppm) -113.36; IR (KBr): 3435, 2955, 2924, 2854, 1719, 1688, 1636, 1607, 1507, 1469, 1255, 1195 cm^{-1} ; HRMS (ESI): calcd. for $\text{C}_{20}\text{H}_{19}\text{FNO}_5\text{S}^+$ [$\text{M} + \text{H}^+$] 404.0962; found 404.0963.

Z-Methyl 2-(((4-fluorobenzoyl)carbamoyl)thio)methyl)-3-(4-fluorophenyl)acrylate (4e):



White solid (97%, 208.2 mg); m.p. 189–191 °C; ^1H NMR (400 MHz, DMSO- d_6): δ (ppm) 3.79 (s, 3H), 4.02 (s, 2H), 7.34 (m, 4H), 7.63 (dd, 2H, $J_1 = 5.6$ Hz, $J_2 = 2.8$ Hz), 7.78 (s, 1H), 8.03 (dd, 2H, $J_1 = 5.2$ Hz, $J_2 = 3.2$ Hz), 11.94 (s, 1H); $^{13}\text{C}\{^1\text{H}\}$ NMR (100 MHz, DMSO- d_6): δ (ppm) 26.8, 52.4, 115.7 (d, $J = 20.8$ Hz), 115.9 (d, $J = 20.3$ Hz), 126.5, 128.3 (d, $J = 2.7$ Hz), 130.7 (d, $J = 3.2$ Hz), 131.4 (d, $J = 9.5$ Hz), 132.0 (d, $J = 8.5$ Hz), 140.7, 161.3, 163.7, 165.5, 166.8, 169.6; ^{19}F NMR (DMSO- d_6 + Hexafluorobenzene): δ (ppm) -111.02, -107.93; IR (KBr): 3440, 2924, 2849, 1713, 1634, 1601, 1508, 1437, 1257, 1195, 1159, 1071 cm^{-1} ; HRMS (ESI): calcd. for $\text{C}_{19}\text{H}_{16}\text{F}_2\text{NO}_4\text{S}^+$ [$\text{M} + \text{H}^+$] 392.0763; found 392.0772.

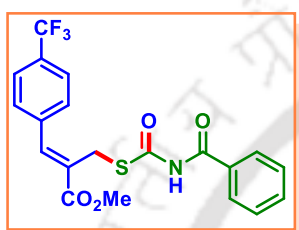
Z-Methyl 3-(4-fluorophenyl)-2-(((4-(trifluoromethyl)benzoyl)carbamoyl)thio)methyl)acrylate (4f):



White solid (96%, 211.6 mg); m.p. 192–194 °C; ^1H NMR (400 MHz, DMSO- d_6): δ (ppm) 3.79 (s, 3H), 4.04 (s, 2H), 7.32 (t, 2H, $J = 8.8$ Hz), 7.62 (dd, 2H, $J_1 = 8.4$ Hz, $J_2 = 8.4$ Hz), 7.79 (s, 1H), 7.89 (d, 2H, $J = 8.4$ Hz), 8.11 (d, 2H, $J = 8.4$ Hz), 12.13 (s, 1H); $^{13}\text{C}\{^1\text{H}\}$ NMR (100 MHz, DMSO- d_6): δ (ppm) 26.8, 52.4, 115.9 (d, $J = 21.6$ Hz), 125.5 (q, $J = 3.6$ Hz), 126.4 (d, $J = 1.2$ Hz), 129.3, 130.8 (d, $J = 3.2$ Hz), 132.0 (d, $J = 8.5$ Hz), 135.8, 140.8, 161.3, 163.8, 165.8, 166.8, 169.5; ^{19}F NMR (DMSO- d_6 + Hexafluorobenzene): δ (ppm) -113.36, -64.00; IR (KBr): 3438,

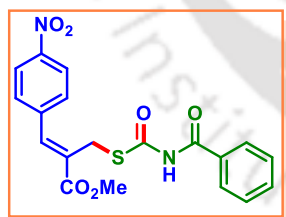
2955, 2922, 2853, 2727, 2632, 2598, 2505, 1441, 1327, 1259, 1184, 1155, 1067 cm^{-1} ; HRMS (ESI): calcd. for $\text{C}_{20}\text{H}_{16}\text{F}_4\text{NO}_4\text{S}^+$ $[\text{M} + \text{H}^+]$ 442.0731; found 442.0741.

Z-methyl 2-(((benzoylcarbamoyl)thio)methyl)-3-(4-(trifluoromethyl)phenyl)acrylate (5a):



White solid (93%, 196.7 mg); m.p. 172–174 °C; ^1H NMR (400 MHz, $\text{DMSO}-d_6$): δ (ppm) 3.80 (s, 3H), 4.02 (s, 2H), 7.50 (t, 2H, $J = 8.0$ Hz), 7.62 (t, 1H, $J = 7.2$ Hz), 7.73 (d, 2H, $J = 8.0$ Hz), 7.81 (d, 3H, $J = 9.6$ Hz), 7.95 (d, 2H, $J = 7.6$ Hz), 11.91 (s, 1H); $^{13}\text{C}\{^1\text{H}\}$ NMR (100 MHz, $\text{DMSO}-d_6$): δ (ppm) 26.6, 52.4, 125.5 (q, $J = 3.6$ Hz), 128.3, 128.6, 129.0, 129.3, 129.4, 130.0, 131.8, 133.1, 138.5, 139.9, 166.57, 166.62, 169.5; ^{19}F NMR ($\text{DMSO}-d_6 + \text{Hexafluorobenzene}$): δ (ppm) -63.68; IR (KBr): 3438, 2956, 2921, 2851, 1722, 1695, 1636, 1471, 1326, 1250, 1107, 1015 cm^{-1} ; HRMS (ESI): calcd. for $\text{C}_{20}\text{H}_{17}\text{F}_3\text{NO}_4\text{S}^+$ $[\text{M} + \text{H}^+]$ 424.0825; found 424.0829.

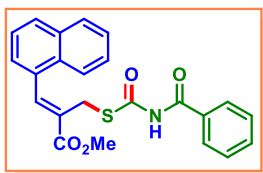
Z-Methyl 2-(((benzoylcarbamoyl)thio)methyl)-3-(4-nitrophenyl)acrylate (6a):



Yellow solid (88%, 176.2 mg); m.p. 183–185 °C; ^1H NMR (400 MHz, $\text{DMSO}-d_6$): δ (ppm) 3.81 (s, 3H), 4.01 (s, 2H), 7.51 (t, 2H, $J = 7.6$ Hz), 7.61 (m, 1H), 7.79 (d, 2H, $J = 8.8$ Hz), 7.84 (s, 1H), 7.93 (t, 2H, $J = 8.4$ Hz), 8.30 (d, 2H, $J = 8.8$ Hz), 11.90 (s, 1H); $^{13}\text{C}\{^1\text{H}\}$ NMR (100 MHz, $\text{DMSO}-d_6$): δ (ppm) 26.5, 52.5, 123.7, 128.3, 128.6, 130.5, 130.6, 131.7, 133.2, 139.1, 141.1, 147.2, 166.4, 166.6, 169.4; IR (KBr): 3434, 2952, 2923, 2851, 1719, 1638, 1541, 1515, 1471, 1344, 1278, 1068 cm^{-1} ; HRMS (ESI): calcd. for $\text{C}_{19}\text{H}_{17}\text{N}_2\text{O}_6\text{S}^+$ $[\text{M} + \text{H}^+]$ 401.0802; found 401.0809.

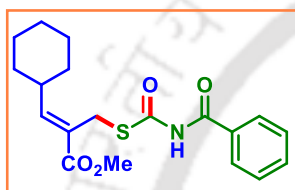
Z-Methyl 2-(((benzoylcarbamoyl)thio)methyl)-3-(naphthalen-1-yl)acrylate (7a):

White solid (95%, 192.3 mg); m.p. 161–163 °C; ^1H NMR (400 MHz, $\text{DMSO}-d_6$): δ (ppm) 3.81 (s, 3H), 4.17 (s, 2H), 7.51 (t, 2H, $J = 7.2$ Hz), 7.56 (m, 2H), 7.64 (m, 2H), 7.94 (t, 6H, $J = 10.0$



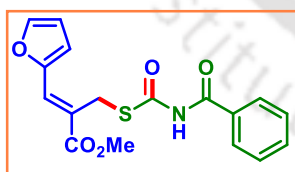
Hz), 8.09 (s, 1H), 11.93 (s, 1H); $^{13}\text{C}\{^1\text{H}\}$ NMR (100 MHz, DMSO- d_6): δ (ppm) 26.9, 52.4, 126.5, 126.8, 127.1, 127.4, 127.5, 127.6, 128.3, 128.4, 128.5, 128.6, 129.8, 131.9, 132.7, 133.0, 133.2, 141.8, 166.7, 167.0, 169.7; IR (KBr): 3439, 2950, 2920, 2853, 1704, 1694, 1638, 1510, 1432, 1259, 1064 cm^{-1} ; HRMS (ESI): calcd. for $\text{C}_{23}\text{H}_{20}\text{NO}_4\text{S}^+$ [$\text{M} + \text{H}^+$] 406.1108; found 406.1118.

Z-Methyl 2-(((benzoylcarbamoyl)thio)methyl)-3-cyclohexylacrylate (8a):



Pale yellow gummy (73%, 131.7 mg); ^1H NMR (400 MHz, CDCl_3): δ (ppm) 1.24 (m, 4H), 1.47 (m, 2H), 1.77 (t, 2H, $J = 9.2$ Hz) 1.89 (d, 2H, $J = 13.2$ Hz), 2.37 (m, 1H), 3.83 (s, 3H), 4.11 (s, 2H), 7.41 (m, 5H), 7.88 (s, 1H), 9.50 (s, 1H); $^{13}\text{C}\{^1\text{H}\}$ NMR (100 MHz, DMSO- d_6): δ (ppm) 25.4, 25.6, 27.7, 28.9, 45.3, 52.5, 126.2, 128.8, 129.4, 129.6, 134.6, 143.6, 167.4, 171.2, 175.8; IR (KBr): 3453, 2955, 2922, 2838, 1729, 1663, 1605, 1435, 1257, 1031 cm^{-1} ; HRMS (ESI): calcd. for $\text{C}_{19}\text{H}_{24}\text{NO}_4\text{S}^+$ [$\text{M} + \text{H}^+$] 362.1421; found 362.1427.

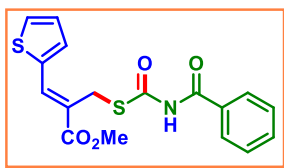
Z-Methyl 2-(((benzoylcarbamoyl)thio)methyl)-3-(furan-2-yl)acrylate (9a):



Yellow solid (81%, 139.7 mg); m.p. 142–144 °C; ^1H NMR (400 MHz, CDCl_3): δ (ppm) 3.83 (s, 3H), 4.36 (s, 2H), 7.11 (dd, 1H, $J_1 = 4.8$ Hz, $J_2 = 5.2$ Hz), 7.38 (d, 1H, $J = 3.6$ Hz), 7.48 (t, 2H, $J = 7.6$ Hz), 7.53 (d, 1H, $J = 4.8$ Hz), 7.59 (t, 1H, $J = 14.4$ Hz), 7.94 (d, 2H, $J = 7.6$ Hz), 8.01 (s, 1H), 9.72 (s, 1H); $^{13}\text{C}\{^1\text{H}\}$ NMR (100 MHz, CDCl_3): δ (ppm) 28.3, 52.7, 122.0, 127.9, 128.0, 129.2, 130.3, 131.2, 131.8, 133.6, 135.8, 137.5, 165.8, 167.6, 172.2; IR (KBr): 3434, 2952, 2925, 2853, 1699, 1662, 1636, 1468, 1436, 1257, 1207, 1072 cm^{-1} ; HRMS (ESI): calcd. for $\text{C}_{17}\text{H}_{16}\text{NO}_5\text{S}^+$ [$\text{M} + \text{H}^+$] 346.0744; found 346.0745.

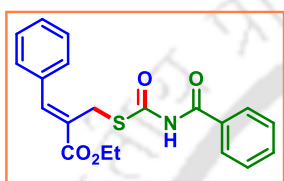
Z-Methyl 2-(((benzoylcarbamoyl)thio)methyl)-3-(thiophen-2-yl)acrylate (10a):

Brown solid (83%, 150.2 mg); m.p. 164–166 °C; ^1H NMR (400 MHz, CDCl_3): δ (ppm) 3.71 (s, 3H), 4.35 (s, 2H), 6.40 (dd, 1H, $J_1 = 3.6$ Hz, $J_2 = 3.6$ Hz), 6.65 (d, 1H, $J = 3.2$ Hz), 7.39 (t, 2H,



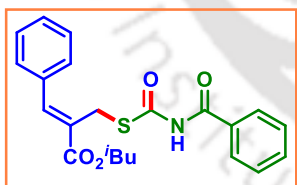
$J = 7.6$ Hz), 7.48 (m, 3H), 7.84 (d, 2H, $J = 7.6$ Hz), 9.59 (s, 1H); $^{13}\text{C}\{^1\text{H}\}$ NMR (100 MHz, CDCl_3): δ (ppm) 28.3, 52.7, 122.0, 127.9, 128.0, 128.1, 129.2, 131.2, 131.8, 133.6, 135.8, 137.5, 165.8, 167.6, 172.2; IR (KBr): 3439, 2952, 2924, 2853, 1700, 1661, 1633, 1506, 1472, 1259, 1191, 1020 cm^{-1} ; HRMS (ESI): calcd. for $\text{C}_{17}\text{H}_{16}\text{NO}_4\text{S}_2^+$ [$\text{M} + \text{H}^+$] 362.0515; found 363.0520.

Z-Ethyl 2-(((benzoylcarbamoyl)thio)methyl)-3-phenylacrylate (11a):



White solid (94%, 173.4 mg); m.p. 149–151 °C; ^1H NMR (400 MHz, $\text{DMSO}-d_6$): δ (ppm) 1.28 (t, 3H, $J = 7.2$ Hz), 4.05 (s, 2H), 4.24 (q, 2H, $J = 7.2$ Hz), 7.48 (m, 7H), 7.63 (t, 1H, $J = 7.2$ Hz), 7.79 (s, 1H), 7.94 (d, 2H, $J = 7.2$ Hz), 11.91 (s, 1H); $^{13}\text{C}\{^1\text{H}\}$ NMR (100 MHz, $\text{DMSO}-d_6$): δ (ppm) 14.1, 26.9, 61.1, 127.0, 128.4, 128.6, 128.9, 129.4, 129.5, 131.8, 133.2, 134.3, 141.7, 166.4, 166.7, 169.6; IR (KBr): 3437, 2955, 2921, 2851, 1708, 1696, 1632, 1462, 1260, 1199, 1074 cm^{-1} ; HRMS (ESI): calcd. for $\text{C}_{20}\text{H}_{20}\text{NO}_4\text{S}^+$ [$\text{M} + \text{H}^+$] 370.1108; found 370.1116.

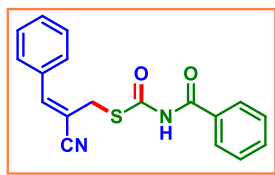
Z-Isobutyl 2-(((benzoylcarbamoyl)thio)methyl)-3-phenylacrylate (12a):



White solid (89%, 165.9 mg); m.p. 168–170 °C; ^1H NMR (400 MHz, $\text{DMSO}-d_6$): δ (ppm) 0.94 (s, 3H), 0.96 (s, 3H), 1.98 (m, 1H), 3.99 (d, 2H, $J = 6.4$ Hz), 4.06 (s, 2H), 7.49 (m, 7H), 7.64 (t, 1H, $J = 7.2$ Hz), 7.81 (s, 1H), 7.95 (t, 2H, $J = 7.2$ Hz), 11.92 (s, 1H); $^{13}\text{C}\{^1\text{H}\}$ NMR (100 MHz, $\text{DMSO}-d_6$): δ (ppm) 18.9, 26.9, 27.4, 70.8, 126.9, 128.4, 128.6, 128.8, 129.4, 129.5, 131.8, 133.2, 134.2, 141.8, 166.3, 166.6, 169.6; IR (KBr): 3436, 2962, 2921, 2851, 1711, 1694, 1636, 1511, 1467, 1259, 1193, 1068 cm^{-1} ; HRMS (ESI): calcd. for $\text{C}_{22}\text{H}_{24}\text{NO}_4\text{S}^+$ [$\text{M} + \text{H}^+$] 398.1421; found 398.1426.

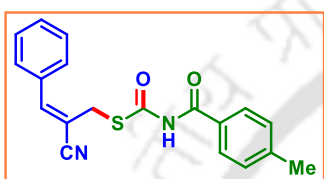
Z-S-(2-Cyano-3-phenylallyl) benzoylcarbamothioate (13a):

White solid (77%, 123.6 mg); m.p. 138–140 °C; ^1H NMR (400 MHz, CDCl_3): δ (ppm) 3.84 (s, 2H), 7.11 (s, 1H), 7.30 (s, 3H), 7.42 (m, 2H), 7.52 (m, 1H), 7.60 (d, 2H, $J = 1.6$ Hz), 7.84 (dd, 2H, $J = 6.8$ Hz), 9.65 (s, 1H); $^{13}\text{C}\{^1\text{H}\}$ NMR (100 MHz, CDCl_3):



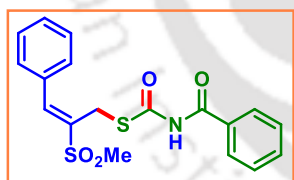
δ (ppm) 34.7, 106.9, 118.0, 128.1, 129.0, 129.1, 129.2, 130.8, 131.6, 133.1, 133.8, 146.3, 166.0, 170.5; IR (KBr): 3448, 2922, 2851, 2215, 1697, 1661, 1643, 1505, 1470, 1180 cm^{-1} ; HRMS (ESI): calcd. for $\text{C}_{18}\text{H}_{15}\text{N}_2\text{O}_2\text{S}^+$ [$\text{M} + \text{H}^+$] 323.0849; found 323.0855.

Z-S-(2-Cyano-3-phenylallyl) (4-methylbenzoyl)carbamothioate (13b):



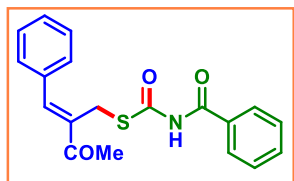
White solid (71%, 119.3 mg); m.p. 173–175 °C; ^1H NMR (400 MHz, CDCl_3): δ (ppm) 2.33 (s, 3H), 3.85 (s, 2H), 7.14 (s, 1H), 7.22 (d, 2H, $J = 8.0$ Hz), 7.32 (d, 4H, $J = 3.2$ Hz), 7.62 (d, 1H, $J = 3.2$ Hz), 7.73 (d, 2H, $J = 8.0$ Hz), 9.44 (s, 1H); $^{13}\text{C}\{^1\text{H}\}$ NMR (100 MHz, CDCl_3): δ (ppm) 21.9, 34.7, 107.0, 118.1, 128.1, 128.7, 129.0, 129.1, 129.9, 130.8, 133.2, 144.9, 146.3, 165.8, 170.4; IR (KBr): 3437, 2986, 2928, 2853, 2212, 1691, 1638, 1610, 1462, 1263, 1198 cm^{-1} ; HRMS (ESI): calcd. for $\text{C}_{19}\text{H}_{17}\text{N}_2\text{O}_2\text{S}^+$ [$\text{M} + \text{H}^+$] 337.1005; found 337.1113.

E-S-(2-(Methylsulfonyl)-3-phenylallyl) benzoylcarbamothioate (14a):



Gummy (69%, 129.4 mg); ^1H NMR (400 MHz, $\text{DMSO}-d_6$): δ (ppm) 3.20 (s, 3H), 4.24 (s, 2H), 7.50–7.55 (m, 5H), 7.63 (dd, 3H, $J_1 = 7.6$ Hz, $J_2 = 7.6$ Hz), 7.73 (s, 1H), 7.95 (t, 2H, $J = 8.4$ Hz), 12.04 (s, 1H); $^{13}\text{C}\{^1\text{H}\}$ NMR (100 MHz, $\text{DMSO}-d_6$): δ (ppm) 25.8, 41.9, 128.4, 128.6, 129.1, 129.8, 130.3, 131.7, 132.6, 133.3, 136.7, 141.1, 166.8, 169.3; IR (KBr): 3418, 3259, 2955, 2925, 2855, 1693, 1628, 1487, 1302, 1256, 1178, 1120, 1025 cm^{-1} ; HRMS (ESI): calcd. for $\text{C}_{18}\text{H}_{18}\text{NO}_4\text{S}_2^+$ [$\text{M} + \text{H}^+$] 376.0672; found 376.0679.

Z-S-(2-Benzylidene-3-oxobutyl) benzoylcarbamothioate (15a):

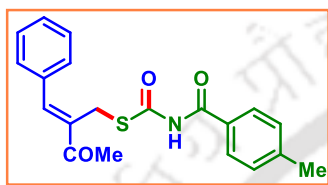


White solid (78%, 132.2 mg); m.p. 172–174 °C; ^1H NMR (400 MHz, CDCl_3): δ (ppm) 2.49 (s, 3H), 4.14 (s, 2H), 7.42 (dd, 5H, $J_1 = 14.4$ Hz, $J_2 = 8.0$ Hz), 7.49 (dd, 3H, $J_1 = 10.8$ Hz, $J_2 = 12.4$ Hz), 7.72 (s, 1H), 7.92 (t, 2H, $J = 8.4$ Hz), 9.91 (s, 1H); $^{13}\text{C}\{^1\text{H}\}$ NMR (100 MHz, CDCl_3): δ (ppm) 26.0, 29.7, 128.0, 128.97,

128.99, 129.7, 130.2, 131.8, 133.5, 134.7, 135.6, 143.8, 165.9, 171.7, 198.4; IR (KBr): 3448, 2983, 2925, 2851, 1664, 1637, 1469, 1381, 1255, 1178, 1024 cm^{-1} ; HRMS (ESI): calcd. for $\text{C}_{19}\text{H}_{18}\text{NO}_3\text{S}^+$ [$\text{M} + \text{H}^+$] 340.1002; found 340.1113.

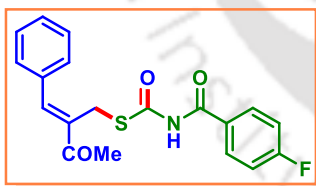
Z-S-(2-Benzylidene-3-oxobutyl) (4-methylbenzoyl)carbamothioate (15b):

White solid (74%, 130.6 mg); m.p. 158–160 °C; ^1H NMR (400 MHz, $\text{DMSO}-d_6$): δ (ppm) 2.40 (s, 3H), 2.53 (s, 3H), 4.03 (s, 2H), 7.35 (d, 2H, $J = 8.4$ Hz), 7.48 (t, 1H, $J = 7.2$ Hz), 7.54 (dd, 2H, $J_1 = 7.6$ Hz, $J_2 = 7.2$ Hz), 7.65 (d, 2H, $J = 7.2$ Hz), 7.90 (s, 1H), 7.92 (d, 2H, $J = 3.2$ Hz), 11.82 (s, 1H); $^{13}\text{C}\{^1\text{H}\}$ NMR (100 MHz, $\text{DMSO}-d_6$): δ (ppm) 21.1, 25.5, 25.9, 127.5, 128.4, 128.8, 129.1, 129.4, 129.6, 134.7, 135.2, 143.3, 143.5, 166.4, 169.9, 198.6; IR (KBr): 3436, 2952, 2923, 2852, 1659, 1636, 1485, 1258, 1025 cm^{-1} ; HRMS (ESI): calcd. for $\text{C}_{20}\text{H}_{20}\text{NO}_3\text{S}^+$ [$\text{M} + \text{H}^+$] 354.1158; found 354.1160.



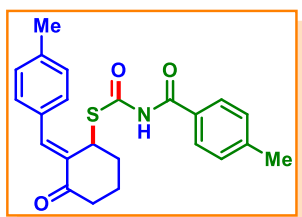
Z-S-(2-Benzylidene-3-oxobutyl) (4-fluorobenzoyl)carbamothioate (15e):

White solid (81%, 144.6 mg); m.p. 138–140 °C; ^1H NMR (400 MHz, $\text{DMSO}-d_6$): δ (ppm) 3.01 (s, 3H), 4.51 (s, 2H), 7.86 (t, 2H, $J = 8.8$ Hz), 7.96 (d, 1H, $J = 7.2$ Hz), 8.01 (t, 2H, $J = 7.6$ Hz), 8.12 (d, 2H, $J = 7.2$ Hz), 8.41 (s, 1H), 8.54–8.58 (m, 2H), 12.40 (s, 1H); $^{13}\text{C}\{^1\text{H}\}$ NMR (100 MHz, $\text{DMSO}-d_6$): δ (ppm) 25.5, 25.8, 115.5, 115.7, 128.8, 129.5, 129.6, 131.3, 131.4, 134.7, 135.1, 143.3, 165.5, 169.9, 198.6; ^{19}F NMR ($\text{DMSO}-d_6 + \text{Hexafluorobenzene}$): δ (ppm) -108.49 (s); IR (KBr): 3432, 2975, 2922, 2851, 1668, 1630, 1453, 1256, 1025 cm^{-1} ; HRMS (ESI): calcd. for $\text{C}_{19}\text{H}_{17}\text{FNO}_3\text{S}^+$ [$\text{M} + \text{H}^+$] 358.0986; found 358.0989.



Z-S-(2-(4-Methylbenzylidene)-3-oxocyclohexyl) (4-methylbenzoyl)carbamothioate (16b):

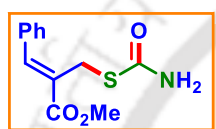
Gummy (55%, 108.1 mg); ^1H NMR (400 MHz, CDCl_3): δ (ppm) 0.83–0.90 (m, 3H), 1.91–1.97 (m, 1H), 2.03–2.11 (m, 1H), 2.32 (s, 3H), 2.40 (s, 3H), 2.73 (d, 1H, $J = 13.6$ Hz), 5.34 (s, 1H), 7.18 (d, 2H, $J = 8.0$ Hz), 7.24 (d, 1H, $J = 7.6$ Hz), 7.41 (d, 2H, $J = 8.0$



(Hz), 7.56 (s, 1H), 7.80 (d, 2H, $J = 8.0$ Hz), 9.37 (s, 1H); $^{13}\text{C}\{^1\text{H}\}$ NMR (100 MHz, CDCl_3): δ (ppm) 19.6, 21.6, 21.8, 29.9, 39.9, 44.3, 128.0, 129.0, 129.7, 129.9, 131.0, 131.9, 133.8, 139.6, 140.1, 144.7, 165.5, 170.5, 200.0; IR (KBr): 3439, 3125, 2956, 2922, 2857, 1668, 1635, 1566, 1453, 1256, 1025 cm^{-1} ; HRMS (ESI): calcd. for $\text{C}_{23}\text{H}_{24}\text{NO}_3\text{S}^+$ [$\text{M} + \text{H}^+$] 394.1471; found 394.1479.

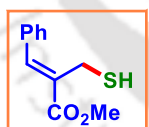
Methyl 2-((carbamoylthio)methyl)-3-phenylacrylate (1ab):

Pale yellow solid (72%, 25.3 mg); m.p. 99–101 °C; ^1H NMR (600 MHz, CDCl_3): δ (ppm) 3.84 (s, 3H), 4.10 (s, 2H), 5.66 (s, 2H), 7.37 (m, 1H), 7.41 (m, 2H), 7.45 (d, 2H, $J = 7.2$ Hz), 7.81 (s, 1H); $^{13}\text{C}\{^1\text{H}\}$ NMR (150 MHz, CDCl_3): δ (ppm) 28.0, 52.6, 127.2, 128.9, 129.5, 129.8, 134.6, 142.8, 167.8, 168.7; IR (KBr): 3459, 3327, 2950, 2924, 2854, 1702, 1662, 1629, 1384, 1268 cm^{-1} ; HRMS (ESI): calcd. for $\text{C}_{12}\text{H}_{14}\text{NO}_3\text{S}^+$ [$\text{M} + \text{H}^+$] 252.0689; found 252.0692.



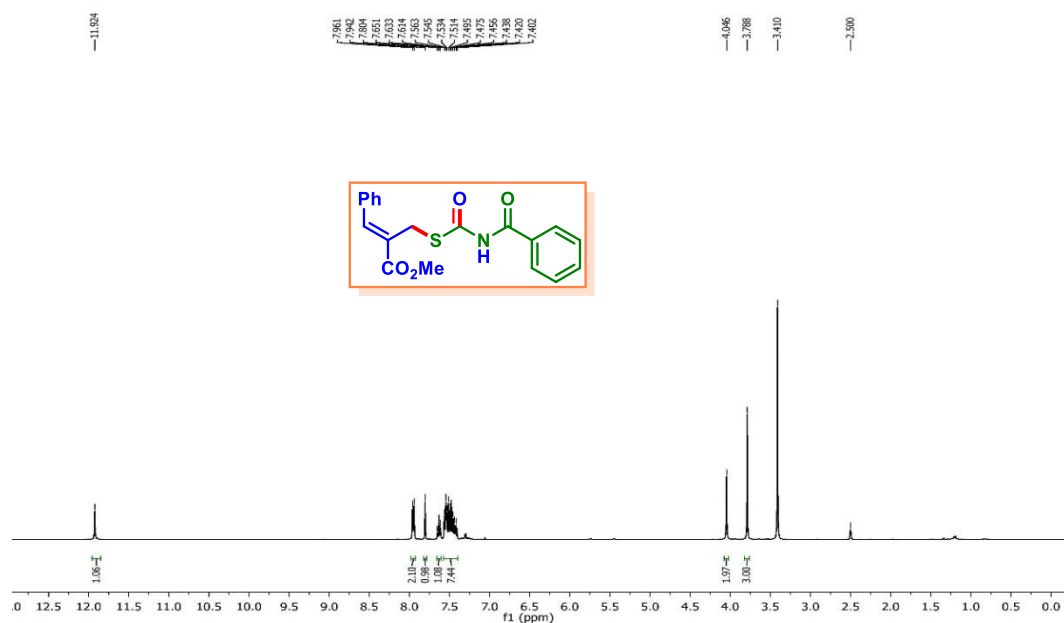
Methyl 2-(mercaptomethyl)-3-phenylacrylate (1ac):

Gummy white solid (79%, 23.1 mg); ^1H NMR (600 MHz, CDCl_3): δ (ppm) 1.65 (s, 1H), 3.74 (s, 2H), 3.84 (s, 3H), 7.36 (d, 1H, $J = 7.8$ Hz), 7.40 (t, 2H, $J = 7.8$ Hz), 7.50 (d, 2H, $J = 7.2$ Hz), 7.76 (s, 1H); $^{13}\text{C}\{^1\text{H}\}$ NMR (150 MHz, CDCl_3): δ (ppm) 30.3, 52.5, 128.8, 128.9, 129.2, 129.9, 135.0, 141.4, 168.0; IR (KBr): 3051, 2950, 2851, 2929, 1712, 1632, 1434, 1265, 1080 cm^{-1} ; HRMS (ESI): calcd. for $\text{C}_{11}\text{H}_{13}\text{O}_2\text{S}^+$ [$\text{M} + \text{H}^+$] 209.0631; found 209.0638.

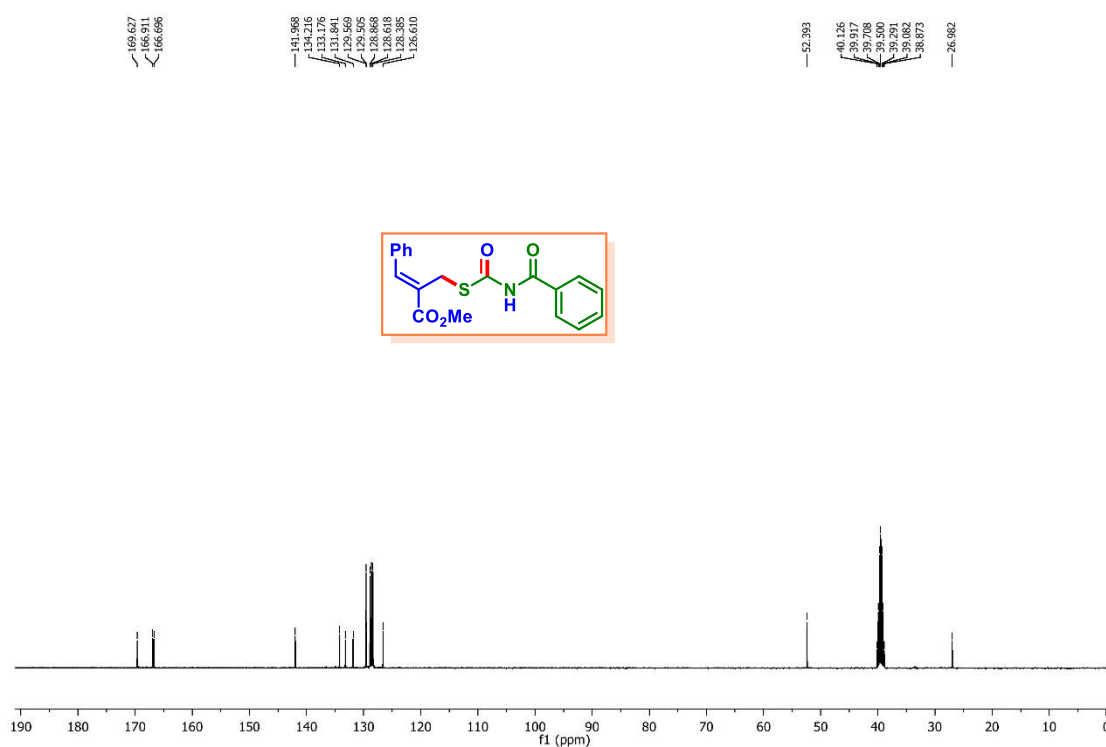


III.7. Representative Spectra

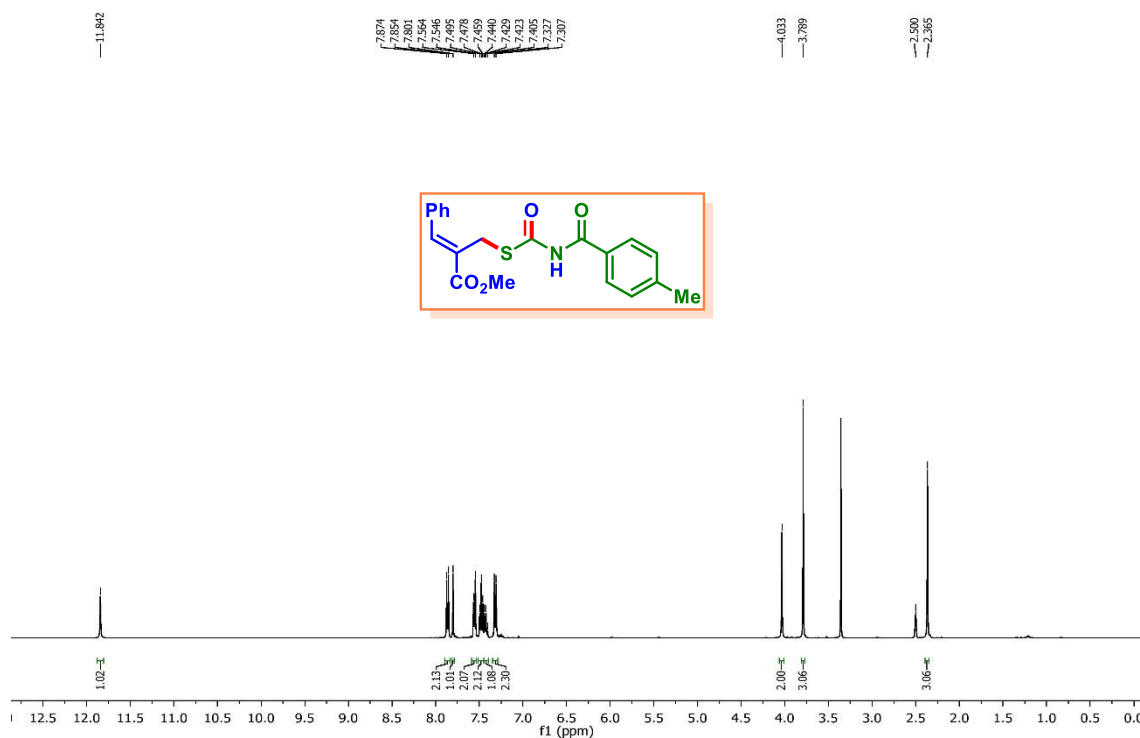
Z-Methyl-2-(((benzoylcarbamoyl)thio)methyl)-3-phenylacrylate (1a): ^1H NMR (400 MHz, $\text{DMSO-}d_6$)



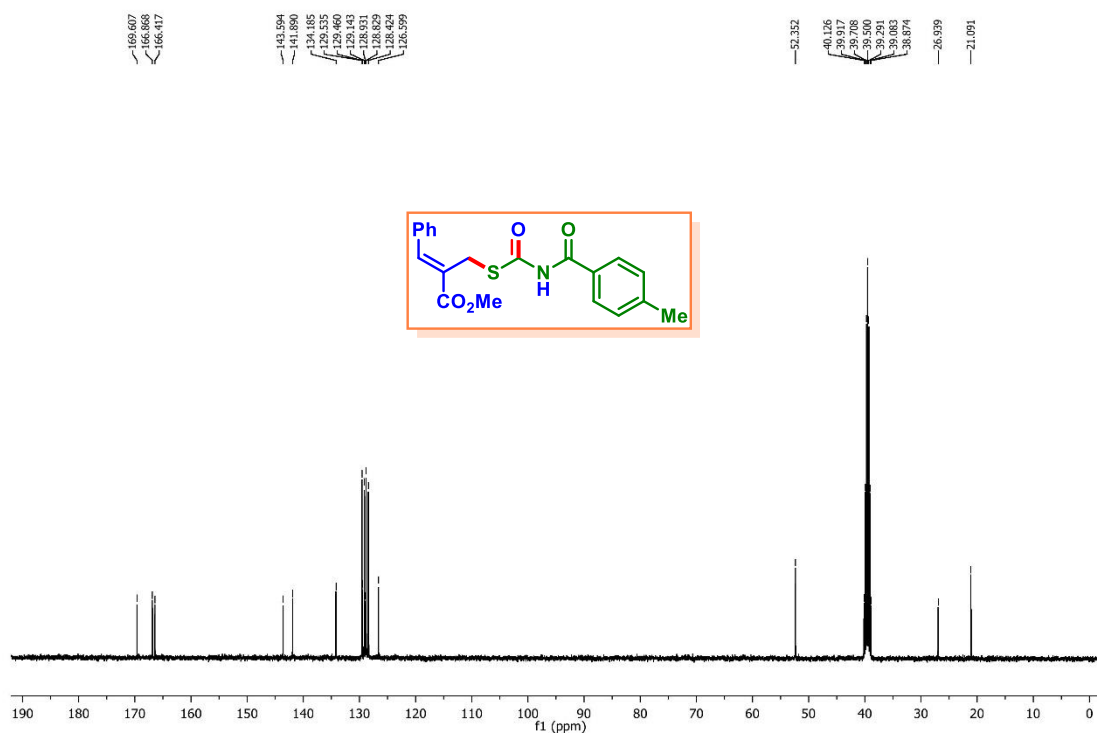
Z-Methyl-2-(((benzoylcarbamoyl)thio)methyl)-3-phenylacrylate (1a): $^{13}\text{C}\{^1\text{H}\}$ NMR (100 MHz, $\text{DMSO-}d_6$)



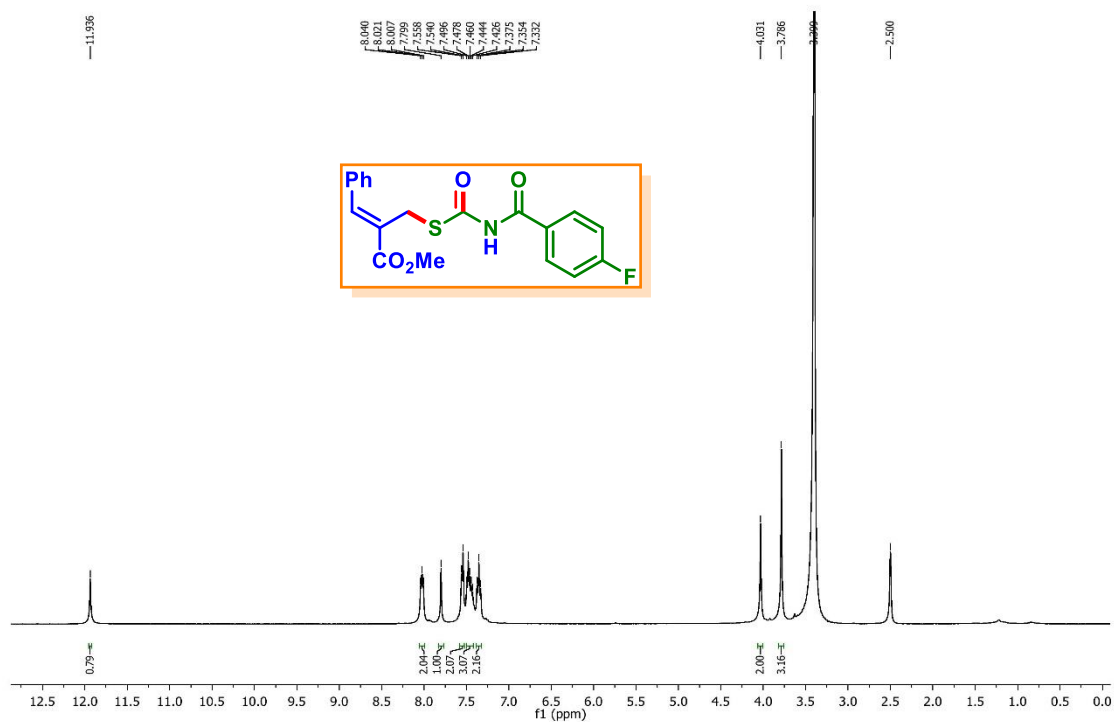
Z-Methyl 2-(((4-methylbenzoyl)carbamoyl)thio)methyl)-3-phenylacrylate (1b): ^1H NMR (400 MHz, $\text{DMSO-}d_6$)



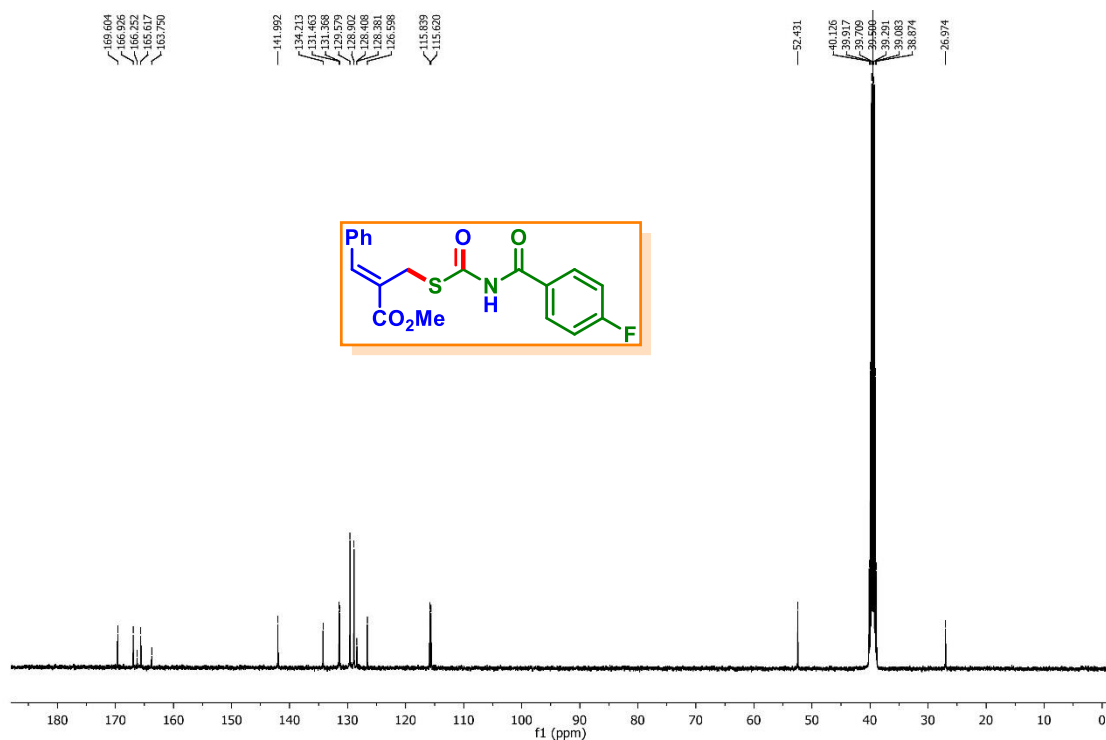
Z-Methyl 2-(((4-methylbenzoyl)carbamoyl)thio)methyl)-3-phenylacrylate (1b): $^{13}\text{C}\{^1\text{H}\}$ NMR (100 MHz, $\text{DMSO-}d_6$)



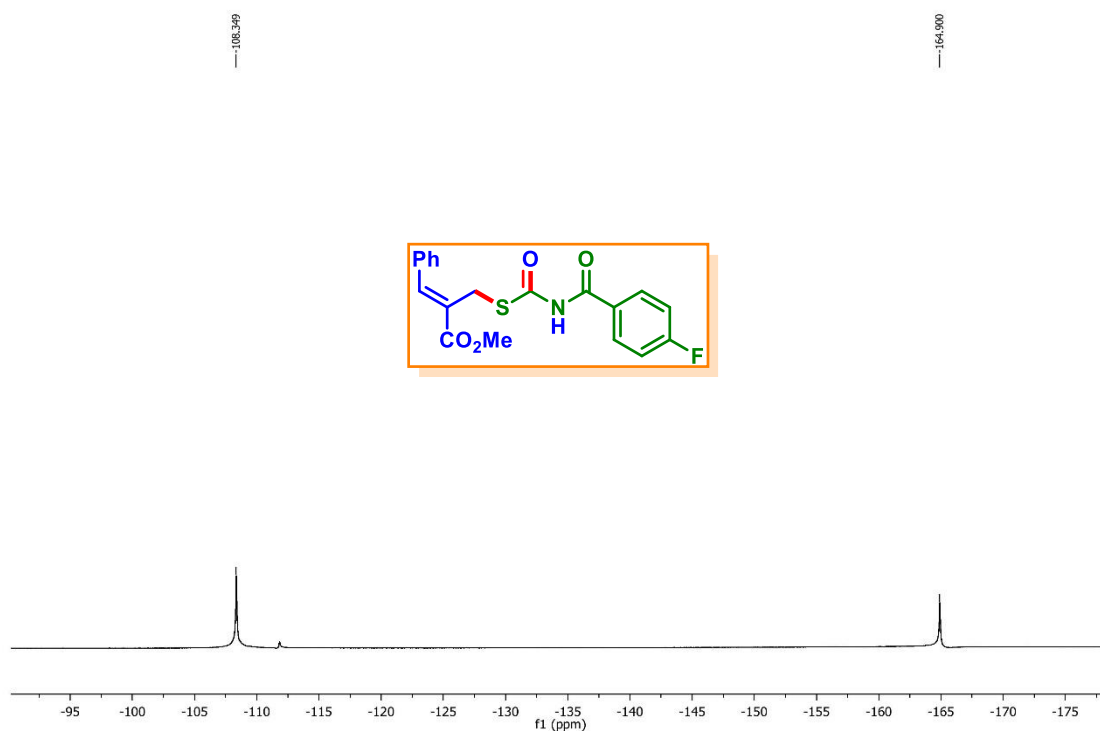
Z-Methyl 2-(((4-fluorobenzoyl)carbamoyl)thio)methyl)-3-phenylacrylate (1e): ^1H NMR (400 MHz, $\text{DMSO-}d_6$)



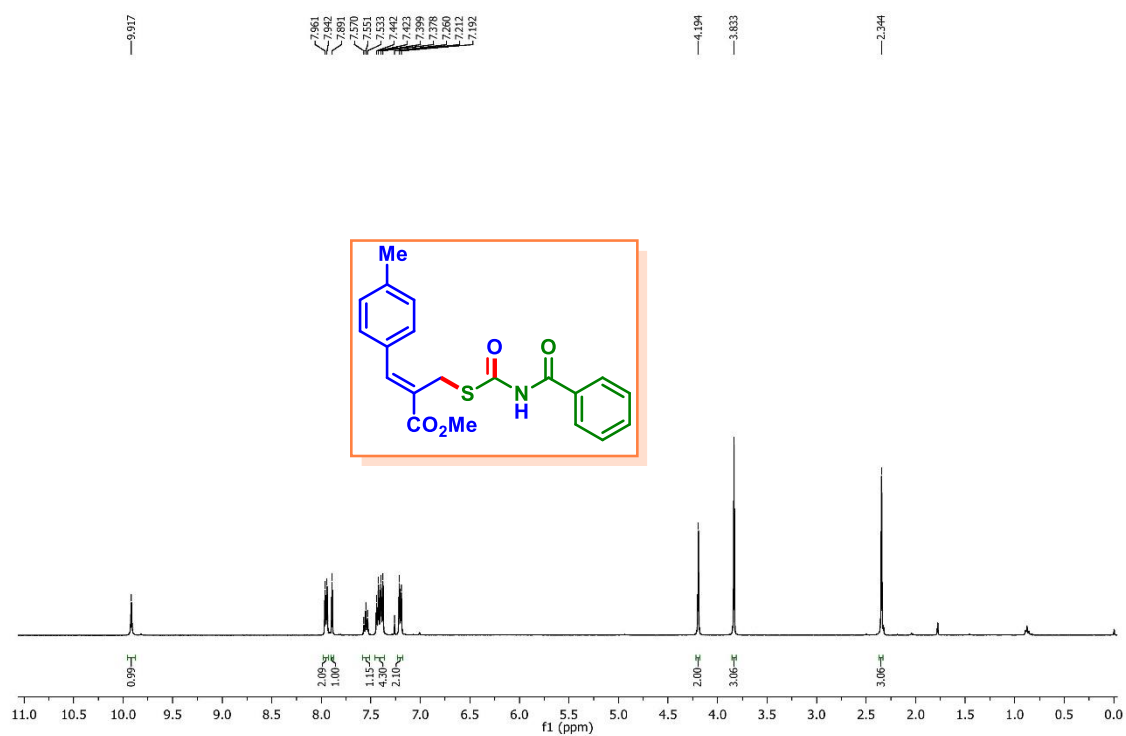
Z-Methyl 2-(((4-fluorobenzoyl)carbamoyl)thio)methyl)-3-phenylacrylate (1e): $^{13}\text{C}\{^1\text{H}\}$ NMR (100 MHz, $\text{DMSO-}d_6$)



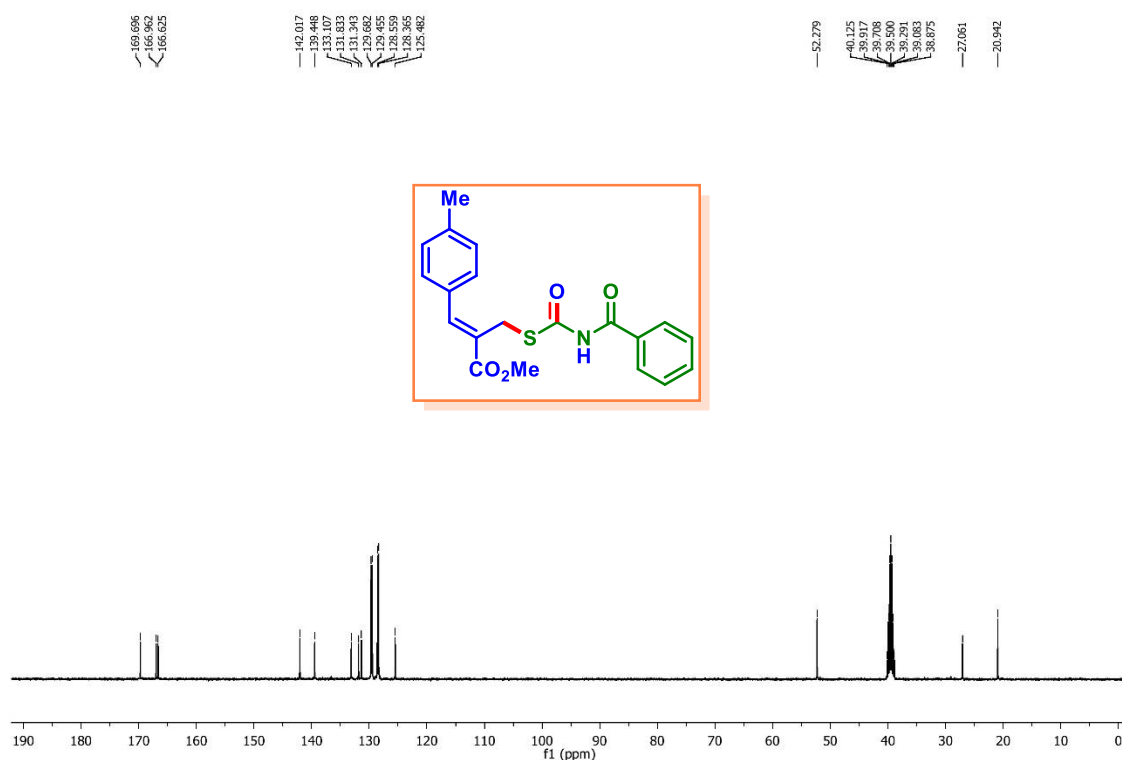
Z-Methyl 2-(((4-fluorobenzoyl)carbamoyl)thio)methyl)-3-phenylacrylate (1e): ^{19}F NMR (DMSO- d_6 + C_6F_6)



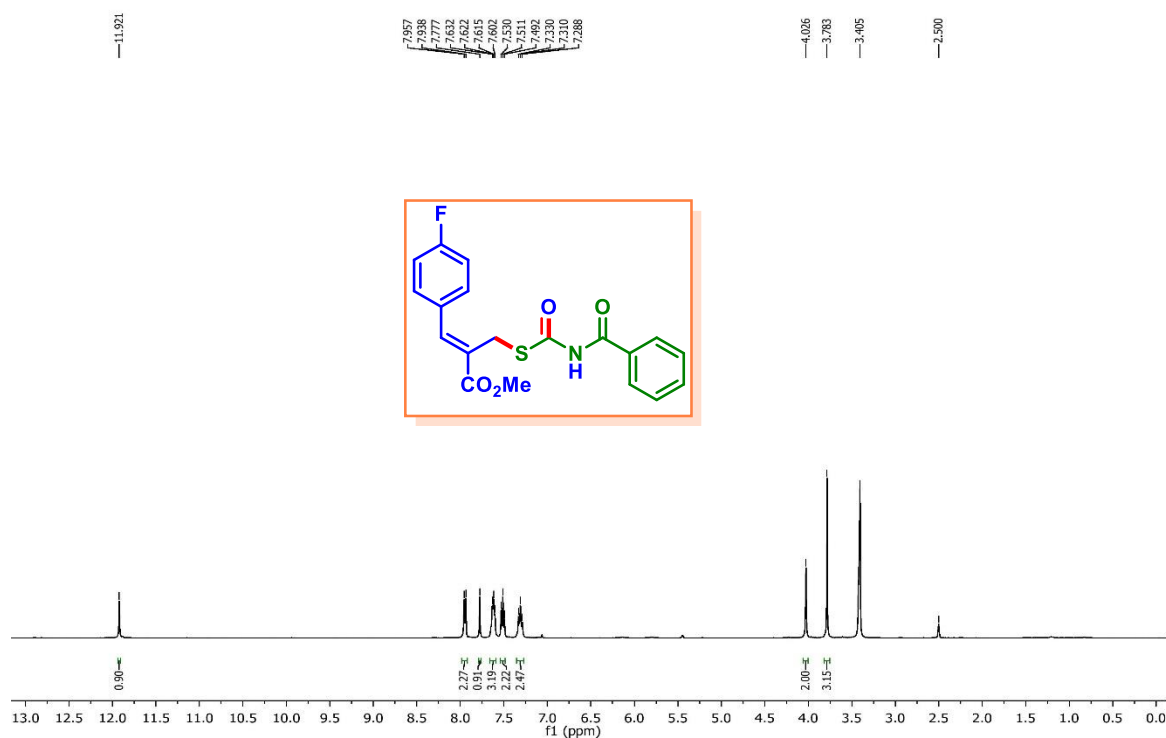
Z-Methyl 2-(((benzoylcarbamoyl)thio)methyl)-3-(*p*-tolyl)acrylate (2a): ^1H NMR (400 MHz, CDCl_3)

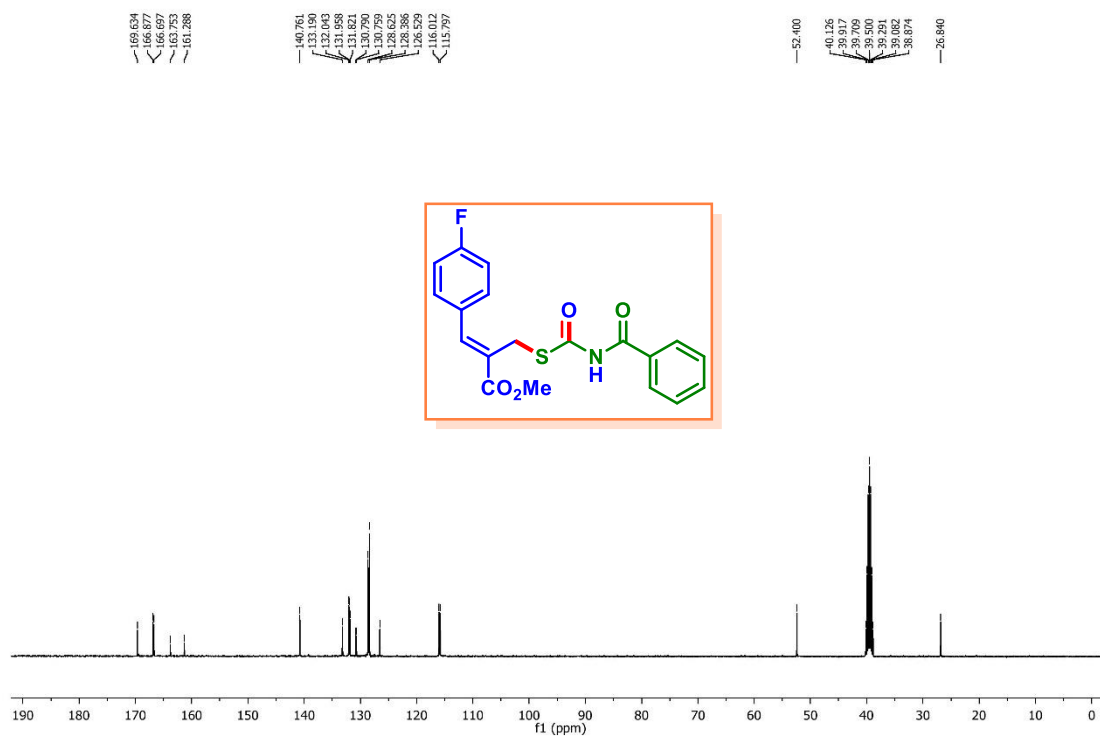
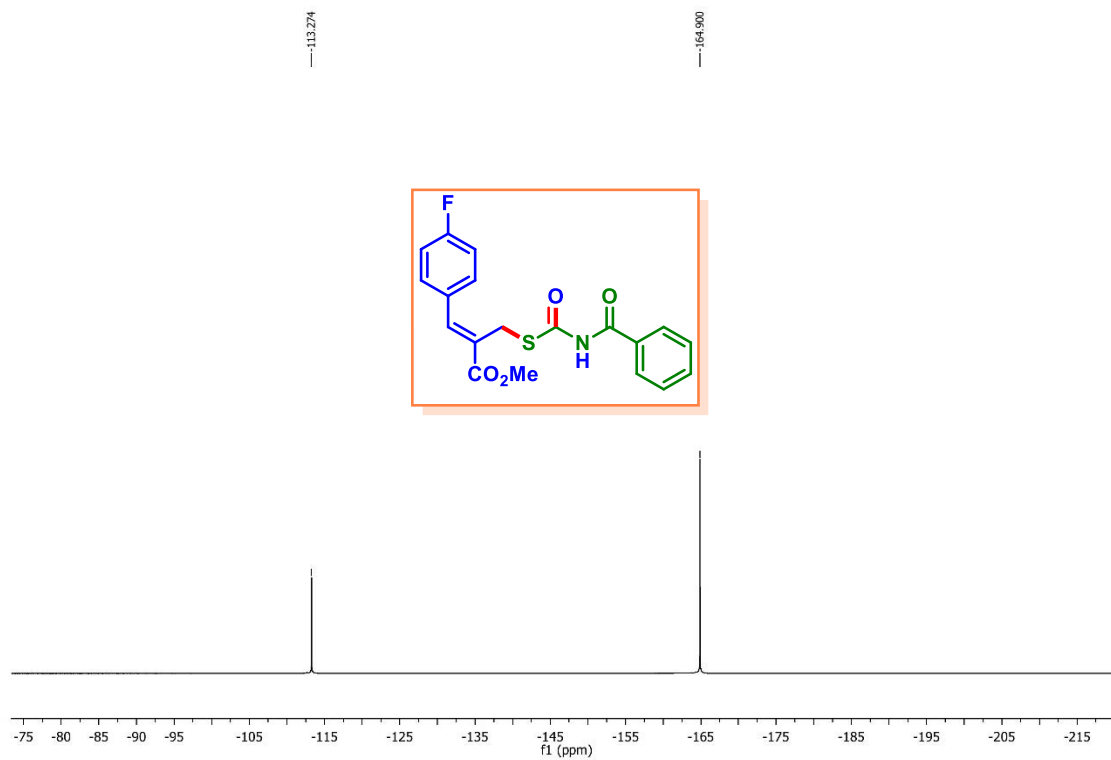


Z-Methyl 2-(((benzoylcarbamoyl)thio)methyl)-3-(*p*-tolyl)acrylate (2a): $^{13}\text{C}\{^1\text{H}\}$ NMR (100 MHz, DMSO- d_6)

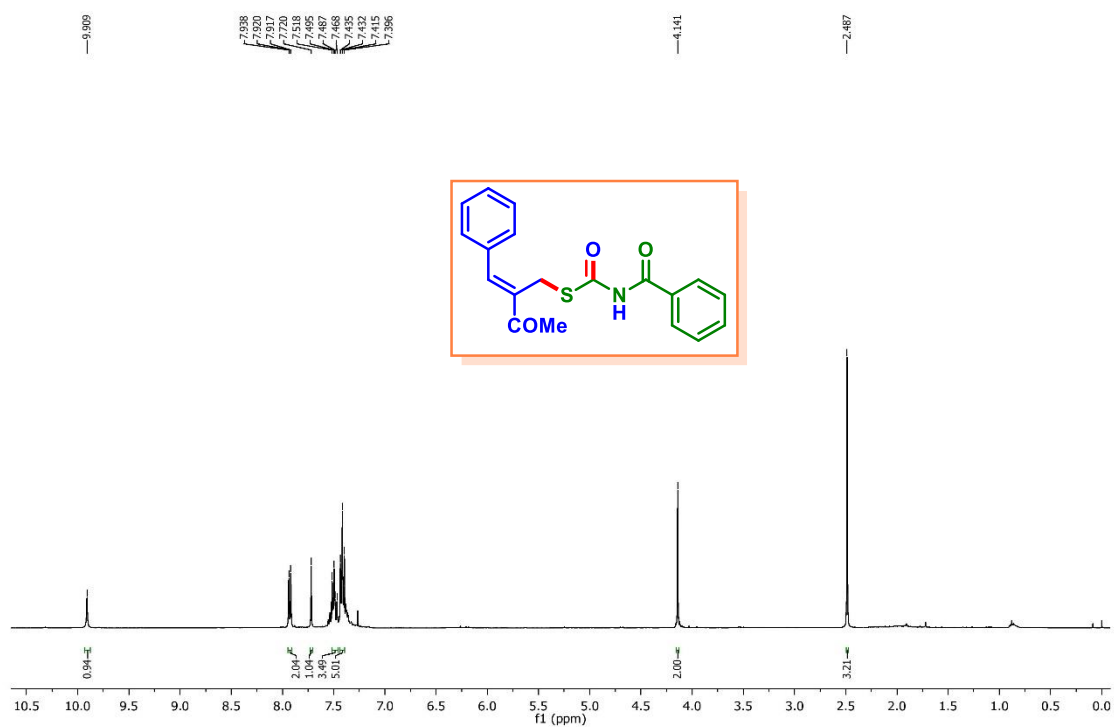


Z-Methyl 2-(((benzoylcarbamoyl)thio)methyl)-3-(4-fluorophenyl)acrylate (4a): ^1H NMR (400 MHz, DMSO- d_6)

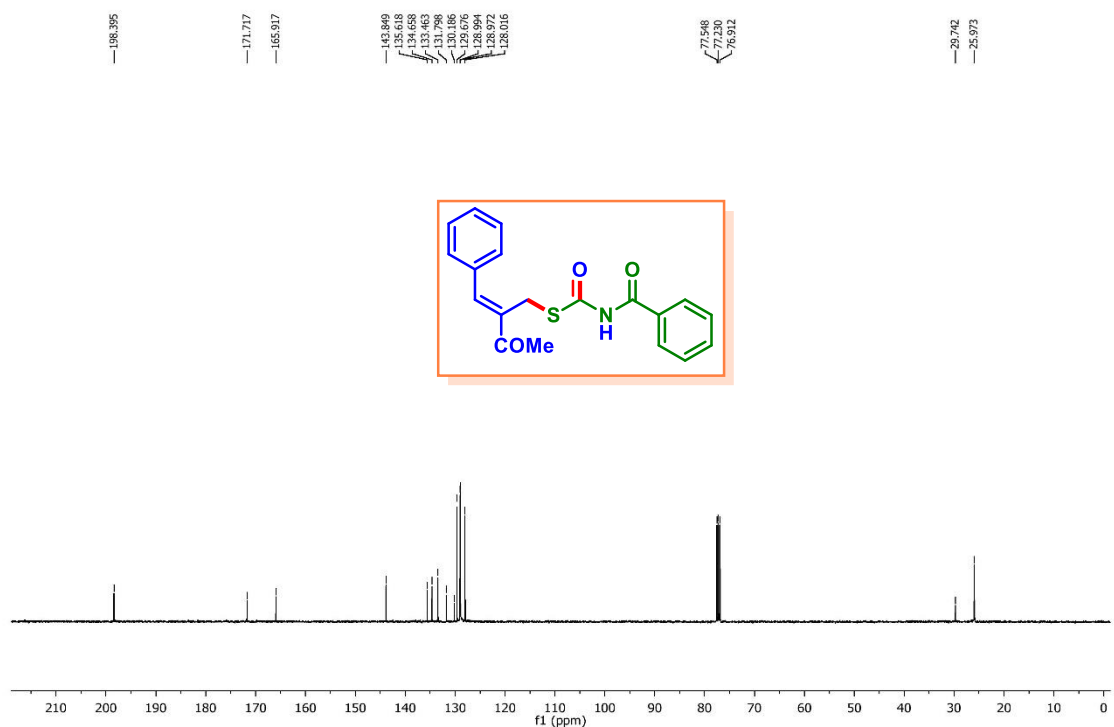


Z-Methyl 2-(((benzoylcarbamoyl)thio)methyl)-3-(4-fluorophenyl)acrylate (4a): $^{13}\text{C}\{^1\text{H}\}$ NMR (100 MHz, $\text{DMSO-}d_6$)**Z-Methyl 2-(((benzoylcarbamoyl)thio)methyl)-3-(4-fluorophenyl)acrylate (4a):** ^{19}F NMR (100 MHz, $\text{DMSO-}d_6$)

Z-S-(2-Benzylidene-3-oxobutyl) benzoylcarbamothioate (15a): ^1H NMR (400 MHz, CDCl_3)



Z-S-(2-Benzylidene-3-oxobutyl) benzoylcarbamothioate (15a): $^{13}\text{C}\{^1\text{H}\}$ NMR (100 MHz, CDCl_3)

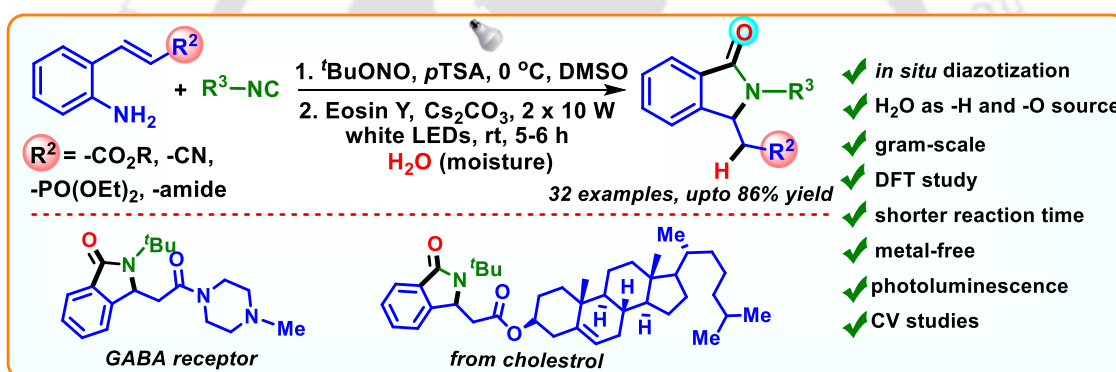




CHAPTER IV



Visible-Light-Driven Isocyanide Insertion to *o*-Alkenylanilines: A Route to Isoindolinone Synthesis



Abstract: A visible-light-mediated intermolecular radical insertion of isocyanides to electron-deficient *o*-alkenylanilines leading to isoindolinone is reported. Deuterium (D_2O) and H_2O^{18} labelling experiments suggest H and O incorporation in the product. The formation of an N-centered radical (NCR) via stepwise PT/ET process was confirmed by radical trapping experiments, photoluminescence, cyclic voltammetry and DFT studies. This photo cascade methodology is overall a redox neutral process featuring metal-free condition and broad substrate scope (32 examples). The synthesis of analogue of GABA receptor antagonist shows the practical utility of this method.



CHAPTER IV

IV. Visible-Light-Driven Isocyanide Insertion to *o*-Alkenylanilines: A Route to Isoindolinone Synthesis**IV.1. Introduction**

The omnipresence of nitrogen-containing heterocycles in bioactive molecules has provided great impetus for chemists to develop efficient methods toward their synthesis.¹ In this regard, visible-light mediated carboamination has turned out to be an alternate paradigm for the synthesis of *N*-heterocycles through *N*-centered radicals (NCRs) formation.²

The quintessential strategies for the generation of NCRs require either homolysis of nitrogen-halogen (N–X, X = Cl, Br, I) or N–H bonds. The activation of a highly stable N–H bond relies on either the stepwise (PT/ET) or concerted transfer of proton and electrons (Proton-Coupled Electron Transfer; PCET). The PCET oxidation comprises the concerted transfer of both proton and electron originating from a single donor to two independent electron acceptors (Brønsted base and one electron oxidant). However, in an adequately strong base, stepwise PT/ET mechanism can predominate over PCET because of substantial equilibrium concentration of the substrate conjugate base present in the solution. Such a mechanism would show selectivity for more acidic bonds. These strategies allows the distinct and exotic bond formations that would otherwise be inaccessible.³

Among nitrogenous heterocycles, isoindolinone (phthalimidines) scaffold having a C(sp³)–N bond represents a growing class of benzo fused γ -lactam natural products. Synthetic and natural isoindolinones are medicinally relevant possessing various biological activities such as inhibitors for the production of tumor necrosis factor (TNF- α), 4 MGR-1 antagonist, anti-tumor, anti-inflammatory, antimicrobial, antioxidant, antifungal, anxiolytic, antiviral etc. (Figure IV.1.1).⁴

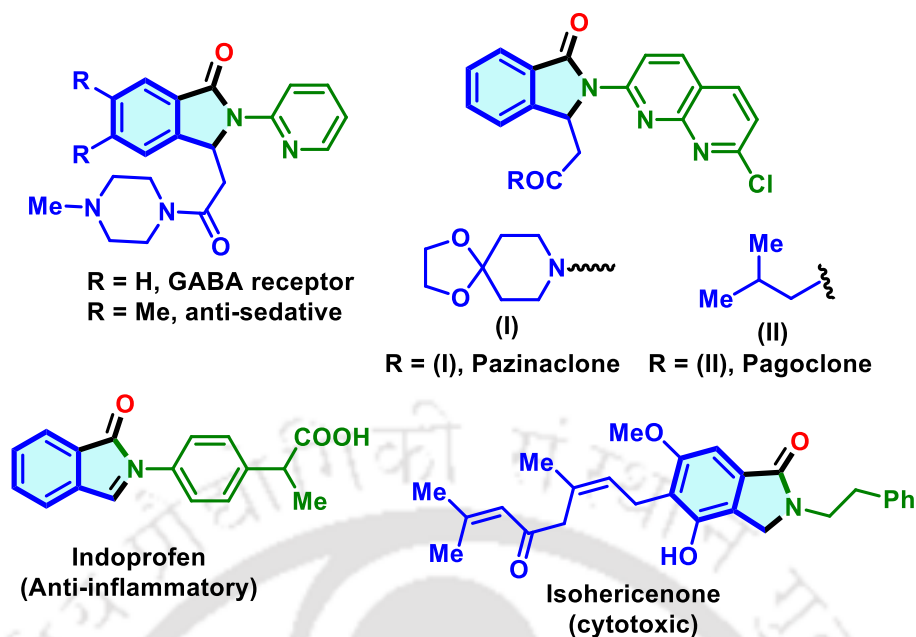


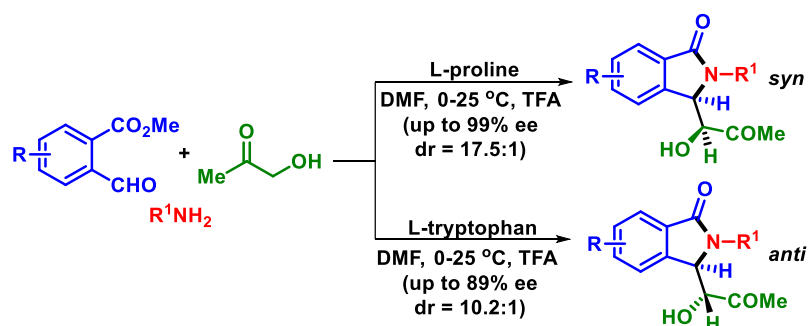
Figure IV.1.1. Representative examples of bioactive isoindolinones.

IV.2. Differential Strategies for Synthesis of Isoindolinones

The prerequisite isoindolinone derivatives are synthesized via lactamization of *o*-(aminomethyl)benzoic acids,⁵ reductive/condensative cyclizations,⁶ halogenation (or direct C–H activation) and cyclization of *o*-methylbenzamides,⁷ and carbonylative strategies.⁸ The C–H functionalization strategies for isoindolinone synthesis requires the use of *N*-substituted benzamides as reactants bearing either activating or directing groups.⁹ Isocyanides are another common synthetic precursor for the synthesis of 3-iminoisoindolinones.¹⁰

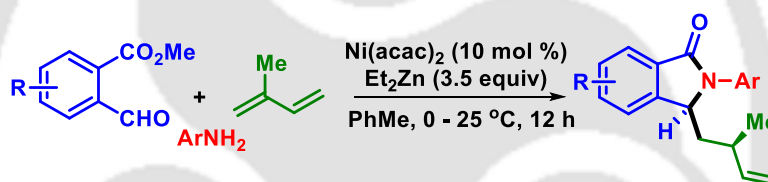
IV.2.1. Synthesis of isoindolinones via lactamization

In 2015, Singh group developed an organocatalytic synthesis of isoindolinones using *o*-formyl methylbenzoates, amines and hydroxyacetone as reacting partners through Mannich–lactamization sequence. Simple amino acids such as L-proline and L-tryptophan were used as inexpensive catalyst. L-proline provides *syn*-selective isoindolinones (up to 99% ee; dr = 17.5:1) whereas, L-tryptophan gave *anti*-selective isoindolinones (up to 89% ee; dr = 10.2:1). The overall transformation involves one C–C and two C–N bond formation in one pot cascade manner, using inexpensive starting material. (Scheme IV.2.1.1).¹¹



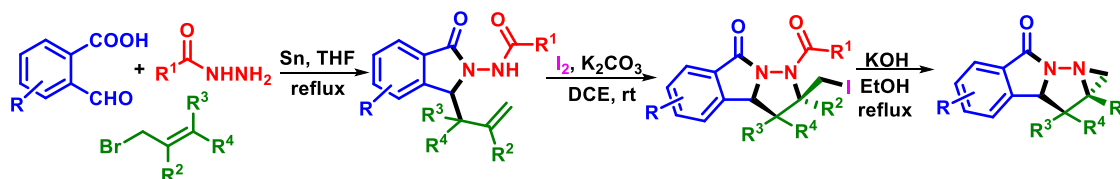
Scheme IV.2.1.1. Enantioselective synthesis of isoindolinones.

Later, the same group reported a Ni(II)-catalyzed stereoselective synthesis of isoindolinones through homoallylation/lactamization of *in situ* generated aldimines and dienes. The aldimines were prepared using *o*-formyl benzoates and primary amines. The reaction proceeds at room temperature giving exclusive 1,3-*syn* selectivity. A stoichiometric amount of Et₂Zn act as a promoter (Scheme IV.2.1.2).¹²



Scheme IV.2.1.2. Synthesis of isoindolinones via homoallylation/lactamization.

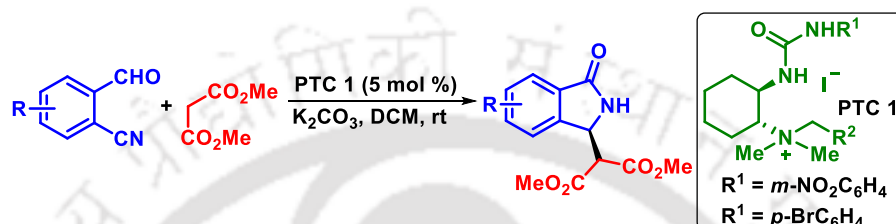
In yet another report, Hu and co-workers disclosed a tin powder promoted route to isoindolinones using 2-formylbenzoic acids, hydrazides, and allyl bromides. The reaction proceeds via condensation followed by allylation and lactamization step. The post synthetic modification of synthesized 3-allylisoindolin-1-ones led to pyrazoloisoindol-8-one derivatives via iodocyclization. Upon treatment with KOH, pyrazoloisoindol-8-one provided more complex tetracyclic compound tetrahydro-4*H*-azirino[1',2':2,3]-pyrazolo[5,1-*a*]isoindol-4-ones (Scheme IV.2.1.3).¹³



Scheme IV.2.1.3. Sn promoted synthesis of isoindolinones.

IV.2.2. Synthesis of isoindolinones via reductive/condensation cyclization

An asymmetric version of isoindolinone synthesis has been disclosed by Massa and co-workers using differentially substituted 2-cyanobenzaldehydes, dimethyl malonate and bifunctional phase-transfer catalyst (PTC). In post synthetic modifications, product (*S*)-2-(1-oxoisoindolin-3-yl)malonate was transformed to Belliotti (*S*)-PD172938 and its derivatives having diverse biological activities (Scheme IV.2.2.1).¹⁴



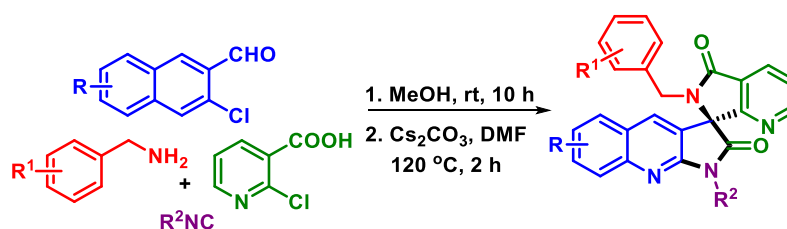
Scheme IV.2.2.1. PTC catalyzed synthesis of isoindolinones.

Huang group reported a four component Ugi reaction for the synthesis of isoindolinones using 2-furaldehydes, amines, isocyanides and 2-(phenylselenanyl)acrylic acids. This one-pot tandem process ensues via condensation, intramolecular Diels-Alder cycloaddition followed by $\text{BF}_3 \cdot \text{OEt}_2$ promoted deselenization-aromatization process (Scheme IV.2.2.2).¹⁵



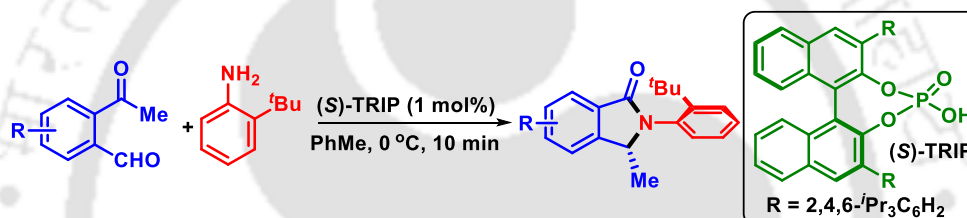
Scheme IV.2.2.2. Synthesis of isoindolinones via Ugi reaction.

A one-pot Ugi reaction is reported by Ghandi *et al.* for the synthesis of spiropyrroloquinoline-isoindolinones using 2-chloroquinoline-3-carbaldehydes, benzylamines, 2-chloronicotinic acid and isocyanides. The mechanism for this metal-free approach involves an Ugi reaction via Mumm rearrangement followed by two intramolecular cyclizations (Scheme IV.2.2.3).¹⁶



Scheme IV.2.2.3. Synthesis of spiropyrroloquinoline-isoindolinones.

In 2017, Seidel *et al.* developed an enantioselective synthesis of isoindolinones using 2-acylbenzaldehydes, anilines as reacting partner and chiral phosphoric acid as a catalyst. Atropisomerism was observed with anilines having $-t\text{Bu}$ group at *o*-position. The reaction is very fast with high enantioselectivity (up to 98 % ee). This strategy was further utilized for the synthesis of Mariline A (Scheme IV.2.2.4).¹⁷

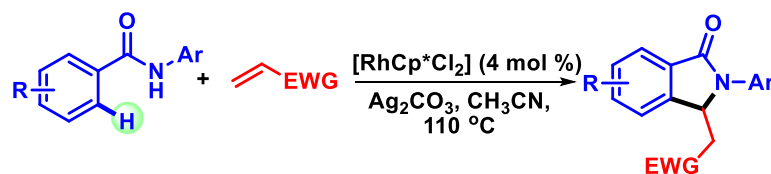


Scheme IV.2.2.4. Biomimetic synthesis of 3-alkyl isoindolinones.

IV.2.3. Synthesis of isoindolinones via C–H activation

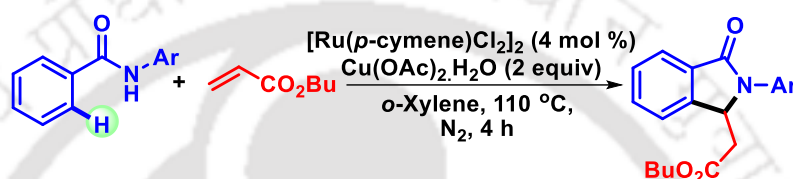
Owing to the pharmacological importance of 3-methyleneisoindolin-1-one frameworks, a variety of strategies have emerged for their synthesis. Among them, transition-metal-catalyzed $\text{C}(\text{sp}^2)\text{--H}$ bond activation has spurred considerable interest for their synthesis. Various groups have developed the coupling reactions of aromatic rings with olefins using Rh, Ru, Pd, Ni, Co, Cu etc. Below are some representative examples of metal catalyzed $\text{C}(\text{sp}^2)\text{--H}$ bond activation involving *N*-substituted benzamides as reactants bearing either activating or directing groups.¹⁸

A Rh(II)-catalyzed synthesis of isoindolinones through oxidative coupling of benzamides/heteroaryl carboxamides with activated and unactivated olefins has been developed by Li group. The *o*-vinylated carboxamides undergoes Michael addition in case of activated olefins (Scheme IV.2.3.1).¹⁹



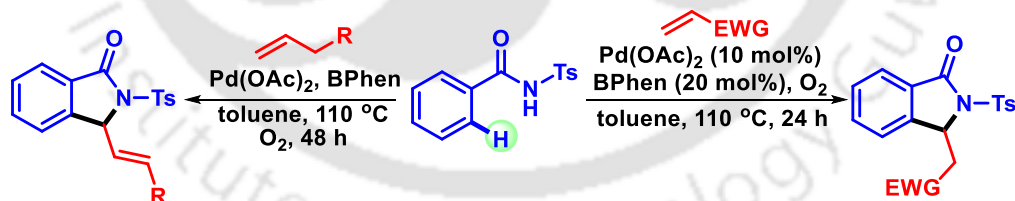
Scheme IV.2.3.1. *Rh(II)-catalyzed synthesis of isoindolinones.*

One of the earliest examples of Ru(II)-catalyzed synthesis of isoindolinones is disclosed by Hashimoto and co-workers. In this oxidative tandem cyclization, $\text{Cu}(\text{OAc})_2 \cdot \text{H}_2\text{O}$ acts as an oxidant (Scheme IV.2.3.2).²⁰



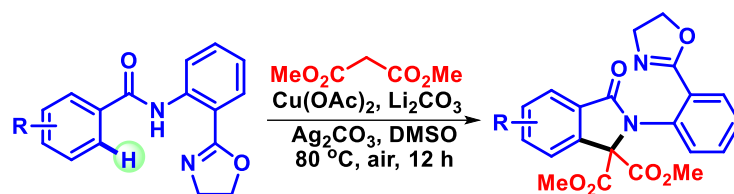
Scheme IV.2.3.2. *Ru(II)-catalyzed synthesis of isoindolinones.*

Zhu *et al.* reported a Pd(II)-catalyzed C–H olefination/annulation of *N*-acylsulfonamides using electron-rich and deficient alkenes. This eco-friendly transformation uses molecular oxygen or air as an oxidant and bathophenanthroline (BPhen) as a ligand. In the case of electron-rich alkenes, the retention and positional shift of the olefinic bond (exclusive *E*-configuration) was observed (Scheme IV.2.3.3).²¹



Scheme IV.2.3.3. *Pd(II)-catalyzed synthesis of isoindolinones.*

In 2015, Yu group used an amide-oxazoline directing group for the synthesis of isoindolinones. The reaction goes through a Cu(II)-catalyzed oxidative coupling between aromatic *ortho*-C–H bonds and malonates followed by an intramolecular oxidative C–N bond formation (Scheme IV.2.3.4).²²



Scheme IV.2.3.4. *Cu(II)-catalyzed synthesis of isoindolinones.*

A step-economical oxidative annulation of *N*-quinolinyl (Q)-substituted benzamides and electron-deficient alkenes was reported by Ackermann group using $\text{Co}(\text{OAc})_2$ as a catalyst and AgOPiv as an oxidant. This $\text{Co}(\text{II})$ -catalyzed C–H/N–H functionalization process yielded isoindolinones in good to moderate yields. Mechanistic studies divulge a carboxylate-assisted irreversible C–H cobaltation process (Scheme IV.2.3.5).²³

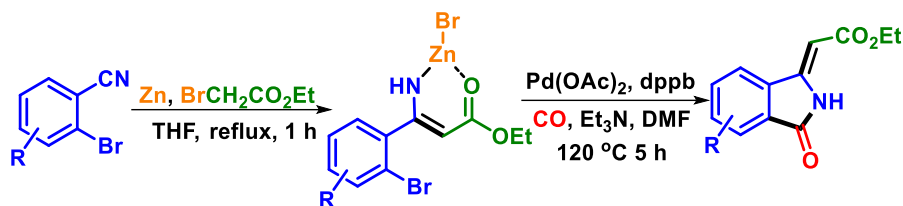


Scheme IV.2.3.5. *Co(II)-catalyzed synthesis of isoindolinones.*

II.2.4. Synthesis of isoindolinones via carbonylation

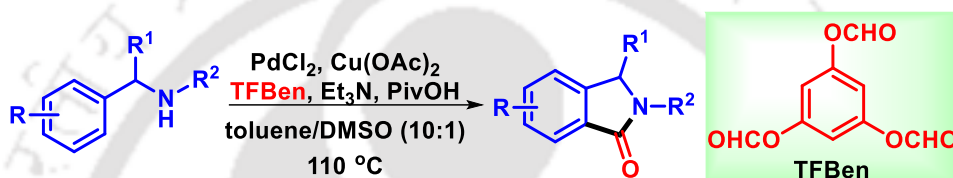
With the remarkable advances over the years, transition metal catalyzed carbonylative reactions has thrived to become a crucial part of contemporary organic chemistry. Carbonylative reactions allows the synthesis of diverse molecular frameworks using inexpensive feedstock *viz.* carbon monoxide (CO), one of the simplest C-1 unit. Various groups have harnessed this strategy for the synthesis of isoindolinones using different CO surrogates.²⁴

A one-pot sequential method for the synthesis of stereo controlled *Z*-3-methyleneisoindolin-1-ones was developed by Lee *et al.* using 2-bromoarylnitriles. This tandem protocol proceeds through Blaise reaction using a Reformatsky reagent ensued by $\text{Pd}(\text{II})$ -catalyzed aminocarbonylation with carbon monoxide at 1 atm pressure (Scheme IV.2.4.1).²⁵



Scheme IV.2.4.1. One-pot sequential synthesis of isoindolinones.

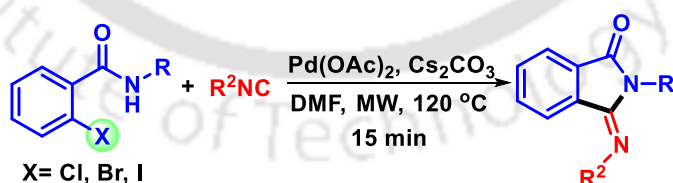
In 2019, Wu and co-workers disclosed a Pd(II) catalyzed isoindolinone synthesis through C–H carbonylation of substituted benzylamines. In this gas-free protocol, benzene-1,3,5-triyl triformate (TFBen) is used as an expedient CO surrogate (Scheme IV.2.4.2).²⁶



Scheme IV.2.4.2. Pd(II)-catalyzed carbonylation of benzylamines.

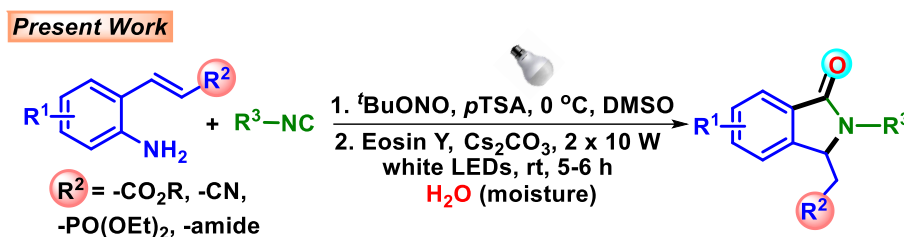
IV.2.5. Synthesis of isoindolinones via metal-catalyzed isocyanide insertion

Chauhan *et al.* described a microwave assisted, Pd(II)-catalyzed isocyanide insertion reaction to render substituted isoindolinones with high stereoselectivity. In this ligand-free domino C–C/C–N coupling reaction, isocyanides and *o*-halogenated amides are used as coupling partners. A large variety of amides are well tolerated, except for *o*-Cl or *o*-Br-substituted amides resulting in lower yields (Scheme IV.2.5.1).²⁷



Scheme IV.2.5.1. Pd(II)-catalyzed isocyanides insertion.

The literature revealed that under metal-free condition, the reaction of aryl diazonium salts and isocyanides generates imidoyl radicals that can be used for subsequent reactions.²⁸ Taking cues from the above-mentioned works, we anticipated that the *in situ* generated 2-alkenylaryldiazonium salts²⁹ could be used as a suitable precursor for the synthesis of isoindolinones (Scheme IV.2.5.2).



Scheme IV.2.5.2 Photocatalytic synthesis of isoindolinones.

IV.3. Present Work

As proof of our concept, a preliminary reaction was conducted between methyl 3-(2-aminophenyl) acrylate (**1**) and *tert*-butyl isocyanide (**a**). Herein, methyl 3-(2-aminophenyl)acrylate (**1**) was first diazotized to the corresponding 2-alkenylaryldiazonium tosylates followed by the addition of *tert*-butyl isocyanide (**a**), eosin Y (2 mol %) as photocatalyst, base Cs_2CO_3 (2 equiv), DMSO (2 mL) and stirred under the irradiation of $2 \times 10\text{ W}$ white LEDs at room temperature. A new compound was isolated in a satisfactory yield of 82%. The IR spectra (peaks at 1683 and 1735 cm^{-1}), ^1H NMR (absence of alkene protons) and $^{13}\text{C}\{^1\text{H}\}$ NMR revealed the product structure to be a benzo-fused lactam. Finally, the single X-ray crystallographic diffraction study of one of the derivatives re-established its structure to be methyl 2-(2-(naphthalen-2-yl)-3-oxoisoindolin-1-yl)acetate (**1d**) (Figure IV.3.1). The analysis of product confirms photocatalytic isocyanide insertion followed by intramolecular cyclization to give the corresponding isoindolinones. To the best of our knowledge, this is the unique report on the visible light-mediated synthesis of isoindolinones using 2-alkenylanilines and isocyanides (Scheme IV.2.5.2).

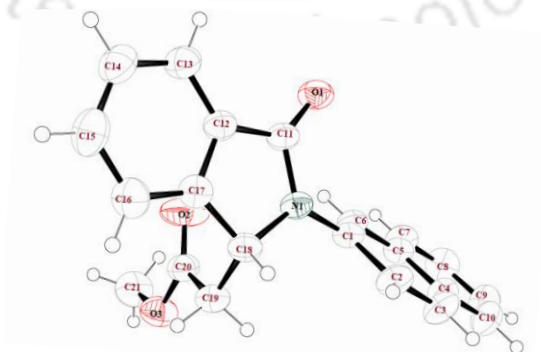
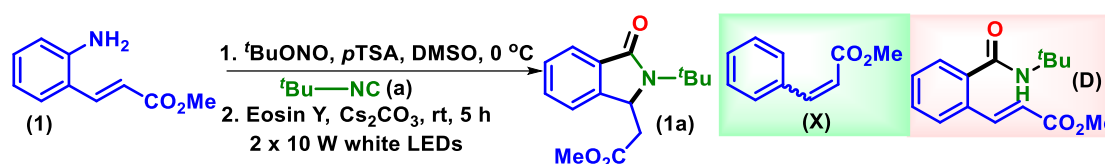


Figure IV.3.1. ORTEP view of **1d**.

Optimizations of Reaction Conditions:

Table IV.3.1. Optimization of the reaction conditions^{a,b}

Entry	Variation from optimal conditions ^[a]	Yield of 1a (%) ^b
1.	none	82
2.	[Ru(bpy) ₃]Cl ₂ and [Ru(bpy) ₃](PF ₆) ₂	81 and 68
3.	Eosin B instead Eosin Y	55
4.	Rose Bengal instead Eosin Y	42
5.	Rhodamin B instead Eosin Y	47
6.	Na ₂ CO ₃ instead of Cs ₂ CO ₃	30
7.	K ₂ CO ₃ instead of Cs ₂ CO ₃	65
8.	^t BuOK instead of Cs ₂ CO ₃	35
9.	DMAP instead of Cs ₂ CO ₃	15
10.	DCM instead of DMSO	60
11.	DMF instead of DMSO	70
12.	CH ₃ CN instead of DMSO	<15
13.	CH ₃ OH instead of DMSO	20
14.	2 x 10 W blue LEDs	68
15.	2 x 10 W green LEDs	53
16.	reaction in dark	N.D.
17.	without Eosin Y	N.D.
18.	without base	N.D.

^aReaction condition: **1** (0.25 mmol), **a** (0.25 mmol), Eosin Y (2 mol %), Cs₂CO₃ (0.5 mmol), DMSO (2 mL) under air for 5 h. ^bIsolated pure product. N.D. = not detected.

In the pursuit to accomplish an appropriate reaction condition for this transformation, extensive optimization studies involving the selection of different catalytic systems, bases and solvents were carried out. Switching the catalytic system to [Ru(bpy)₃]Cl₂ (81%) and [Ru(bpy)₃](PF₆)₂ (68%) failed to improve the product yield (Table IV.3.1, entry 2). The low-cost and commercial availability of organic dyes makes them attractive substitutes to transition metal-based photoredox catalysts.³⁰ Albeit the yield was comparable to that of [Ru(bpy)₃]Cl₂ (81%), further optimizations were carried out using organic dyes. The use of organic dyes such as eosin B, Rose Bengal, and Rhodamine B (Table IV.3.1, entries 3-5) gave inferior yields compared to eosin Y. Screening of other inorganic bases, such as Na₂CO₃, K₂CO₃, and ^tBuOK, instead of Cs₂CO₃ had a detrimental influence on the yield (Table IV.3.1, entries 6-8). Similarly, the

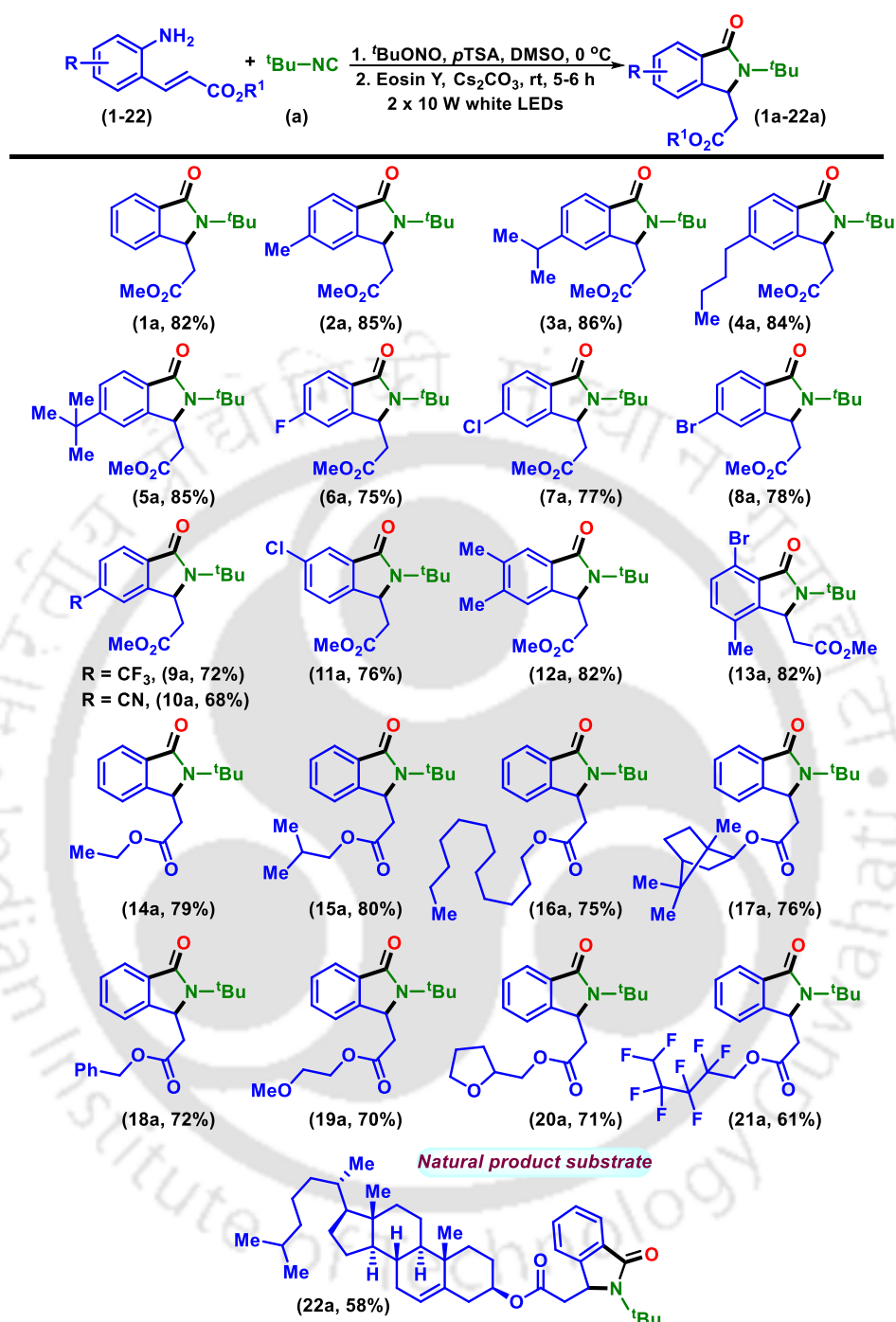
use of organic base DMAP failed to improve the product yield (Table IV.3.1, entry 9). During the solvent screening, DMSO (82%) was found optimal compared to other solvents such as DCM (60%), DMF (70%), CH₃CN (<15%) and CH₃OH (20%) tested (Table IV.3.1, entries 10-13). The nitriles and isonitriles are functional isomers. Due to this both have the tendency to form nitrilium intermediate upon reaction with diazonium salts. The lower yield obtained in CH₃CN and CH₃OH might be due to their competing reaction with the diazotized product, providing a multitude of products in present case.^{28d,e} To check the effect of wavelength and intensity of the light, the standard reaction was carried out in 2 x 10 W blue (430 nm) and green (513 nm) LEDs. Both the LEDs failed to improve the reaction yield beyond 68% (Table IV.3.1, entry 14 and 15). The use of green light is a better choice for the excitation of EY which is confirmed from the emission spectra of eosin Y in DMSO solvent (543 nm). The reaction performed well in white LED (82%) as well as blue LED (68%). The ineffectiveness of the intense blue light might be due to the decomposition of 2-alkenylaryldiazonium tosylate (**1'**). Control experiments revealed that eosin Y, base and light are indispensable for this transformation (Table IV.3.1, entries 16-18). In reactions with the omission of any one of the components (light, eosin Y, or base) deaminated alkene (**X**) and an un-cyclized amide (**D**) were isolated as major products. In the absence of light, a deaminated alkene (**X**, 30%) and an un-cyclized amide (**D**, 49%) were obtained as major products (Table IV.3.1, entry 16). Hence, the light is assisting in the formation of aryl radical intermediate (**A**) followed by the isocyanide insertion. After the omission of EY, the un-cyclized amide (**D**, 73%) was obtained as the major product and deaminated alkene (**X**, 12%) as minor product (Table IV.3.1, entry 17). This suggests the non-involvement of eosin Y in the first step (dediazotization) but has a definite role in the amidyl radical formation in the subsequent step. In absence of base, the deaminated alkene (**X**, 92%) was obtained exclusively (Table IV.3.1, entry 18). Apart from light, diazonium salts are known to generate aryl radicals more efficiently in the presence of base with evolution of acid. This acid later helps in the hydrolysis of nitrilium intermediates to corresponding amides.^{29d-e} For all the reactions, proper aeration was provided using a fan and the surrounding temperature was just about the room temperature (~28 °C), thereby approving the photochemical nature of this protocol (Figure IV.3.2).



Figure IV.3.2. Reaction set-up from front (left) and top view (right).

Substrate Scope for Isoindolinones Synthesis:

With the optimized condition in hand, this protocol was subsequently applied for various *o*-alkenylanilines using different isocyanides. At first, the scope of differently substituted *o*-alkenylanilines (**1-22**) was tested with *tert*-butyl isocyanide (**a**) and the results are summarized in Scheme IV.3.1. Various *o*-alkenylanilines possessing electron neutral and electron-donating groups such as $-H$ (**1**), *p*-Me (**2**), *p*-*i*Pr (**3**), *p*-*n*Bu (**4**), *p*-*t*Bu (**5**) were efficiently converted to their desired products **1a** (82%), **2a** (85%), **3a** (86%), **4a** (84%) and **5a** (85%) respectively in excellent yields. This protocol was equally successful for *o*-alkenylanilines having electron-withdrawing substituents such as *p*-F (**6**), *p*-Cl (**7**), *p*-Br (**8**), *p*-CF₃ (**9**), *p*-CN (**10**) and *m*-Cl (**11**) affording their corresponding isoindolinones **6a** (75%), **7a** (77%), **8a** (78%), **9a** (72%), **10a** (68%) and **11a** (76%) in good yields (Scheme IV.3.1). In particular, the tolerance of halogen and $-CN$ group opened new avenues for further derivatization. Apart from the mono-substituted *o*-alkenylanilines, the use of di-substituted *o*-alkenylanilines (**12-13**) were compatible for this transformation (Scheme IV.3.1). After successfully demonstrating the present strategy with methyl acrylate, other acrylates such as Et (**14**), *t*Bu (**15**), dodecyl (**16**), isoborenyl (**17**), benzyl (**18**), 2-methoxyethyl (**19**), and 2-methyl tetrahydrofuran (**20**) were also well-tolerated irrespective of their electronic nature and steric effect. Notably, octafluoropentyl acrylate (**21**) gave its anticipated isoindolinone (**21a**) in a 61% yield. This methodology was equally successful for a cholesteryl acrylate (**22**) giving the desired product (**22a**, 58%) in an acceptable yield (Scheme IV.3.1).

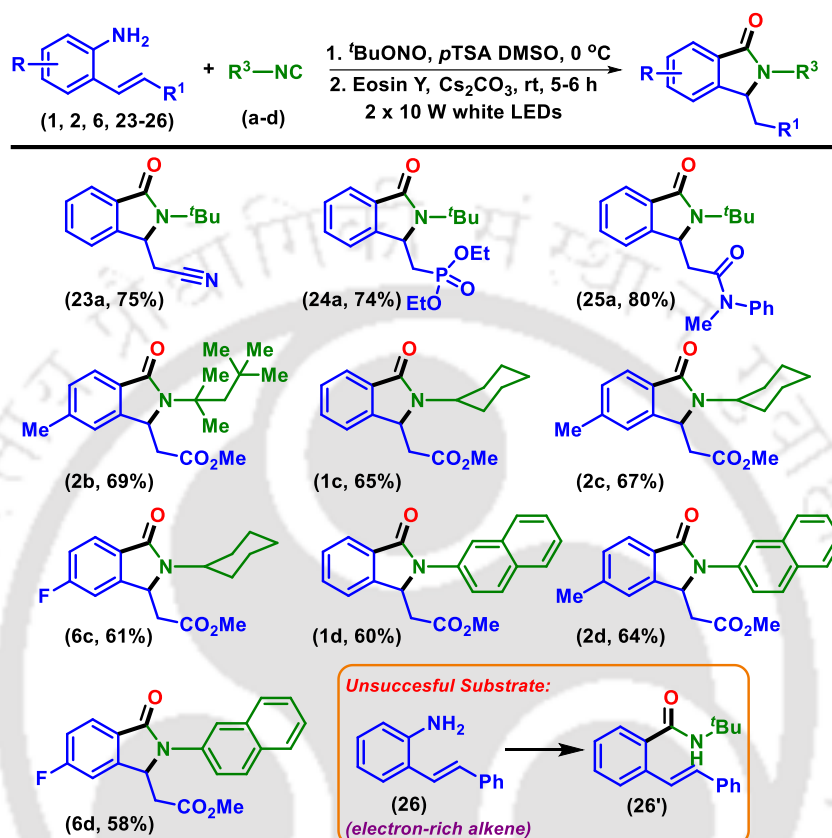
Scheme IV.3.1. Scope of various *o*-alkenylanilines with *tert*-butyl isocyanide^{a,b}

^aReaction conditions: **1-22** (0.5 mmol), **a** (0.5 mmol), Cs₂CO₃ (1 mmol), Eosin Y (2 mol %), DMSO (2 mL) under irradiation of 2 x 10 W white LEDs, 5-6 h. ^bIsolated yield of pure product.

Next, the viability of the reaction was tested by replacing the ester group with –CN (**23**), diethyl vinylphosphonate {PO(OEt)₂} (**24**), and *N*-methyl-*N*-phenylacrylamide (**25**) (Scheme IV.3.2). To our delight, these substrates were found compatible, yielding the corresponding products in 74-80% yields. In literature, alkenes having diethyl vinylphosphonate (**24**) and amide (**25**) functionality are hardly ever used for the synthesis

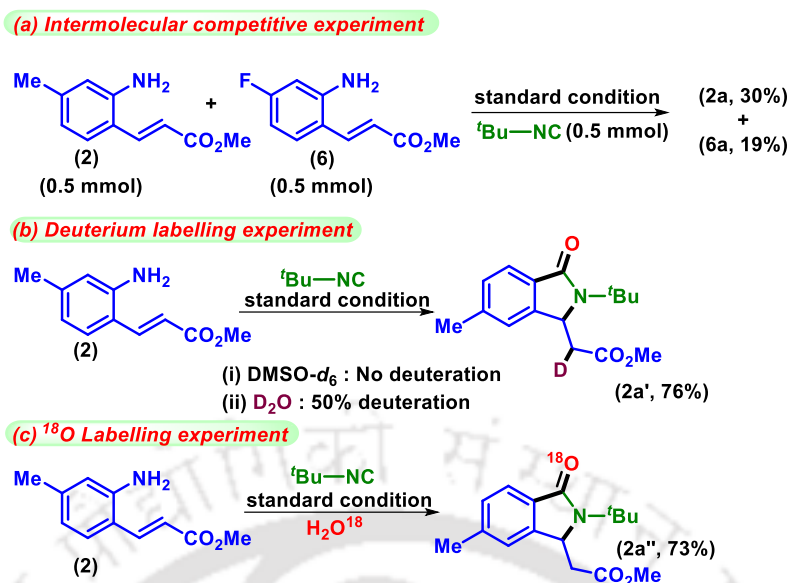
of isoindolinones. The generality of this method was further extended by reacting branched (**b**), cyclic (**c**), and polyaromatic isocyanides (**d**) with different *o*-alkenylanilines.

Scheme IV.3.2. Scope of various *o*-alkenylanilines with different isocyanides^{a,b}



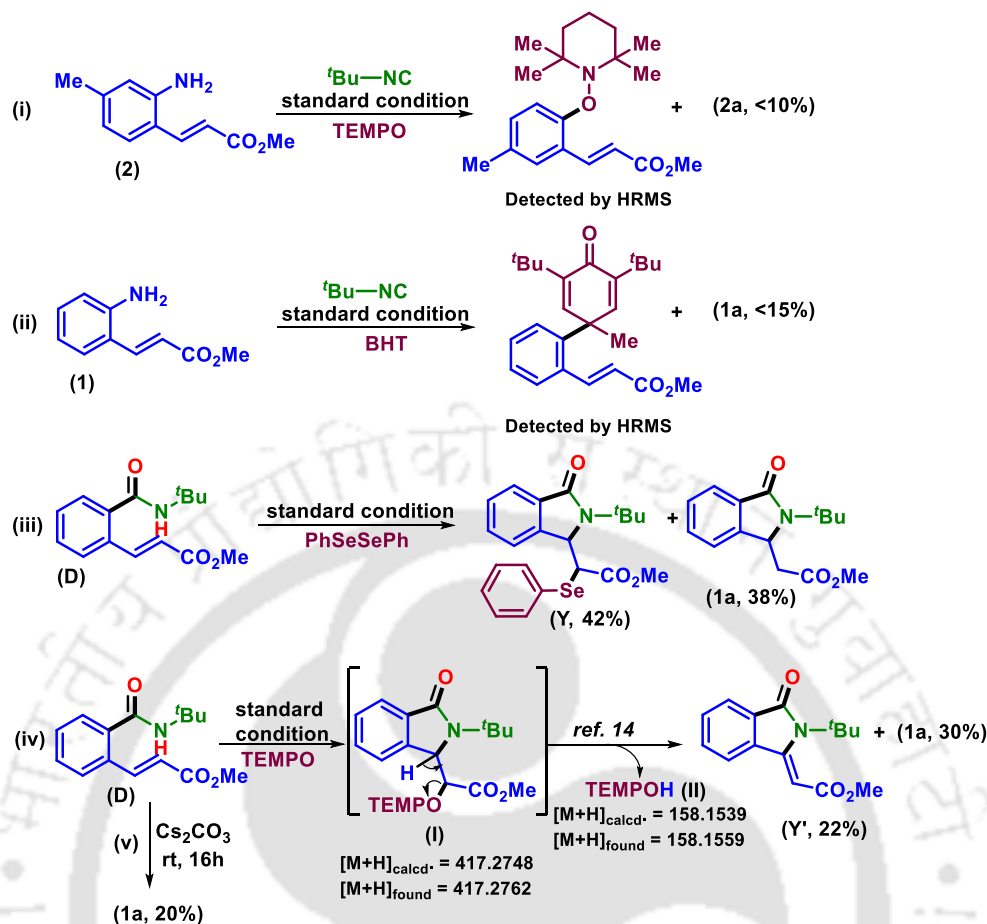
^aReaction conditions: **1**, **2**, **6**, **23-25** (0.5 mmol), **a-d** (0.5 mmol), Cs₂CO₃ (1 mmol), eosin Y (2 mol %), DMSO (2 mL) under irradiation of 2 x 10 W white LEDs, 5-6 h. ^bIsolated yield of product.

Though the reactivity of *tert*-octyl isocyanide (**b**) is similar to *tert*-butyl isocyanide, its corresponding product (**2b**, 69%) was obtained in a modest yield. Likewise, cyclohexyl isocyanide (**c**) also proved to be effective with *o*-alkenylanilines (**1**, **2**, **6**), producing **1c** (65%), **2c** (67%) and **6c** (61%) in good yields. When 2-naphthyl isocyanide (**d**) was reacted with *o*-alkenylanilines having -H (**1**), -Me (**2**) and -F (**6**) substituents, their respective isoindolinones **1d** (60%), **2d** (64%) and **6d** (58%) were obtained in acceptable yields (Scheme IV.3.2). However, the reaction with an electron-rich alkene *viz.* 2-styrylaniline (**26**) under the standard conditions failed to give the desired isoindolinone even after 24 h. However, the corresponding carboxamide (**26'**) was isolated in an 83% yield. The $E_{1/2 \text{ oxd}}$ (+1.48 V *vs.* SCE) of **26'** was found to be higher than the $E_{1/2 \text{ red}}$ (+0.83 V *vs.* SCE) of excited EY. The higher $E_{1/2 \text{ oxd}}$ of **26'** prevents the ET process and further cyclization in the case of 2-styrylaniline (**26**) (Scheme IV.3.2).



Scheme IV.3.3. Intermolecular competitive and mechanistic investigation.

After synthesizing a library of isoindolinones, a few control experiments were conducted to get a better insight into the mechanism. To see the electronic effect of substituents on *o*-alkenylanilines, an equimolar mixture of methyl *E*-3-(2-amino-5-methylphenyl)acrylate (**2**) and methyl *E*-3-(2-amino-5-fluorophenyl)acrylate (**6**) was reacted with *tert*-butyl isocyanide (**a**). The yields obtained for *p*-Me (**2**) substituted isoindolinone (**2a**, 30%) was higher than *p*-F (**6**) isoindolinone (**6a**, 19%) which indicates that *o*-alkenylanilines possessing EDGs show better reactivity (Scheme IV.3.3a). This observation is in agreement with the yield pattern obtained in Scheme IV.3.1. The lower yields obtained for substrates bearing EWG (**6-11**) compared to EDG (**1-5**) might be due to the $-M$ and $-I$ effect of EWGs which possibly destabilize the radical intermediate (**A**) as proposed in Scheme IV.3.5. To unearth the origin of extra hydrogen in the product, two independent reactions were carried out, one using DMSO- d_6 (1 mL) and another in a mixture of DMSO and D_2O (10 equiv). In the former, no deuterium incorporation was observed {Scheme IV.3.3b, (i)}, while in the latter, isoindolinone (**2a'**) was obtained in 76% yield with 50% deuteration at α to the ester group {Scheme IV.3.3b, (ii)}. This confirms that the moisture present in solvent (DMSO) is the possible source of hydrogen. To ascertain the origin of the carbonyl oxygen in the product, a reaction was carried out in the presence of 1 equiv of H_2O^{18} which gave an ^{18}O -labelled isoindolinone (**2a''**) in 73% yield. This confirms water to be the source of carbonyl oxygen (Scheme IV.3.3c).



Scheme IV.3.4. Radical trapping experiments.

The reaction in the presence of radical scavenger 2,2,6,6-tetramethylpiperidine-1-oxyl (TEMPO, 1 equiv) and 2,6-di-*tert*butyl-4-methyl phenol (BHT, 1 equiv) turned out to be messy, and the desired product was obtained in <math><15\%</math> yield, confirming the radical nature of the present photochemical approach {Scheme IV.3.4, (i), (ii)}. The formation of trapped TEMPO and BHT adducts of aryl radical intermediate (A) was confirmed by HRMS analysis of the reaction mixture. From intermediate D the reaction can either proceed via radical or an anionic pathway (aza-Michael addition). To ascertain the radical nature of the reaction, a radical-trapping experiment was conducted using pre-synthesized D and diphenyl diselenide. The reaction furnished a mixture of 1a (38%) and a selenide adduct (Y, 42%) {Scheme IV.3.4, (iii)}. While, in the presence of TEMPO, the formation of TEMPO eliminated alkene (Y') along with the detection of intermediates (I) and TEMPOH (II) (by HRMS) supports the radical nature of the reaction. Further, the formation of the adduct (I), along with (Y') and TEMPOH can only happen if there is a formation of an amidyl radical (E). If the reaction proceeds via an exclusive anionic path one cannot account for the formation of any of these intermediates. An anionic

mechanism would only give isoindolinone **1a** {Scheme IV.3.4, (iv)}.^{2ij,31} The reaction of carboxamide **D** in the absence of EY and light gave only 20% of isoindolinone (**1a**) after 16 h {Scheme IV.3.4, (v)}. This suggests that in addition to the anionic mechanism (Scheme IV.3.5, path-II), a predominant radical path is operating concurrently under this photochemical condition. Both light and the photocatalyst are assisting in accelerating the reaction (5 h) and improving the product (**1a**) yield (82%) as opposed to a 20% yield obtained after 16 h under non-photochemical conditions.

To confirm the photochemical nature of the reaction, Stern-Volmer (SV) quenching experiments of eosin Y (EY) were performed using pre-synthesized 2-alkenyl carboxamide intermediate (**D**) (Figure IV.3.3).^{3f,h-k} The cyclization of intermediate (**D**) can occur either through direct reductive quenching or stepwise PT/ET process. Thus, the quenching experiments were carried out in the presence and absence of Cs₂CO₃. The fluorescence maxima of EY-DMSO solution (0.033 mM) was observed at 561 nm when excited at 543 nm. For each quenching experiment, 10 μL of 0.1 M solution of **D** (quencher) was added sequentially. However, no significant change in the fluorescence intensity of EY was observed which rules out the direct reductive quenching of EY by intermediate **D** (Figure IV.3.3a). This hinted that the reaction might be going through the stepwise PT/ET process. To confirm this, another set of quenching experiments was carried out in which 10 μL aqueous solution of Cs₂CO₃ (0.01 M) was added. After the one-time addition of the base, the intensity of the peak at 547 nm (shifted from 561 nm after addition of base) gradually decreases with the sequential addition of the quencher **D** (10 μL of 0.1 M) (Figure. IV.3.3b). A linear quenching was observed in the Stern-Volmer plot (Figure IV.3.3c). This indicates the electron transfer between excited state of eosin Y (EY*) and **D** where Cs₂CO₃ is acting as a Brønsted base and helping in the stepwise PT/ET pathway for the generation of an amidyl radical (**E**). These observations were further supported by the redox potential of **D** in the presence and absence of base. In the absence of a base, no clear peak was observed in the CV plot (Figure IV.3.3d). However, on the addition of equivalence of Cs₂CO₃, the $E_{1/2 \text{ oxd}}$ of **D** was found to be +0.286 V vs. SCE (+0.33 V vs. Ag/AgCl sat. KCl), which is lower than the $E_{1/2 \text{ red}}$ of excited EY, *i.e.*, +0.83 V vs. SCE (Figure IV.3.3e). This confirms the base mediated PT/ET process between the excited state of eosin Y (EY*) and **D** to generate EY⁻ radical anion and an amidyl radical (**E**).

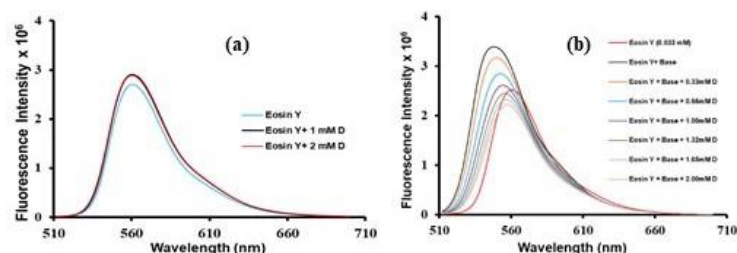


Figure 2a. Quenching of EY fluorescence emission in the presence of **D** when excited at 543 nm.

Figure 2b. Quenching of EY fluorescence emission in presence of base **D** when excited at 543 nm.

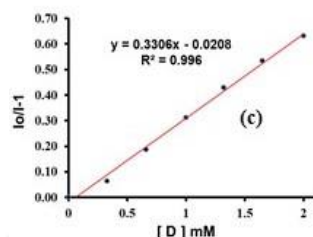


Figure 2c. Stern-Volmer plot **D** and base. A linear quenching was observed.

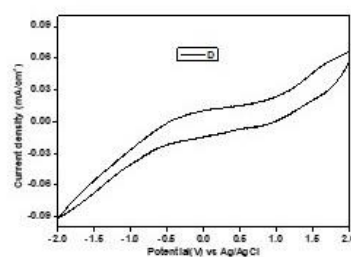


Figure 2d. Cyclic voltammetry plot for **D** in absence of base.

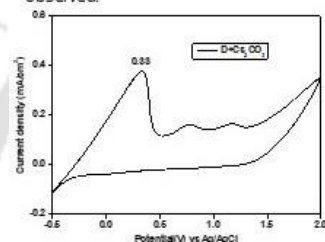


Figure 2e. Cyclic voltammetry plot for **D** in presence of base.

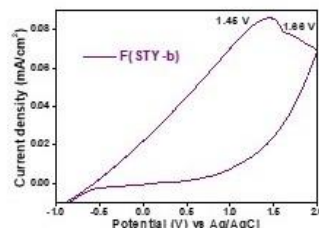
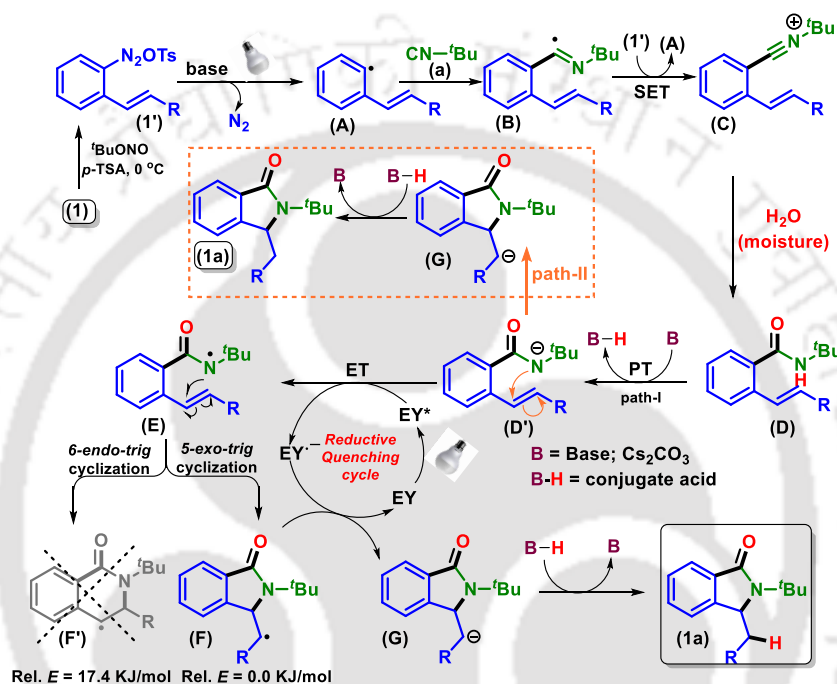


Figure 2f. CV plot for **26'** in presence of base.

Figure IV.3.3. Stern-Volmer and CV results.

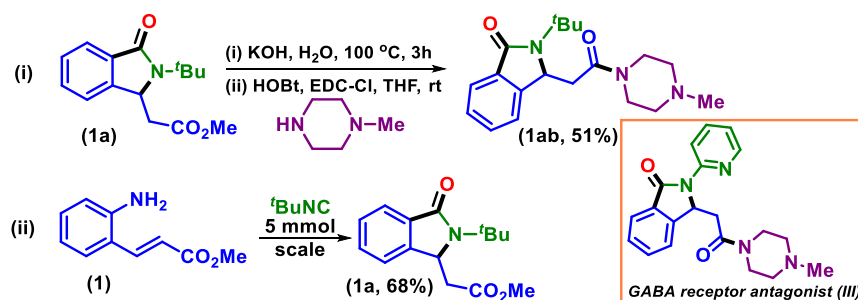
Based on the above experimental results and literature precedents,^{3f,h-k,30} a plausible mechanism is proposed for this photochemical reaction (Scheme IV.3.5). Initially, the *in situ* generated 2-alkenyl arenediazonium salt (**1'**) forms an aryl radical (**A**) via a visible-light-induced deamination process^{29c,d} The aryl radical (**A**) is then trapped by isocyanide (**a**) to give an imidoyl radical (**B**) followed by a single electron transfer (SET) between 2-alkenyl arenediazonium salt (**1'**) and **B** to give a nitrilium intermediate (**C**) and aryl radical (**A**). The nucleophilic addition of water and concurrent tautomerization gives a 2-alkenyl carboxamide species (**D**). As evident from the Stern-Volmer (SV) and CV experiments, the carbonate base induces PT from 2-alkenyl carboxamide (**D**) to give intermediate **D'** followed by ET between the excited state of eosin Y (**EY***) and **D'** to give an amidyl radical (**E**) and a radical anion of eosin Y (**EY⁻**). The intermediate **E** can undergo 5-*exo-trig* or 6-*endo-trig* cyclization. The DFT calculations energetically favours the formation of **F** (5-*exo-trig*) instead of **F'** (6-*endo-trig*) by 17.4 KJ/mol. Thus, a 5-*exo-trig* cyclization of **E** gives intermediate (**F**) which is reduced by radical anion of eosin Y

to give intermediate (**G**), thereby maintaining the reductive catalytic cycle of eosin Y. Finally, the intermediate (**G**) abstracts a proton from the conjugate acid of base (**B-H**) to give the corresponding isoindolinone (**1a**) (Scheme IV.3.5). Based on the control experiment {Scheme IV.3.4, (v)} it is apparent that without photochemical conditions an anionic reaction pathway cannot be completely ruled out (path-II). Notably, the present photocatalytic cycle is a redox-neutral process without the addition of any external oxidant.



Scheme IV.3.5. Plausible mechanism for synthesis of isoindolinones.

To demonstrate the synthetic utility of the isoindolinone products, **1a** was transformed to a useful analogue (**1ab**) of a GABA receptor antagonist (**III**) {Scheme IV.3.6 (i)}. To check the scalability of the present protocol, a standard reaction was carried out at a 5 mmol scale. Delightfully, the anticipated isoindolinone (**1a**) was obtained in 68% yield {Scheme IV.3.6 (ii)}.



Scheme IV.3.6. Post-synthetic modification and gram-scale synthesis.

In conclusion, we have demonstrated a photocatalytic approach for accessing isoindolinones via PT/ET-assisted amidyl radical formation. The photochemical nature of this protocol was confirmed by SV and CV experiments. Mechanistic investigations confirm water as –H and –O sources. This photo cascade methodology is overall a redox neutral process featuring metal-free condition and substrate scope is demonstrated with 32 examples. This method is amenable to gram-scale synthesis. The practical utility of the present protocol is demonstrated by synthesizing analogue of GABA receptor antagonist.

IV.4. Experimental Section

IV.4.1. General Information: All the compounds were commercial grade and used without further purification. HPLC grade solvents were purchase from commercial source. Organic extracts were dried over anhydrous sodium sulfate. Solvents were removed in a rotary evaporator under reduced pressure. Silica gel (60–120 mesh size) was used for the column chromatography. Reactions were monitored by TLC on silica gel 60 F₂₅₄ (0.25 mm). All NMR spectras were recorded in CDCl₃ with tetramethylsilane (TMS) as an internal standard for ¹H NMR (400, 500 and 600 MHz) and CDCl₃ solvent as an internal standard for ¹³C{¹H} NMR (100, 125 and 150 MHz). NMR. Both ¹H and ¹³C{¹H} NMR spectra were referenced to the residual CDCl₃ (δ 7.260 and 77.230 ppm). HRMS spectra were recorded using ESI mode (Q-TOF MS Analyzer). IR spectra were recorded in KBr or neat in FT-IR spectra.

IV.4.2. Crytallographic Description

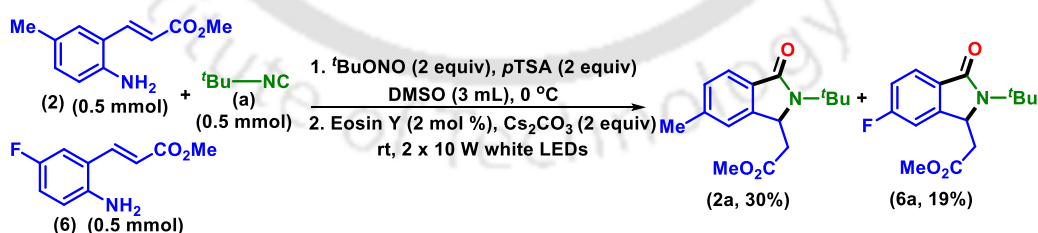
CCDC Number for Compound 1d: CCDC-2102335 contains the supplementary crystallographic data for this paper. These data can be obtained free of charge from The Cambridge Crystallographic Data Centre via www.ccdc.cam.ac.uk/data_request/cif.

Crystallographic Description of Methyl 2-(2-(naphthalen-2-yl)-3-oxoisindolin-1-yl)acetate (1d): C₂₁H₁₇NO₃, colorless rod-shape; crystal dimensions 0.11 x 0.06 x 0.05 mm; $M_r = 331.36$; monoclinic; space group P 2₁/c; $a = 17.0695(7)$, $b = 5.9841(2)$, $c = 17.1635 \text{ \AA}$; $\alpha = 90^\circ$, $\beta = 107.945(4)$, $\gamma = 90^\circ$, $V = 1667.89(12) \text{ \AA}^3$; $Z = 4$; $\rho_{\text{calcd}} = 1.320 \text{ g/cm}^3$; $\mu = 0.089 \text{ mm}^{-1}$, $F(000) = 696.0$, reflection collected / unique = 3624 / 2412, refinement method = full-matrix least-squares on F^2 , final R indices [$I > 2\sigma(I)$]: $R_1 =$

0.0782, $wR_2 = 0.2424$, R indices (all data): $R_1 = 0.1022$, $wR_2 = 0.2180$, goodness of fit = 0.992.

IV.4.3. General Procedure for Synthesis of 2-(2-(*tert*-Butyl)-3-oxoisindolin-1-yl)acetate (1a): To an oven-dried 10 mL screw-cap borosilicate vial, methyl *E*-3-(2-aminophenyl)acrylate (**1**) (0.5 mmol, 88.5 mg), *tert*-butyl nitrite (0.5 mmol, 51.5 mg), *p*-toluenesulfonic acid (0.5 mmol, 96.0 mg), DMSO (2 mL) were taken and the reaction mixture was stirred in an ice bath for 30 mins. After completion of the reaction (as indicated by the disappearance of **1** in TLC analysis) the vial was taken out from the bath. To this diazotized mixture, eosin Y (2 mol %, 6.47 mg), *tert*-butyl isocyanide (**a**) (0.5 mmol, 41.5 mg), Cs_2CO_3 (2 equiv, 325.8 mg) were added and the reaction mixture was stirred at room temperature for 5 h, tentatively at a distance of ~6-8 cm from two 10 W white LED bulbs. After completion of the reaction (monitored by TLC analysis), the solvent was removed in vacuum and the mixture was admixed with 20 mL ethyl acetate and sequentially washed with brine solution (2 x 10 mL) and aqueous NaHCO_3 (1 x 10 mL). The organic layer was dried over anhydrous Na_2SO_4 , and the solvent was evaporated under reduced pressure. The crude residue thus obtained was purified by column chromatography over silica gel (60–120 mesh) using hexane and ethyl acetate (17:3) as eluent to afford methyl 2-(2-(*tert*-butyl)-3-oxoisindolin-1-yl)acetate (**1a**) in 82% yield. The identity and purity of the product was confirmed by spectroscopic analysis.

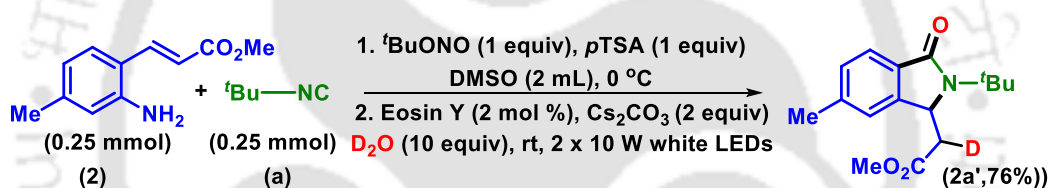
IV.4.4. Intermolecular Competitive Experiment



To an oven-dried 10 mL screw-cap borosilicate vial, methyl *E*-3-(2-amino-5-methylphenyl)acrylate (**2**) (0.5 mmol, 95.5 mg), methyl *E*-3-(2-amino-5-fluorophenyl)acrylate (**6**) (0.5 mmol, 97.5 mg), *tert*-butyl nitrite (1 mmol, 2 equiv, 103 mg), *p*-toluenesulfonic acid (1 mmol, 2 equiv, 190 mg), DMSO (3 mL) were taken and the reaction mixture was stirred in an ice bath for 30 mins. After completion of the reaction (as indicated by the disappearance of **2** and **6** in TLC analysis) the vial was taken out

from the bath. To this diazotized mixture, eosin Y (2 mol %, 6.47 mg), *tert*-butyl isocyanide (**a**) (0.5 mmol, 1 equiv, 41.5 mg), Cs₂CO₃ (2 equiv, 325 mg) were added and the reaction mixture was stirred at room temperature for 6 h, tentatively at a distance of ~6-8 cm from two 10 W white LED bulbs. After completion of the reaction (monitored by TLC analysis), the solvent was removed *in vacuo* and the mixture was admixed with 20 mL ethyl acetate and sequentially washed with brine solution (2 x 10 mL) and aqueous NaHCO₃ (1 x 10 mL). The organic layer was dried over anhydrous Na₂SO₄, and the solvent was evaporated under reduced pressure. The crude residue thus obtained was purified by column chromatography over silica gel (60-120 mesh) using hexane and ethyl acetate (17:3) as eluent to afford methyl 2-(2-(*tert*-butyl)-6-methyl-3-oxoisindolin-1-yl)acetate (**2a**, 30%) and methyl 2-(2-(*tert*-butyl)-6-fluoro-3-oxoisindolin-1-yl)acetate (**6a**, 19%).

IV.4.5. Deuterium Labelling Experiment



To an oven-dried 10 mL screw-cap borosilicate vial, methyl *E*-3-(2-amino-4-methylphenyl)acrylate (**2**) (0.25 mmol, 47.7 mg), *tert*-butyl nitrite (0.25 mmol, 1 equiv 25.7 mg), *p*-toluenesulfonic acid (0.25 mmol, 1 equiv 48.0 mg), DMSO (1.5 mL) were taken and the reaction mixture was stirred in an ice bath for 30 mins. After completion of the reaction (as indicated by the disappearance of **2** in TLC analysis) the vial was taken out from the bath. To this diazotized mixture, eosin Y (2 mol %, 3.23 mg), *tert*-butyl isocyanide (**a**) (0.25 mmol, 20.2 mg), Cs₂CO₃ (2 equiv, 162.5 mg) were added and the reaction mixture was stirred at room temperature for 5 h, tentatively at a distance of ~6-8 cm from two 10 W white LED bulbs. After completion of the reaction (monitored by TLC analysis), the solvent was removed *in vacuo* and the mixture was admixed with 20 mL ethyl acetate and sequentially washed with brine solution (2 x 10 mL) and aqueous NaHCO₃ (1 x 10 mL). The organic layer was dried over anhydrous Na₂SO₄, and the solvent was evaporated under reduced pressure. The crude residue thus obtained was purified by column chromatography over silica gel (60-120 mesh) using hexane and ethyl acetate (17:3) as eluent to afford [*d*]-2-(2-(*tert*-butyl)-6-methyl-3-oxoisindolin-1-

yl)acetate (**2a'**) in 76% yield. The extent of H/D exchange was calculated from ^1H NMR (Figure IV.5.1) and ESI-MS (Figure IV.5.2) analyses.

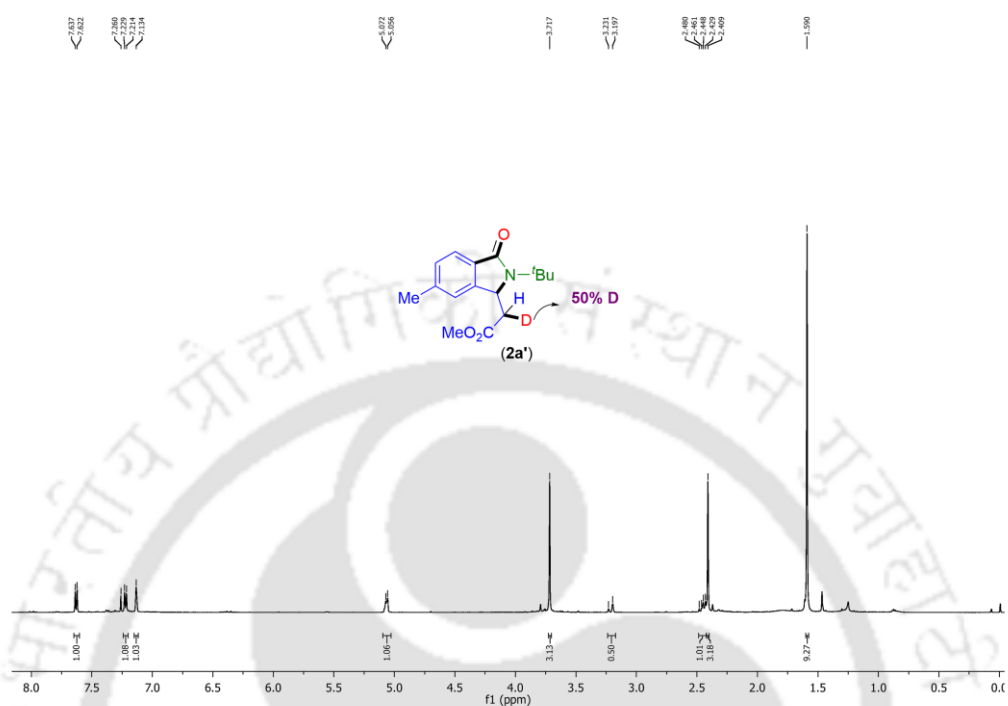


Figure IV.5.1. ^1H NMR spectra of **2a'** (CDCl_3 , 500 MHz).

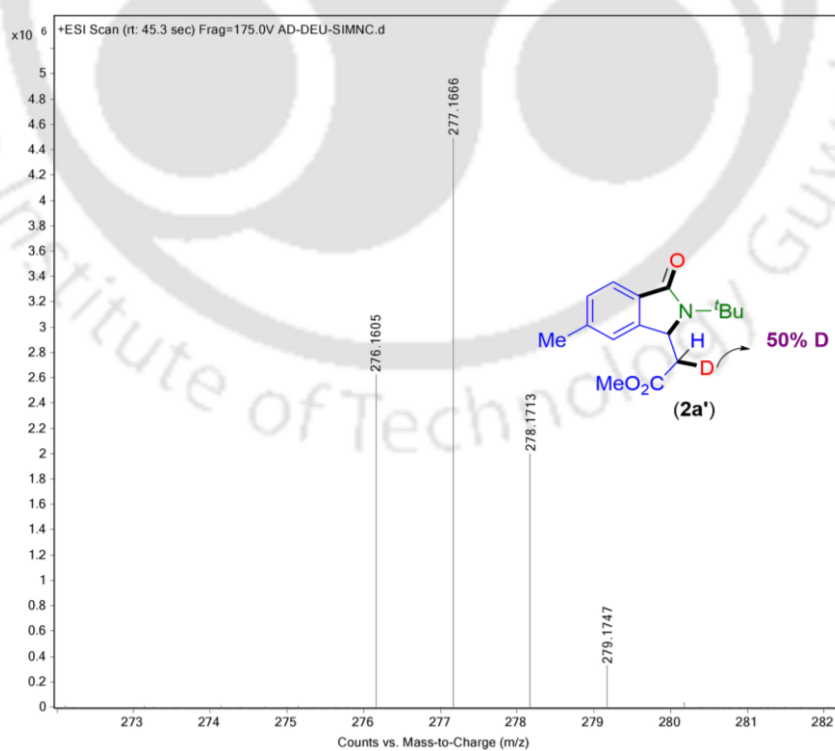
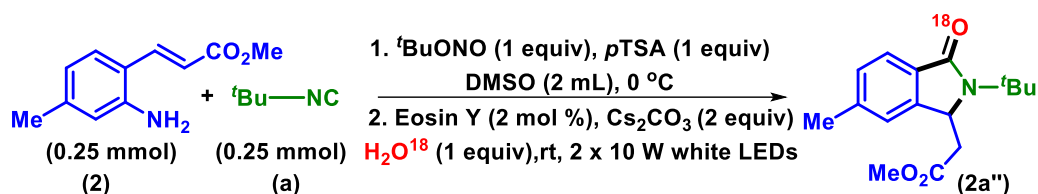


Figure IV.5.2. ESI-MS spectra of deuterated **2a'**.

IV.4.6. ^{18}O Labelling Experiment

To an oven-dried 10 mL screw-cap borosilicate vial, methyl *E*-3-(2-aminophenyl)acrylate (**1**) (0.25 mmol, 47.7 mg), *tert*-butyl nitrite (0.25 mmol, 1 equiv, 25 mg), *p*-toluenesulfonic acid (0.25 mmol, 1 equiv, 48.0 mg), DMSO (1.5 mL) were taken and the reaction mixture was stirred in an ice bath for 30 mins. After completion of the reaction (as indicated by the disappearance of **2** in TLC analysis) the vial was taken out from the bath. To this diazotized mixture, eosin Y (2 mol %, 3.23 mg), *tert*-butyl isocyanide (**a**) (0.25 mmol, 1 equiv, 20.2 mg), Cs_2CO_3 (2 equiv, 162.5 mg) were added and the reaction mixture was stirred at room temperature for 5 h, tentatively at a distance of ~6-8 cm from two 10 W white LED bulbs. After completion of the reaction (monitored by TLC analysis), the solvent was removed *in vacuo* and the mixture was admixed with 20 mL ethyl acetate and sequentially washed with brine solution (2 x 10 mL) and aqueous NaHCO_3 (1 x 10 mL). The organic layer was dried over anhydrous Na_2SO_4 , and the solvent was evaporated under reduced pressure. The crude residue thus obtained was purified by column chromatography over silica gel (60-120 mesh) using hexane and ethyl acetate (17:3) as eluent to afford methyl 2-(2-(*tert*-butyl)-6-methyl-3-oxoisindolin-1-yl)acetate (**2a''**) in 73% yield. The formation of ^{18}O -labeled isoindolinone (**2a''**) was confirmed by spectroscopic and HRMS analysis. In $^{13}\text{C}\{^1\text{H}\}$ NMR, **2a''** shows two signals (δ 168.145 and 168.115 ppm) due to both labelled and unlabeled carbonyl groups (amide) of isoindolinone (Figure IV.6.1). Further, the HRMS analysis also confirms the formation of ^{18}O -labeled isoindolinone (**2a''**) (Figure IV.6.2). This confirms that water is the source of carbonyl oxygen.

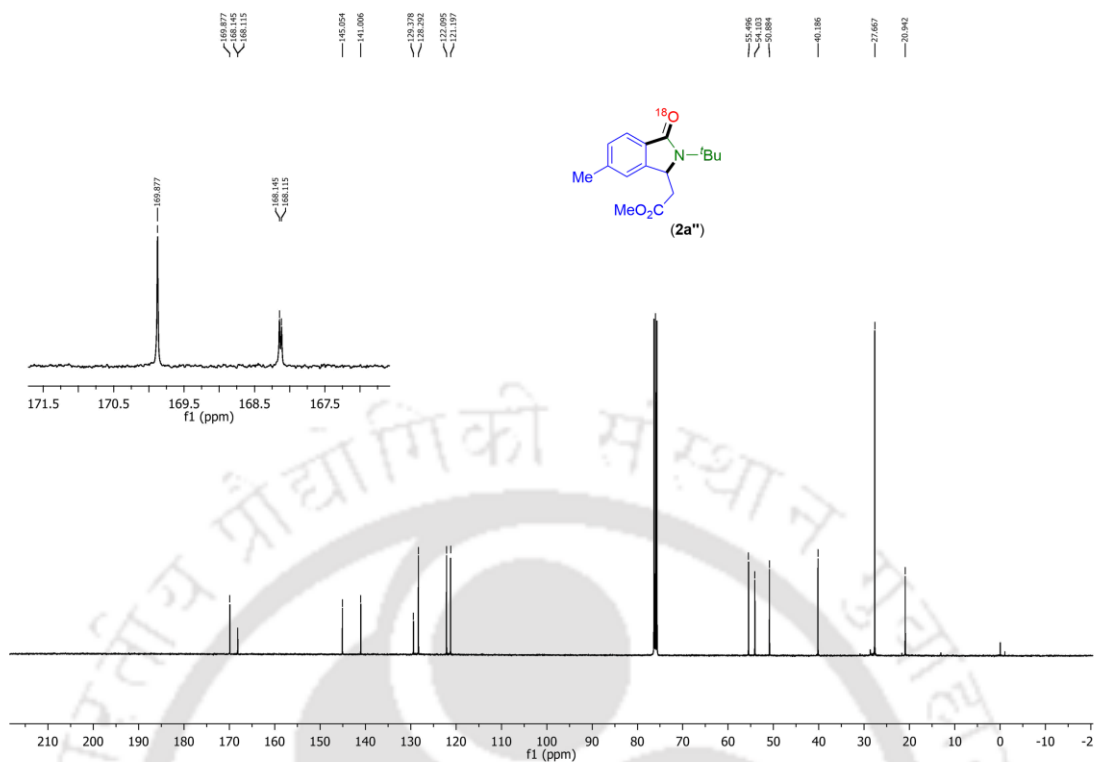


Figure IV.4.6.1. $^{13}\text{C}\{^1\text{H}\}$ NMR spectra of ^{18}O labelled isoindolinone ($2a''$).

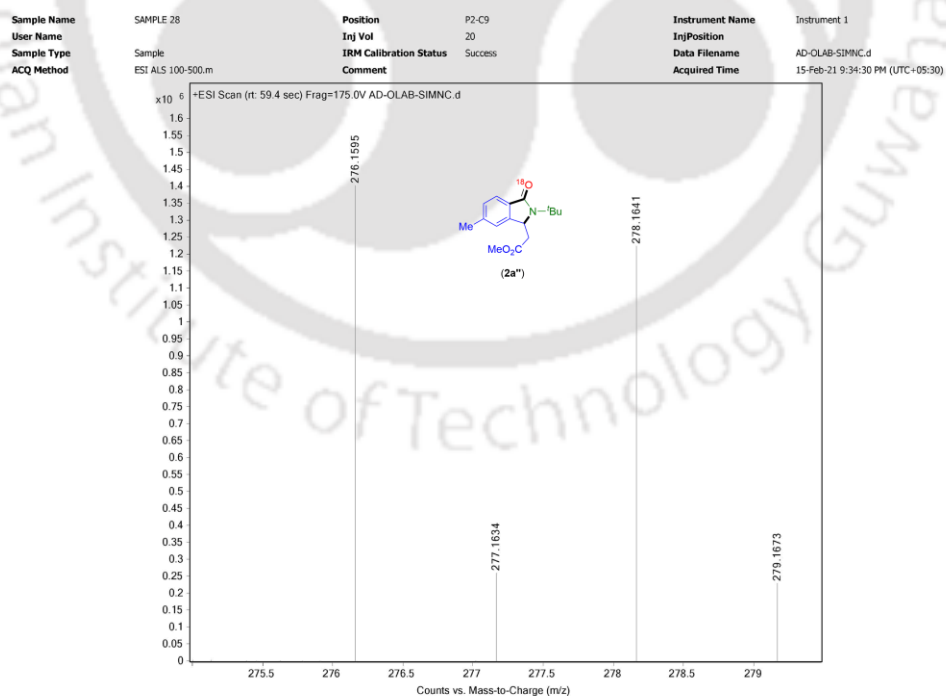
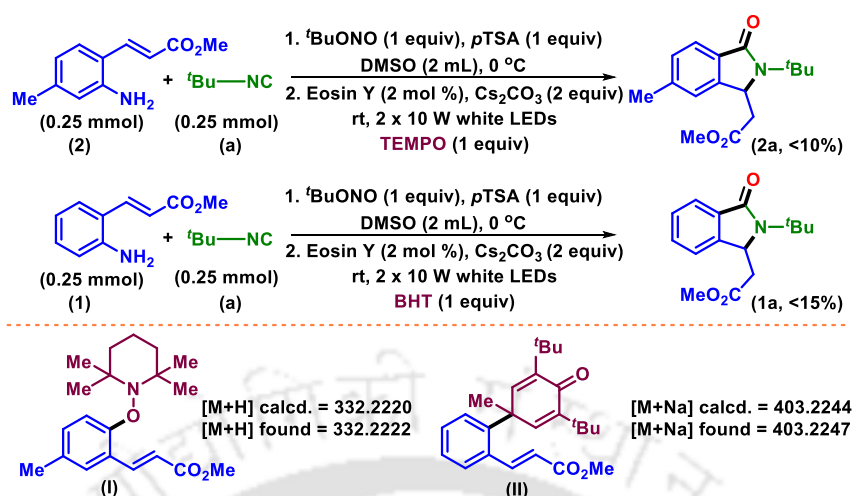


Figure IV.4.6.2 ESI-MS spectra of ^{18}O labelled isoindolinone ($2a''$).

IV.4.7. Radical-trapping Experiment



For this experiment, two sets of reactions were carried out. In reaction (i), methyl (*E*)-3-(2-amino-4-methylphenyl)acrylate (**2**) (0.25 mmol, 47.7 mg), *tert*-butyl nitrite (0.25 mmol, 25.7 mg), *p*-toluenesulfonic acid (0.25 mmol, 48.0 mg), DMSO (1.5 mL) were taken and the reaction mixture was stirred in an ice bath for 30 mins. After completion of the reaction (as indicated by the disappearance of **2** in TLC analysis) the vial was taken out from the bath. To this diazotized mixture, eosin Y (2 mol %, 3.23 mg), *tert*-butyl isocyanide (**a**) (0.25 mmol, 1 equiv, 20.2 mg), Cs₂CO₃ (2 equiv, 162.5 mg), 2,2,6,6-tetramethylpiperidine 1-oxyl (TEMPO) (1 equiv, 78 mg) were added and the reaction mixture was stirred at room temperature for 5 h, tentatively at a distance of ~6–8 cm from two 10 W white LED bulbs. A small aliquot of the reaction mixture was withdrawn at different intervals (5 min, 10 min and 15 min) and diluted with 60:40 CH₃CN: H₂O mixture (1 mL) and subjected to HRMS. The HRMS analysis of this reaction aliquot shows HRMS values for TEMPO adduct (**I**) (Figure IV.4.7.1). This observation infers the generation of aryl radical (**A**) after the deamination process.

In reaction (ii), methyl *E*-3-(2-aminophenyl)acrylate (**1**) (0.25 mmol, 44.2 mg), *tert*-butyl nitrite (0.25 mmol, 1 equiv, 25.7 mg), *p*-toluenesulfonic acid (0.25 mmol, 1 equiv, 48.0 mg), DMSO (1.5 mL) were taken and the reaction mixture was stirred in an ice bath for 30 mins. After completion of the reaction (as indicated by the disappearance of **1** in TLC analysis) the vial was taken out from the bath. To this diazotized mixture, eosin Y (2 mol %, 3.23 mg), *tert*-butyl isocyanide (**a**) (0.25 mmol, 1 equiv, 20.2 mg), Cs₂CO₃ (2 equiv, 162.5 mg), 2,6-di-*tert*-butyl-4-methylphenol (BHT) (1 equiv, 110 mg) were added and the reaction mixture was stirred at room temperature for 5 h, tentatively at a distance

of ~6-8 cm from two 10 W white LED bulbs. A small aliquot of the reaction mixture was withdrawn at different intervals (5 min, 10 min and 15 min) and diluted with 60:40 CH₃CN : H₂O mixture (1 mL) and subjected to HRMS. The HRMS analysis of this reaction aliquot shows mass values for BHT adduct (**II**) (Figure IV.4.7.2). This observation further confirms the generation of aryl radical (**A**) after the deamination process.

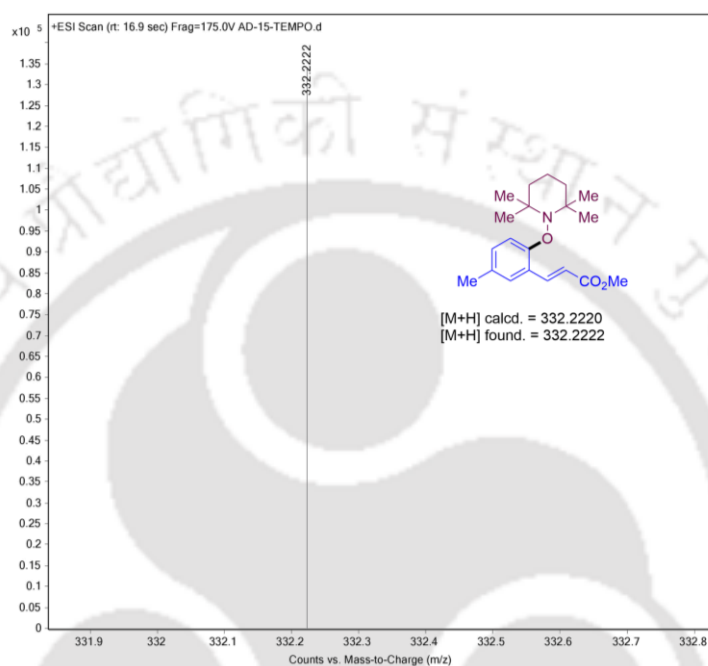


Figure IV.4.7.1. HRMS spectra of TEMPO-adduct (**I**).

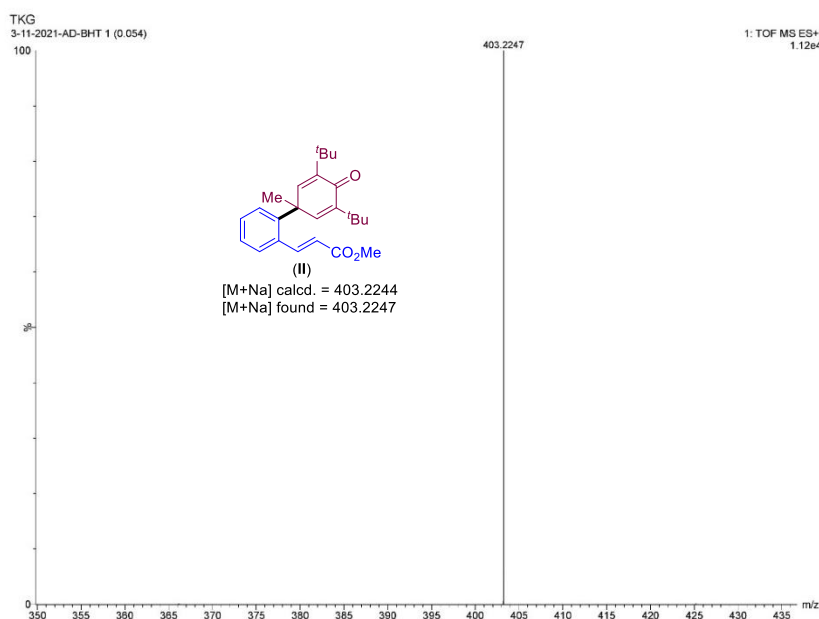
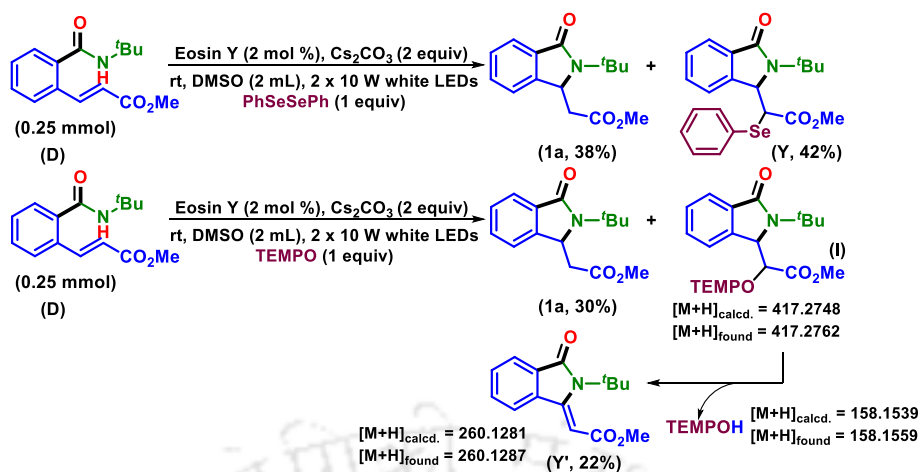


Figure IV.4.7.2. HRMS spectra of BHT-adduct (**II**).



To an oven-dried 10 mL screw-cap borosilicate vial, methyl 3-(2-(*tert*-butylcarbamoyl)phenyl)acrylate (**D**) (0.25 mmol, 65.0 mg), eosin Y (2 mol %, 3.23 mg), Cs₂CO₃ (2 equiv, 162.5 mg), PhSeSePh (1 equiv), DMSO (2 mL) were added and the reaction mixture was stirred at room temperature for 2 h, tentatively at a distance of ~6-8 cm from two 10 W white LED bulbs. After completion of the reaction (monitored by TLC analysis), the solvent was removed *in vacuo* and the mixture was admixed with 20 mL ethyl acetate and sequentially washed with brine solution (2 x 10 mL) and aqueous NaHCO₃ (1 x 10 mL). The organic layer was dried over anhydrous Na₂SO₄, and the solvent was evaporated under reduced pressure. The crude residue thus obtained was purified by column chromatography over silica gel (60-120 mesh) using hexane and ethyl acetate (9:1) as eluent to afford methyl 2-(2-(*tert*-butyl)-3-oxoisindolin-1-yl)-2-(phenylselanyl)acetate (**Y**) in 42% yield. The identity and purity of the product was confirmed by spectroscopic analysis (Figure IV.4.7.3-5).

In reaction (ii), methyl 3-(2-(*tert*-butylcarbamoyl)phenyl)acrylate (**D**) (0.25 mmol, 65.0 mg), eosin Y (2 mol %, 3.23 mg), Cs₂CO₃ (2 equiv, 162.5 mg), TEMPO (1 equiv), DMSO (2 mL) were added and the reaction mixture was stirred at room temperature for 2 h, tentatively at a distance of ~6-8 cm from two 10 W white LED bulbs. A small aliquot of the reaction mixture was withdrawn at 15 min and diluted with 60:40 CH₃CN : H₂O mixture (1 mL) and subjected to HRMS. The HRMS analysis of this reaction aliquot shows mass values for TEMPO adduct (**I**), TEMPOH and **Y'**. This observation further confirms the generation of amidyl radical (**E**) and subsequent C-radical (**F**). After completion of the reaction (monitored by TLC analysis), the solvent was removed *in vacuo* and the mixture was admixed with 20 mL ethyl acetate and sequentially washed with brine solution (2 x 10 mL) and aqueous NaHCO₃ (1 x 10 mL). The organic layer

was dried over anhydrous Na_2SO_4 , and the solvent was evaporated under reduced pressure. The crude residue thus obtained was purified by column chromatography over silica gel (60-120 mesh) using hexane and ethyl acetate (1:35) as eluent to afford methyl (*Z*)-2-(2-(*tert*-butyl)-3-oxoisindolin-1-ylidene)acetate (**Y'**) in 22% yield. The identity and purity of the product was confirmed by spectroscopic analysis (Figure IV.4.7.6-10).

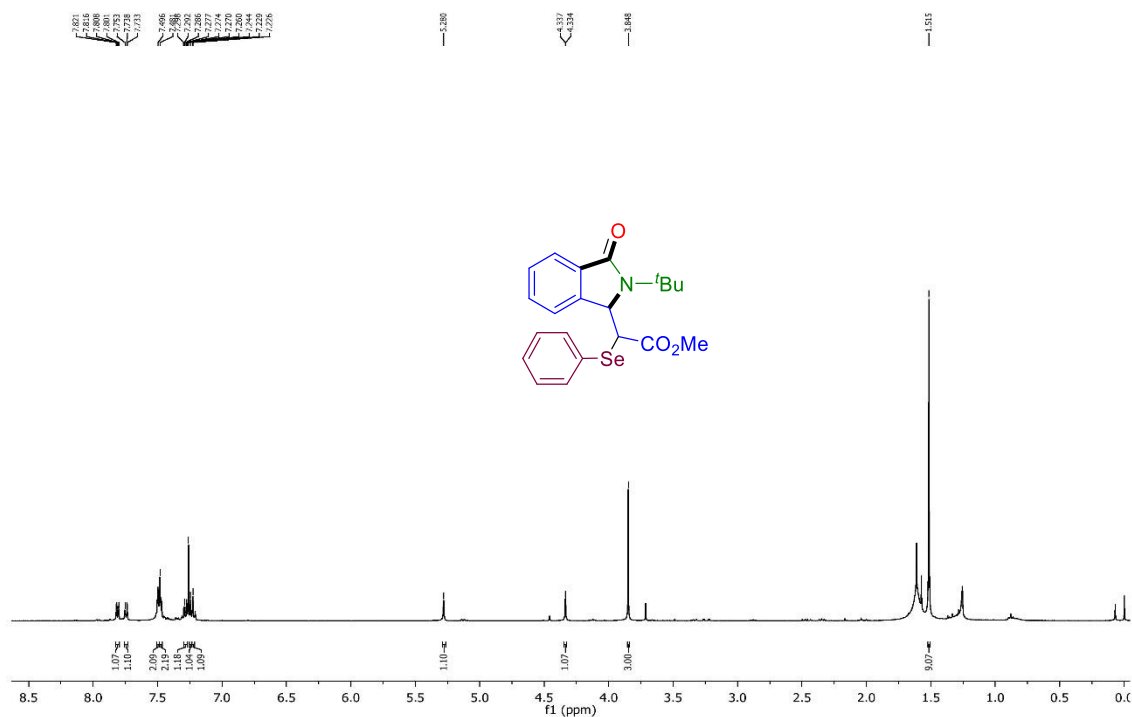


Figure IV.4.7.3. ^1H NMR spectra of selenide adduct **Y** (400 MHz, CDCl_3).

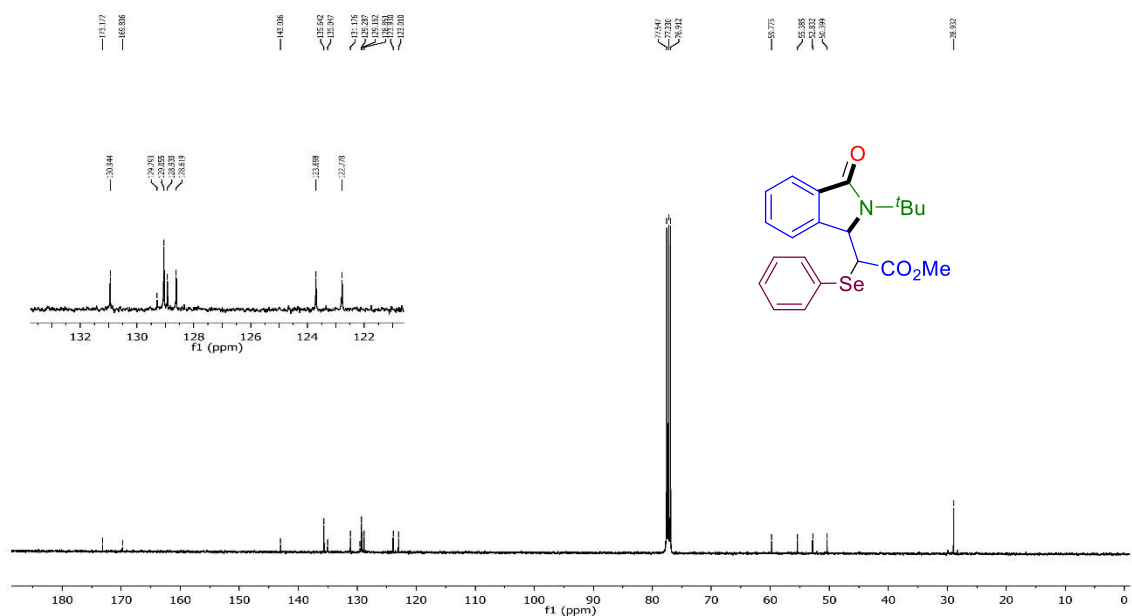


Figure IV.4.7.4. $^{13}\text{C}\{^1\text{H}\}$ NMR spectra of selenide adduct **Y** (100 MHz, CDCl_3).

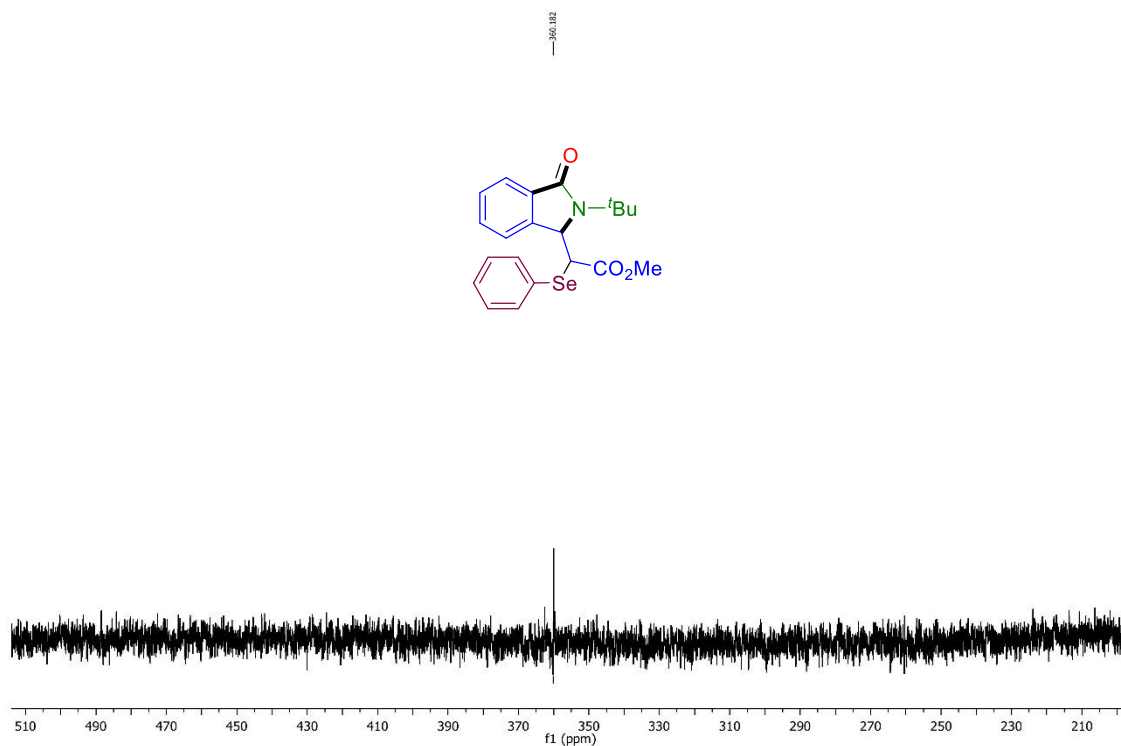


Figure IV.4.7.5. ^{77}Se NMR spectra of selenide adduct Y (500 MHz, CDCl_3).

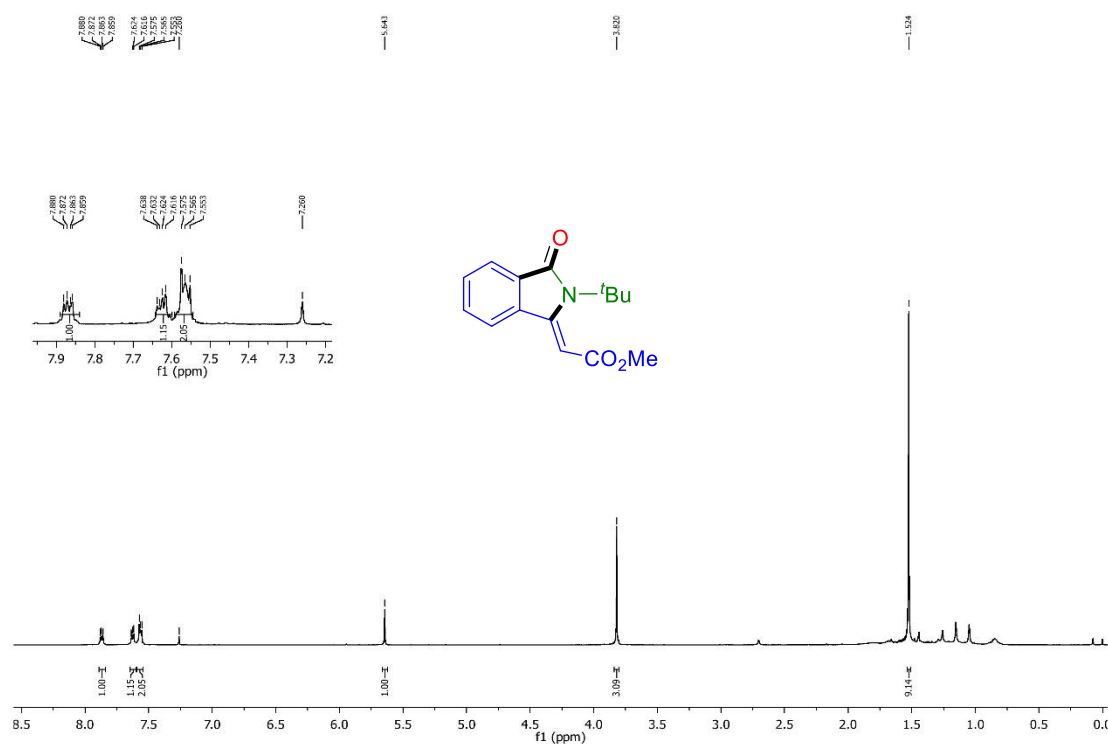


Figure IV.4.7.6. ^1H NMR spectra of TEMPO adduct Y' (400 MHz, CDCl_3).

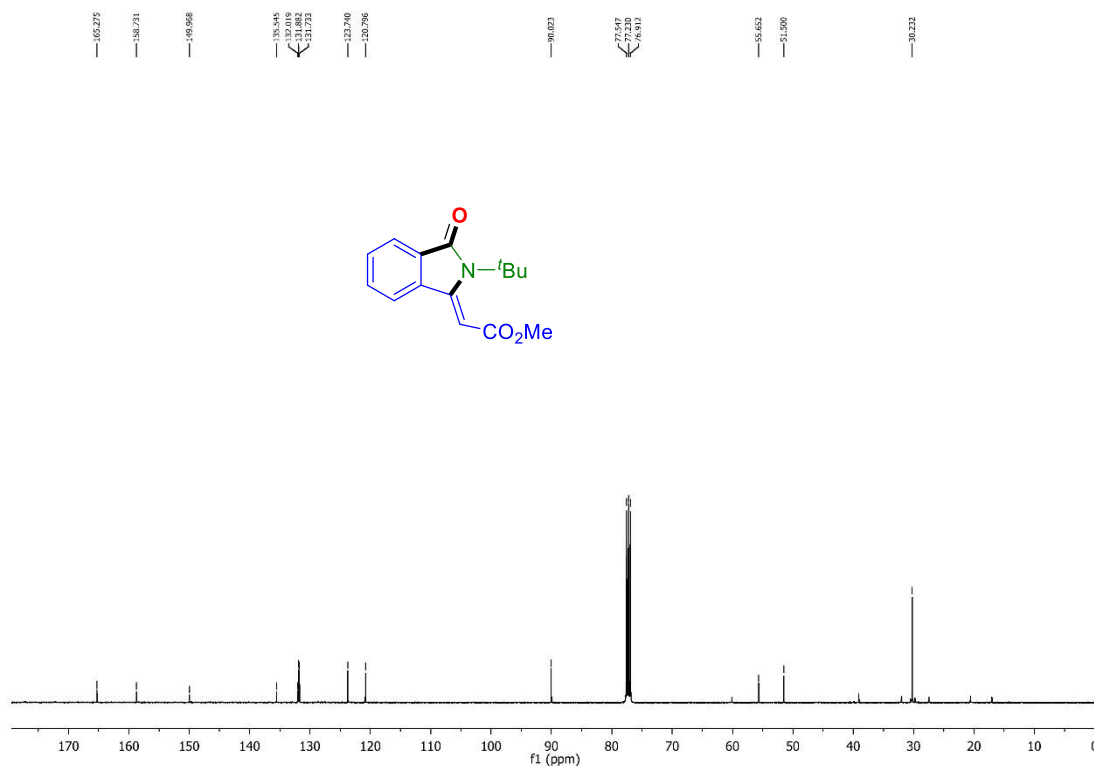


Figure IV.4.7.7. ¹³C NMR spectra of TEMPO adduct Y' (100 MHz, CDCl₃).

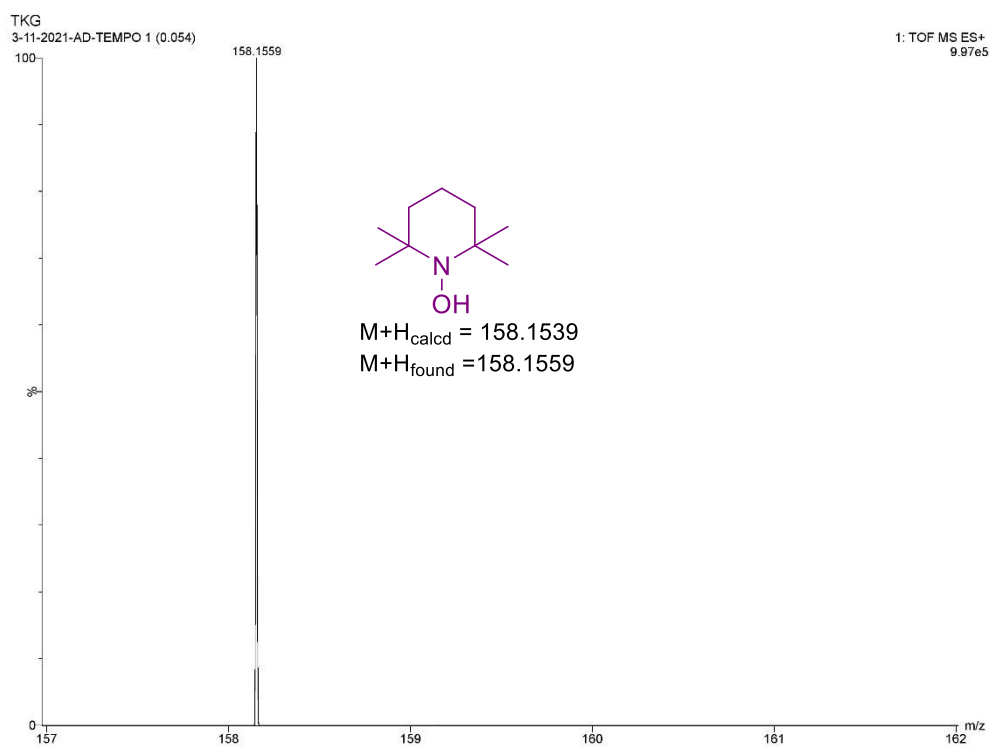


Figure IV.4.7.8. HRMS spectra of TEMPOH.

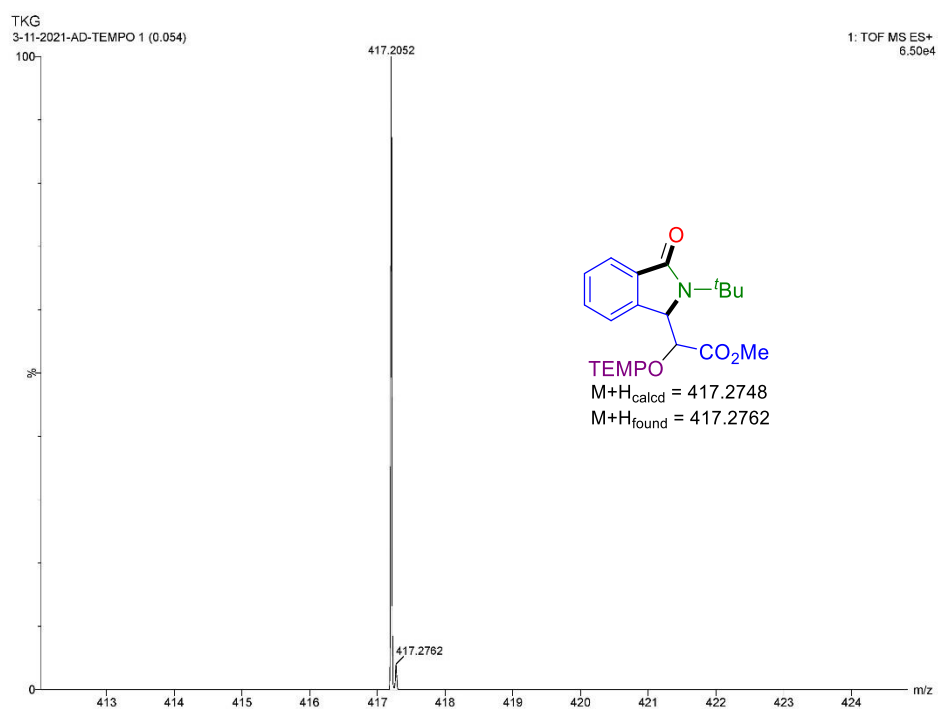


Figure IV.4.7.9. HRMS spectra of TEMPO-adduct (I).

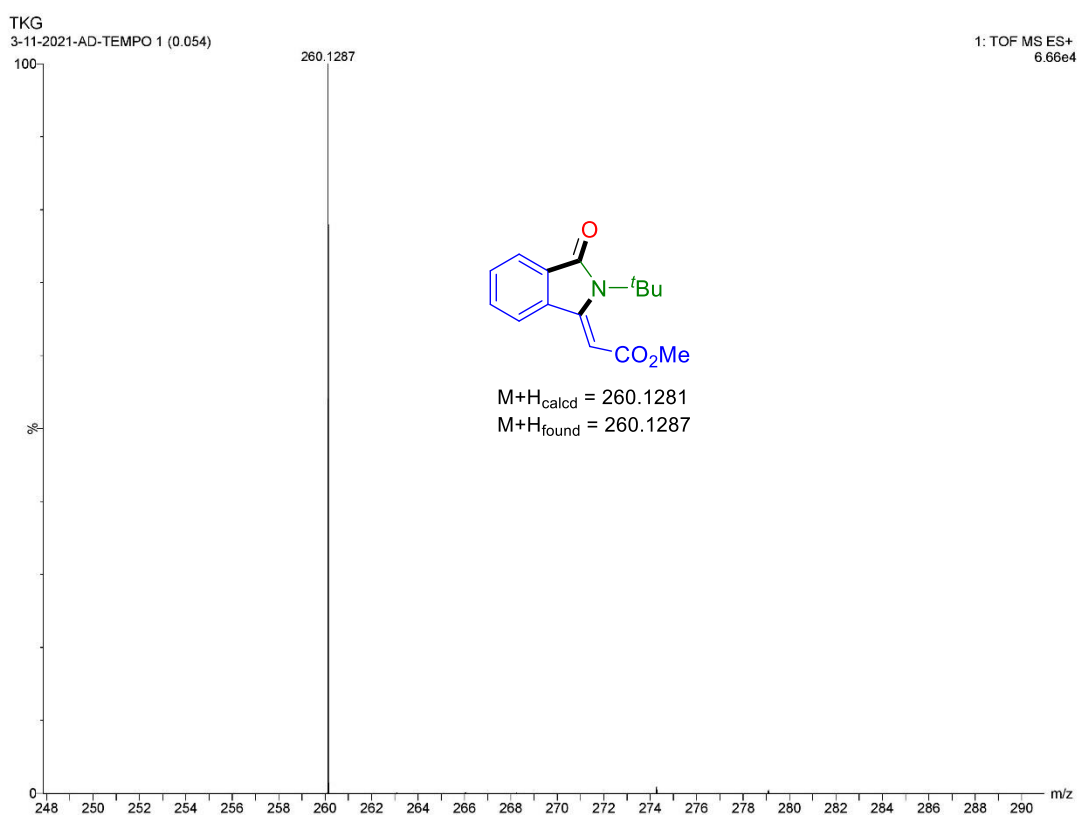


Figure IV.4.7.10. HRMS spectra of Y'.

IV.4.8. Stern-Volmer Quenching Studies

UV-visible spectroscopy of reaction solution was recorded on a SHIMADZU UV3600 UV-visible spectrophotometer. The 0.01 M sample was prepared by mixing eosin Y in DMSO in a light path quartz UV cuvette. The UV-visible spectroscopy indicated that the maximum absorption wavelength of the reaction solution was found to be 543 nm. The absorption was collected and the results are shown in Figure IV.4.8.1.

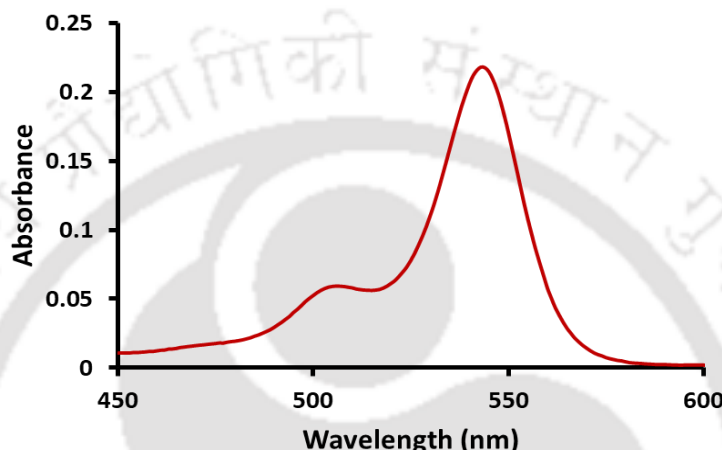


Figure IV.4. 8.1. UV-vis spectra of eosin Y in DMSO (0.01 M).

Next, the fluorescence emission intensity of the reaction solution was recorded on a Fluoromax-4600 spectrofluorimeter. At first, we investigated the excitation and emission spectra of the photocatalyst eosin Y. The excitation wavelength was fixed at 543 nm, and the emission wavelength was measured at 561 nm. At first, the quenching experiment was carried out in absence of Cs_2CO_3 . For this experiment, 0.01 M eosin Y solution was prepared in DMSO. The concentration of methyl *E*-3-(2-(*tert*-butylcarbamoyl)phenyl)acrylate (**D**) (quencher) stock solution is 1 M in DMSO. For each quenching experiment, 10 μL of *E*-3-(2-(*tert*-butylcarbamoyl)phenyl)acrylate (**D**) stock solution was titrated to a mixed solution of eosin Y (0.033 mM). Then the emission intensity was collected and the results are presented in Figure IV.4.8.2. As evident from Figure IV.4.8.2, no significant change in the fluorescence intensity of EY was observed which rules out the direct reductive quenching of EY by intermediate **D**.

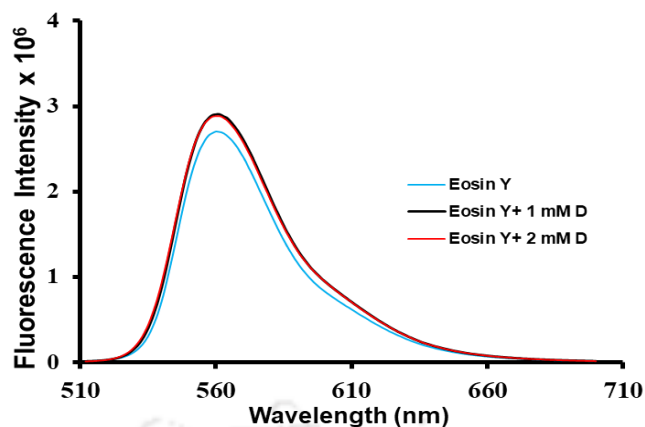


Figure IV.4.8.2. Quenching of eosin Y fluorescence emission in the presence of *E*-3-(2-(*tert*-butylcarbamoyl)phenyl)acrylate (**D**) when excited at 543 nm.

In the second set of experiments, 0.01 M aqueous solution of Cs_2CO_3 was prepared. The concentration of methyl *E*-3-(2-(*tert*-butylcarbamoyl)phenyl)acrylate (**D**) (quencher) stock solution is 0.1 M in DMSO. First, 10 μL of Cs_2CO_3 solution was added and the emission maxima was shifted from 561 to 547 nm. After that, 10 μL of *E*-3-(2-(*tert*-butylcarbamoyl)phenyl)acrylate (**D**) stock solution was titrated to a mixed solution of eosin Y (0.033 mM). The emission intensity was collected and the results are presented in Figure IV.4.8.3. As evident from Figure IV.4.8.3, a gradual decrease in the fluorescence intensity of EY was observed which confirms that Cs_2CO_3 is acting as a Brønsted base and helping in the PT/ET pathway for the generation of amidyl radical **E** from *E*-3-(2-(*tert*-butylcarbamoyl)phenyl)acrylate (**D**).

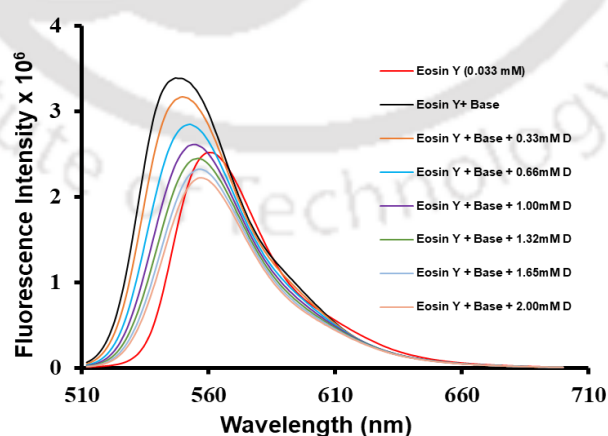


Figure IV.4.8.3. Quenching of eosin Y fluorescence emission in the presence of base and *E*-3-(2-(*tert*-butylcarbamoyl)phenyl)acrylate (**D**) when excited at 543 nm.

In presence of a base, fluorescence quenching phenomenon of eosin Y under various concentrations of *E*-3-(2-(*tert*-butylcarbamoyl)phenyl)acrylate was demonstrated in Stern-Volmer graph using the equation $I_0/I_t = 1 + K_{SV} [Q]$ where I_0 and I_t are integrated emission intensity in the absence and presence of quencher and K_{SV} are quenching constant. As evident from Figure IV.4.8.4, a linear quenching was observed which confirms Cs_2CO_3 is acting as a Brønsted base and helping in the PT/ET pathway for the generation of an amidyl radical (**E**) from *E*-3-(2-(*tert*-butylcarbamoyl)phenyl)acrylate (**D**).

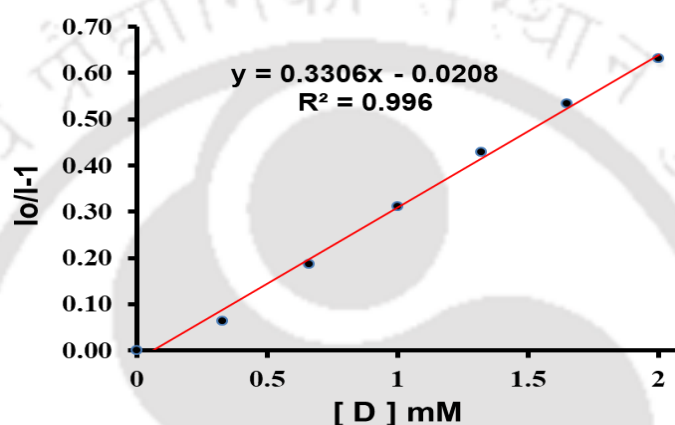


Figure IV.4.8.4. Stern-Volmer plot in presence of *E*-3-(2-(*tert*-butylcarbamoyl)phenyl)acrylate (**D**) and base. A linear quenching was observed.

IV.4.9. Cyclic Voltammetry Experiments

All the PEC measurements were characterized with the help of an electrochemical workstation with model number CHI1120B having a three-electrode system. The three-electrode cell configuration comprised a glassy carbon, a platinum wire and Ag(s)/AgCl (0.01 M) as the working, auxiliary, and reference electrodes respectively. The supporting electrolyte used was tetraethylammonium hexafluorophosphate $(\text{C}_2\text{H}_5)_4\text{N}(\text{PF}_6)$. Samples were prepared with a substrate concentration of 0.01 M in a 0.1 M TEAHFP in the acetonitrile electrolyte solution. In absence of base, no clear peak for *E*-3-(2-(*tert*-butylcarbamoyl)phenyl)acrylate (**D**) was observed (Figure IV.4.9.1). However, on the addition of equivalence of Cs_2CO_3 , the $E_{1/2 \text{ oxd}}$ of **D** was found to be +0.286 V vs. SCE (+0.33 V vs. Ag/AgCl sat. KCl), which is lower than the $E_{1/2 \text{ red}}$ of excited EY, i.e., +0.83 V vs. SCE (Figure IV.4.9.2). This confirms base mediated PT/ET between the excited state of eosin Y (EY^*) and **D** to generate $\text{EY}^{\cdot -}$ radical anion and an amidyl radical (**E**).

The reaction with an electron-rich alkene *viz.* 2-styrylaniline (**26**) stopped at corresponding carboxamide (**26'**, 83%) step. To find out the exact reason, the $E_{1/2 \text{ oxd}}$ of **26'** was calculated in presence of Cs_2CO_3 . The $E_{1/2 \text{ oxd}}$ of **26'** (+1.48 V *vs.* SCE) is higher than the $E_{1/2 \text{ red}}$ of excited EY (+0.83 V *vs.* SCE) which prevents the ET process and the further cyclization (Figure IV.4.9.3).

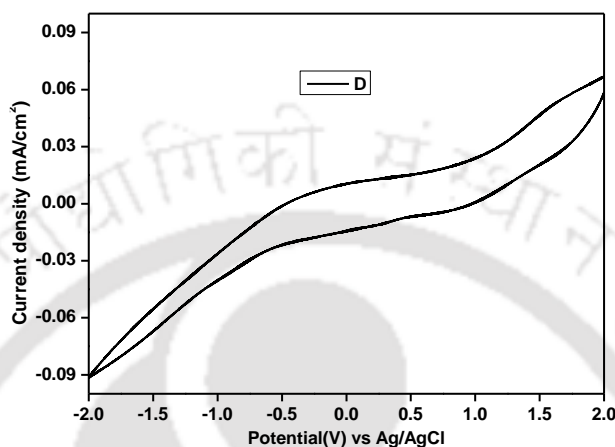


Figure IV.4.9.1. Cyclic voltammery plot for **D** in absence of base.

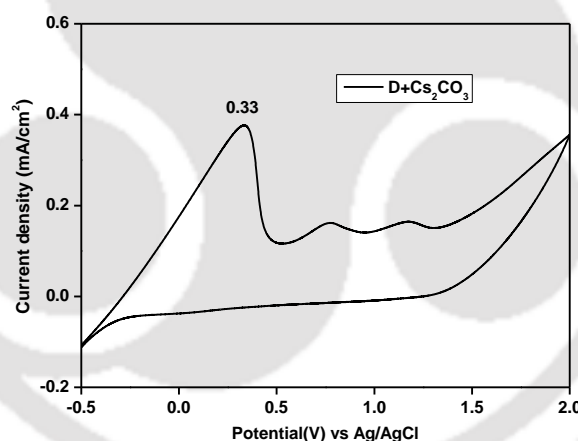


Figure IV.4.9.2. Cyclic voltammery plot for **D** in presence of Cs_2CO_3 .

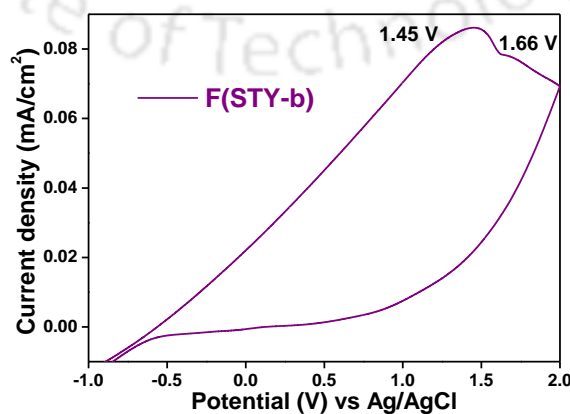
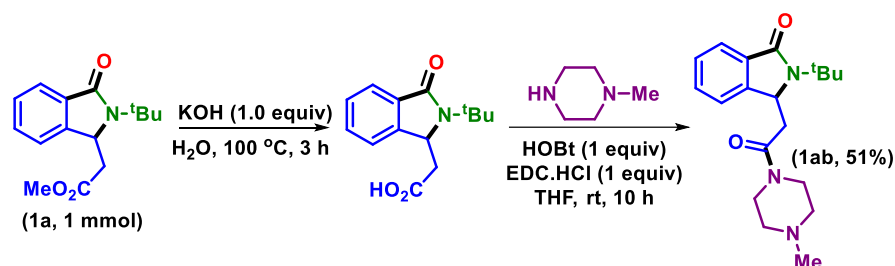


Figure IV.4.9.3. Cyclic voltammery plot for **26'** in presence of Cs_2CO_3 .

IV.4.10. Post-Synthetic Modification



Isoindolinone (**1a**, 1 mmol) was treated with KOH (1.0 equiv) and heated in oil bath at 100 °C for 3 h. The reaction mixture was diluted with water and the pH was maintained between 2-3 using conc. HCl. The reaction mixture was diluted with 30 mL of CHCl₃, the layers were separated and the organic layer was washed with aqueous saturated brine solution and dried over Na₂SO₄. The organic layer was concentrated under reduced pressure. The crude material so obtained was treated with HOBT (1.0 equiv), EDC-HCl (1.0 equiv) and *N*-methylpiperazine in THF at room temperature for 10 h. Progress of the reaction was monitored by TLC analysis; after complete consumption of starting material, the reaction mixture was diluted with 30 mL of CHCl₃, and filtered through a Celite pad. The filtrate was diluted with water (15 mL). The layers were separated, and the organic layer was washed with aqueous saturated brine solution and dried over Na₂SO₄. The organic layer was concentrated under reduced pressure. The crude material so obtained was purified by column chromatography on silica gel (60-120) (CHCl₃/MeOH; 95/5). The structure and purity of the synthesized products **1ab** was confirmed by comparison of their physical and spectral data.

IV.4.11. DFT Study

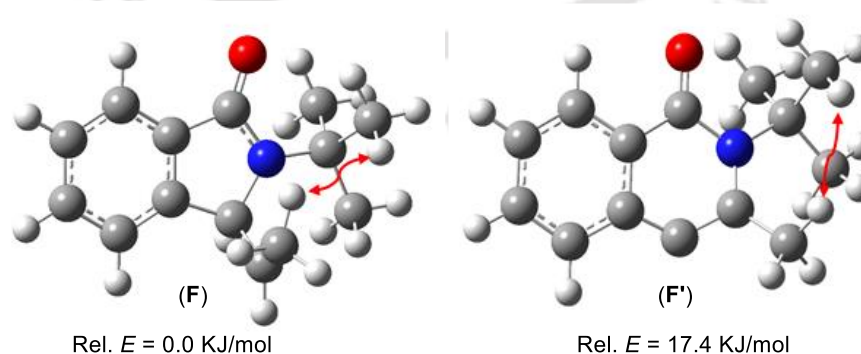
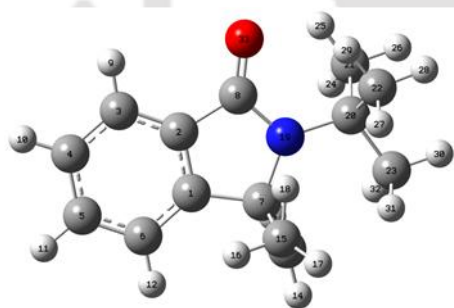


Figure IV.4.11.1. Geometries optimized at CAM-B3LYP level of theory.

To account for the relative stability of the five (F) and six membered ring (F') DFT calculations were carried using Gaussian 09 computational package. The DFT

calculations energetically favours the formation of **F** (*5-exo-trig*) instead of **F'** (*6-endo-trig*) by 17.4 KJ/mol. The extra stability of the former may be attributed to the stabilization of free radical by delocalization with carbonyl group. Moreover, in the optimized geometries of two possibilities, the two H-H distances (H32-H21 and H32-H25 2.72, 2.58 and 2.32, 3.31 Å respectively) were found longer in case of **F** which reflects the minimized steric hindrance in the said structure.

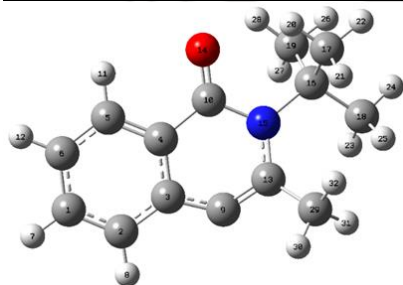
Computational method: In this work all, theoretical calculations were carried out at the density functional theory (DFT) level of theory, performed by using Gaussian 09 computational package.³² The geometries of the reactants, transition states and products were fully optimized by employing CAM-B3LYP exchange correlation functional in conjugation with 6-311++G (d, p) basis set [2, 3]. The neutral molecules were treated as closed-shell systems, while for the free radical open-shell system optimizations were carried out using a spin unrestricted wave function. The optimized geometries were subjected to frequency analysis to justify that the transition state structures possessing one imaginary frequency and no imaginary frequency for ground states geometries.



Coordinates

Center Numb	Atomic Number	Coordinates (Angstroms)		
		X	Y	Z
1	6	-1.253555	0.281901	0.303183
2	6	-1.026443	-0.969525	-0.320702
3	6	-2.005046	-1.942166	-0.470115
4	6	-3.296057	-1.690168	0.044942
5	6	-3.541717	-0.486381	0.723116
6	6	-2.530768	0.495156	0.856862
7	6	-0.086609	1.215388	0.311551
8	6	0.404698	-1.170971	-0.577596
9	1	-1.746237	-2.882276	-0.941534
10	1	-4.070438	-2.438858	-0.055891
11	1	-4.510828	-0.288146	1.162799
12	1	-2.767217	1.405263	1.399757
13	6	-0.339285	2.539845	-0.113359
14	1	0.432242	3.223847	0.238353

15	6	-1.317736	3.274660	-1.115097
16	1	-2.115895	3.756011	-0.555714
17	1	-0.772853	4.050802	-1.661184
18	1	-1.746952	2.587665	-1.849855
19	7	1.099655	-0.044099	-0.318127
20	6	2.442054	-0.077637	0.266245
21	6	2.474487	-0.968080	1.521440
22	6	3.413863	-0.657502	-0.793809
23	6	2.776782	1.388368	0.574170
24	1	1.767273	-0.605857	2.273286
25	1	2.208338	-1.990460	1.238907
26	1	3.478206	-0.961557	1.954607
27	1	3.372550	-0.054354	-1.703558
28	1	4.441618	-0.659027	-0.416815
29	1	3.090422	-1.670968	-1.027199
30	1	3.812348	1.499833	0.919736
31	1	2.651618	1.979408	-0.334439
32	1	2.098726	1.763445	1.341195
33	8	0.883531	-2.263712	-0.971545
34	1	0.176020	1.332535	1.342183



Center Atomic Coordinates (Angstroms)
Number Number X Y Z

1	6	-5.707134	-1.792083	-0.197548
2	6	-4.428605	-1.999213	-0.736199
3	6	-3.400592	-1.102911	-0.425174
4	6	-3.684627	0.082500	0.244139
5	6	-4.930672	0.256696	0.856980
6	6	-5.944970	-0.688011	0.638481
7	1	-6.498691	-2.477475	-0.417947
8	1	-4.238298	-2.842054	-1.367311
9	6	-1.952776	-1.383436	-0.823849
10	6	-2.631169	1.223093	0.253307
11	1	-5.113011	1.110378	1.475752
12	1	-6.901251	-0.563694	1.102133
13	6	-0.934102	-0.261701	-0.591852
14	8	-2.855586	2.258519	0.932351
15	7	-1.367156	1.132227	-0.536945
16	6	-0.338729	1.936129	0.139056
17	6	-0.121119	1.397196	1.565168
18	6	0.981214	1.849298	-0.649495

19	6	-0.798880	3.404078	0.209686
20	1	-1.038222	1.457527	2.113057
21	1	0.198597	0.377258	1.516094
22	1	0.627465	1.982349	2.057224
23	1	0.830018	2.223751	-1.640365
24	1	1.729797	2.434451	-0.157440
25	1	1.300930	0.829360	-0.698569
26	1	-0.050297	3.989231	0.701741
27	1	-0.950076	3.778531	-0.781185
28	1	-1.715983	3.464409	0.757575
29	6	0.550134	-0.608059	-0.371211
30	1	0.627391	-1.574629	0.081195
31	1	1.058944	-0.613121	-1.312480
32	1	0.995320	0.122924	0.270952

IV.5. References

- (1) (a) Vitaku, E.; Smith, D. T.; Njardarson, J. T. *J. Med. Chem.* **2014**, *57*, 10257. (b) Kerru, N.; Gummidi, L.; Maddila, S.; Gangu, K. K.; Jonnalagadda, S. B. *Molecules* **2020**, *25*, 1909. (c) Zhang, B.; Studer, A. *Chem. Soc. Rev.* **2015**, *44*, 3505. (d) Liu, J.; Jiang, J.; Zheng, L.; Liu, Z. Q. *Adv. Synth. Catal.* **2020**, *362*, 4876. (e) Kumar, D.; Jain, S. K. *Curr. Med. Chem.* **2016**, *23*, 4338.
- (2) (a) Festa, A. A.; Voskressensky, L. G.; Van der Eycken, E. V. *Chem. Soc. Rev.* **2019**, *48*, 4401. (b) Dhiya, A. K.; Monga, A. Sharma, A. *Org. Chem. Front.* **2021**, *8*, 1657. (c) Chen, J. R.; Hu, X. Q.; Lu, L. Q.; Xiao, W. J. *Acc. Chem. Res.* **2016**, *49*, 1911. (d) Wang, P.; Zhao, Q.; Xiao, W.; Chen, J. *Green Synth. Catal.* **2020**, *1*, 42. (e) Pawlowski, R.; Stanek, F.; Stodulski, M. *Molecules* **2019**, *24*, 1533. (f) Karkas, M. D. *ACS Catal.* **2017**, *7*, 4999. (g) Singh, S.; Roy, V.J.; Dagar, N.; Sen, P. P.; Roy, S. R. *Adv. Synth. Catal.* **2021**, *363*, 937. (h) Zard, S. Z. *Chem. Soc. Rev.* **2008**, *37*, 1603. (i) Hu, X. Q.; Qi, X.; Chen, J. R.; Zhao, Q. Q.; Wei, Q.; Lan, Y.; Xiao, W. J. *Nat. Commun.* **2016**, *7*, 11188. (j) Chen, Z. Y.; Wu, L. Y.; Fang, H. S.; Zhang, T.; Mao, Z. F.; Zou, Y.; Zhang, X. J.; Yan, M. *Adv. Synth. Catal.* **2017**, *359*, 3894.
- (3) (a) Jia, J.; Ho, Y. A.; Bülow, R. F.; Rueping, M. *Chem. Eur. J.* **2018**, *24*, 14054. (b) Davies, J.; Svejstrup, T. D.; Reina, D. F.; Sheikh, N. S.; Leonori, D. *J. Am. Chem. Soc.* **2016**, *138*, 8092. (c) Reina, D. F.; Dauncey, E. M.; Morcillo, S. P.; Svejstrup, T. D.; Popescu, M. V.; Douglas, J. J.; Sheikh, N. S.; Leonori, D. *Eur. J. Org. Chem.* **2017**, *2017*, 2108. (d) Musacchio, A. J.; Nguyen, L. Q.; Beard, G. H.;

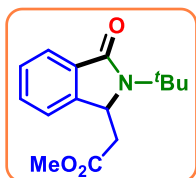
- Knowles, R. R. *J. Am. Chem. Soc.* **2014**, *136*, 12217. (e) Gao, Q. S.; Niu, Z.; Chen, Y.; Sun, J.; Han, W. Y.; Wang, J. Y.; Yu, M.; Zhou, M. D. *Org. Lett.* **2021**, *23*, 6153. (f) Zheng, S.; Gutiérrez-Bonet, A.; Molander, G. A. *Chem.* **2019**, *5*, 339. (g) Zheng, S.; Zhang, S. Q.; Saeednia, B.; Zhou, J.; Anna, J. M.; Hong, X.; Molander, G. A. *Chem. Sci.* **2020**, *11*, 4131. (h) Choi, G. J.; Knowles, R. R. *J. Am. Chem. Soc.* **2015**, *137*, 9226. (i) Miller, D. C.; Choi, G. J.; Orbe, H. S.; Knowles, R. R. *J. Am. Chem. Soc.* **2015**, *137*, 13492. (j) Zhao, Q.-Q.; Li, M.; Xue, X.-S.; Chen, J.-R.; Xiao, W.-J. *Org. Lett.* **2019**, *21*, 3861. (k) Murray, P. R. D.; Cox, J. H.; Chiappini, N. D.; Roos, C. B.; McLoughlin, E. A.; Hejna, B. G.; Nguyen, S. T.; Ripberger, H. H.; Ganley, J. M.; Tsui, E.; Shin, N. Y.; Koronkiewicz, B.; Qiu, G.; Knowles, R. R. *Chem. Rev.* **2022**, *122*, 2017.
- (4) (a) Boger, D. L.; Lee, J. K.; Goldberg, J.; Jin, Q. *J. Org. Chem.* **2000**, *65*, 1467. (b) Chia, Y. C.; Chang, F. R.; Teng, C. M.; Wu, Y. C. *J. Nat. Prod.* **2000**, *63*, 1160. (c) Honma, T.; Hayashi, K.; Aoyama, T.; Hashimoto, Machida, N.; Fukasawa, T. K.; Iwama, T.; Ikeura, C.; Ikuta, M.; Suzuki-Takahashi, I. *J. Med. Chem.* **2001**, *44*, 4615.
- (5) (a) Hu, X. Q.; Hou, Y. X.; Liu, Z. K.; Gao, Y. *Org. Chem. Front.* **2021**, *8*, 915. (b) Shi, L.; Hu, L.; Wang, J.; Cao, X.; Gu, H. *Org. Lett.* **2012**, *14*, 1876. (c) Guo, S.; Xie, Y.; Hu, X.; Xia, C.; Huang, H. *Angew. Chem. Int. Ed.* **2010**, *49*, 2728. (d) Ray, S. K.; Sadhu, M. M.; Biswas, R. G.; Unhale, R. A.; Singh, V. K. *Org. Lett.* **2019**, *21*, 417. (e) Zhang, H.; Leng, Y.; Liu W.; Duan, W. *Synth. Commun.* **2012**, *42*, 1115. (f) Dhanasekaran, S.; Kayet, A.; Suneja, A.; Bisai, V.; Singh, V. K. *Org. Lett.* **2015**, *17*, 2780. (g) Meng, J.-L.; Jiao, T.-Q.; Chen, Y.-H.; Fu, R.; Zhang, S.-S.; Zhao, Q.; Feng, C.-G.; Lin, G.-Q. *Tetrahedron Lett.* **2018**, *59*, 1564.
- (6) (a) Comins, D. L.; Schilling, S.; Zhang, Y. *Org. Lett.* **2005**, *7*, 95. (b) Wehlan, H.; Jezek, E.; Lebrasseur, N.; Pavé, G.; Roulland, E.; White, A. J.; Burrows, J. N.; Barrett, A. G. *J. Org. Chem.* **2006**, *71*, 8151. (c) Dhanasekaran, S.; Bisai, V.; Unhale, R. A.; Suneja, A.; Singh, V. K. *Org. Lett.* **2014**, *16*, 6068. (d) Mun, B.; Kim, S.; Yoon, H.; K. Lee, H. Y. *J. Org. Chem.* **2017**, *82*, 6349.
- (7) (a) Verma, A.; Patel, S.; Kumar, A.; Yadav, A.; Kumar, S.; Jana, S.; Sharma, S.; Prasad, C. D.; Kumar, S. *Chem. Commun.* **2015**, *51*, 1371. (b) Zhu, C.; Liang, Y.; Hong, X.; Sun, H.; Sun, W. Y.; Houk, K. N.; Shi, Z. *J. Am. Chem. Soc.* **2015**, *137*,

7564. (c) Yamamoto, C.; Takamatsu, K.; Hirano, K.; Miura, M. *J. Org. Chem.* **2016**, *81*, 7675. (d) Bedford, R. B.; Bowen, J. G.; Méndez-Gálvez, C. *J. Org. Chem.* **2017**, *82*, 1719. (e) Nozawa-Kumada, K.; Kadokawa, J.; Kameyama, T.; Kondo, Y. *Org. Lett.* **2015**, *17*, 4479.
- (8) (a) Lukasevics, L.; Cizikovs, A.; Grigorjeva, L. *Org. Lett.* **2020**, *22*, 2720. (b) Lukasevics, L.; Grigorjeva, L. *Org. Biomol. Chem.* **2020**, *18*, 7460. (c) Ling, F.; Ai, C.; Lv, Y.; Zhong, W. *Adv. Synth. Catal.* **2017**, *359*, 3707. (d) Cheng, X. F.; Wang, T.; Li, Y.; Wu, Y.; Sheng, J.; Wang, R.; Li, C.; Bian, K. J.; Wang, X. S. *Org. Lett.* **2018**, *20*, 6530. (e) Wang, C.; Zhang, L.; Chen, C.; Han, J.; Yao, Y.; Zhao, Y. *Chem. Sci.* **2015**, *6*, 4610. (f) Png, Z. M.; Cabrera-Pardo, J. R.; Cadahía, J. P.; Gaunt, M. J. *Chem. Sci.* **2018**, *9*, 7628. (g) Zhang, C.; Ding, Y.; Gao, Y.; Li, S.; Li, G. *Org. Lett.* **2018**, *20*, 2595–2598. (h) Das, D.; Bhanage, B. M. *Adv. Synth. Catal.* **2020**, *362*, 3022. (i) Barrio, P.; Ibáñez, I.; Herrera, L.; Román, R.; Catalán, S.; Fustero, S. *Chem. Eur. J.* **2015**, *21*, 11579.
- (9) (a) Manoharan, R.; Jeganmohan, M. *Chem. Commun.* **2015**, *51*, 2929. (b) Kumar, M.; Verma, S.; Verma, A. K. *Org. Lett.* **2020**, *22*, 4620. (c) Zheng, X. X.; Du, C.; Zhao, X. M.; Zhu, X.; Suo, J. F.; Hao, X. Q.; Niu, J. L.; Song, M. P. *J. Org. Chem.* **2016**, *81*, 4002. (d) Wang, S. M.; Li, C.; Leng, J.; Bukhari, S. N. A.; Qin, H. L.; *Org. Chem. Front.* **2018**, *5*, 1411. (e) Li, X. H.; Gong, J. F.; Song, M. P. *Org. Biomol. Chem.* **2021**, *19*, 5876.
- (10) (a) Liu, Y.-J.; Xu, H.; Kong, W.-J.; Shang, M.; Dai, H.-X.; Yu, J.-Q. *Nature* **2014**, *515*, 389. (b) Wang, D.; Cai, S.; Ben, R.; Zhou, Y.; Li, X.; Zhao, J.; Wei, W.; Qian, Y. *Synthesis* **2014**, *46*, 2045. (c) Zhu, C.; Xie, W.; Falck, J. R. *Chem. Eur. J.* **2011**, *17*, 12591. (d) Reddy, K. N.; Subhadra, U.; Sridhar, B.; Subba Reddy, B. V. *Org. Biomol. Chem.* **2018**, *16*, 2522. (e) Hao, W.; Tian, J.; Li, W.; Shi, R.; Huang, Z.; Lei, A. *Chem. Asian J.* **2016**, *11*, 1664. (f) Takamatsu, K.; Hirano, K.; Miura, M. *Org. Lett.* **2015**, *17*, 4066. (g) Gu, Z.-Y.; Liu, C.-G.; Wang, S.-Y.; Ji, S.-J. *J. Org. Chem.* **2017**, *82*, 2223. (h) Kalsi, D.; Barsu, N.; Sundararaju, B.; *Chem. Eur. J.* **2018**, *24*, 2360. (j) Zhao, H.; Shao, X.; Qing, Z.; Wang, T.; Chen, X.; Yang, H.; Zhai, H. *Adv. Synth. Catal.* **2019**, *361*, 1678. (k) Wang, J.; Liu, Y.; Xiong, Z.; Zhong, L.; Ding, S.; Li, L.; Zhao, H.; Chen, C.; Shang, Y. *Chem. Commun.* **2020**, *56*, 3249. (l) Pathare, R. S.; Sharma, S.; Elagandhula, S.; Saini, V.; Sawant, D.

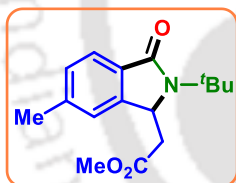
- M.; Yadav, M.; Sharon, A.; Khan, S.; Pardasani, R. T. *Eur. J. Org. Chem.* **2016**, 5579.
- (11) Bisai, V.; Unhale, R. A.; Suneja, A.; Dhanasekaran, S.; Singh, V. K. *Org. Lett.* **2015**, *17*, 2102.
- (12) Karmakar, R.; Suneja, A.; Bisai, V.; Singh, V. K. *Org. Lett.* **2015**, *17*, 5650.
- (13) Wang, X.; Huang, D.; Wang, K.-H.; Su, Y.; Hu, Y. *J. Org. Chem.* **2019**, *84*, 6946.
- (14) Mola, A. D.; Tiffner, M.; Scorzelli, F.; Palombi, L.; Filosa, R.; Caprariis, P. D.; Waser, M.; Massa, A. *Beilstein J. Org. Chem.* **2015**, *11*, 2591.
- (15) Huang, X.; Xu, J. *J. Org. Chem.* **2009**, *74*, 8859.
- (16) Ghandi, M.; Zarezadeh, N.; Abbasi, A. *Org. Biomol. Chem.* **2015**, *13*, 8211.
- (17) Min, C.; Lin, Y.; Seidel D. *Angew. Chem. Int. Ed.* **2017**, *56*, 15353.
- (18) Savela, R.; Méndez-Gálvez, C. *Chem. Eur. J.* **2021**, *27*, 5344.
- (19) Wang, F.; Song, G.; Li, X. *Org. Lett.* **2010**, *12*, 5430.
- (20) Hashimoto, Y.; Ueyama, T.; Fukutani, T.; Hirano, K.; Satoh, T.; Miura, M. *Chem. Lett.* **2011**, *40*, 1165.
- (21) Zhu, C.; Falck, J. R. *Org. Lett.* **2011**, *13*, 1214.
- (22) Wang, H.-L.; Shang, M.; Sun, S.-Z.; Zhou, Z.-L.; Laforteza, B. N.; Dai, H.-X.; Yu, J.-Q. *Org. Lett.* **2015**, *17*, 1228.
- (23) Ma, W.; Ackermann, L. *ACS Catal.* **2015**, *5*, 2822.
- (24) (a) Wu, X.-F.; Neumann, H.; Beller M. *Chem. Rev.* **2013**, *113*, 1. (b) Perrone, S.; Troisi, L.; Salomone, A. *Eur. J. Org. Chem.* **2019**, 4626. (c) Shen, C.; Wu, X.-F. *Chem. Eur. J.* **2017**, *23*, 2973.
- (25) Xuan, Z.; Jung, D. J.; Jeon, H. J.; Lee, S.-G. *J. Org. Chem.* **2016**, *81*, 10094.
- (26) Fu, L.-Y.; Ying, J.; Qi, X.; Peng, J.-B.; Wu, X.-F. *J. Org. Chem.* **2019**, *84*, 1421.
- (27) Tyagi, V.; Khan, S.; Chauhan, P. M. S. *Synlett* **2013**, *24*, 645.
- (28) (a) Liu, Y. J.; Xu, H.; Kong, W. J.; Shang, M.; Dai, H. X.; Yu, J. Q. *Nature* **2014**, *515*, 389. (b) Wang, D.; Cai, S.; Ben, R.; Zhou, Y.; Li, X.; Zhao, J.; Wei, W.; Qian, Y. *Synthesis* **2014**, *46*, 2045. (c) Takamatsu, K.; Hirano, K.; Miura, M. *Org. Lett.* **2015**, *17*, 4066. (d) Lygin, A. V.; de Meijere, A. *Angew. Chem. Int. Ed.* **2010**, *49*, 9094. (e) Singh, A. K.; Yadav, V. K.; Yadav, L. D. S. *Indian J. Chem.* **2019**, *58B*, 140. (f) Zhan, Y.; Chen, Z. *Tetrahedron Lett.* **2018**, *59*, 4183.
- (29) (a) F. X. Felpin, S. Sengupta, *Chem. Soc. Rev.* **2019**, *48*, 1150. (b) X. Zhang, Y. Mei, Y. Li, J. Hu, D. Huang, Y. Bi, *Asian J. Org. Chem.* **2021**, *10*, 453. (c) U. M.

- V. Basavanag, A. D. Santos, L. E. Kaim, R. Gámez-Montaño, L. Grimaud, *Angew. Chem. Int. Ed.* **2013**, *52*, 7194. (d) Z. Xia, Q. A. Zhu, *Org. Lett.* **2013**, *15*, 4110. (e) Malacarne, M. Protti, S. M. Fagnoni, *Adv. Synth. Catal.* **2017**, *359*, 3826.
- (30) (a) Hari, D. P.; König, B. *Chem. Commun.* **2014**, *50*, 6688. (b) Majek, M.; Filace, F.; Von Wangelin, A. J. Beilstein *J. Org. Chem.* **2014**, *10*, 981. (c) Srivastava, V. Singh, P. P. *RSC Adv.* **2017**, *7*, 31377. (d) Bosveli, A.; Montagnon, T.; Kalaitzakis, D.; Vassilikogiannakis, G; *Org. Biomol. Chem.* **2021**, *19*, 3303. (e) Yan, D. M.; Zhao, Q. Q.; Rao, L.; Chen, J. R.; Xiao, W. J. *Chem. Eur. J.* **2018**, *24*, 16895. (f) Zou, S.; Geng, S.; Chen, L.; Wang, H.; Huang, F. *Org. Biomol. Chem.* **2019**, *17*, 380. (g) Yu, X.; Zhou, F. J. Chen, W. Xiao, *Acta. Chimica Sinica.* **2017**, *75*, 86. (h) Sahoo, A. K.; Dahiya, A.; Das, B.; Behera, A.; Patel, B. K. *J. Org. Chem.* **2021**, *86*, 11968.
- (31) (a) Maity, S.; Manna, S.; Rana, S.; Naveen, T.; Mallick, A.; Maiti, D. *J. Am. Chem. Soc.* **2013**, *135*, 3355. (b) Zhu, X.; Wang, Y. F.; Ren, W.; Zhang, F. L.; Chiba, S. *Org. Lett.* **2013**, *15*, 3214.
- (32) I. Frisch, M. J.; Trucks, G. W.; Schlegel, H. B.; Scuseria, G. E.; Robb, M. A.;Cheeseman, J. R.; Scalmani, G.; Barone, V.; Mennucci, B.; Petersson, G. A.; Nakatsuji, H. Caricato, M. Li, X.;H. Hratchian, P.; Izmaylov, A. F.; Bloino, J.; Zheng, G.; Sonnenberg, J. L.; Hada,M.; Ehara, M.; Toyota, K.; Fukuda, R.; Hasegawa, J.; Ishida, M.; Nakajima, T.; Honda, Y.;Kitao, O.; Nakai, H.; Vreven, T.; Montgomery, J. A.; Peralta, Jr., J. E.; Ogliaro,F.; Bearpark, M.; Heyd, J. J.; Brothers, E.; Kudin, K. N.; Staroverov, V. N.; Kobayashi, R.; Normand, J.; Raghavachari, K.; Rendell, A.; Burant, J. C.; Iyengar, S. S.; Tomasi, J.; Cossi, M.; Rega, N.; Millam, J. M.; Klene, M.; Knox, J. E.; Cross, J. B.; Bakken, V.; Adamo, C.; Jaramillo, J.; Gomperts, R.; Stratmann, R. E.; Yazyev, O.; Austin, A. J.; Cammi, R.; Pomelli, C.; Ochterski, J. W.; Martin, R. L.; Morokuma, K.; Zakrzewski, V. G.; Voth, G. A.; Salvador, P.; Dannenberg, J. J.; Dapprich,S.; Daniels, A. D.; Farkas, Ö.; Foresman,J. B.; Ortiz, J. V.; Cioslowski, J.; Fox, D. J.; Gaussian 09; Gaussian, Inc.: Wallingford CT, **2009**.

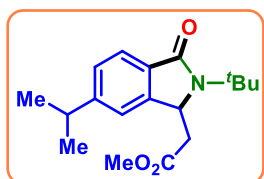
IV.6. Spectral Data

Methyl 2-(2-(*tert*-butyl)-3-oxoisindolin-1-yl)acetate (1a):

Yellow gummy (107 mg, 82% yield); ^1H NMR (CDCl_3 , 400 MHz): δ 1.51 (s, 9H), 2.36 (dd, 1H, $J_1 = 16.4$ Hz, $J_2 = 5.6$ Hz), 3.15 (dd, 1H, $J_1 = 16.0$ Hz, $J_2 = 2.0$ Hz), 3.16 (s, 3H), 5.04 (dd, 1H, $J_1 = 9.2$ Hz, $J_2 = 2.4$ Hz), 7.25 (d, 1H, $J = 7.2$ Hz), 7.31-7.35 (m, 1H), 7.40-7.36 (m, 1H), 7.66 (d, 1H, $J = 6.8$ Hz); $^{13}\text{C}\{^1\text{H}\}$ NMR (CDCl_3 , 100 MHz): δ 28.8, 41.3, 52.1, 55.4, 56.9, 122.0, 123.5, 128.5, 131.6, 133.1, 145.8, 169.2, 171.0; IR (KBr, cm^{-1}): 3065, 2959, 2854, 1735, 1683, 1436, 1381, 1066; HRMS (ESI): calcd. for $\text{C}_{15}\text{H}_{20}\text{NO}_3^+$ [$\text{M} + \text{H}^+$] 262.1438; found 262.1438.

Methyl 2-(2-(*tert*-butyl)-6-methyl-3-oxoisindolin-1-yl)acetate (2a):

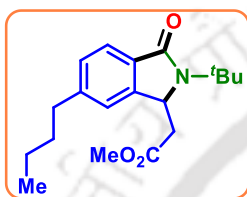
Yellow gummy (116 mg, 85% yield); ^1H NMR (CDCl_3 , 400 MHz): δ 1.59 (s, 9H), 2.41 (s, 3H), 2.45 (dd, 1H, $J_1 = 16.0$ Hz, $J_2 = 9.2$ Hz), 3.21 (dd, 1H, $J_1 = 16.4$ Hz, $J_2 = 2.8$ Hz), 3.72 (s, 3H), 5.07 (dd, 1H, $J_1 = 9.6$ Hz, $J_2 = 2.8$ Hz), 7.13 (s, 1H), 7.22 (d, 1H, $J = 7.6$ Hz), 7.63 (d, 1H, $J = 7.6$ Hz); $^{13}\text{C}\{^1\text{H}\}$ NMR (CDCl_3 , 100 MHz): δ 22.2, 28.9, 41.4, 52.1, 55.3, 56.7, 122.4, 123.3, 129.5, 130.5, 142.2, 146.2, 169.4, 171.1; IR (KBr, cm^{-1}): 3054, 2962, 2924, 1734, 1682, 1378, 1275, 1138; HRMS (ESI): calcd. for $\text{C}_{16}\text{H}_{22}\text{NO}_3^+$ [$\text{M} + \text{H}^+$] 276.1594; found 276.1591.

Methyl 2-(2-(*tert*-butyl)-6-isopropyl-3-oxoisindolin-1-yl)acetate (3a):

Yellow gummy (130 mg, 86% yield); ^1H NMR (CDCl_3 , 600 MHz): δ 1.25 (d, 3H, $J = 2.4$ Hz), 1.26 (d, 3H, $J = 2.4$ Hz), 1.60 (s, 9H), 2.44 (dd, 1H, $J_1 = 15.6$ Hz, $J_2 = 9.0$ Hz), 3.00-2.93 (m, 1H), 3.25 (dd, 1H, $J_1 = 15.6$ Hz, $J_2 = 2.4$ Hz), 3.73 (s, 3H), 5.10 (dd, 1H, $J_1 = 9.6$ Hz, $J_2 = 3.0$ Hz), 7.18 (s, 1H), 7.30-7.28 (m, 1H), 7.67 (d, 1H, $J = 7.8$ Hz); $^{13}\text{C}\{^1\text{H}\}$ NMR (CDCl_3 , 150 MHz): δ 24.16, 24.21, 28.9, 34.7, 41.6, 52.1, 55.3, 56.9,

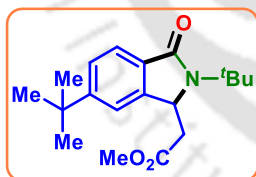
119.8, 123.4, 127.1, 130.9, 146.1, 153.2, 169.3, 171.1; IR (KBr, cm^{-1}): 3051, 2961, 2865, 1735, 1687, 1379, 1264, 1156; HRMS (ESI): calcd. for $\text{C}_{18}\text{H}_{26}\text{NO}_3^+$ [$\text{M} + \text{H}^+$] 304.1907; found 304.1907.

Methyl 2-(2-(*tert*-butyl)-6-butyl-3-oxoisindolin-1-yl)acetate (4a):



Red gummy (133 mg, 84% yield); ^1H NMR (CDCl_3 , 600 MHz): δ 0.90 (t, 3H, $J = 7.2$ Hz), 1.32 (dd, 2H, $J_1 = 15.0$ Hz, $J_2 = 7.8$ Hz), 1.57-1.53 (m, 2H), 1.58 (s, 9H), 2.43 (dd, 1H, $J_1 = 16.2$ Hz, $J_2 = 9.6$ Hz), 2.64 (t, 2H, $J = 7.8$ Hz), 3.22 (dd, 1H, $J_1 = 15.6$ Hz, $J_2 = 2.4$ Hz), 3.70 (s, 3H), 5.08 (dd, 1H, $J_1 = 9.6$ Hz, $J_2 = 2.4$ Hz), 7.12 (s, 1H), 7.22 (d, 1H, $J = 7.8$ Hz), 7.63 (d, 1H, $J = 7.2$ Hz); $^{13}\text{C}\{^1\text{H}\}$ NMR (CDCl_3 , 150 MHz): δ 14.1, 22.4, 28.8, 33.8, 36.2, 41.5, 52.1, 55.3, 56.8, 121.8, 123.3, 128.9, 130.7, 146.1, 147.3, 169.3, 171.1; IR (KBr, cm^{-1}): 2961, 2905, 2868, 1735, 1686, 1459, 1364, 1158; HRMS (ESI): calcd. for $\text{C}_{19}\text{H}_{28}\text{NO}_3^+$ [$\text{M} + \text{H}^+$] 318.2064; found 318.2084.

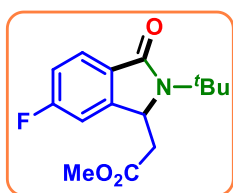
Methyl 2-(2,6-di-*tert*-butyl-3-oxoisindolin-1-yl)acetate (5a):



Brown gummy (134 mg, 85% yield); ^1H NMR (CDCl_3 , 600 MHz): δ 1.31 (s, 9H), 1.59 (s, 9H), 2.40 (dd, 1H, $J_1 = 16.2$ Hz, $J_2 = 9.6$ Hz), 3.24 (dd, 1H, $J_1 = 16.2$ Hz, $J_2 = 3.0$ Hz), 3.72 (s, 3H), 5.10 (dd, 1H, $J_1 = 10.2$ Hz, $J_2 = 3.0$ Hz), 7.33 (s, 1H), 7.45 (dd, 1H, $J_1 = 7.8$ Hz, $J_2 = 1.2$ Hz), 7.67 (d, 1H, $J = 8.4$ Hz); $^{13}\text{C}\{^1\text{H}\}$ NMR (CDCl_3 , 150 MHz): δ 28.9, 31.6, 35.5, 41.7, 52.1, 55.3, 57.0, 118.7, 123.1, 125.9, 130.5, 145.8, 155.5, 169.3, 171.2; IR (KBr, cm^{-1}): 3054, 2962, 2843, 1735, 1686, 1375, 1264, 1046; HRMS (ESI): calcd. for $\text{C}_{19}\text{H}_{28}\text{NO}_3^+$ [$\text{M} + \text{H}^+$] 318.2064; found 318.2057.

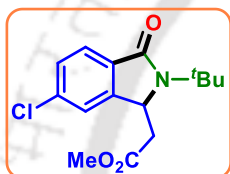
Methyl 2-(2-(*tert*-butyl)-6-fluoro-3-oxoisindolin-1-yl)acetate (6a):

As a yellow solid (104 mg, 75% yield); mp 56-58 $^\circ\text{C}$; ^1H NMR (CDCl_3 , 400 MHz): δ 1.58 (s, 9H), 2.44 (dd, 1H, $J_1 = 16.8$ Hz, $J_2 = 5.6$ Hz), 3.23 (dd, 1H, $J_1 = 16.4$ Hz, $J_2 = 2.8$ Hz), 3.72 (s, 3H), 5.08 (dd, 1H, $J_1 = 9.6$ Hz, $J_2 = 2.8$ Hz), 7.12-7.05 (m,



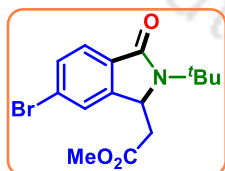
2H), 7.72 (dd, 1H, $J_1 = 8.4$ Hz, $J_2 = 5.2$ Hz); $^{13}\text{C}\{^1\text{H}\}$ NMR (CDCl_3 , 100 MHz): δ 28.8, 41.1, 52.3, 55.6, 56.5 (d, $J = 2.6$ Hz), 109.5 (d, $J = 24.5$ Hz), 116.1 (d, $J = 23.3$ Hz), 125.5 (d, $J = 9.6$ Hz), 129.1 (d, $J = 2.0$ Hz), 148.0 (d, $J = 9.7$ Hz), 163.9 (d, $J = 249$ Hz), 168.2, 170.8; ^{19}F NMR (CDCl_3 , 376 MHz): δ -107.36; IR (KBr, cm^{-1}): 3054, 2957, 2868, 1734, 1686, 1488, 1367, 1264, 1216, 1154; HRMS (ESI): calcd. for $\text{C}_{15}\text{H}_{19}\text{FNO}_3^+$ [$\text{M} + \text{H}^+$] 280.1343; found 280.1343.

Methyl 2-(2-(tert-butyl)-6-chloro-3-oxoisindolin-1-yl)acetate (7a):

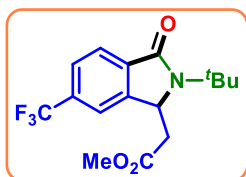


As a black solid (113 mg, 77% yield); mp 66–68 °C; ^1H NMR (CDCl_3 , 400 MHz): δ 1.59 (s, 9H), 2.46 (dd, 1H, $J_1 = 16.8$ Hz, $J_2 = 9.6$ Hz), 3.23 (dd, 1H, $J_1 = 16.4$ Hz, $J_2 = 2.4$ Hz), 3.73 (s, 3H), 5.09 (dd, 1H, $J_1 = 9.6$ Hz, $J_2 = 2.4$ Hz), 7.39 (dd, 2H, $J_1 = 8.0$ Hz, $J_2 = 4.0$ Hz), 7.67 (d, 1H, $J = 8.0$ Hz); $^{13}\text{C}\{^1\text{H}\}$ NMR (CDCl_3 , 100 MHz): δ 28.8, 41.0, 52.3, 55.6, 56.5, 122.6, 124.8, 129.1, 131.6, 137.9, 147.4, 168.1, 170.8; IR (KBr, cm^{-1}): 3051, 2962, 2837, 1733, 1684, 1366, 1264, 1150, 1070; HRMS (ESI): calcd. for $\text{C}_{15}\text{H}_{19}\text{ClNO}_3^+$ [$\text{M} + \text{H}^+$] 296.1048; found 296.1050.

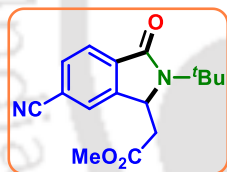
Methyl 2-(6-bromo-2-(tert-butyl)-3-oxoisindolin-1-yl)acetate (8a):



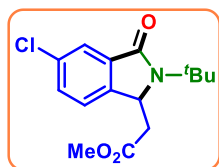
Red gummy (132 mg, 78% yield); ^1H NMR (CDCl_3 , 600 MHz): δ 1.56 (s, 9H), 2.44 (dd, 1H, $J_1 = 16.2$ Hz, $J_2 = 9.0$ Hz), 3.20 (dd, 1H, $J_1 = 16.8$ Hz, $J_2 = 9.0$ Hz), 3.70 (s, 3H), 5.07 (dd, 1H, $J_1 = 9.6$ Hz, $J_2 = 1.8$ Hz), 7.52 (d, 2H, $J = 10.8$ Hz), 7.58 (d, 1H, $J = 8.4$ Hz); $^{13}\text{C}\{^1\text{H}\}$ NMR (CDCl_3 , 150 MHz): δ 28.7, 40.9, 52.2, 55.5, 56.4, 124.9, 125.5, 126.2, 131.9, 132.0, 147.5, 168.1, 170.7; IR (KBr, cm^{-1}): 3059, 2979, 2870, 1734, 1689, 1436, 1377, 1264, 1150, 1046; HRMS (ESI): calcd. for $\text{C}_{15}\text{H}_{19}\text{BrNO}_3^+$ [$\text{M} + \text{H}^+$] 340.0543; found 340.0543.

Methyl 2-(2-(*tert*-butyl)-3-oxo-6-(trifluoromethyl)isoindolin-1-yl)acetate (9a):

As a red solid (118 mg, 72% yield); mp 58–60 °C; ^1H NMR (CDCl_3 , 400 MHz): δ 1.59 (s, 9H), 2.47 (dd, 1H, $J_1 = 16.4$ Hz, $J_2 = 9.2$ Hz), 3.26 (dd, 1H, $J_1 = 16.4$ Hz, $J_2 = 2.4$ Hz), 3.70 (s, 3H), 5.17 (dd, 1H, $J_1 = 9.6$ Hz, $J_2 = 2.8$ Hz), 7.64 (s, 1H), 7.68 (d, 1H, $J = 8.0$ Hz), 7.84 (d, 1H, $J = 8.0$ Hz); $^{13}\text{C}\{^1\text{H}\}$ NMR (CDCl_3 , 100 MHz): δ 28.7, 40.9, 52.2, 55.8, 56.9, 119.5 (q, $J = 15.6$), 122.6, 124.1, 125.8 (q, $J = 14.8$ Hz), 133.5 (q, $J = 128.4$ Hz), 136.4, 146.1, 167.7, 170.6; ^{19}F NMR (CDCl_3 , 376 MHz): δ -62.31; IR (KBr, cm^{-1}): 3051, 2979, 2930, 1737, 1693, 1437, 1325, 1264, 1167, 1059; HRMS (ESI): calcd. for $\text{C}_{16}\text{H}_{19}\text{F}_3\text{NO}_3^+$ [$\text{M} + \text{H}^+$] 330.1312; found 330.1315.

Methyl 2-(2-(*tert*-butyl)-6-cyano-3-oxoisoindolin-1-yl)acetate (10a):

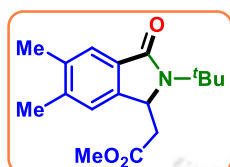
As a yellow solid (97 mg, 68% yield); mp 127–129 °C; ^1H NMR (CDCl_3 , 400 MHz): δ 1.58 (s, 9H), 2.45 (dd, 1H, $J_1 = 16.8$ Hz, $J_2 = 9.2$ Hz), 3.25 (dd, 1H, $J_1 = 16.8$ Hz, $J_2 = 2.4$ Hz), 3.70 (s, 3H), 5.15 (dd, 1H, $J_1 = 9.2$ Hz, $J_2 = 2.0$ Hz), 7.70 (d, 2H, $J = 8.4$ Hz), 7.82 (d, 1H, $J = 7.6$ Hz); $^{13}\text{C}\{^1\text{H}\}$ NMR (CDCl_3 , 100 MHz): δ 28.6, 40.5, 52.3, 55.9, 56.7, 114.9, 118.5, 124.2, 126.4, 132.6, 137.0, 146.1, 167.0, 170.4; IR (KBr, cm^{-1}): 3056, 2983, 2832, 2299, 1732, 1682, 1467, 1328, 1264, 1150, 1045; HRMS (ESI): calcd. for $\text{C}_{16}\text{H}_{19}\text{N}_2\text{O}_3^+$ [$\text{M} + \text{H}^+$] 287.1390; found 287.1397.

Methyl 2-(2-(*tert*-butyl)-5-chloro-3-oxoisoindolin-1-yl)acetate (11a):

As a yellow solid (112 mg, 76% yield); mp 145–147 °C; ^1H NMR (CDCl_3 , 400 MHz): δ 1.57 (s, 9H), 2.42 (dd, 1H, $J_1 = 16.2$ Hz, $J_2 = 9.6$ Hz), 3.21 (dd, 1H, $J_1 = 16.8$ Hz, $J_2 = 3.0$ Hz), 3.68 (s, 3H), 5.08 (dd, 1H, $J_1 = 9.6$ Hz, $J_2 = 2.4$ Hz), 7.28 (d, 1H, $J = 8.4$ Hz), 7.40 (dd, 1H, $J_1 = 7.8$ Hz, $J_2 = 1.2$ Hz), 7.68 (s, 1H); $^{13}\text{C}\{^1\text{H}\}$ NMR (CDCl_3 , 100 MHz): δ 28.7, 41.0, 52.2, 55.6, 56.6, 123.4, 123.5, 131.7, 134.7, 134.9, 143.9, 167.7, 170.7; IR (KBr, cm^{-1}): 3075, 2983, 2868, 1734, 1687, 1426,

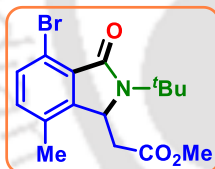
1375, 1264, 1045; HRMS (ESI): calcd. for $C_{15}H_{19}ClNO_3^+$ [$M + H^+$] 296.1048; found 296.1048.

Methyl 2-(2-(*tert*-butyl)-5,6-dimethyl-3-oxoisindolin-1-yl)acetate (12a):



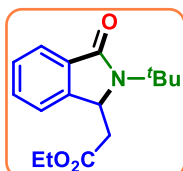
As a yellow solid (118 mg, 82% yield); mp 89–91 °C; 1H NMR ($CDCl_3$, 400 MHz): δ 1.57 (s, 9H), 2.28 (s, 3H), 2.29 (s, 3H), 2.41 (dd, 1H, $J_1 = 16.2$ Hz, $J_2 = 9.6$ Hz), 3.20 (dd, 1H, $J_1 = 16.2$ Hz, $J_2 = 3.2$ Hz), 3.71 (s, 3H), 5.03 (dd, 1H, $J_1 = 9.0$ Hz, $J_2 = 2.4$ Hz), 7.08 (s, 1H), 7.49 (s, 1H); $^{13}C\{^1H\}$ NMR ($CDCl_3$, 100 MHz): δ 20.1, 20.7, 28.8, 41.5, 52.0, 55.2, 56.5, 122.8, 124.0, 130.9, 137.2, 140.9, 143.8, 169.5, 171.1; IR (KBr, cm^{-1}): 3046, 2976, 2813, 1735, 1683, 1436, 1376, 1264, 1215, 1045; HRMS (ESI): calcd. for $C_{17}H_{24}NO_3^+$ [$M + H^+$] 290.1751; found 290.1753.

Methyl 2-(4-bromo-2-(*tert*-butyl)-7-methyl-3-oxoisindolin-1-yl)acetate (13a):



As a yellow solid (141 mg, 80% yield); mp 86–88 °C; 1H NMR ($CDCl_3$, 600 MHz): δ 1.54 (s, 9H), 2.33 (s, 3H), 2.40 (dd, 1H, $J_1 = 16.2$ Hz, $J_2 = 8.0$ Hz), 3.15 (d, 1H, $J = 10.2$ Hz), 3.68 (s, 3H), 4.97 (d, 1H, $J = 9.0$ Hz), 7.05 (s, 1H), 7.33 (s, 1H); $^{13}C\{^1H\}$ NMR ($CDCl_3$, 150 MHz): δ 21.5, 28.7, 41.2, 52.1, 55.2, 55.5, 118.1, 121.7, 127.3, 134.1, 143.5, 148.7, 167.0, 170.8; IR (KBr, cm^{-1}): 3048, 2960, 2888, 1736, 1685, 1376, 1264, 1150, 1053; HRMS (ESI): calcd. for $C_{16}H_{21}BrNO_3^+$ [$M + H^+$] 354.0699; found 354.0699.

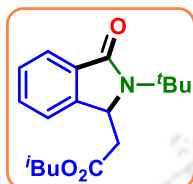
Ethyl 2-(2-(*tert*-butyl)-3-oxoisindolin-1-yl)acetate (14a):



Yellow gummy (108 mg, 79% yield); 1H NMR ($CDCl_3$, 400 MHz): δ 1.20 (t, 3H, $J = 7.0$ Hz), 1.60 (s, 9H), 2.47 (dd, 1H, $J_1 = 16.0$ Hz, $J_2 = 9.2$ Hz), 3.21 (dd, 1H, $J_1 = 16.0$ Hz, $J_2 = 2.4$ Hz), 4.14 (m, 2H), 5.12 (dd, 1H, $J_1 = 8.8$ Hz, $J_2 = 2.4$ Hz), 7.36 (d, 1H, $J = 7.6$ Hz), 7.42–7.39 (m, 1H), 7.49–7.44 (m, 1H), 7.75 (d, 1H, $J = 7.2$ Hz); $^{13}C\{^1H\}$ NMR ($CDCl_3$, 100 MHz): δ 14.3, 28.8, 41.5, 55.4, 57.0, 61.1, 122.0, 123.4, 128.5, 131.6, 133.2, 145.8, 169.2, 170.4; IR (KBr, cm^{-1}): 3048, 2981, 2839, 1731,

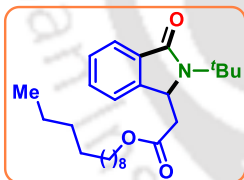
1684, 1467, 1368, 1264, 1152, 1037; HRMS (ESI): calcd. for $C_{16}H_{22}NO_3^+$ $[M + H^+]$ 276.1594; found 276.1599.

Isobutyl 2-(2-(*tert*-butyl)-3-oxoisindolin-1-yl)acetate (15a):



Brown gummy (121 mg, 80% yield); 1H NMR ($CDCl_3$, 400 MHz): δ 0.86 (d, 3H, $J = 4.8$ Hz), 0.88 (d, 3H, $J = 4.8$ Hz), 1.61 (s, 9H), 1.90-1.84 (m, 1H), 2.47 (dd, 1H, $J_1 = 9.2$ Hz, $J_2 = 9.2$ Hz), 3.24 (dd, 1H, $J_1 = 16.0$ Hz, $J_2 = 2.4$ Hz), 3.92-3.84 (m, 2H), 5.12 (dd, 1H, $J_1 = 9.6$ Hz, $J_2 = 2.8$ Hz), 7.35 (d, 1H, $J = 7.2$ Hz), 7.48-7.39 (m, 2H), 7.75 (d, 1H, $J = 7.2$ Hz); $^{13}C\{^1H\}$ NMR ($CDCl_3$, 100 MHz): δ 19.21, 19.23, 27.8, 28.8, 41.5, 55.4, 57.0, 71.3, 122.0, 123.5, 128.5, 131.6, 133.1, 145.9, 169.2, 170.6; IR (KBr, cm^{-1}): 3054, 2984, 2870, 1732, 1685, 1264, 1046; HRMS (ESI): calcd. for $C_{18}H_{26}NO_3^+$ $[M + H^+]$ 304.1907; found 304.1907.

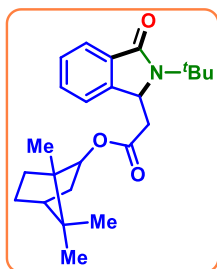
Dodecyl 2-(2-(*tert*-butyl)-3-oxoisindolin-1-yl)acetate (16a):



Red gummy (155 mg, 75% yield); 1H NMR ($CDCl_3$, 500 MHz): δ 0.87 (t, 3H, $J = 7.0$ Hz), 1.25 (s, 20H), 1.61 (s, 9H), 2.48 (dd, 1H, $J_1 = 16.0$ Hz, $J_2 = 9.8$ Hz), 3.22 (dd, 1H, $J_1 = 16.0$ Hz, $J_2 = 2.5$ Hz), 4.09 (t, 2H, $J = 7.5$ Hz), 5.12 (dd, 1H, $J_1 = 9.0$ Hz, $J_2 = 2.5$ Hz), 7.36 (d, 1H, $J = 7.5$ Hz), 7.42 (t, 1H, $J = 7.5$ Hz), 7.44 (t, 1H, $J = 7.5$ Hz), 7.76 (d, 1H, $J = 7.0$ Hz); $^{13}C\{^1H\}$ NMR ($CDCl_3$, 125 MHz): δ 14.3, 22.9, 28.7, 28.9, 29.4, 29.6, 29.65, 29.70, 29.8, 29.9, 32.1, 33.0, 41.5, 55.4, 57.0, 65.4, 122.0, 123.5, 128.5, 131.6, 133.2, 145.9, 169.2, 170.6; IR (KBr, cm^{-1}): 3065, 2925, 2851, 1732, 1688, 1264, 1045; HRMS (ESI): calcd. for $C_{26}H_{42}NO_3^+$ $[M + H^+]$ 416.3159; found 416.3164.

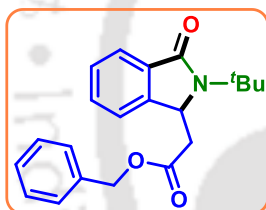
(1R,4S)-1,7,7-Trimethylbicyclo[2.2.1]heptan-2-yl 2-(2-(*tert*-butyl)-3-oxoisindolin-1-yl)acetate (17a):

Yellow gummy (145 mg, 76% yield); 1H NMR ($CDCl_3$, 400 MHz): δ 0.77 (d, 3H, $J = 13.2$ Hz), 0.80 (s, 3H), 0.85 (d, 3H, $J = 7.2$ Hz), 1.12-1.01 (m, 2H), 1.17 (d, 1H, $J = 7.6$ Hz), 1.60 (s,



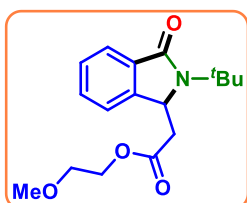
9H), 1.71-1.65 (m, 2H), 1.87-1.77 (m, 2H), 2.40-2.33 (m, 1H), 3.20 (dd, 1H, $J_1 = 15.6$ Hz, $J_2 = 2.4$ Hz), 4.79-4.70 (m, 1H), 5.11 (dd, 1H, $J_1 = 9.6$ Hz, $J_2 = 2.0$ Hz), 7.34 (d, 1H, $J = 7.2$ Hz), 7.46-7.38 (m, 2H), 7.74 (d, 1H, $J = 7.2$ Hz); $^{13}\text{C}\{^1\text{H}\}$ NMR (CDCl_3 , 100 MHz): δ 11.7, 20.0, 20.2, 27.1, 28.8, 33.9, 39.0, 41.8, 45.1, 47.1, 48.8, 55.4, 57.1, 82.1, 121.9, 123.5, 128.4, 131.6, 133.0, 145.9, 169.1, 170.0; IR (KBr, cm^{-1}): 3056, 2955, 2924, 1708, 1636, 1534, 1275, 1173, 1053; HRMS (ESI): calcd. for $\text{C}_{24}\text{H}_{34}\text{NO}_3^+$ [$\text{M} + \text{H}^+$] 384.2533; found 384.2533.

Benzyl 2-(2-(*tert*-butyl)-3-oxoisoindolin-1-yl)acetate (18a):



Brown gummy (121 mg, 72% yield); ^1H NMR (CDCl_3 , 400 MHz): δ 1.52 (s, 9H), 2.43 (dd, 1H, $J_1 = 16.0$ Hz, $J_2 = 9.6$ Hz), 3.20 (dd, 1H, $J_1 = 16.0$ Hz, $J_2 = 2.4$ Hz), 5.04 (d, 1H, $J = 2.4$ Hz), 5.07 (s, 2H), 7.16 (dd, 1H, $J_1 = 8.4$ Hz, $J_2 = 3.2$ Hz), 7.23 (dd, 2H, $J_1 = 5.2$ Hz, $J_2 = 2.8$ Hz), 7.27 (t, 3H, $J = 6.4$ Hz), 7.31 (dd, 2H, $J_1 = 5.2$ Hz, $J_2 = 2.8$ Hz), 7.66 (t, 1H, $J = 5.6$ Hz); $^{13}\text{C}\{^1\text{H}\}$ NMR (CDCl_3 , 100 MHz): δ 28.8, 41.5, 55.4, 57.0, 67.0, 122.0, 123.5, 128.5, 128.68, 128.70, 128.8, 131.6, 133.1, 135.4, 145.7, 169.2, 170.3; IR (KBr, cm^{-1}): 3051, 2979, 2851, 1732, 1685, 1365, 1264, 1154, 1045; HRMS (ESI): calcd. for $\text{C}_{21}\text{H}_{24}\text{NO}_3^+$ [$\text{M} + \text{H}^+$] 338.1751; found 338.1752.

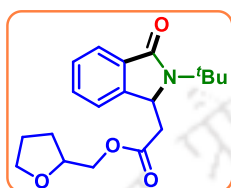
2-Methoxyethyl 2-(2-(*tert*-butyl)-3-oxoisoindolin-1-yl)acetate (19a):



Red gummy (106 mg, 70% yield); ^1H NMR (CDCl_3 , 600 MHz): δ 1.61 (s, 9H), 2.51 (dd, 1H, $J_1 = 16.2$ Hz, $J_2 = 9.6$ Hz), 3.28 (dd, 1H, $J_1 = 16.8$ Hz, $J_2 = 2.4$ Hz), 3.35 (s, 3H), 3.53-3.56 (m, 2H), 4.24-4.28 (m, 2H), 5.14 (dd, 1H, $J_1 = 9.6$ Hz, $J_2 = 2.4$ Hz), 7.40 (d, 1H, $J_1 = 7.2$ Hz), 7.43 (d, 1H, $J = 7.2$ Hz), 7.46 (dd, 1H, $J_1 = 7.2$ Hz, $J_2 = 0.6$ Hz), 7.76 (d, 1H, $J = 7.2$ Hz); $^{13}\text{C}\{^1\text{H}\}$ NMR (CDCl_3 , 150 MHz): δ 28.9, 41.4, 55.4, 56.9, 59.2, 64.1, 70.4, 122.1, 123.5, 128.5, 131.6, 133.1, 145.8, 169.2, 170.5; IR (KBr, cm^{-1}): 3054, 2989, 2871, 1733, 1686,

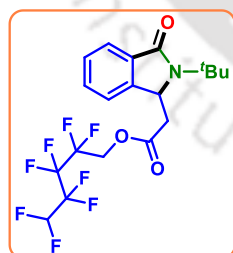
1373, 1264, 1048; HRMS (ESI): calcd. for $C_{17}H_{24}NO_4^+$ $[M+H^+]$ 306.1700; found 306.1700.

Tetrahydrofuran-2-yl-methyl 2-(2-(*tert*-butyl)-3-oxoisindolin-1-yl)acetate (20a):



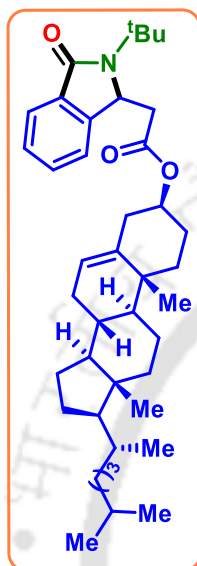
Red gummy (117 mg, 71% yield); 1H NMR ($CDCl_3$, 600 MHz): δ 1.54-1.47 (m, 1H), 1.58 (s, 9H), 1.86 (dd, 2H, $J_1 = 14.0$ Hz, $J_2 = 6.8$ Hz), 1.94 (dd, 1H, $J_1 = 12.4$ Hz, $J_2 = 6.0$ Hz), 2.47 (dd, 1H, $J_1 = 16.4$ Hz, $J_2 = 9.6$ Hz), 3.29-3.23 (m, 1H), 3.74 (dd, 1H, $J_1 = 14.8$ Hz, $J_2 = 7.6$ Hz), 3.82 (dd, 1H, $J_1 = 16.0$ Hz, $J_2 = 8.4$ Hz), 4.07-3.99 (m, 2H), 4.16 (t, 1H, $J = 7.6$ Hz), 5.11 (d, 1H, $J = 8.4$ Hz), 7.38 (t, 2H, $J = 8.0$ Hz), 7.44 (t, 1H, $J = 7.2$ Hz), 7.72 (d, 1H, $J = 7.2$ Hz); $^{13}C\{^1H\}$ NMR ($CDCl_3$, 150 MHz): δ 25.7, 28.1, 28.8, 41.3, 55.3, 56.8, 66.9, 68.5, 76.3, 123.4, 128.4, 131.54, 131.56, 133.0, 145.7, 169.1, 170.4; IR (KBr, cm^{-1}): 3051, 2955, 2881, 1729, 1688, 1456, 1369, 1264, 1161, 1052; HRMS (ESI): calcd. for $C_{19}H_{26}NO_4^+$ $[M + H^+]$ 332.1856; found 332.1859.

2,2,3,3,4,4,5,5-Octafluoropentyl 2-(2-(*tert*-butyl)-3-oxoisindolin-1-yl)acetate (21a):



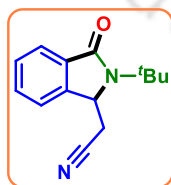
Yellow gummy (140 mg, 61% yield); 1H NMR ($CDCl_3$, 500 MHz): δ 1.62 (s, 9H), 2.69 (dd, 1H, $J_1 = 17.0$ Hz, $J_2 = 9.0$ Hz), 2.76 (s, 1H), 3.34 (dd, 1H, $J_1 = 11.5$ Hz, $J_2 = 2.5$ Hz), 4.73 (d, 1H, $J = 13.5$ Hz), 5.16 (dd, 1H, $J_1 = 8.5$ Hz, $J_2 = 2.0$ Hz), 6.51 (d, 1H, $J = 16.0$ Hz), 7.53 (s, 1H), 7.63 (d, 1H, $J = 7.5$ Hz), 7.79 (dd, 2H, $J_1 = 13.0$ Hz, $J_2 = 5.5$ Hz); $^{13}C\{^1H\}$ NMR ($CDCl_3$, 125 MHz): δ 28.8, 40.6, 55.9, 56.4, 59.8 (t, $J = 104$ Hz), 108.5 (m), 107.8 (m), 109.8 (m), 116.8, 118.1, 121.6, 124.3, 129.1, 135.3, 137.4, 146.3, 165.0, 168.9; $^{19}F\{^{13}C\}$ NMR ($CDCl_3$, 470 MHz): δ -137.2, -129.9, -125.3, -119.6; IR (KBr, cm^{-1}): 3060, 2986, 2842, 1733, 1688, 1374, 1264, 1170, 1045, 982; ESI-MS: calcd. for $C_{19}H_{20}F_8NO_3^+$ $[M + H^+]$ 462.1310; found 462.1435

(3S,8S,9S,10R,13R,14S,17R)-10,13-dimethyl-17-((R)-4-methylpentan-2-yl)-2,3,4,7,8,9,10,11,12,13,14,15,16,17-Tetradecahydro-1H-cyclopenta[*a*]phenanthren-3-yl 2-(2-(*tert*-butyl)-3-oxoisindolin-1-yl)acetate (22a):

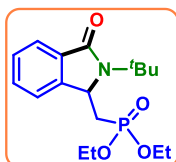


Yellow gummy (178 mg, 58% yield); ^1H NMR (CDCl_3 , 500 MHz): δ 0.86 (d, 9H, $J = 6.5$ Hz), 0.91 (d, 3H, $J = 6.5$ Hz), 0.98 (s, 3H), 1.07 (d, 2H, $J = 10.5$ Hz), 1.13 (dd, 4H, $J_1 = 12.5$ Hz, $J_2 = 7.5$ Hz), 1.26 (s, 4H), 1.34 (t, 4H, $J = 6.0$ Hz), 1.46 (d, 3H, $J = 14.0$ Hz), 1.52 (dd, 3H, $J_1 = 13.0$ Hz, $J_2 = 6.0$ Hz), 1.61 (s, 9H), 1.85-1.76 (m, 4H), 1.97 (d, 2H, $J = 22.0$ Hz), 2.03 (d, 1H, $J = 9.0$ Hz), 2.26-2.13 (m, 2H), 2.54-2.49 (m, 1H), 3.18 (d, 1H, $J = 16.0$ Hz), 5.11 (d, 1H, $J = 8.5$ Hz), 5.36 (s, 1H), 7.38 (d, 1H, $J = 7.5$ Hz), 7.42 (t, 1H, $J = 7.5$ Hz), 7.49-7.46 (m, 1H), 7.76 (d, 1H, $J = 7.5$ Hz); $^{13}\text{C}\{^1\text{H}\}$ NMR (CDCl_3 , 125 MHz): δ 12.0, 18.9, 19.5, 21.2, 22.8, 23.0, 24.0, 24.5, 27.8, 27.9, 28.2, 28.4, 28.9, 32.07, 32.11, 36.0, 36.4, 36.8, 37.1, 38.2, 39.7, 40.0, 41.7, 42.5, 50.3, 53.6, 55.4, 56.4, 56.9, 57.1, 75.0, 122.1, 123.1, 123.5, 128.5, 131.5, 133.4, 139.6, 145.8, 169.3, 169.8; IR (KBr, cm^{-1}): 3054, 2934, 2862, 1732, 1688, 1373, 1264, 1046; HRMS (ESI): calcd. for $\text{C}_{41}\text{H}_{62}\text{NO}_3^+$ [$\text{M} + \text{H}^+$] 616.4724; found 616.4735.

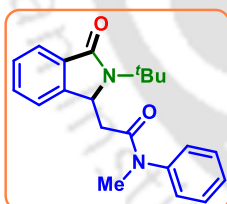
2-(2-(*tert*-Butyl)-3-oxoisindolin-1-yl)acetonitrile (23a):



Brown solid (85 mg, 75% yield); mp 141–143 °C; ^1H NMR (CDCl_3 , 400 MHz): δ 1.60 (s, 9H), 2.84 (dd, 1H, $J_1 = 17.2$ Hz, $J_2 = 7.2$ Hz), 3.14 (dd, 1H, $J_1 = 16.8$ Hz, $J_2 = 2.4$ Hz), 4.91 (dd, 1H, $J_1 = 7.2$ Hz, $J_2 = 2.4$ Hz), 7.48 (t, 1H, $J = 6.8$ Hz), 7.57-7.51 (m, 2H), 7.78 (d, 1H, $J = 7.2$ Hz); $^{13}\text{C}\{^1\text{H}\}$ NMR (CDCl_3 , 100 MHz): δ 26.3, 28.8, 55.6, 55.9, 115.6, 121.8, 123.8, 129.4, 132.1, 133.2, 143.1, 169.0; IR (KBr, cm^{-1}): 3003, 2943, 2885, 2294, 1636, 1442, 1375, 1038; HRMS (ESI): calcd. for $\text{C}_{14}\text{H}_{17}\text{N}_2\text{O}^+$ [$\text{M} + \text{H}^+$] 229.1335; found 229.1336.

Diethyl ((2-(*tert*-butyl)-3-oxoisindolin-1-yl)methyl)phosphonate (24a):

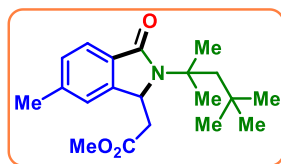
Red gummy (125 mg, 74% yield); ^1H NMR (CDCl_3 , 500 MHz): δ 1.27 (t, 3H, $J = 7.5$ Hz), 1.32 (t, 3H, $J = 7.0$ Hz), 1.61 (s, 9H), 2.09-2.01 (m, 1H), 2.66 (dd, 1H, $J_1 = 21.5$ Hz, $J_2 = 16.0$ Hz), 4.02 (dd, 2H, $J_1 = 15.0$ Hz, $J_2 = 7.5$ Hz), 4.14-4.09 (m, 2H), 5.02 (dd, 1H, $J_1 = 15.0$ Hz, $J_2 = 10.0$ Hz), 7.41 (t, 1H, $J = 7.5$ Hz), 7.50 (t, 1H, $J = 8.0$ Hz), 7.73 (d, 1H, $J = 7.0$ Hz), 7.82 (d, 1H, $J = 7.2$ Hz); $^{13}\text{C}\{^1\text{H}\}$ NMR (CDCl_3 , 125 MHz): δ 15.4 (d, $J = 8.9$ Hz), 27.7, 32.0 (d, $J = 137.0$ Hz), 54.4, 60.8 (d, $J = 9.0$ Hz), 60.9 (d, $J = 7.1$ Hz), 122.0 (d, $J = 5.1$ Hz), 127.3, 130.3, 131.1 (d, $J = 10$ Hz), 131.8, 144.7, 168.1; $^{31}\text{P}\{^{13}\text{C}\}$ NMR (CDCl_3 , 202 MHz): δ 26.2; IR (KBr, cm^{-1}): 3056, 2981, 2911, 1683, 1468, 1379, 1119, 1025; HRMS (ESI): calcd. for $\text{C}_{17}\text{H}_{27}\text{NO}_4\text{P}^+$ [$\text{M} + \text{H}^+$] 340.1672; found 340.1673.

2-(2-(*tert*-Butyl)-3-oxoisindolin-1-yl)-*N*-methyl-*N*-phenylacetamide (25a):

As a yellow solid (134 mg, 80% yield); mp 168–170 °C; ^1H NMR (CDCl_3 , 500 MHz): δ 1.41 (s, 9H), 1.94 (dd, 1H, $J_1 = 15.5$ Hz, $J_2 = 10.0$ Hz), 2.89 (d, 1H, $J = 15.5$ Hz), 3.24 (s, 3H), 5.21 (d, 1H, $J = 10.0$ Hz), 6.77 (d, 2H, $J = 6.0$ Hz), 7.18 (d, 3H, $J = 6.5$ Hz), 7.32 (t, 1H, $J = 7.0$ Hz), 7.42 (dd, 2H, $J_1 = 12.5$ Hz, $J_2 = 7.5$ Hz), 7.61 (d, 1H, $J = 7.0$ Hz); $^{13}\text{C}\{^1\text{H}\}$ NMR (CDCl_3 , 125 MHz): δ 28.7, 37.3, 41.5, 55.0, 57.7, 122.4, 123.2, 127.1, 128.15, 128.23, 130.0, 131.2, 132.9, 143.3, 146.5, 168.9, 169.7; IR (KBr, cm^{-1}): 3054, 2984, 2871, 1681, 1650, 1496, 1264, 1042; HRMS (ESI): calcd. for $\text{C}_{21}\text{H}_{25}\text{N}_2\text{O}_2^+$ [$\text{M} + \text{H}^+$] 337.1911; found 337.1906.

Methyl 2-(6-methyl-3-oxo-2-(2,4,4-trimethylpentan-2-yl)isoindolin-1-yl)acetate (2b):

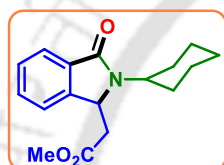
Yellow gummy (114 mg, 69% yield); ^1H NMR (CDCl_3 , 400 MHz): δ 0.89 (s, 9H), 1.45 (d, 1H, $J = 14.8$ Hz), 1.63 (s, 6H), 2.39 (s, 3H), 2.45 (dd, 1H, $J_1 = 16.8$ Hz, $J_2 = 9.2$ Hz), 2.85 (d, 1H, $J = 14.8$ Hz), 3.23 (dd, 1H, $J_1 = 16.4$ Hz, $J_2 = 2.4$ Hz), 3.72 (s, 3H), 5.08 (dd, 1H, $J_1 = 9.2$ Hz, $J_2 = 2.0$ Hz), 7.12 (s, 1H),



7.20 (d, 1H, $J = 7.6$ Hz), 7.61 (d, 1H, $J = 7.6$ Hz); $^{13}\text{C}\{^1\text{H}\}$ NMR (CDCl_3 , 100 MHz): δ 22.1, 27.9, 30.8, 31.5, 31.7, 41.6, 50.6, 52.1, 57.1, 59.3, 122.3, 123.3, 129.5, 130.7, 171.2, 142.2, 146.2, 169.5; IR (KBr, cm^{-1}): 3057, 2954, 2882, 1733, 1686, 1264, 1125; HRMS (ESI): calcd. for $\text{C}_{20}\text{H}_{30}\text{NO}_3^+$ [$\text{M} + \text{H}^+$] 332.2220; found 332.2211.

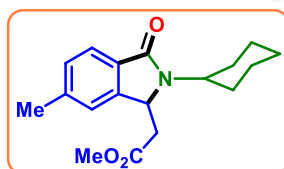
Methyl 2-(2-cyclohexyl-3-oxoisindolin-1-yl)acetate (1c):

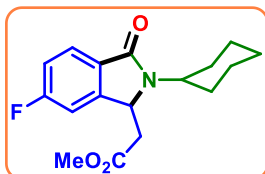
Brown gummy (93 mg, 65% yield); ^1H NMR (CDCl_3 , 400 MHz): δ 1.26-1.19 (m, 1H), 1.40-1.30 (m, 2H), 1.72 (t, 2H, $J = 12.8$ Hz), 1.89-1.77 (m, 4H), 2.06-1.96 (m, 1H), 2.55 (dd, 1H, $J_1 = 16.4$ Hz, $J_2 = 8.8$ Hz), 3.11 (dd, 1H, $J_1 = 16.4$ Hz, $J_2 = 4.4$ Hz), 3.74 (s, 3H), 3.82-3.75 (m, 1H), 4.98 (dd, 1H, $J_1 = 8.8$ Hz, $J_2 = 4.4$ Hz), 7.36 (d, 1H, $J = 7.6$ Hz), 7.44 (t, 1H, $J = 6.8$ Hz), 7.51-7.42 (m, 2H), 7.80 (d, 1H, $J = 6.8$ Hz); $^{13}\text{C}\{^1\text{H}\}$ NMR (CDCl_3 , 100 MHz): δ 25.7, 26.3, 26.4, 30.9, 31.4, 39.2, 52.2, 54.0, 56.7, 122.3, 123.7, 128.7, 131.7, 132.8, 145.3, 168.5, 171.2; IR (KBr, cm^{-1}): 3041, 2932, 2855, 1735, 1686, 1469, 1372, 1264, 1045; HRMS (ESI): calcd. for $\text{C}_{17}\text{H}_{22}\text{NO}_3^+$ [$\text{M} + \text{H}^+$] 288.1594; found 288.1603.



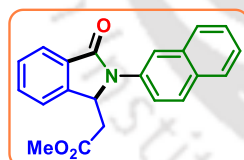
Methyl 2-(2-cyclohexyl-6-methyl-3-oxoisindolin-1-yl)acetate (2c):

As a yellow solid (100 mg, 67% yield); ^1H NMR (CDCl_3 , 400 MHz): δ 1.23-1.15 (m, 2H), 1.41-1.27 (m, 2H), 1.68 (d, 1H, $J = 12.4$ Hz), 1.88-1.77 (m, 4H), 2.04-1.94 (m, 1H), 2.41 (s, 3H), 2.53 (dd, 1H, $J_1 = 16.0$ Hz, $J_2 = 8.4$ Hz), 3.07 (dd, 1H, $J_1 = 16.0$ Hz, $J_2 = 4.0$ Hz), 3.73 (s, 3H), 3.80-3.76 (m, 1H), 4.92 (dd, 1H, $J_1 = 8.8$ Hz, $J_2 = 4.0$ Hz), 7.14 (s, 1H), 7.23 (d, 1H, $J = 7.6$ Hz), 7.67 (d, 1H, $J = 7.6$ Hz); $^{13}\text{C}\{^1\text{H}\}$ NMR (CDCl_3 , 125 MHz): δ 22.1, 25.6, 26.3, 26.4, 30.9, 31.4, 39.2, 52.2, 53.9, 56.4, 122.8, 123.4, 129.6, 130.1, 142.2, 145.7, 168.6, 171.2; IR (KBr, cm^{-1}): 3048, 2930, 2855, 1735, 1684, 1401, 1371, 1264, 1163, 1045; HRMS (ESI): calcd. for $\text{C}_{18}\text{H}_{24}\text{NO}_3^+$ [$\text{M} + \text{H}^+$] 302.1751; found 302.1752.

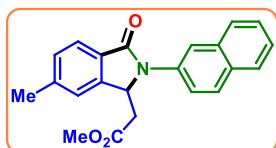


Methyl 2-(2-cyclohexyl-6-fluoro-3-oxoisindolin-1-yl)acetate (6c):

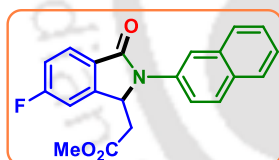
As a red solid (93 mg, 61% yield); mp 87–89 °C; ^1H NMR (CDCl_3 , 400 MHz): δ 1.25-1.18 (m, 1H), 1.43-1.30 (m, 2H), 1.90-1.75 (m, 6H), 2.03-1.96 (m, 1H), 2.53 (dd, 1H, $J_1 = 16.4$ Hz, $J_2 = 8.4$ Hz), 3.12 (dd, 1H, $J_1 = 16.4$ Hz, $J_2 = 4.0$ Hz), 3.75 (s, 3H), 3.80-3.76 (m, 1H), 4.95 (dd, 1H, $J_1 = 9.2$ Hz, $J_2 = 4.0$ Hz), 7.16-7.08 (m, 2H), 7.77 (dd, 1H, $J_1 = 8.4$ Hz, $J_2 = 8.4$ Hz); $^{13}\text{C}\{^1\text{H}\}$ NMR (CDCl_3 , 100 MHz): δ 25.6, 26.2, 26.4, 30.9, 31.5, 38.9, 52.4, 54.1, 56.2 (d, $J = 2.7$ Hz), 110.0 (d, $J = 24.5$ Hz), 116.3 (d, $J = 23.3$ Hz), 125.6 (d, $J = 9.6$ Hz), 128.8 (d, $J = 2.1$ Hz), 147.6 (d, $J = 9.7$ Hz), 164.0 (d, $J = 249.4$ Hz), 167.5, 171.0; $^{19}\text{F}\{^{13}\text{C}\}$ NMR (CDCl_3 , 376 MHz): δ -107.28; IR (KBr, cm^{-1}): 3077, 2936, 2850, 1734, 1684, 1470, 1264, 1166; HRMS (ESI): calcd. for $\text{C}_{17}\text{H}_{21}\text{FNO}_3^+$ [$\text{M} + \text{H}^+$] 306.1500; found 306.1505.

Methyl 2-(2-(naphthalen-2-yl)-3-oxoisindolin-1-yl)acetate (1d):

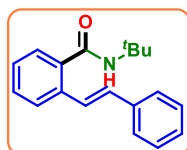
As a red solid (99 mg, 60% yield); mp 138–140 °C; ^1H NMR (CDCl_3 , 400 MHz): δ 2.54 (dd, 1H, $J_1 = 16.4$ Hz, $J_2 = 8.8$ Hz), 2.99 (dd, 1H, $J_1 = 16.0$ Hz, $J_2 = 4.0$ Hz), 3.59 (s, 3H), 5.73 (dd, 1H, $J_1 = 8.8$ Hz, $J_2 = 4.0$ Hz), 7.51-7.46 (m, 2H), 7.57-7.52 (m, 2H), 7.64-7.60 (m, 1H), 7.79 (dd, 1H, $J_1 = 8.8$ Hz, $J_2 = 2.0$ Hz), 7.86-7.84 (m, 2H), 7.93 (d, 1H, $J = 8.8$ Hz), 7.98 (d, 2H, $J = 6.8$ Hz); $^{13}\text{C}\{^1\text{H}\}$ NMR (CDCl_3 , 100 MHz): δ 37.8, 52.2, 57.9, 121.8, 122.77, 122.78, 124.5, 126.1, 126.8, 127.8, 128.0, 129.2, 129.3, 131.6, 132.0, 132.6, 133.8, 134.2, 144.4, 167.2, 171.1; IR (KBr, cm^{-1}): 3054, 2986, 2866, 1733, 1698, 1264, 1100, 1045; HRMS (ESI): calcd. for $\text{C}_{21}\text{H}_{18}\text{NO}_3^+$ [$\text{M} + \text{H}^+$] 332.1281; found 332.1281.

Methyl 2-(6-methyl-2-(naphthalen-2-yl)-3-oxoisindolin-1-yl)acetate (2d):

As a red solid (180.4 mg, 64% yield); mp 168–170 °C; ^1H NMR (CDCl_3 , 400 MHz): δ 2.49 (s, 3H), 2.54 (t, 1H, $J = 6.8$ Hz), 2.97 (dd, 1H, $J_1 = 16.4$ Hz, $J_2 = 3.6$ Hz), 3.60 (s, 3H), 5.68 (d, 1H, $J = 4.8$ Hz), 7.35 (d, 2H, $J = 8.0$ Hz), 7.49 (t, 2H, $J = 6.4$ Hz), 7.79 (d, 1H, $J = 8.4$ Hz), 7.85 (d, 3H, $J = 6.4$ Hz), 7.93 (t, 2H, $J = 8.8$ Hz); $^{13}\text{C}\{^1\text{H}\}$ NMR (CDCl_3 , 100 MHz): δ 22.3, 37.8, 52.1, 57.6, 121.6, 122.8, 123.2, 124.3, 126.0, 126.7, 127.8, 128.0, 129.3, 129.4, 130.2, 131.5, 133.8, 134.3, 143.4, 144.8, 167.3, 171.2; IR (KBr, cm^{-1}): 3054, 2949, 2846, 1734, 1702, 1600, 1388, 1264, 1045; HRMS (ESI): calcd. for $\text{C}_{22}\text{H}_{20}\text{NO}_3^+$ [$\text{M} + \text{H}^+$] 346.1438; found 346.1440.

Methyl 2-(6-fluoro-2-(naphthalen-2-yl)-3-oxoisindolin-1-yl)acetate (6d):

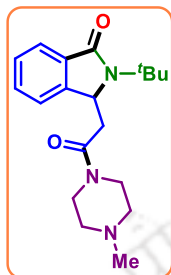
As a red solid (101 mg, 58% yield); mp 150–152 °C; ^1H NMR (CDCl_3 , 400 MHz): δ 2.53 (dd, 1H, $J_1 = 16.4$ Hz, $J_2 = 9.2$ Hz), 3.01 (dd, 1H, $J_1 = 16.8$ Hz, $J_2 = 4.0$ Hz), 3.63 (s, 3H), 5.70 (dd, 1H, $J_1 = 9.2$ Hz, $J_2 = 4.0$ Hz), 7.30–7.23 (m, 3H), 7.54–7.47 (m, 2H), 7.86 (d, 2H, $J = 7.2$ Hz), 7.97–7.92 (m, 3H); $^{13}\text{C}\{^1\text{H}\}$ NMR (CDCl_3 , 100 MHz): δ 37.6, 52.3, 57.5 (d, $J = 2.6$ Hz), 110.4 (d, $J = 24.6$ Hz), 117.0 (d, $J = 23.3$ Hz), 121.8, 122.7, 126.3, 126.6 (d, $J = 9.7$ Hz), 126.9, 127.9, 128.0, 128.10, 128.12, 129.5, 131.7, 133.8 (d, $J = 16.0$ Hz), 146.9 (d, $J = 9.9$ Hz), 164.5 (d, $J = 250.9$ Hz), 166.2, 171.0; IR (KBr, cm^{-1}): 3051, 2974, 2836, 1734, 1623, 1390, 1264, 1045; HRMS (ESI): calcd. for $\text{C}_{21}\text{H}_{17}\text{FNO}_3^+$ [$\text{M} + \text{H}^+$] 350.1187; found 350.1181.

***N*-(*tert*-butyl)-2-styrylbenzamide (26')**

Brown gummy (108 mg, 83% yield); ^1H NMR (CDCl_3 , 400 MHz): δ 1.38 (s, 9H), 5.57 (s, 1H), 6.96 (d, 1H, $J = 12.4$ Hz), 7.21–7.17 (m, 2H), 7.31–7.26 (m, 4H), 7.37 (dd, 1H, $J_1 = 6.4$ Hz, $J_2 = 0.8$ Hz), 7.42 (d, 2H, $J = 7.2$ Hz), 7.57 (d, 1H, $J = 8.0$ Hz); $^{13}\text{C}\{^1\text{H}\}$ NMR (CDCl_3 , 100 MHz): δ 29.1, 52.3, 126.1,

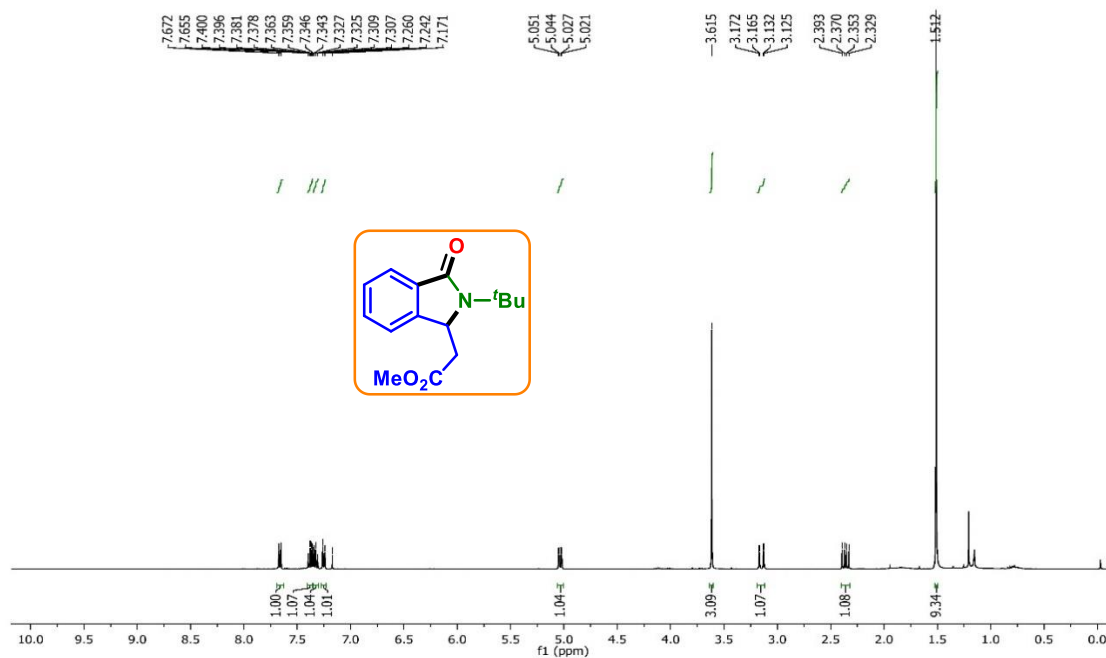
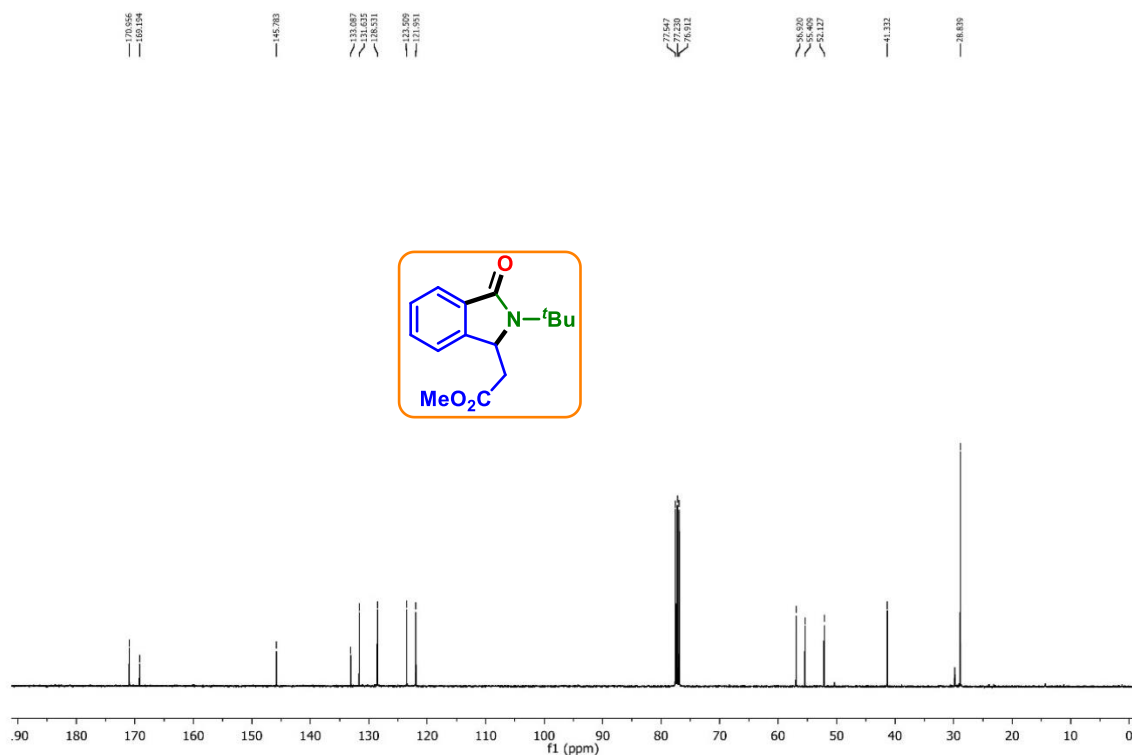
126.2, 126.8, 127.6, 127.7, 128.1, 128.9, 130.0, 131.3, 135.1, 137.20, 13.23, 169.2.

2-(*tert*-Butyl)-3-(2-(4-methylpiperazin-1-yl)-2-oxoethyl)isoindolin-1-one (1ab):

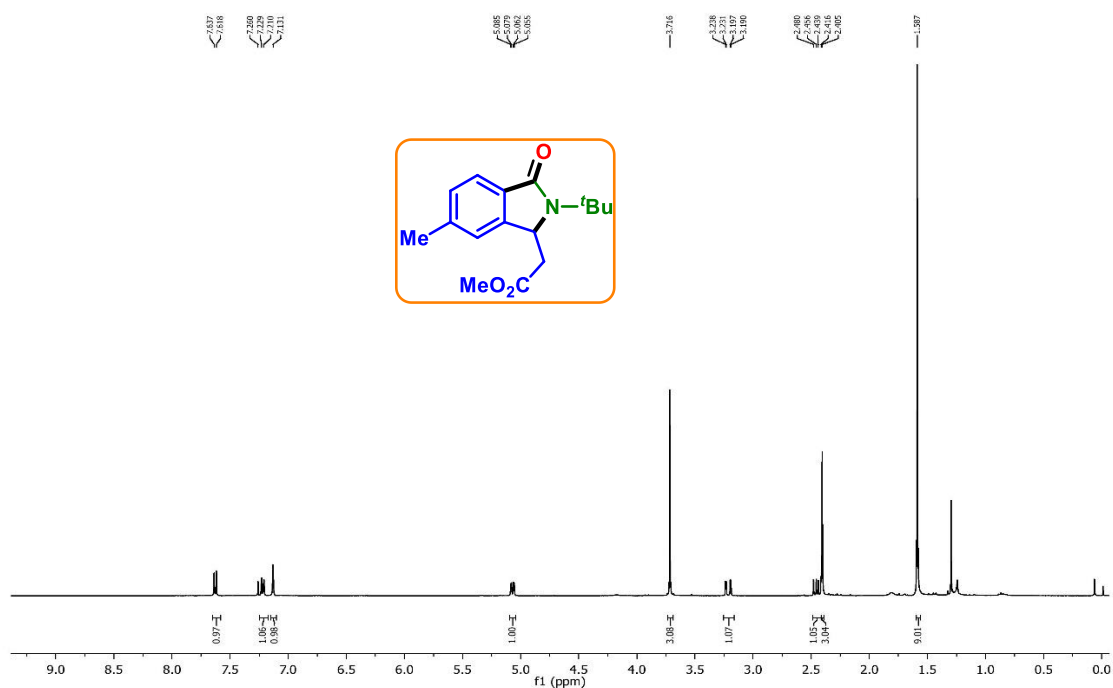


Yellow gummy (168 mg, 51% yield); ^1H NMR (CDCl_3 , 500 MHz): δ 1.53 (s, 9H), 2.11 (s, 3H), 2.19 (s, 3H), 2.35-2.23 (m, 4H), 3.07 (dd, 1H, $J_1 = 16.0$ Hz, $J_2 = 1.5$ Hz), 3.22 (t, 2H, $J = 22.0$ Hz), 3.60 (s, 3H), 3.66 (s, 3H), 5.30 (t, 1H, $J = 9.5$ Hz), 7.34 (d, 3H, $J = 10.0$ Hz), 7.65 (s, 1H); $^{13}\text{C}\{^1\text{H}\}$ NMR (CDCl_3 , 125 MHz): δ 28.7, 39.8, 40.8, 45.3, 45.8, 54.5, 54.8, 55.1, 57.5, 122.5, 123.1, 128.1, 131.3, 132.6, 146.5, 168.0, 168.9; IR (KBr, cm^{-1}): 3081, 2971, 2853, 1690, 1683, 1437, 1381, 1264, 1066; HRMS (ESI): calcd. for $\text{C}_{15}\text{H}_{20}\text{NO}_3^+$ [$\text{M} + \text{H}^+$] 330.2176; found 330.2176.

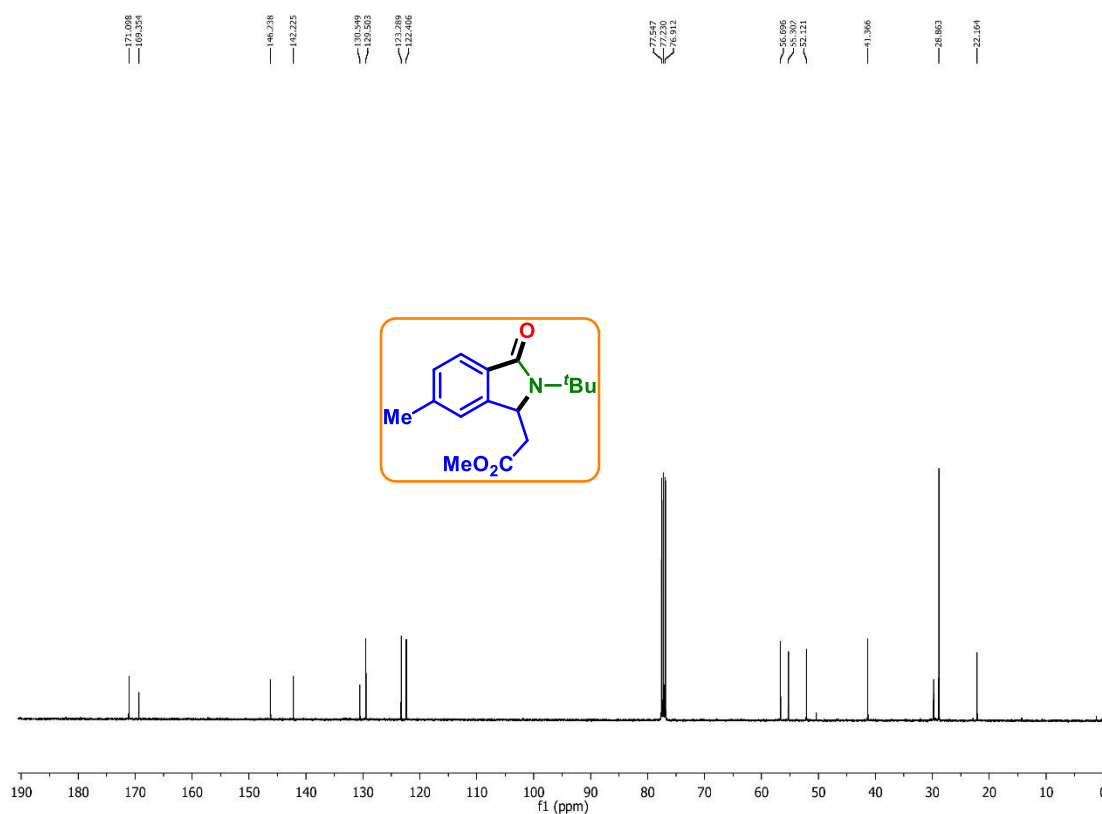
IV.7. Representative Spectra

Methyl 2-(2-(*tert*-butyl)-3-oxoisindolin-1-yl)acetate (**1a**): ^1H NMR (CDCl_3 , 400 MHz)Methyl 2-(2-(*tert*-butyl)-3-oxoisindolin-1-yl)acetate (**1a**): ^{13}C $\{^1\text{H}\}$ NMR (CDCl_3 , 100 MHz)

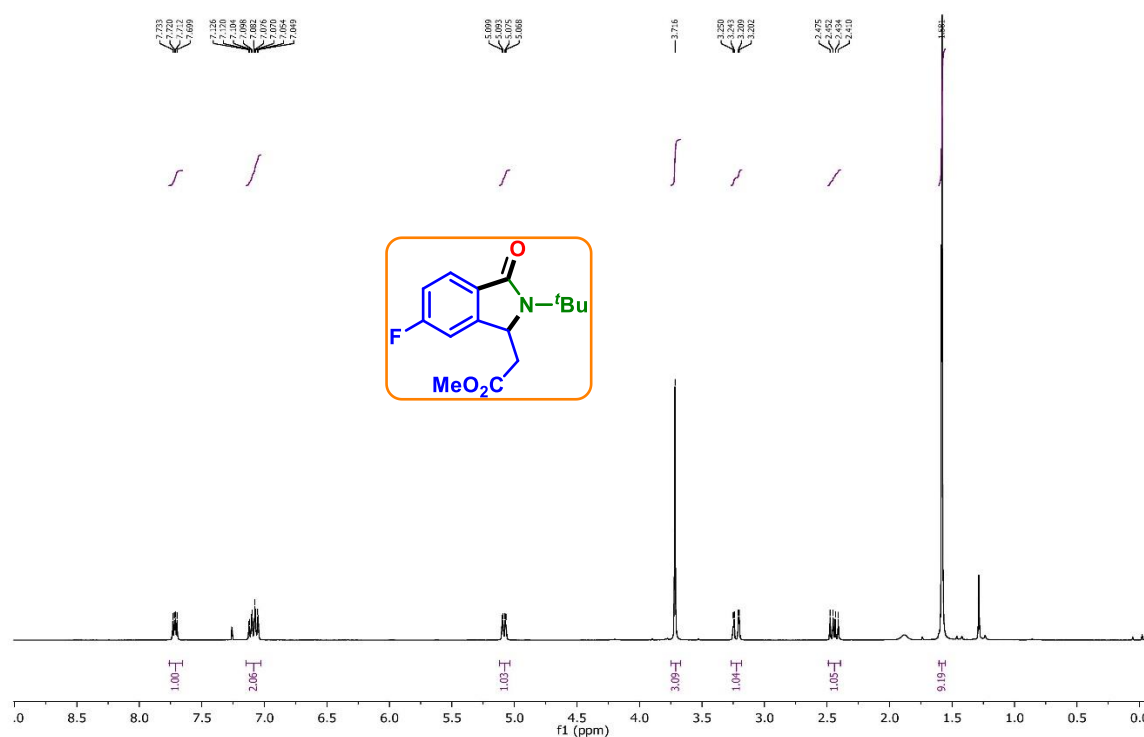
Methyl 2-(2-(*tert*-butyl)-6-methyl-3-oxoisindolin-1-yl)acetate (**2a**): ^1H NMR (CDCl_3 , 400 MHz)



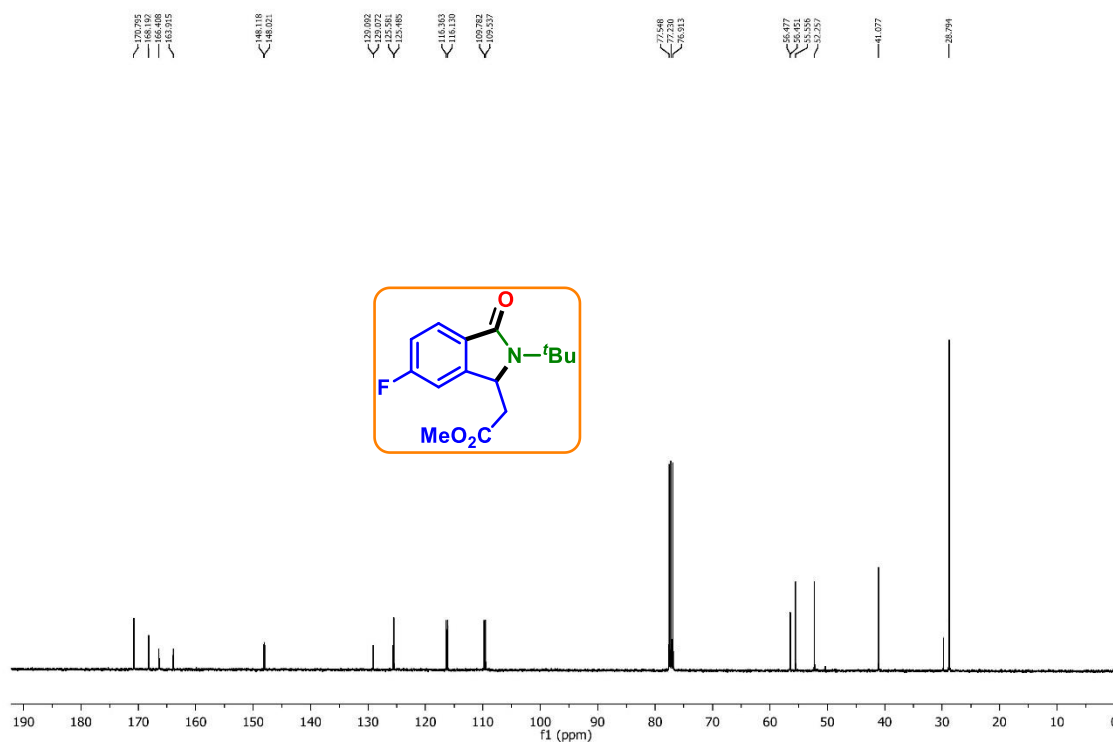
Methyl 2-(2-(*tert*-butyl)-6-methyl-3-oxoisindolin-1-yl)acetate (**2a**): $^{13}\text{C}\{^1\text{H}\}$ NMR (CDCl_3 , 100 MHz)



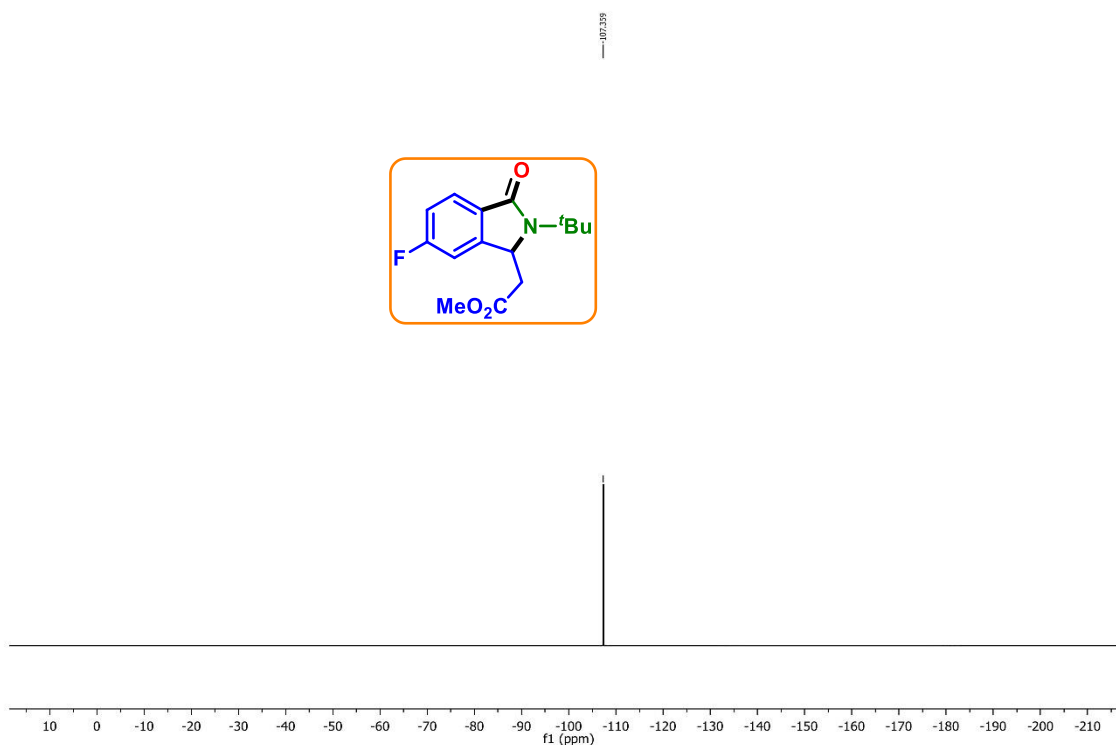
Methyl 2-(2-(*tert*-butyl)-6-fluoro-3-oxoisindolin-1-yl)acetate (6a): ^1H NMR (CDCl_3 , 400 MHz)



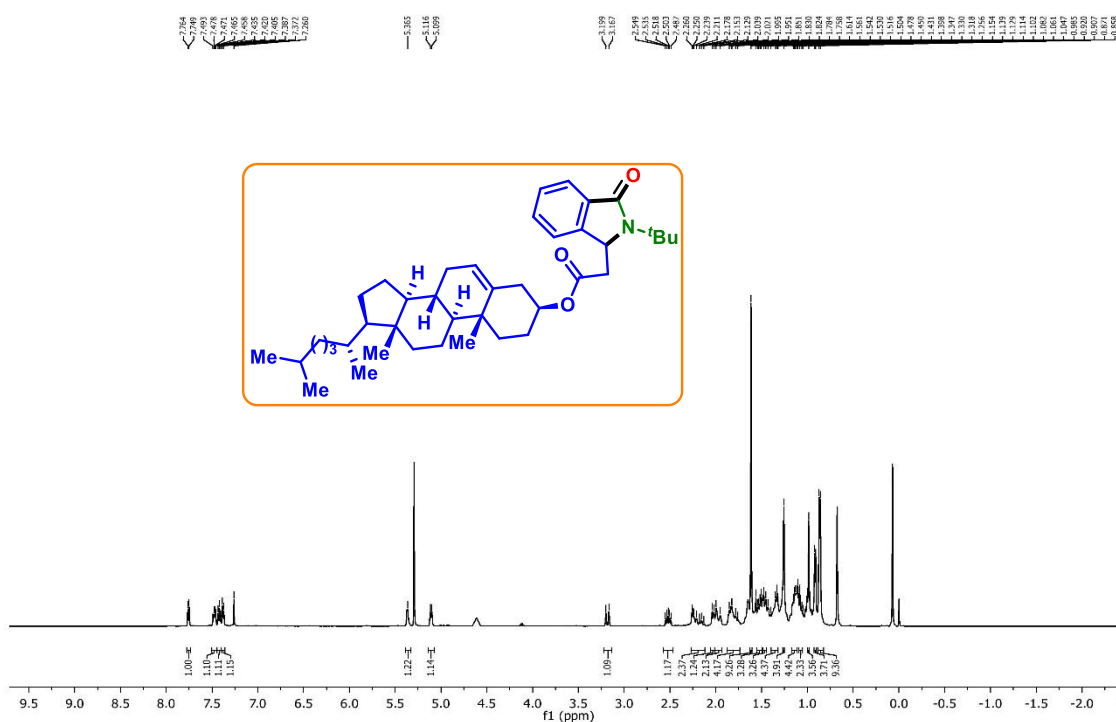
Methyl 2-(2-(*tert*-butyl)-6-fluoro-3-oxoisindolin-1-yl)acetate (6a): ^1H NMR (CDCl_3 , 400 MHz)



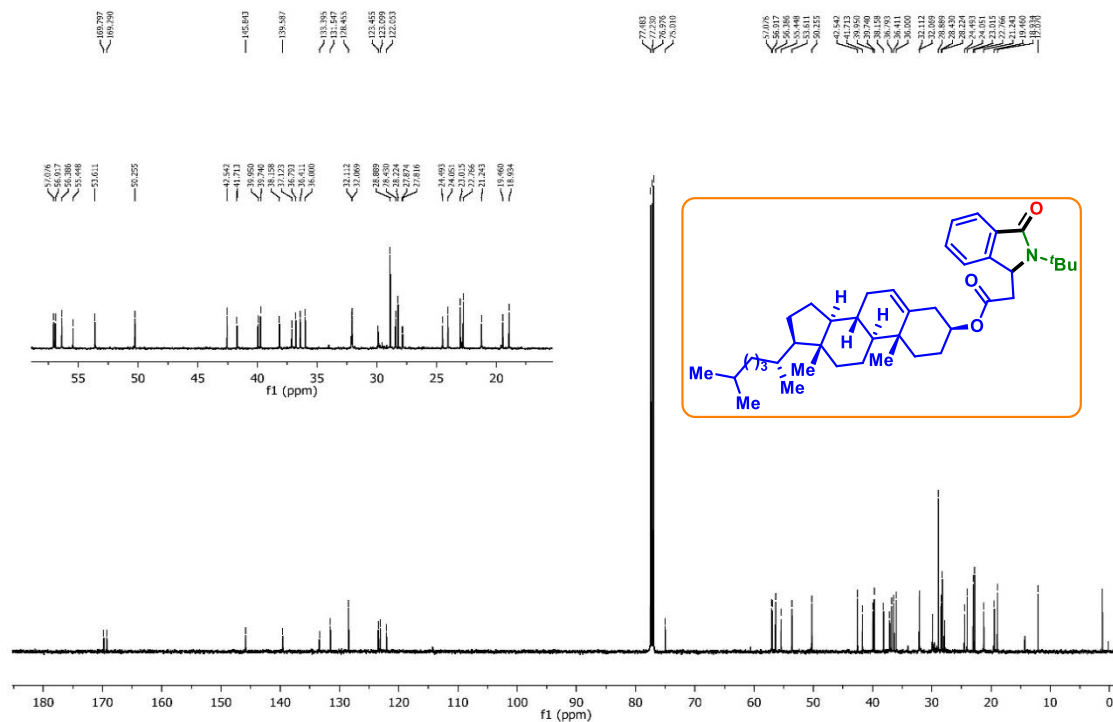
Methyl 2-(2-(*tert*-butyl)-6-fluoro-3-oxoisindolin-1-yl)acetate (6a): ^{19}F NMR (CDCl_3 , 376 MHz)



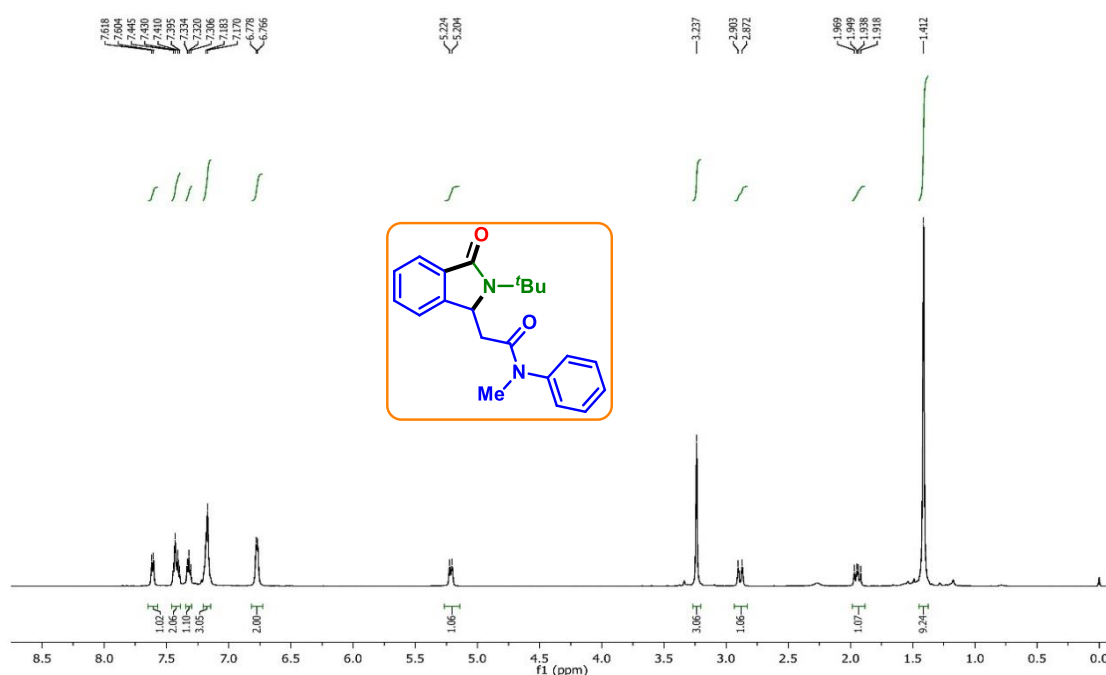
(3*S*,8*S*,9*S*,10*R*,13*R*,14*S*,17*R*)-10,13-Dimethyl-17-((*R*)-4-methylpentan-2-yl)-2,3,4,7,8,9,10,11,12,13,14,15,16,17-Tetradecahydro-1*H*-cyclopenta[*a*]phenanthren-3-yl 2-(2-(*tert*-butyl)-3-oxoisindolin-1-yl)acetate (22a): ^1H NMR (CDCl_3 , 500 MHz)



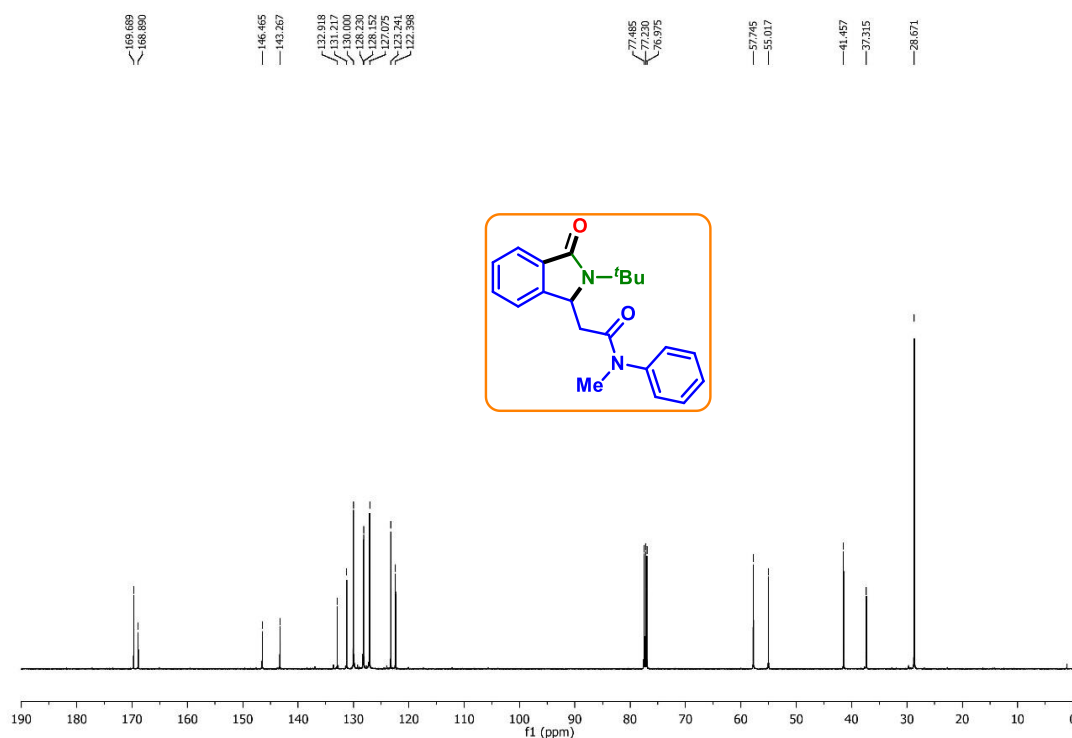
(3*S*,8*S*,9*S*,10*R*,13*R*,14*S*,17*R*)-10,13-Dimethyl-17-((*R*)-4-methylpentan-2-yl)-2,3,4,7,8,9,10,11,12,13,14,15,16,17-Tetradecahydro-1*H*-cyclopenta[*a*]phenanthren-3-yl 2-(2-(*tert*-butyl)-3-oxoisindolin-1-yl)acetate (22a): $^{13}\text{C}\{^1\text{H}\}$ NMR (CDCl_3 , 125 MHz)



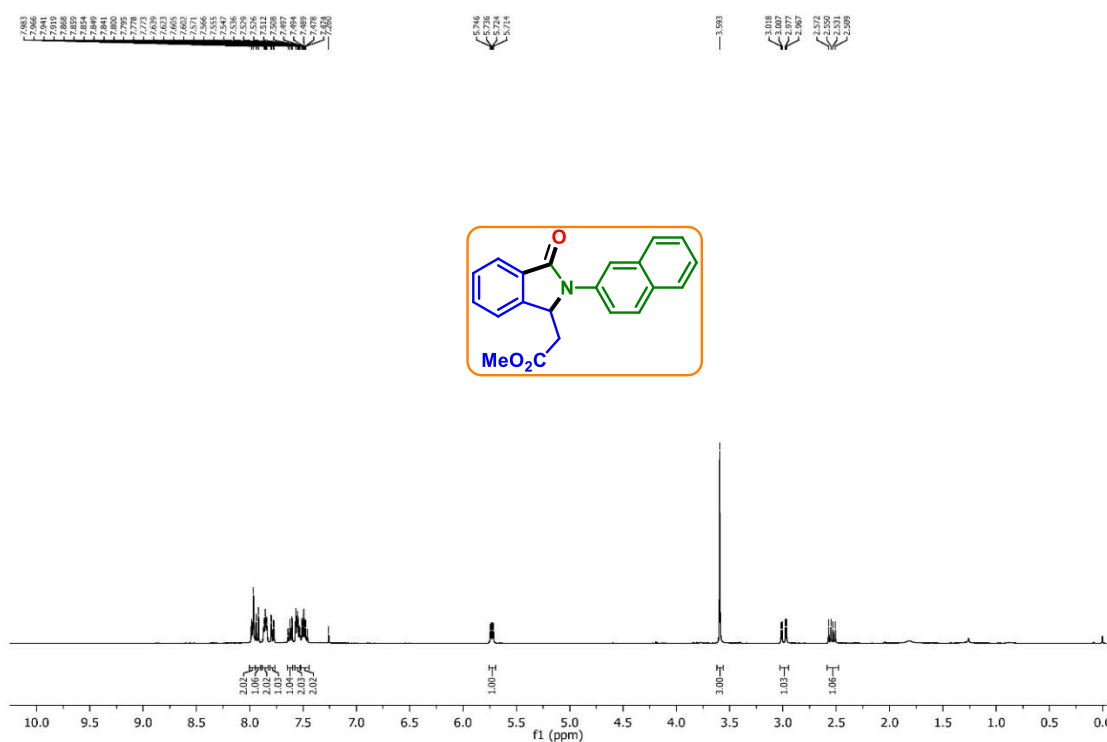
2-(2-(*tert*-Butyl)-3-oxoisindolin-1-yl)-*N*-methyl-*N*-phenylacetamide (25a): ^1H NMR (CDCl_3 , 500 MHz)



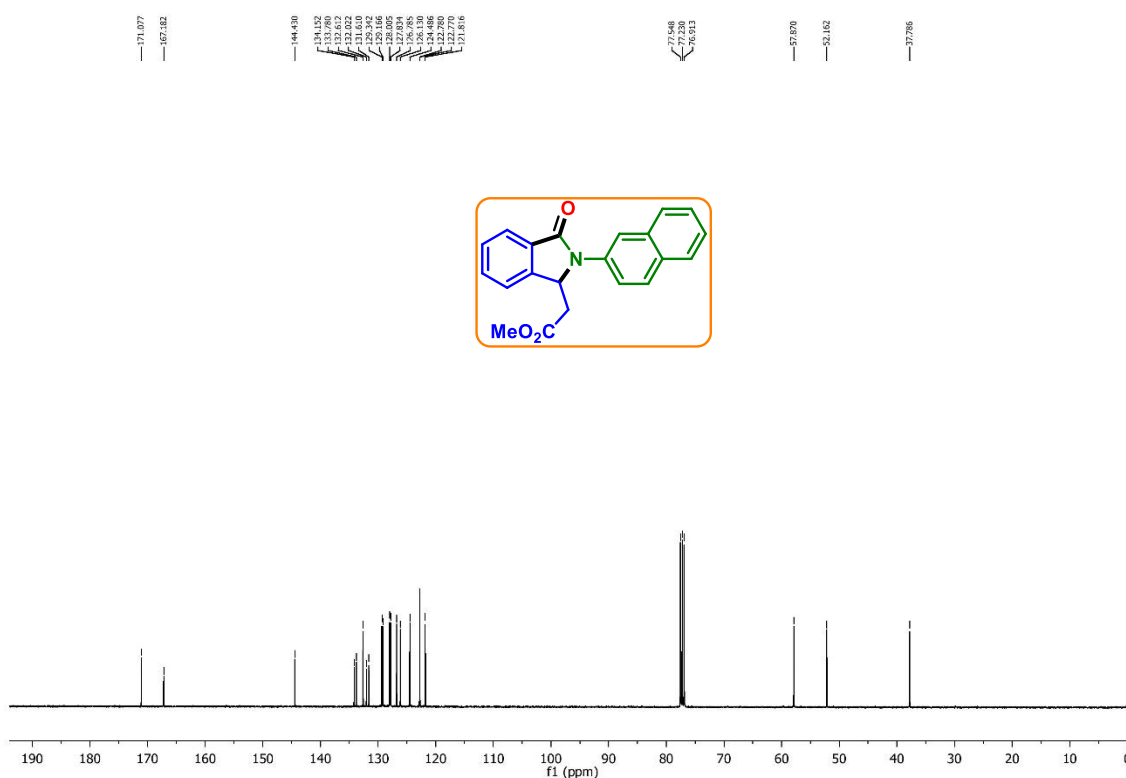
2-(2-(*tert*-Butyl)-3-oxoisindolin-1-yl)-*N*-methyl-*N*-phenylacetamide (25a): $^{13}\text{C}\{^1\text{H}\}$ NMR (CDCl_3 , 125 MHz)



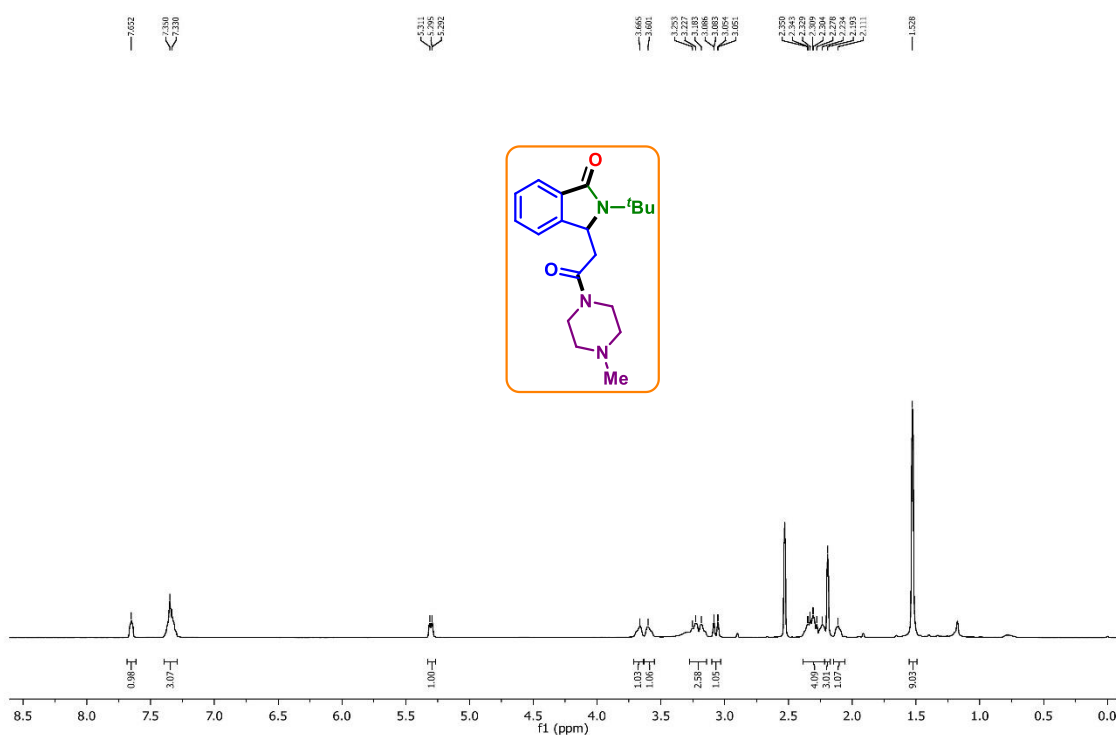
Methyl 2-(2-(naphthalen-2-yl)-3-oxoisindolin-1-yl)acetate (1d): ^1H NMR (CDCl_3 , 400 MHz)



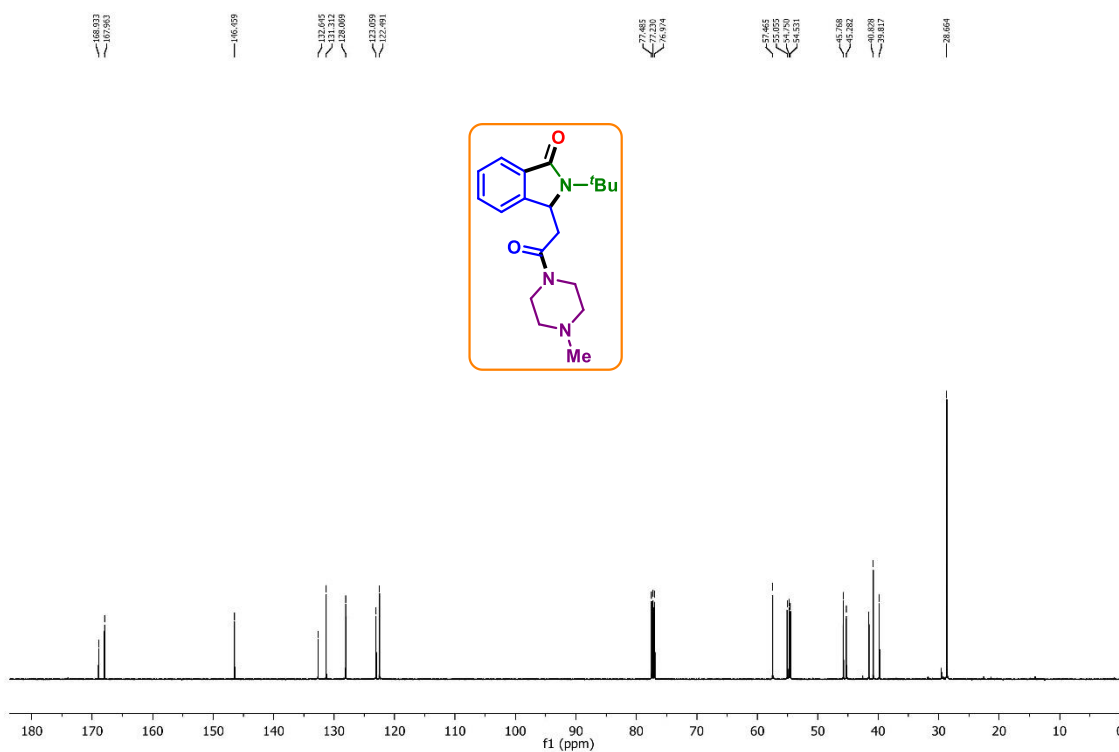
Methyl 2-(2-(naphthalen-2-yl)-3-oxoisindolin-1-yl)acetate (**1d**): $^{13}\text{C}\{^1\text{H}\}$ NMR (CDCl₃, 100 MHz)



2-(*tert*-Butyl)-3-(2-(4-methylpiperazin-1-yl)-2-oxoethyl)isoindolin-1-one (**1ab**): ^1H NMR, 500 MHz, CDCl₃)



2-(*tert*-Butyl)-3-(2-(4-methylpiperazin-1-yl)-2-oxoethyl)isoindolin-1-one (1a**b**): ^{13}C NMR, 125 MHz, CDCl_3)



List of Publications:

Research Articles

- (1) A cascade synthesis of *S*-allyl benzoylcarbamothioates via Mumm-type rearrangement. **Anjali Dahiya**, Wajid Ali, Tipu Alam and Bhisma K. Patel, *Org. Biomol. Chem.* **2018**, *16*, 7787. (**I. F. = 3.87**)
- (2) Cascade Synthesis of Dihydrobenzofurans and Aurones via Palladium-Catalyzed Isocyanides Insertion into 2-Halophenoxy Acrylates. Wajid Ali, **Anjali Dahiya** and Bhisma K. Patel, *Adv. Synth. Catal.* **2018**, *360*, 1232. (**I. F. = 5.85**)
- (3) Catalyst and Solvent Free Domino Ring Opening Cyclization: A Greener and Atom Economic Route to 2-Iminothiazolidines. **Anjali Dahiya**, Wajid Ali and Bhisma K. Patel, *ACS Sustainable Chem. Eng.*, **2018**, *6*, 4272. (**I. F. = 8.19**)
- (4) Microwave-Assisted Cascade Strategy for the Synthesis of Indolo[2,3-*b*]quinolines from 2-(Phenylethynyl)anilines and Aryl Isothiocyanates. Wajid Ali, **Anjali Dahiya**, Ramdhari Pandey, Tipu Alam, and Bhisma K. Patel, *J. Org. Chem.* **2017**, *82*, 2089. (**I. F. = 4.35**)
- (5) Visible Light-Mediated C2-Quaternarization of *N*-Alkyl Indoles through Oxidative Dearomatization using Ir(III) Catalyst. Gaurav Shukla, **Anjali Dahiya**, Tipu Alam, Prof. Bhisma K. Patel, *Asian J. Org. Chem.* **2019**, *8*, 2243. (**I. F. = 3.31**)
- (6) Visible-Light Induced Difunctionalization of Styrenes: Synthesis of *N*-Hydroxybenzimidoyl Cyanides. Tipu Alam, Amitava Rakshit, Pakiza Begum, **Anjali Dahiya**, Prof. Bhisma K. Patel, *Org. Lett.* **2020**, *22*, 3728. (**I. F. = 6.00**)
- (7) Visible-Light-Mediated Regioselective Difunctionalization of Alkynes: Expedient Route for Synthesis of *Z*- β -Carboxy Vinylsulfones. Ashish Kumar Sahoo, **Anjali Dahiya**, Bubul Das and Bhisma K. Patel, *J. Org. Chem.*, **2021**, *86*, 11968. (**I. F. = 4.35**)
- (8) An Expedient Route to Tricyanovinylindoles and Indolylmaleimides from *o*-Alkynylanilines Utilizing DMSO as One-Carbon Synthone. Nikita Chakraborty, **Anjali Dahiya**, Amitava Rakshit, Anju Modi and Bhisma K. Patel, *Org. Biomol. Chem.*, **2021**, *19*, 6847. (**I. F. = 3.87**)
- (9) Cu (II)-Promoted Cascade Synthesis of Fused Imidazo-Pyridine-Carbonitriles. Amitava Rakshit, Hirendrath Dhara, Tipu Alam, **Anjali Dahiya**, Bhisma K. Patel, *J. Org. Chem.*, **2021**, *86*, 17504. (**I. F. = 4.35**)

- (10) Visible-Light-Driven Isocyanide Insertion to *o*-Alkenylanilines: A Route to Isoindolinone Synthesis. **Anjali Dahiya**, Bubul Das, Ashish K. Sahoo, Bhisma K. Patel, *Adv. Synth. Catal.*, **2022**, 364, 966. (**I. F. = 5.85**)
- (11) Visible-Light-Mediated Synthesis of Thio-Functionalized Pyrroles. Ashish K. Sahoo, Amitava Rakshit, Anjali Dahiya, Bhisma K. Patel, *Org. Lett.* **2022**, 24, 1918. (**I. F. = 6.00**)

Review Articles

- (1) *tert*-Butyl Nitrite (TBN), a Multitasking Reagent in Organic Synthesis. **Anjali Dahiya**, Ashish Kumar Sahoo, Tipu Alam, Prof. Bhisma K. Patel, *Chem. Asian J.*, **2019**, 14, 4454. (**I. F. = 4.56**)
- (2) The Rich Legacy and Bright Future of Transition-Metal Catalyzed Peroxide Based Radical Reactions. **Anjali Dahiya**, Prof. Bhisma K. Patel, *Chem. Rec.* **2021**, 21, 3589 (**I. F. = 6.77**)
- (3) The renaissance of alkali metabisulfites as SO₂ surrogate. Ashish Kumar Sahoo, **Anjali Dahiya**, Amitava Rakshit, Prof. Bhisma K. Patel, *Syn Open.* **2021**, 5, 232.
- (4) Updates on hypervalent-iodine reagents: metal-free functionalisation of alkenes, alkynes and heterocycles. Anjali Dahiya, Ashish K. Sahoo, Nikita Chakraborty, Bubul Das, Bhisma K. Patel, *Org. Biomol. Chem.*, **2022**, 20, 2005. (**I. F. = 3.87**)

Book Chapters

- (1) Photocatalytic Degradation of Organic Dyes Using Heterogeneous Catalysts. **Anjali Dahiya**, Prof. Bhisma K. Patel. In: Photocatalytic Degradation of Dyes: Current Trends and Future Perspectives. Ed. Sushma Dave, Jayashankar Das, Maulin P. Shah, *Elsevier*, **2020**, 43-90.
- (2) Biological Methods for Textile Dyes Removal from Wastewaters. Ashish Kumar Sahoo, **Anjali Dahiya**, Prof. Bhisma K. Patel. In: Development in Wastewater Treatment Research and Processes. Ed. Susana Rodriguez-Couto, Maulin Shah, Jayanta Biswas, *Elsevier*, **2020**, 127-151.
- (3) Conventional Liquid Biofuels. Bubul Das, Ashish Kumar Sahoo, **Anjali Dahiya**, Prof. Bhisma K. Patel. In: Bio-Clean Energy Technologies Vol. II. Ed. Pankaj

Chowdhary, Soumya Pandit, Namita Khanna *Springer Nature*, 2020 (*Manuscript Submitted*).

- (4) Heterogeneous Photocatalytic Degradation of Dyes: Fundamental Principles and its Application. Bubul Das, Hirendranath Dhara, Anjali Dahiya, Bhisma K. Patel. In: Trends and Contemporary Technology for Photocatalytic Degradation of Dyes. Ed. Susma Dave *Springer Nature*, 2021 (*Manuscript Submitted*).

